PilVax: A novel peptide carrier for the development of vaccines against tuberculosis

Samuel Douglas Blanchett

A thesis submitted in fulfilment of the requirements for the degree of

Doctor of Philosophy

Department of Molecular Medicine and Pathology

The University of Auckland

2019

Abstract

PilVax is a peptide delivery strategy for the generation of highly specific mucosal immune responses. The food-grade bacterium *Lactococcus lactis* (*L. lacti*s) is used to express selected peptides engineered within the *Streptococcus pyogenes* (*S. pyogenes*) pilus, allowing for peptide amplification, stabilization, and enhanced immunogenicity.

The present study aimed to demonstrate the suitability of PilVax for the generation of novel peptide vaccines against tuberculosis.

Selected peptides (B cell and T cell epitopes), derived from tuberculosis vaccine targets ESAT-6 and Ag85B, were genetically engineered into loop regions of the pilus backbone subunit and expressed in *L. lactis*. Western blots and flow cytometry confirmed pilus formation on *L. lactis*. Mice were vaccinated the PilVax constructs and the B cell response analysed by ELISA while T cell responses were analysed by flow cytometry.

Moderate serum and titers of anti-peptide IgG and IgA were detected confirming the ability to produce antibodies against the cognate peptide. Peptide specific IgA was also detected across a number of mucosal sites sampled. However it remains to be seen whether these antibodies are protective. In PilVax-Ag85B vaccinated mice, peptide specific CD4+ T cells were detected at levels similar to when mice were immunised with BCG. This has been repeated and the same trend has been seen with similar levels of Ag85B peptide specific CD4+ T cells detected. However no ESAT-6 peptide specific CD4+ T cells were detected.

Vaccination with PilVax resulted in the large scale proliferation of CD3+CD4-CD8- T cells. Analysis of cytokine production following stimulation with the cognate peptide showed the major cytokine producing cells to be CD4+ T cells (INF-γ) and CD3+CD4-CD8- T cells (IL-17) in PilVax-Ag85B and BCG vaccinated mice.

This study provides insight into the humoral and cellular immune responses generated by PilVax vaccination and has identified at least one construct that will be used in future protection studies.

Acknowledgements

Firstly I would like to thank Thomas, without whom none of this would have been possible. I first joined the Proft lab as a summer student in 2012 and have been lucky enough to be able to come back and work on PilVax. These have been some of the most challenging, but most rewarding years of my life and I am incredibly grateful for the opportunity.

To Jace, over my time in the group you have been nothing but helpful and supportive for which I will be eternally thankful. The time and effort you have put into helping me with lab work and reading while still maintaining a phenomenal amount of lab work yourself is nothing short of inspirational.

To Catherine, I would like to thank you for you for your friendship in the lab especially when our work was so closely aligned in PilVax related projects. I am truly thankful you were willing to answer my questions at any time, even if it was just checking that 10 x 10 is indeed 100.

I would also like to thank other members of the Proft group and I&I, past and present for their friendship and support over the years, in particular Sky, Adrina, Haniyeh, Reuben, Alana, and Claire.

At the University of Otago I would like to thank Dr Joanna Kirman whose expertise and guidance have enabled me to carry out a large portion of my work in her lab. I would also like to thank Anthony Major for his help in the lab and logistical help. To Brin, thank you for your patience and teaching while I was visiting Otago. I could not have done what I did in Dunedin without your experience and guidance.

To Jeremy and Mei Lin, thank you for being good friends over the last few years both in the office and on excursions. You are the best thing to have happened to the lab.

To Mel, you have been there since day one when it all started at O'Rorke, and we've finally come out the other side almost eight years later. I couldn't have made it this far without you.

To Ashley, James, Lisa, Onalee, Nelson and Tucker, from aqua, the various harvests, to New Year's Eve by the fire, many of my best memories over the last few years have involved you. Thank you for the distractions from the lab.

To my family, thank you. Thank you to Trish and Nana for the support and helping push me over the finish line. Thank to Laura for always being there to provide advice and a good conversation even from the other side of the world. To Bob, Ollie and Jack for selflessly always being there.

Thank you Mum for the support and belief from the beginning.

Table of Contents

List of Figures

List of Tables

Chapter 1. Introduction

1.1. Tuberculosis

Tuberculosis (TB) is a disease caused by *Mycobacterium tuberculosis (Mtb)* which often results in granuloma formation in the affected tissue followed by caseous lesions that lead to cavity formation. Pulmonary TB is of the greatest concern. TB in the bone and joints is also a significant burden of disease with the United States' (US) Centres for Disease control (CDC) estimating 10% of extra pulmonary cases in the US are bone and joint infections. The disease has affected humans for approximately 70,000 years and continues to have a significant impact on human health across the globe (Cambier, Falkow, & Ramakrishnan, 2014).

1.1.1 ***Causative agent: Mycobacterium tuberculosis***

First identified as the causative agent of TB by Robert Koch in 1882, *Mtb* is an expert human pathogen establishing long term infections in the host through a complex infection process (Gordon & Parish, 2018). The bacteria is Gram positive however it has a unique thick and waxy cell wall structure. *Mtb* has an outer lipid membrane containing high levels of lipids and mycolic acid which is reflected in the bacteria's genome where 9% of the genes are dedicated to lipid metabolism (Gordon & Parish, 2018). In addition to its unusual cell wall, it also replicates extremely slowly dividing once every 24 hours, compared to other species that can replicate every hour or less (Cambier et al., 2014).

1.1.2 ***Tuberculosis epidemiology***

Humans are the reservoir for the *Mtb*, with transmission occurring by fine aerosol droplets. Less than 10 bacterium are required to establish infection.

In 2017 there were 10 million new cases of TB infection presented to national health authorities across the globe. TB caused 1.6 million deaths in 2017 alone with the majority of these being in HIV negative people (1.3 million). Additionally, 1.23 billion people are estimated to have latent TB infections and are all at risk of developing active TB in their life time (WorldHealthOrganisation, 2018).

The global distribution of the disease is not uniform (figure 1.1). There is an estimated rate of 10 cases per 100, 000 in high income countries, while the majority of low income countries face rates of 150-400 cases per 100, 000. However in the most affected nations these rates can reach as high as 500+ per 100, 000 seen in parts of Mozambique and South Africa which also have a persistent HIV epidemic (WorldHealthOrganisation, 2018). The challenges many of the most affected countries face differ depending on geographic locations. Antibiotic resistance is particularly common in ex-Soviet bloc countries such as Azerbaijan, Belarus and Kazakhstan. Despite having relatively low incident rates, these countries have a high burden of multi drug resistant cases where initial treatment hasn't resulted in complete eradication. Meanwhile many sub Saharan African nations that have extremely high incident rates are also dealing with a HIV co infection as well. The different challenges faced highlight a need for continued global cooperation in trying to control this disease (WorldHealthOrganisation, 2018).

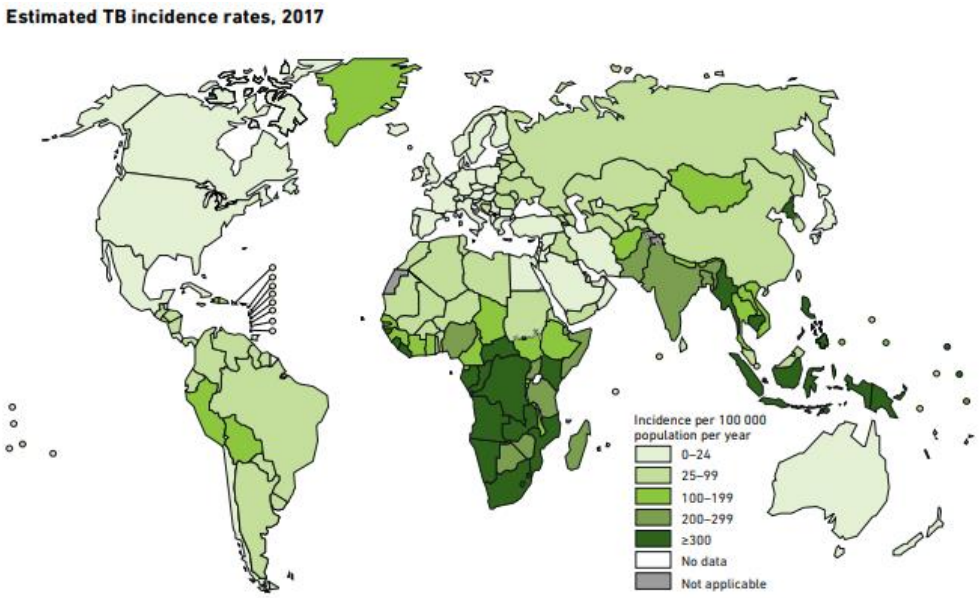

Figure 1.1: Global prevalence of TB incidences (Source: 2018 World Health Organisation annual Global tuberculosis report, reproduced with permission).

Bacteria continue to develop resistance to antibiotics and *Mtb* is no exception. There were 558, 000 cases of rifampicin resistant *Mtb* cases estimated in 2018, up from 490, 000 cases in 2017, a 110% increase. Although the overall number of cases is slowly falling, the proportion of cases that are antibiotic resistant is increasing. The overall rate of decline is below the level required to meet WHO goals (agreed to by all UN member states) of eradication by 2030. To meet this goal urgent action is required in the form of policy change or the discovery of new treatments or vaccines (WorldHealthOrganisation, 2018).

Worldwide funding for TB prevention strategies has more than doubled the last decade, however TB remains in the top 10 causes of death globally, and is the leading cause of death by a single infectious agent. The WHO has stated there is an urgent need for an effective vaccine to prevent TB disease due to the risk posed by the rise of drug resistant strains, the huge amount of people already infected that are at risk of developing active TB over their life

time, and the highly contagious nature of the bacteria. The WHO has gone as far to describe TB as a global health emergency (WorldHealthOrganisation, 2018).

1.1.3 ***Mtb pathogenesis***

Mtb is spread by fine aerosol droplets with less than 10 bacteria required for infection. This low dose allows the bacteria to establish successful entry into the host in the lower respiratory tract (W. F. Wells, Ratcliffe, & Grumb, 1948). Once the bacteria is inside the alveolar, it avoids detection by virtue of one of the lipids expressed in its cell wall. Phthiocerol dimycoceroserate (PDIM) is a lipid that prevents the toll like receptors (TLRs) of the innate immune system from recognising the myriad of pathogen associated molecular patterns (PAMPs) on the surface of *Mtb*. The importance of this lipid in host evasion is critical as all pathogenic strains of *Mtb* possess this despite its metabolic burden to produce (Onwueme, Vos, Zurita, Ferreras, & Quadri, 2005).

Once inside the host and effectively masked from the immune system, *Mtb* utilises phenolic glycolipids (PGL) to attract macrophages. This induces chemokine ligand 2 (CCL2) signalling in the host (Siegrist & Bertozzi, 2014). PGLs are not as essential to virulence as PDIM as these genes are not found in all clinical isolates. However, the recruitment of macrophages greatly increases the chance *Mtb* will reach its niche, the cytosol or endosomes of macrophages (Reed et al., 2004; van der Wel et al., 2007). Uptake by macrophages allows the bacteria to travel into deeper tissue and across epithelial barriers further establishing infection (Cambier et al., 2014).

Mtb grows intracellularly in infected macrophages, which then undergo apoptotic cell death. This is followed by recruitment of more macrophages to the site of infection. Both process are modulated by the early secreted antigen (ESAT-6) protein, (discussed later on) resulting in the formation of a granuloma. In forming a granuloma, macrophages attempt to contain the lesion, but in effect also provide a niche for *Mtb* survival and latency (Cambier et al., 2014).

Macrophages inside the granuloma that are infected continue to die by either apoptosis or necrosis. After apoptotic death, viable *Mtb* contained within the macrophage are engulfed by an incoming macrophage. Following necrotic death of a macrophage, *Mtb* is released into the extracellular core of the granuloma which provides a rich growth environment for the bacteria. The conditions that promote necrosis of the lesion are poorly characterised, but the bacteria is contagious when the necrotic cores leak into the airways allowing for aerosolisation and thus transmission (Cambier et al., 2014).

1.1.4 ***Adaptive immune response Mtb***

The use of the terms innate and adaptive immune system is controversial as they attempt to confine immune cells within an easily definable role. However, as the immune response is a spectrum of cellular responses there lies a difficulty in classifying the two as distinct entities. The cells of each 'compartment' interact with each other to a significant extent making distinguishing the two with accuracy and consistency difficult. For simplicity these terms were used throughout this thesis to provide an insight into where on the spectrum of immune responses the relevant cells were.

T cells are thought to be the main mediator of protection against *Mtb*, with CD4+ T cells being the main component of protection. This is evident in diseases that result in depletion of CD4+ T cells, such as HIV where infected patients are more susceptible to rapid advance of the disease (Pape et al., 1983). The role of CD8+ T cells has not been well characterised as protection can be conferred though adoptive transfer of CD4+ memory T cells from antigen experienced mice. The same study also showed long term memory cells are the key mediators of protection (Orme, 1988). However protection to *Mtb* is only conferred by memory T cells in recipient mice that are immune deficient (Orme & Collins, 1983). While this model of adoptive transfer has been highly utilised, there are concerns surrounding the use of these

models as transfer of CD4+ T cells from BCG vaccinated mice into immunodefiicent mice resulted in recipient mice developing severe colitis (Ancelet, Rich, Delahunt, & Kirman, 2012). Moreover, cells transferred from naive mice protected against an intranasal BCG challenge equally as well as antigen experienced donor cells suggesting the protection may not be due to antigen specificity, but a heighted immune state as a result of the transferred cells (Ancelet et al., 2012).

Further studies have characterised the phenotype of the CD4+ T cells implicated in *Mtb* infection with the phenotypes and localisation summarised in table 1.1.

Table 1.1: CD4+ memory T cell subsets and a selection of their phenotypic markers.

	$T_{Central\ Memory}$	$T_{Effector\ Memory}$	$T_{Resident\ Memory}$
Phenotype	CD44+ $CD62L^{hi}$ $CD69^{lo}$	CD44+ $CD62L^{lo}$ $CD69^{lo}$	CD44+ $CD62L^{lo}$ $CD69^{hi}$
Localisation	Lymphoid organs	Peripheral and circulating	Lung

In naïve T cells CD44 is rapidly upregulated upon exposure to an invading pathogen and remains upregulated following the clearance of the pathogen. This prolonged upregulation makes CD44 a suitable marker of antigen experienced T cells (Baaten, Li, & Bradley, 2010). Additionally, CD44 plays a key role in induction of a long lived, antigen specific population. In a murine model CD44 upregulated the survival of CD4+ cells in the absence of specific antigens. Conversely, in CD44 deficient mice, effector cells rapidly undergo apoptosis after multiple rounds of division, suggesting CD44 is required to signal cells to progress toward a memory phenotype (Baaten et al., 2010).

CD62L is a cell surface marker present in naïve T cells that plays a key role in lymphocyte homing as a CD62L knockout mouse model demonstrated impaired lymphocyte homing to not only the site of infection, but lymphoid tissue as well (Arbonés et al., 1994). Upon activation of the naïve cell the ADAM17 enzyme cleaves the receptor at the K283-S284 site resulting in shedding of the marker from the cell surface (A. Chen, Engel, & Tedder, 1995). In antigen experienced T cells CD62L can be upregulated again. The presence of CD62L in CD44+ T cells is implicated in tissue homing and can be used to distinguish T_{CM} (central memory) cells from T_{EM} (effector memory) cells as it enables cells to access the lymph nodes from the blood (Park & Kupper, 2015; S. Yang, Liu, Wang, Rosenberg, & Morgan, 2011). While CCR7 is often used in conjunction with CD62L to identify memory T cell subsets, CD62L is expressed more consistently and has been identified as a better discriminatory marker of T cell subsets than CCR7 (Unsoeld & Pircher, 2005).

T_{CM} (central memory) cells have demonstrated to be able to transfer protection against *Mtb* infection in adoptive transfer studies while T_{EM} (effector memory) cells have not been able to show the same ability. This is possibly due to the higher replicative capacity T_{CM} (central memory) cells, and their longevity compared to T_{EM} (effector memory) (Orme, 2010; Vogelzang et al., 2014; Wherry et al., 2003). The route of vaccine delivery also plays a key role in the driving the immune response to these different CD4+ T cell phenotypes. Aerosol delivery of BCG vaccination in a non-human primate study generated a high proportion of T_{CM} cells compared to intradermal BCG vaccine that drives T_{EM} responses (Orme, 2010). However the findings of these studies identifying the T_{CM} as mediators of protection need to be viewed with caution following the findings of Ancelet et al 2012. The process of adoptive transfer itself into immunodeficient may be responsible for a heighted immune state and thus the reason for the protection observed (Ancelet et al., 2012). Adoptive transfer studies should include a control group where recipient mice receive naïve cells to ensure protection is not able to be

attributed to the transfer process itself, or the immunogenic state of the lymphopenic recipient mice.

CD69 is a cell surface marker that has been implicated in a wide variety of functions from immune activation to metabolic processes (Cibrian & Sanchez-Madrid, 2017). The marker is absent in naïve lymphocytes but rapidly upregulated following activation (Sancho, Gómez, & Sánchez-Madrid, 2005). The presence of this marker in antigen experienced T cells is implicated in tissue retention. CD69 upregulation is associated with down regulation of sphingosine-1-phosphate receptor $S1P_1$, diminishing the ability of the cell to migrate along the sphingosine-1-phosphate gradient thus preventing a return to circulation (Mackay et al., 2015). CD69 thereby aids in the identification of T_{RM} (resident memory) cells (Mackay et al., 2015; Park & Kupper, 2015). In a tuberculosis context, T_{RM} cells are confined to the lungs and are persistent following BCG vaccination. They confer the ability to provide protection in studies where migration of other types of memory T cells is inhibited, suggesting this population of lung resident cells is capable of providing protection in their own right (Connor et al., 2010). The ability of these cells to protect in an adoptive transfer free model provides strong evidence of a role for T_{RM} cells in *Mtb* protection.

Canonically it has been thought the humoral immune response was more specific for the targeting of extra cellular pathogens. However antibodies against a toxin from the intra-cellular bacteria *Listeria monocytogenes* (*L. monocytogenes*) have challenged this theory. The pore forming toxin listerolysin O (llo) facilitates cytosolic translocation of *L. monocytogenes* within infected macrophages. Administration of monoclonal antibodies against llo in *L. monocytogenes* infected mice decreased the bacterial burden and increased the clearance of bacteria in these mice. This occurred independently of INF-γ, and Fc receptor signalling as it

was demonstrated macrophages are able to uptake antibodies from the external environment at concentrations that are physiologically possible (Edelson & Unanue, 2001).

Mtb and *L. monoytogenes* are both intracellular pathogens that escape phagosome maturation. The ability of antibodies against llo to increase clearance of the bacteria suggests that perhaps they could have the same effect against a similar toxin in *Mtb* such as ESAT-6, or indeed other *Mtb* proteins. Canonically it has been thought the humoral immune response was more specific for the targeting of extra cellular pathogens through the production of antibodies (Thakur, Mikkelsen, & Jungersen, 2019).However antibodies against a toxin from the intra-cellular bacteria Listeria monocytogenes (*L. monocytogenes*) have challenged this theory. The pore forming toxin listerolysin O (llo) facilitates cytosolic translocation of L. monocytogenes within infected macrophages. Administration of monoclonal antibodies against llo in *L. monocytogenes* infected mice decreased the bacterial burden and increased the clearance of bacteria in these mice. This occurred independently of INF-γ, and Fc receptor signalling as it was demonstrated macrophages are able to uptake antibodies from the external environment at concentrations that are physiologically possible (Edelson & Unanue, 2001).

Antibodies isolated from patients with latent tuberculosis exhibited an altered antibody glycosylation profile compared with antibodies isolated from patients with active tuberculosis. This altered profile affected the functionality of the antibodies with those from latent tuberculosis patients exhibiting greater macrophage activation and intracellular killing, directly postulating a role for antibodies in the control of *Mtb* infection (Lu et al., 2016) . *Mtb* and *L. monoytogenes* are both intracellular pathogens that escape phagosome maturation. The ability of antibodies against llo to increase clearance of the bacteria suggests that perhaps they could have the same effect against a similar toxin in *Mtb* such as ESAT-6, or indeed other *Mtb* proteins.

A number of pre-clinical studies have measured an increase in *Mtb* specific antibodies following vaccination with the relevant antigen, largely from the antigen 85 complex of proteins. (Giri, Verma, & Khuller, 2006; Kohama et al., 2008). These studies have identified an increase in antigen specific IgG antibodies that have been associated with a reduction in bacterial load upon *Mtb* challenge. The protection offered is comparable to BCG vaccination. However these studies have not extensively established the role T cell activation played in these vaccinations, nor the role of antibody class switching, rather identifying IgG subtypes. The role of IgA should not be underestimated as it has been shown to be vital to protection as IgA deficient mice are more susceptible to *Mtb* infection (Rodríguez et al., 2005). Additionally, passive immunisation is able to be carried out with the transfer of anti-*Mtb* protein α-crystallin IgA which results in transient immunity (Williams et al., 2004).

Though the T cell response to *Mtb* is not fully understood, it has been seen as a key component in the containment of the bacteria with one 1996 review of TB literature claiming 'antibodies have no role' in protection (Rook & Hernandez-Pando, 1996). However the interplay between the different components of the immune system has become more evident especially in *Mtb* infection. Evidence of this is seen in a study where B cell deficient mice immunised with BCG are not able to generate the protective responses that are usually seen, and the ability of the T cells to respond is diminished (Kondratieva et al., 2010). Combined with the previously discussed results, this shows future research should focus on the generation of immune responses to both T and B cell epitopes.

1.2. Current vaccine and treatment

1.2.1 ***Bacillus Calmette-Guerin (BCG) Vaccine***

Currently the only licensed TB vaccine is the Bacille Calmette Guerin (BCG) vaccine that is a live attenuated strain of *Mycobacterium bovis* (*M. bovis*), the bovine equivalent of *Mtb.* The

strain was created between 1908 and 1919 by Calmette and Guerin after 231 passages of virulent *M. bovis* in culture media. Continual cultivation led to spontaneous attenuation and the inability to cause disease in cattle or humans. (Oettinger, Jorgensen, Ladefoged, Haslov, & Andersen, 1999). Attenuation was a result of the complete deletion of the 1kB chromosomal region of difference 1 (RD1) in BCG strains that contains many of the virulence genes in *Mtb* (Berthet, Rasmussen, Rosenkrands, Andersen, & Gicquel, 1998; Mahairas, Sabo, Hickey, Singh, & Stover, 1996).

As this is one of the oldest vaccines in the world, more people have been immunised with BCG than any other vaccine. Its exact mechanism of protection however remains unknown, and its efficacy has been the subject of extensive debate (Lienhardt & Zumla; Ritz & Curtis, 2009). Immunisation with BCG has been reported as reducing the risk of all TB diseases by up to 50%. It does however provide almost complete protection against non-pulmonary TB diseases such as meningitis and proves to be particularly effective in preventing all manifestations of *Mtb* infection in children (Andersen & Doherty, 2005; Colditz, Brewer, Berkey, & et al., 1994). Despite this, many studies report the efficacy of BCG vaccine in preventing pulmonary disease in adults as anywhere from 0 to 80% as well as reporting geographic differences in protection levels (Lienhardt & Zumla; Ritz & Curtis, 2009).

The observed geographic differences in efficacy could be due to differences in how BCG strains have been cultured. For example, studies have shown one strain of *M. bovis* that is cultured in two different media results in distinct humoral response in mice (Petricevich et al., 2001; Ritz & Curtis, 2009). When the initial strain was developed in France, it was sent across the globe to meet demand for vaccine doses. Over the last century these bacteria have likely diverged significantly resulting in different populations being vaccinated with different strains of BCG (Andersen & Doherty, 2005; Ritz & Curtis, 2009). It is also possible that BCG strains

have been cultured *in vitro* for too long and are now so significantly distinct from virulent strains that they no longer confer protection against infections (Lienhardt & Zumla).

There is also evidence to suggest the initial intradermal BCG administration during infancy is not sufficient to provide lifelong protection and perhaps only lasts about 10-20 years (Andersen & Doherty, 2005; Sterne, Rodrigues, & Guedes, 1998). Initial vaccination does cause significant reductions in incidences in all manifestations of *Mtb* infection in infants and young children. However the highest risk age groups for pulmonary disease development in countries with a high TB disease burden is the 25-35 year old age bracket. This correlates with the suggestion of a limited term of immunity (Andersen & Doherty, 2005). This in itself provides challenges for the development of new vaccines since the BCG vaccination is effective at prevention of infant and childhood disease. A new vaccine targeting adult pulmonary TB will not necessarily replace BCG, but either act as a booster, or in its own right, being able to replace the protective effects of BCG (Andersen & Doherty, 2005).

Exposure at a young age to non *Mtb* environmental mycobacteria is also seen as a potential explanation for the lack of life long efficacy of BCG vaccination. There are various species of environmental mycobacteria at tropical latitudes found in both soil and water samples. Exposure to those mycobacterium species could result in rapid clearance of *M. bovis* in the BCG vaccine preventing an appropriate, sustained immunological response to vaccination (Andersen & Doherty, 2005; Lienhardt & Zumla). Where individuals are pre-screened for previous mycobacteria exposure using the tuberculin skin test, BCG induced protection is bimodal. High levels of protection are achieved in naïve individuals, whereas antigen experienced individuals do not achieve the same degree of protection (Andersen & Doherty, 2005; Lienhardt & Zumla). This suggests sensitisation to mycobacteria may be playing a role in the BCG ‘failure’ in epidemic areas.

Maternal infection with *Mtb* is another source of sensitisation as *in utero* exposure to mycobacterial antigens diminished the effects of the BCG vaccine in both human and mouse models (Malhotra et al., 1997; Rahman, Dégano, Singh, & Fernández, 2010). In the most recent example of this, latent maternal infection with *Mtb* was correlated with a diminished infant T cell response following BCG immunisation in a Ugandan cohort. (Mawa et al., 2015). Due to the high failure rate of BCG in tropical countries, this is being further characterised with larger study cohorts in Uganda.

In spite of these factors, the WHO still recommends intradermal neonatal BCG vaccination. However on account of the BCG vaccine being inadequate to control and eradicate pulmonary TB in adults, there is still a need to develop more effective vaccines against *Mtb.*

It is still possible to treat *Mtb* infection however rising antibiotic resistance threatens the long term viability of this route of therapeutic intervention. Provided the infecting strain of *Mtb* is not drug resistant, current WHO guidelines for treatment for TB is prolonged and expensive limiting its effectiveness in developing countries. New infections involves taking a daily cocktail of Isoniazid/Rifampicin/Pyrazinamide/Ethambutol for two months. Followed by four months of Isoniazid/Rifampicin taken daily.

Rifampin acts by inhibiting the DNA dependent RNA polymerase of *Mtb*. Resistance occurs when spontaneous point mutations occur within a well-defined 81 base pair region of the β-subunit of the RNA polymerase (rpoB). A single point mutation, such as at codon 526, can result in minimum inhibitory concentration of at least >32 μg/mL from a baseline of 1 μg/mL in wild type *Mtb* (Schön et al., 2009; Somoskovi, Parsons, & Salfinger, 2001).

Isoniazid is a prodrug that is activated *in vivo* and affects the mycobacterial catalase-peroxidase gene *katG* that provides *Mtb* with oxidative protection against host anti-microbial agents (Schön et al., 2009; Ying Zhang, Heym, Allen, Young, & Cole, 1992). Resistance occurs most

frequently through Ser315Thr mutation whereby the *katG* enzyme maintains over 50% of its catalase-peroxidase activity without activating isoniazid (Rouse, DeVito, Li, Byer, & Morris, 1996). There are a variety of potential mutation sites found that do not all offer the same level of resistance to the antibiotic (Rouse et al., 1996). The minimum inhibitory concentration in resistant strains generally increases from a baseline of 0.2 µg/mL in wild type to 4-8 µg/mL (Schön et al., 2009)

Ethambutol is a bacteriostatic agent that disrupts the formation of arabinogalactan and lipoarabinomannan, vital components of cell wall in *Mtb.* Resistance to this antibiotic has been associated with mutations in a cluster of genes, termed *embA*, *embB*, and *embC.* (Telenti et al., 1997). *embA* and *embB* encode arabinosyl transferase enzymes critical to the synthesis of arabinogalactan while *embC* encodes an enzyme involved in the arabinosylation of lipoarabinomannan (Berg et al., 2005; Escuyer et al., 2001). While ethambutol's interaction with the enzymes is not fully characterised, resistance occurs as a result of point mutations within these enzymes. The most common being at codon 306 of *embB* (Cuevas-Cordoba et al., 2015). This can increase the minimum inhibitory concentration from 5 µg/mL in wild type *Mtb* to >8 µg/mL (Schön et al., 2009).

Pyrazinamide is highly effective against semi dormant *Mtb* and is a nicotinamide analog that, like isoniazid, is a pro drug requiring activation *in vivo*. The pro drug is converted to pyrazinoic acid by the intracellular *Mtb* enzyme pyrazinamidase which then accumulates in the cytosol due to an inefficient *Mtb* efflux system (Y. Zhang, Scorpio, Nikaido, & Sun, 1999). The accumulation of cytosolic pyrazinoic is thought to lower the pH to the point where it inactivates fatty acid synthase I, disrupting cell wall synthesis (Zimhony, Cox, Welch, Vilcheze, & Jacobs, 2000). Resistance occurs primarily due to point mutations in the promoter region of the *pncA (*pyrazinamidase) gene. *M. bovis* is naturally resistant due to a C-G mutation at codon 169 however resistance in *Mtb* resistance strains is due diverse single point mutations found

throughout *pncA* (Scorpio & Zhang, 1996). Other mechanisms of resistance have developed as there are strains that do not contain *pncA* mutations. Proposed mechanisms of action include improved efflux of pyrazinoic acid, reduced uptake of pyrazinamide or even altered regulation of pncA expression (Raynaud et al., 1999).

These drugs are recommended as a cocktail in *Mtb* treatment to reduce the chance of resistance developing to any of the individual components, and to shorten the length of treatment. For example, Rifampin and pyrazinamide in combination are able to reduce the time taken for sterilization time from 1 year to six months (Grosset, 1978).

Treatment of all new infections requires at least monthly patient monitoring to ensure compliance and monitor any adverse effects of the antibiotic cocktails. In the USA, the CDC estimates this treatment to costs US$47, 000 in direct and indirect costs per case. Treatment of multi drug resistant, and extensively drug resistance TB is estimated at US$300, 000, and US$710, 000 respectively on a per case basis.

Multidrug resistant and extensively drug resistant cases of TB are assed on a case by case basis to determine the best course of treatment. The selection of drugs is based on a stepwise selection process of what the bacteria might be susceptible to which is again assessed in a case specific manner. Latent TB can be treated with Rifapentine and isoniazid taken once a week for 12 weeks.

1.3. Vaccines in clinical trials

Vaccines are the most cost effective and effective means of controlling and eradicating diseases. A vaccine against *Mtb* that is more effective than BCG is highly sought after and there is a significant amount of research surrounding *Mtb* vaccine development. However progress to clinical trials has been slow due to the difficulties in understanding *Mtb*

pathogenicity and finding what targets offer the most protection. The current most advanced candidates are based on whole cell bacteria, like the BCG vaccine. These candidates have varying aims, whether they be therapeutic, prophylactic, or boost vaccinations for BCG. In total there are 13 vaccine candidates in the pipeline three viral vectors, three protein/adjuvant, and seven live or whole cell based vaccines (figure 1.2).

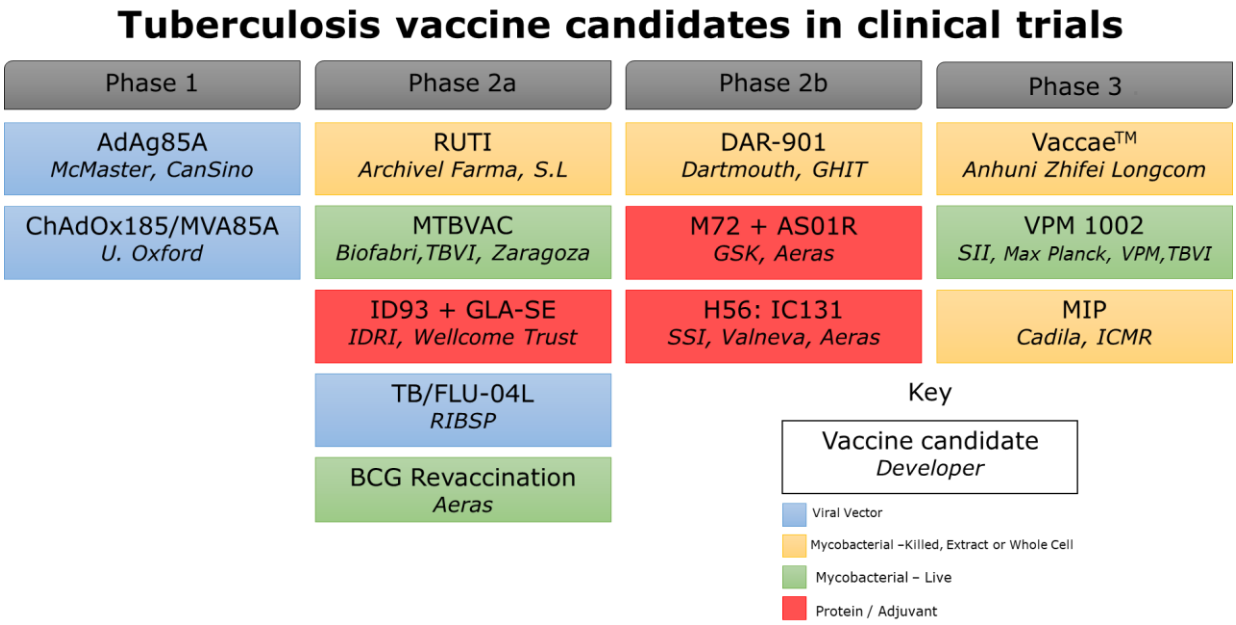

Figure 1.2: Pipeline of current clinical trials for *Mtb* vaccines (Adapted from the Tuberculosis Vaccine Initiative).

1.3.1 ***Vaccines in phase III clinical trials***

Vaccae™ is comprised of heat killed *Mycobacterium vaccae*, a non-pathogenic soil bacteria (Huang & Hsieh, 2017). Early studies with this species have shown that administration has therapeutic effects in patients with multi drug resistant TB. Patients exhibited increased bacterial clearance rates in the sputum in the early stages of chemotherapy administration compared with non-treated patients (J. Stanford, Stanford, & Grange, 2004) (Huang & Hsieh, 2017). The vaccine acts by driving a T_h1 immune response which is critical for the clearance of *Mtb*. One dose has been sufficient to see this effect in parts of South America and the Middle East, however multiple doses have been required to achieve the same effect in South Africa.

This difference is theorised to be due to the state of the immune system in patients where local microbes and persistent parasitic infections drive a T_h2 cell immune response that requires more boosts to overcome (J. Stanford et al., 2004; J. L. Stanford, Stanford, Grange, Lan, & Etemadi, 2001). The increase in boosts does come along with a decrease in compliance with less than 55% of patients receiving the second and subsequent doses (J. Stanford et al., 2004).

In naïve mice, vaccination with heat killed *M. vaccae* results in the production of CD8+ T cells that are able to be re-stimulated following incubation of spleenocytes with *M. vaccace* or *Mtb.* This indicates protection is mediated by a memory CD8+ T cell phenotype. These CD8+ T cells produce large amounts of INF-γ (Skinner et al., 1997). Mouse studies have also showed administration of heat killed *M. vaccae* in mice already infected with *Mtb* increased the number of CD3+ and CD4+ cells. There was a significant increase in the number of INF-γ producing CD4+ T cells observed and a reduction in the IL-4 producing CD4+ cells (Xu et al., 2009). The superior immune response seen in mice vaccinated with live *M. vaccae* compared to BCG vaccinated mice is also due to a higher production of TNFα and IFN-γ (L. Zhang et al., 2016). Protection appears to be through the increase of TNFa and IFN-γ production, as well as an increase in the overall number of CD4+ and CD8+ T cells.

Vaccae™ is already licenced in China for therapeutic treatment in patients that already have tuberculosis (Huang & Hsieh, 2017). However most recent trial of this candidate vaccines protective capacity has been conducted in China to assess the efficacy of Vaccae™ in preventing TB in groups at high risk of infection. Vaccae™ was administered intra muscularly as a 1 mL solution once every two weeks for a total of 6 doses. The study has concluded but is awaiting release of results.

The MIP vaccine consists of heat killed environmental bacteria *Mycobacterium indicus pranni.* MIP has also seen a high level of therapeutic success in patients with difficult to treat, and drug

resistance TB (Scriba et al., 2016; Sharma et al., 2017). In the most recent trial, individuals with multi drug resistant *Mtb* were given conventional treatment (according to WHO guidelines) together with an intradermal dose $5x10^8$ heat killed MPI. This was administered once every two weeks for a total of two months. Treatment groups achieved a slightly higher rate of sputum smear conversion than placebo groups (Sharma et al., 2017).

Investigation of immune responses to MIP vaccination has shown the mechanism of protection is mediated by TLR-4 induction. TLR-4 activation significantly increases pro-inflammatory cytokines such as TNFα, and induces significant increase in NO generation. TLR-4 blocking completely diminished MIP mediated generation of the protective mechanisms identified (Das et al., 2016). MIP has also shown potential to be an effective booster to BCG vaccination. BCG vaccination with a MIP boost results in a one log reduction of bacterial load compared to BCG vaccination alone. This is potentially due to the induction of cytokines (such as IL-2, INFγ and IL-17) as well as a higher number of polyfunctional T cells which have been correlated with a reduction in bacterial load. BCG/MIP vaccination also resulted in a higher number of cells infiltrating and residing in the lungs indicating the importance of any *Mtb* vaccine requiring a large number of resident lung specific cells (Saqib et al., 2016).

The only prophylactic vaccine in phase III clinical trials is the VPM1002 vaccine which is a recombinant form of BCG administered as a single dose live vaccine. In this construct the BCG urease C gene has been replaced with the listeriolysin O (llo) gene from *L. monocytogenes* (Nieuwenhuizen et al., 2017). Urease C drives the neutralisation of the phagosomes through production of ammonia and promotes prolonged survival of the BCG strains in the phagosome. The llo gene encodes a pore forming toxin that allows *L. monocytogenes* to escape the phagosome and persist in the cytosol of infected cells. Replacement of the Urease C gene with llo in BCG confers the ability to escape the phagosome. Bacterial material in the cytosol, as well as caspases released from the phagosome trigger apoptosis. This results in antigen

presentation on both MHC class I and II molecules. Antigen presentation on both classes of MHC has shown to improve the immune response in mice against unmodified BCG strains (Nieuwenhuizen et al., 2017).

Compared to BCG vaccination, VPM1002 results in increased, and sustained protection against *Mtb* infection (Desel et al., 2011; Vogelzang et al., 2014). VPM1002 vaccination induces a significant population of IL-17 secreting CD4+ T cells while BCG vaccination lacks this cell population. Additionally VPM1002 also results in a higher proportion of multifunctional T cells in terms of cytokines with production of INF-γ , TNFα, IL-2 and IL-17 and combinations thereof being predominant in VPM1002 vaccinated mice (Desel et al., 2011). This vaccine also results in a higher production of *Mtb* specific antibodies, although passive immunization with these antibodies alone did not impact *Mtb* progression indicating they perhaps play a role in conjunction with other sections of the immune response in *Mtb* control (Vogelzang et al., 2014). However protection is able to be mediated independently of these antibodies as shown by adoptive transfer, where T_{CM} cells alone rather than T_{EM} were able to confer protection. Interestingly this adoptive transfer model contradicts previous studies where protection is achieved where transfer of naïve cells did not result in protection (Vogelzang et al., 2014). This model however did not test T_{RM} cells which reside in the lungs and have been suggested to play a role in protection (Clark, 2015; Sakai et al., 2014). The presence of a INF-γ producing tissue resident memory subset, and a T cell subset that can rapidly home to tissue such as T_{CM} cells following expansion have been reported as critical to *Mtb* protection (Sakai et al., 2014; Vogelzang et al., 2014). The most recent trial for this vaccine started in 2018 in India and is scheduled to conclude in mid-2020 (Nieuwenhuizen et al., 2017).

1.3.2 ***Vaccines in phase 2b clinical trials***

Mycobacterium obuense is an environmental bacterium that also featured in the abandoned SRL-172 vaccine (von Reyn et al., 2017). In its trial SRL-172 was administered as a series of five intradermal doses and led to a reduction in culture confirmed TB of 39% in HIV infected individuals. However the method of production was not scalable to be economically viable and was later abandoned. DAR-901 is comprised of the same bacterium, however, it is grown in broth and production of the vaccine is easily scalable. The most recent DAR-901 trial involved three intradermal vaccinations with 1 mg of the heat killed bacteria which was well tolerated amongst the cohort. These vaccinations resulted in the production of a significant amount of INF-γ in response to *Mycobacterium obuense* and *Mtb* cell lysates, as well as a significant humoral response to *Mtb* antigens (von Reyn et al., 2017). These results mean DAR-901 will progress to further trials.

However in contrast to other vaccinations in trials to date, DAR-901 does not result in the induction of cytokines to a higher degree compared to BCG. The vaccine does however show an increase in the number of polyfunctional T cells secreting IFNγ, IL-2, IL-7, largely of a terminally differentiated T_{EM} phenotype (Masonou et al., 2019). These results suggest a major increase in cytokine production compared to BCG is not necessarily a correlate of protection as inferred in a large number of vaccine studies and highlights the difficulty in identifying a universal correlate of protection in *Mtb* vaccine development. Protective effects have been attributed to T_{EM} cells however the difference in the phenotype of memory cell identified as providing protection differs to the VPM1002 vaccine again highlighting the difficulty in identifying a correlate of protection (Masonou et al., 2019; Vogelzang et al., 2014).

The other two vaccine candidates phase 2b clinical trials are subunit vaccines which are based on ESAT-6 and Ag85B proteins. Delivery of these, and other subunit vaccines in other phases of trials are primarily as part of a viral vector. Replication deficient adenovirus or vaccinia

virus are used to express the protein of interest as these viruses are potent mucosal adjuvants. Subunit vaccines that do not utilise the adjuvant properties of viral vectors are delivered with an alternative adjuvant (Andersen & Kaufmann, 2014).

H56 is a fusion protein consisting of the proteins Ag85B, ESAT-6 and an antigen associated with latent infection, Rv2660c. The fusion protein is co administered with IC31, a synthetic oligodeoxynucleotide agonist of TLR 9 (Lin et al., 2012; Olafsdottir, Lingnau, Nagy, & Jonsdottir, 2009). This vaccine is designed to act as a boost to BCG. In one study macaques were vaccinated intradermally with BCG, followed by two 50 µg intramuscular doses of H56. The results showed vaccination was able to reduce the rate of disease and efficiently contain the *Mtb* following challenge (Lin et al., 2012). A recent human trial carried out in South Africa administered various concentrations of the vaccine intramuscularly. This study determined the optimal schedule for production of long lived Ag85B and ESAT-6 specific CD4+ T cells is 3 intramuscular doses of 5 µg H56 + 500 nmol IC31. Vaccination was found to drive a T_h1 cellular response with a large number of peptide specific CD4+ T cells detected (Suliman et al., 2019).

In murine studies, H56 induces a high proportion of polyfunctional T cells that express IFNγ, IL-2 and TNFα cells following stimulation with each of the individual components of the vaccine (Aagaard et al., 2009) . Interestingly the proportion of polyfunctional cells is increased in response to a lower vaccine dose which correlates with a greater reduction in pulmonary bacterial load compared to vaccination with a higher dose (Aagaard et al., 2009). This effect that is also seen in human trials suggesting more care needs to be put into the optimisation of vaccine doses (Luabeya et al., 2015). This data shows a factor that should be considered in determining the protection is assessing the memory recall response to different doses of a given vaccine to determine the most appropriate dose and not just assessing the initial cytokine response to a given vaccine (Aagaard et al., 2009). Protection in mice has been attributed to

H56 antigen specific cells that localise to and reside in the lung following vaccination that rapidly proliferate when challenged (J. S. Woodworth et al., 2017). In the first human trial, the predominant cytokine secreting memory cells were of a T_{CM} phenotype implicating these cells in protection, similar to the VMP1002 vaccine (Luabeya et al., 2015; Vogelzang et al., 2014). Antigen specific IgG antibodies have also been noted as present in human studies however their importance not analysed (Luabeya et al., 2015). Since the vaccine has been shown to be safe and immunogenic in humans further studies will be carried out.

The other advanced protein subunit vaccine is the M72 formulation. This vaccine is a fusion of the *Mtb* antigen Mtb39A and Mtb32A administered with the $AS02_A$ adjuvant. Mtb32A is a constitutively expressed serine protease while Mtb39A is a putative immune evasion virulence factor that is also constitutively expressed. The two proteins are highly immunogenic *Mtb* antigens that have no homologues in other mycobacteria species (Skeiky et al., 2004). $AS02_A$ is an oil in water emulsion with monophosphoryl lipid A and extract from *Quillaja saponaria* bark (Leroux-Roels et al., 2010) The most recent trial of this vaccine was carried out with patients in Kenya, Zambia, and South Africa among *Mtb* infected, but HIV negative individuals. Two doses were administered two weeks apart intramuscularly and were well tolerated with a low number of adverse events. M72 administration also showed some level of protection as there was a reduction in the progression of latent to active TB among the vaccine cohort compared to the placebo group (Van Der Meeren et al., 2018). M72 vaccination results in a sustained number of antigen specific CD4+ T cells as measured by cytokine re-stimulation. The major cytokine producing cells are polyfunctional producing various combinations of IFNγ, IL-2, IL-7 and TNFα consistent with other candidate vaccines (Penn-Nicholson et al., 2015). M72 vaccination has also demonstrated sustained CD8+ T cells, natural killer cell activation, and specific antibodies, though the implications of these have not been characterised (Penn-Nicholson et al., 2015).

Despite the importance of antibodies in control of *Mtb* infection, the pre-clinical data from the vaccines in clinical trials largely fail to address the role of antibodies in the protection seen from their vaccines and focus on the cytokine and T cell responses. Antibody data is poorly characterized in terms of functionality and epitope specificity with the information confined to the supplementary data.

1.4. Tuberculosis vaccine antigens

Two proteins have been identified as potent immune cell stimulators that are produced in high quantities in the early culture filtrates. ESAT-6 and the antigen 85 enzymes have been the focus of extensive research with the aim of understanding their role in pathogenesis and how they may be used as targets for vaccination. The two proteins have already seen successful use in the H56 vaccine, and various other pre-clinical vaccine candidates.

1.4.1 ***Early Secreted Antigen (ESAT-6)***

ESAT-6 is a 6 kDa protein encoded on the RD1 region of *Mtb* that contains a large number of virulence genes. The absence of the RD1 region in BCG strains is a key reason they are not as virulent as wild type *M. bovis* which do not produce ESAT-6. BCG virulence is restored upon complementation with the RD1 region and subsequent ESAT-6 production allowing for escape form phagosome and localisation to the cytosol (Berthet et al., 1998; Harboe, Oettinger, Wiker, Rosenkrands, & Andersen, 1996; D. Houben et al., 2012; Mahairas et al., 1996). The importance of ESAT-6 is demonstrated in the generation of *Mtb* strains that carry mutations which abolish either production or secretion of ESAT-6. These strains are no longer pathogenic or able to establish infection (Peng & Sun, 2016). ESAT-6 is an extremely potent T cell stimulant. Memory T cells from mice previously exposed to *Mtb* generate large quantities of INF-γ when exposed to this protein (Andersen, Andersen, Sorensen, & Nagai, 1995). The

importance of ESAT-6 in *Mtb* virulence and its immunogenicity make it a good target for vaccination.

Neutralising antibodies against the llo toxin of *L. monocytogenes* are able to increase the clearance of the bacteria in infected mice (Edelson & Unanue, 2001). Since ESAT-6 and llo are both pore forming toxins that facilitate escape form the phagosome, antibodies against ESAT-6 may assist in clearance of *Mtb*. ESAT-6 is also a potent T cell antigen with numerous immunomodulatory effects. As such, T cells and antibodies specific for ESAT-6 may be beneficial in *Mtb* immunity. These properties make it a protein of interest in vaccine design.

1.4.1.1 ***Expression of ESAT-6***

ESAT-6 is under the control of a di-cistronic operon that also promotes the 10 kDa culture filtrate protein (cfp-10). These proteins associate following production and are exported form the *Mtb* cell via the ESX1 type VII secretion system. Cfp-10 largely appears to act as a chaperone for export as ESAT-6 lacks a signal peptide and they dissociate following secretion. ESAT-6 was first identified as a major component in the early growth phase of *Mtb*, though transcriptional analysis has revealed it is produced in non-replicating bacteria as well as active bacteria (Berthet et al., 1998; Haile, Bjune, & Wiker, 2002). The disctronic operon is regulated by a two component regulator system where PhoP is the effector response regulator. Phop is activated by a sensor histidine kinase that is phosphorylated in response to external stimuli, however the stimuli is unknown (Ryndak, Wang, & Smith, 2008).

1.4.1.2 ***Function of ESAT-6***

The major functions of ESAT-6 are pore formation and immune modulation. Virulent *Mtb* strains translocate to the cytosol of the macrophage and ESAT-6 is a pore forming toxin that facilitates this escape from the phagosome (van der Wel et al., 2007). In addition to this, ESAT-6 may also facilitate *Mtb* spreading through the alveolar wall in a phagocyte independent manner. The protein has the ability to anchor to pneumocytes expressing laminin and damage

not only the cell but the basement membrane. Such damage allows *Mtb* to disseminate through the alveolar walls (Kinhikar et al., 2010).

ESAT-6 has two hydrophobic α helixes that are approximately 50 Å in length (figure 1.3). This corresponds with the typical depth of a lipid bilayer, suggesting these are inserted into phagosome membrane (E. N. Houben, Korotkov, & Bitter, 2014; Ma, Keil, & Sun, 2015). The host substrates required for ESAT-6 binding have yet to be completely elucidated, however it does show strong association with 1,2 dimyristoryl-sn-glycero-3-phosphocoline (DMPC) cholesterol and laminin (Kinhikar et al., 2010; van der Wel et al., 2007).

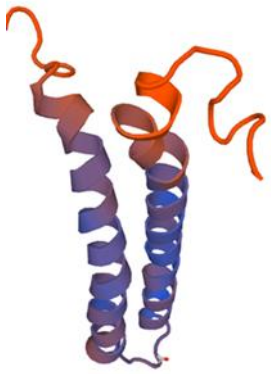

Figure 1.3: Structure of ESAT-6 depicted using SWISS model.

Labelling of ESAT-6 at various positions with markers that fluoresce when in contact with lipid membranes allowed for mapping of the transmembrane domains, and provide direct evidence ESAT-6 is inserted into the phagosome membrane. Additional studies have shown the long flexible C and N terminal regions of ESAT-6 play a critical role in the ability of the protein to insert into the membrane. Truncated recombinant ESAT-6 proteins without the C and or N terminal region do not insert into to the membrane The C and N terminals themselves do not insert into the membrane, but may function in anchoring ESAT-6 to the membrane, or perhaps even linking ESAT-6 into an oligomer for membrane insertion (Ma et al., 2015). The estimated pore size formed by purified ESAT-6 in red blood cells is 4.5 nm while ESAT-6 is

only 95 amino acids suggesting it likely forms an oligomer to facilitate escape from the phagosome through a transmembrane pore (Ma et al., 2015; Smith et al., 2008).

ESAT-6 also has a number of immunomodulatory effects. Incubation of THP-1 cells (human monocytes differentiated into macrophages in this instance) with ESAT-6 induced significant apoptosis of the cells. Real time PCR analysis revealed this to be due to up regulation of caspases 1,3,5,7 and 8. Incubation of cells with an *Mtb* mutant strain that does not produce ESAT-6 did not result in significant levels of apoptosis of THP-1 cells (Derrick & Morris, 2007). Apoptosis of macrophages is advantageous to *Mtb* in the early stages of infection as it results in the recruitment of more macrophages. These immune cells are critical in the formation of granulomas which are vital in successfully establishing infection.

To further recruit macrophages to the site of infection and to promote establishment of granulomas, ESAT-6 also modulates the expression of chemokines in epithelial cells. The protein induces expression of matrix metalloprotease 9 (MMP9) in epithelial cells neighbouring infected macrophages. This chemokine attracts macrophages to the site of infection (Volkman et al., 2010). ESAT-6 also down regulates the expression of the β-2 microglobulin that diminishes expression of MHC class I molecules (Sreejit et al., 2014).

1.4.2 ***The antigen 85 enzymes***

The antigen 85 enzymes, Ag85A (30 kDa), Ag85B (31.5 kDa) and Ag85C (32 kDa) proteins comprise over 40% of the proteins secreted by *Mtb* (Andersen, Askgaard, Ljungqvist, Bentzon, & Heron, 1991; Sorensen, Nagai, Houen, Andersen, & Andersen, 1995; Wiker & Harboe, 1992). These proteins are hyper conserved among strains of *Mtb* indicating a significant role in basic cell function. These proteins are also found in non-pathogenic strains of *Mtb* and even other mycobacterial species as they are not encoded on the RD1 region. As such they are also found in BCG strains of *M. bovis* were they share significant homology. For example the

Ag85B gene in *Mtb* and *M. bovis* differ at only 5 bases. (Content et al., 1991; Fuchs et al., 2014; Harth, Lee, Wang, Clemens, & Horwitz, 1996).

M. bovis deficient in Ag85B were unable to infect macrophages *in vitro* suggesting a role in the virulence of pathogenic strains where combination with other virulence factors aids in the establishment of infection (Prendergast et al., 2016). The Antigen 85 enzymes also elicit production of significant amounts of INF-γ from antigen experienced cells (Andersen et al., 1991). As these proteins are highly immunogenic and appear to play a role in pathogenesis they have been the subject of extensive research in the pursuit of a suitable vaccine candidate.

1.4.2.1 ***Expression***

The three antigen 85 enzymes are encoded at separate locations under separate promoters. In strains that carry mutations which disrupt one antigen 85 gene, production of the other two proteins is not affected. Despite the fact these proteins are regulated and exported separately, the proteins are found in a constant 3:2:1 (B:A:C) ratio during a two to three week growth phase (Armitige, Jagannath, Wanger, & Norris, 2000; Harth et al., 1996). As the Ag85B protein is produced in the largest amount, it is thought to be of the most importance.

1.4.2.2 ***Function***

The major functions of the Ag85 proteins are fibronectin binding and mycoltransferase activity. The proteins act individually, however, they function in the same manner owing to the significant homology between the proteins. It has been suggested the presence of three essentially redundant genes resulted from a gene duplication event in ancient mycobacteria species (Wiker & Harboe, 1992).

One of the earliest functions of these proteins that was identified was fibronectin biding, thus these three genes are termed *fbpA, fbpB,* and *fbpC* (Belisle et al., 1997; Peake, Gooley, & Britton, 1993). The enzymes have also shown to promote binding and uptake of *Mtb* into

macrophages (Abou-Zeid et al., 1988; Peake et al., 1993). Using multiple overlapping peptides of the Ag85B as an example, it was revealed the fibronectin reactive epitope lies within the N terminus at the predicted collagen biding domain (Peake et al., 1993).

In situ labelling of the Ag85B enzyme has revealed the protein is associated with the cell wall of mycobacteria while a significant proportion of the protein is secreted into the early phase culture filtrates (Peake et al., 1993). Cell wall association of the protein is likely due to the protein also acting as a mycolytransferase, performing a vital function in the final stages of mycobacterial cell wall assembly (Belisle et al., 1997). The cell wall of mycobacterial species consists mostly of the covalently linked mycolic acids D-arabino-D-galactan complemented with peptidoglycans and glycolips. These lipids shield the bacteria from harsh environments and significantly contribute to the persistence of *Mtb* (Belisle et al., 1997; Brennan & Nikaido, 1995). The Ag85 proteins catalyse transesterification of α,α'-trehalose monomycolate (TMM) to α,α'-trehalose dimycolate (TDM) during the production of cell wall components.

Since the production of cell wall components are critical to bacterial survival, targeting cell wall biogenesis by inhibiting this pathway is an attractive prospect despite the redundancy of the three enzymes. The homology of the enzymes suggests that targeting of one enzyme may also affect the other enzymes. This is seen in suppression growth of *Mycobateria avarium* when incubated with competitive inhibitors of Ag85B (Belisle et al., 1997). Additionally, knock out mutations of one enzyme also affects the ability of the bacteria to grow and survive. An *Mtb* Ag85A knockout significantly hinders the ability of the bacteria to growth in nutrient poor media compared to the wild type (Armitige et al., 2000).The *fbpA* mutants also exhibited poor survival in murine macrophages. TDM in the cell wall enhances trafficking of the bacteria to the acidic compartments of the macrophage. Cell wall TDM produced by the antigen 85 enzymes may play an important role arresting phagosome maturation and subsequent bacterial survival (Armitige et al., 2000; Gomes et al., 1999).

1.5. The need for prophylactic vaccines

Even with the number of TB vaccines currently undergoing clinical trials the most advanced vaccines are eliciting therapeutic effects rather than preventative strategies. The most advanced prophylacitic vaccine to have advanced through to clinical trials was a subunit vaccine utilising a replication deficient modified vaccinia virus Ankara (MVA85A). This vaccine expressed the Ag85A protein form the antigen 85 enzymes of *Mtb*. MVA85A was also the first vaccine designed as a booster to BCG (Mwau et al., 2004; Tameris et al., 2013). MVA85A resulted in promising levels of immunogenicity and boosted pre-existing BCG immune responses in early studies. However it failed to provide any additional benefits over vaccination with BCG alone in infants. This was despite the apparent success of the vaccine in eliciting high levels of immune responses such as INF-γ (Tameris et al., 2013). The results seen here have called into question using INF-γ only as a correlate of protection. It is important to note however that though this vaccine may not be able to replace or enhance the protection provided by BCG vaccination in infants, it may have uses in other populations and is currently in clinical trials in HIV^+ patients (Andersen & Kaufmann, 2014).

The heat killed whole cell vaccines (Vaccae™ and MIP) have not been demonstrated to be prophylactic. They do however seem promising for the therapeutic treatment of existing infections, especially those that are difficult to treat. Such vaccines could be incredibly valuable to ex-Soviet Bloc countries that have a high burden of these cases. These candidates are also limited by their requirement for multiple doses, as are the subunit vaccines which can decrease compliance. However multiple doses are required for successful protection against a number of other diseases, and this may be the only way to treat *Mtb*. The intradermal and intramuscular methods used in these vaccines are however technically challenging. Given the major burden of disease is in low income countries, easier, alternative methods of vaccine delivery are an attractive prospect. The route of delivery will also effect on the efficacy of the vaccine. This is

seen in subunit vaccinations where intra nasal delivery of Ag85B can elicit higher levels of protection than intramuscular delivery (Giri et al., 2006; Palma et al., 2008).

1.6. Peptide vaccines

Traditional vaccines contain live attenuated or inactivated microorganisms that can elicit protective immunity to subsequent infections. However these vaccines can contain hundreds to thousands of proteins whereas quite often the main antigenic determinant is just one or two epitopes within a single protein (Azmi, Ahmad Fuaad, Skwarczynski, & Toth, 2014; Li et al., 2014). The excess of proteins may induce allergenic or adverse reactions thus removal of these are desirable in vaccine development. BCG vaccination results in hardness surrounding the injection site followed by a raised blister in most people. This can develop into an ulcer that takes weeks to heal accompanied by fever and headaches. Reducing such adverse effects would be beneficial to future vaccine design. Peptide vaccines can be as small as 20 to 30 amino acids and have many advantages over conventional vaccines including increased safety (Azmi et al., 2014; Li et al., 2014). Other significant benefits of peptide vaccines include the low cost (critical in the development of *Mtb* vaccines where the highest burden is in low income nations) and the ability to specifically target disease. Despite this potential however, as of 2015 there were no FDA approved peptide vaccines despite the large number of potential candidates making it to clinical trials (H. Yang & Kim, 2015). The most common cause of failure has been due to the lack of efficacy of the peptide. On their own, peptides are subject to degradation and poor bioavailability limiting the presentation of the target to antigen presenting cells without providing an appropriate danger signal (Pilon et al., 2013; Rezvani et al., 2011; H. Yang & Kim, 2015).

Despite the limitations of peptide vaccines, a 2000 study by Weinreich Olsen et al demonstrated protection against TB can be generated from vaccines containing single synthetic peptides

provided a suitable delivery system to instigate and appropriate, but also prolonged immune response is used. Analysis of peptides from the two major antigenic proteins of *Mtb*, ESAT-6 and Ag85B has shown the feasibility of eliciting protective immune responses from peptides derived from these proteins.

1.6.1 ***Antigenic peptides of ESAT-6***

Epitope mapping using overlapping peptides 20-23 amino acids long spanning the entire protein have been used to determine the major epitopes of ESAT-6. These were determined by analysis of INF-γ production in response to a particular ESAT-6 peptide, or the ability of antibodies to recognise these peptides. (Kanaujia, Motzel, Garcia, Andersen, & Gennaro, 2004; A. S. Mustafa et al., 2000).

Vaccination of mice with ESAT-6 $_{1-20}$ or ESAT-6 $_{51-70}$ and an adjuvant resulted in the production of large amounts of INF-γ when T cells were then exposed to the full ESAT-6 protein. Results from this study also indicated the peptide/adjuvant vaccinations were able to induce protective immunity similar to levels seen in BCG vaccinated mice using this particular model (Olsen, Hansen, Holm, & Andersen, 2000). In C57BL/6 mice the N terminus peptides induce the highest amounts of INF-γ production and mapping of this epitope has narrowed down the core residues as ESAT-6 $_{1-20}$ (Brandt, Oettinger, Holm, Andersen, & Andersen, 1996). However in humans this has proven to be more variable with recognition of T cell epitopes differing across the globe suggesting that genetic variability plays a role in the dominant epitopes. Lymphocytes from Danish *Mtb* patients predominantly recognised the epitope in the C terminal (ESAT-6 $_{72-95)}$, Ethiopian patients in the middle of the protein (ESAT-6 $_{42-75}$) and German patients in the N terminus residues (ESAT-6 $_{1-30}$) (A. S. Mustafa et al., 2000).

Given the increasing awareness of the importance of antibodies in *Mtb* infection, B cell epitopes selection should also be taken into consideration when choosing peptides to use.

Analysis of serum from non-human primates infected with *Mtb* indicates the presence of antibodies against the ESAT-6 protein. Using the same overlapping peptides used in previous epitope mapping studies, antibody response was skewed towards peptides from the C terminus of the protein, with antibodies recognising the ESAT-6_{51-70} and ESAT-6_{72-95} peptides being the most common. (Kanaujia et al., 2004).

1.6.2 ***Antigenic peptides of the Ag85B enzymes***

Epitope mapping of the Ag85 enzymes was carried out by infecting mice with *Mtb* or a DNA vaccine containing *fbpA*, *fbpB*, and *fbpC*. Spleenocytes were re-stimulated with peptides from all three proteins and the production of IL-2 and INF-γ in response to stimulation by a number of peptides from across these proteins (Huygen et al., 1994) (D'Souza et al., 2003). The Ag85A and Ag85B share 77% homology so it is perhaps not surprising that the dominant T cell epitope is same peptide, from residues 241-260 (D'Souza et al., 2003). IL-2 and INF-γ are present in significant amounts when stimulated with the dominant Ag85A and Ag85B epitope in both *Mtb* infected and vaccinated mice (D'Souza et al., 2003). The Ag85C however does not share the same level of homology and differs in its dominant epitope. The dominant epitope of Ag85C was determined through re-stimulation of spleenocytes from vaccinated mice, however this same epitope was not able to stimulate a detectable cytokine response in *Mtb* infected mice. Ag85C is produced in the lowest amount in *Mtb* thus the protein may not have been produced in sufficient quantities for immune recognition, or this assay may not have been sensitive enough to the response in *Mtb* infected mice. As Ag85B is produced in the largest amounts many vaccines have focused on this protein. Indeed vaccination with a fusion Ag85B protein has demonstrated the ability of Ag85B residues 241-255 to generate specific CD4+ T cells that are able to protection against *Mtb* challenge in a mouse model (Bennekov et al., 2006). In contrast the B cell epitopes of the Ag85 enzymes have not been as well characterised.

Given the identification of the core peptides that generate specific immune responses to the ESAT-6 and Ag85 enzymes, it is in theoretically possible to vaccinate with just these core peptides. However the limitations of peptide vaccines will need to be overcome and the peptides delivered with an adjuvant that's not only immunogenic, but also protects the peptide from degradation.

1.7. *L lactis* vaccines

L. lactis is a vaccine carrier of interest for mucosal vaccines. The bacteria has been used in the food industry for decades and has generally regarded as safe (GRAS) status. *L. lactis* is easy to grow in large quantities quickly, and cheaply. The species is cleared quickly in both mice and humans as it is a non-commensal and does not colonise (Bahey-El-Din, 2012). The species has also shown it is able to generate systemic and local antigen specific IgA responses following intransal immunisation when the bacteria are expressing heterologous protein (J. M. Wells & Mercenier, 2008).

Mucosal administration of *L. lactis* vaccines induces a strong mucosal immune response against the target of interest which in some cases has been showed to induce protective immunity (Bermudez-Humaran et al., 2004; Corthesy, Boris, Isler, Grangette, & Mercenier, 2005; Dieye et al., 2003; Mannam, Jones, & Geller, 2004). However the location where the target antigen is expressed has a significant effect on the immune response. A study investigating the response to a human papillomavirus antigen found that the immune response against the antigen is significantly higher when it is anchored to the cell wall of *L. lactis*, rather than secreted by the bacteria (Bermudez-Humaran et al., 2004). This suggests the antigen of interest needs to be presented to the APCs in close association with *L. lactis* to elicit the greatest immune response.

L. lactis vaccines have been shown to provide protection against *Streptococcus pneumonia*, a bacterium that colonises the respiratory tract. Intranasal delivery of 10^8 *L. lactis* expressing *Streptococcus pneumonia* proteins for five days was able to stimulate innate and specific immune responses in the respiratory mucosa. This included increased production of pro inflammatory cytokines (such as TNFα) that increased the effectiveness of the innate immune system. There was also the production of specific immune responses with activation of the humoral immune response evident in the production of local (bronchiole alveolar lavage (BAL) and systemic (serum) specific IgG and IgA. These immune responses resulted in the increased clearance of bacteria form the lungs and blood as well as reducing injury seen in the lungs (Villena, Medina, Vintiñi, & Alvarez, 2008).

Contemporary vaccine design needs to take into account the ability of the vaccine to stimulate a strong local response to where the target pathogen is likely to be first encountered or resides. In the case of *Mtb* this is going to require a targeting of mucosal immunity in the respiratory tract (Bahey-El-Din, 2012; Mercenier, Muller-Alouf, & Grangette, 2000).

Preclinical studies of *Mtb* vaccine candidates administered intranasally have shown improved protection compared to intradermal or intramuscular administration. The interaction of the respiratory mucosa could explain these findings. It is therefore conceivable that delivery of *Mtb* proteins or peptides in *L. lactis* could enhance the mucosal immune response in the respiratory tract and provide protection against TB.

1.7.1 ***Intransal vaccine delivery***

Intranasal vaccine delivery follows a global trend towards needle free vaccine administration (Giudice & Campbell, 2006). The motivation being ease of delivery, reduction in cost and increases in safety and compliance, particularly relevant in the developing world (Giudice & Campbell, 2006). Targeting the mucosa is highly effective as an estimated 80% of all immune

cells are localised to the mucosal associated lymphoid tissue (MALT) (Holmgren & Czerkinsky, 2005; Yusuf & Kett, 2017). One of the major functions of this arm of the immune system is protecting the mucosa (and by extension the host) from colonisation by invading microbes (Holmgren & Czerkinsky, 2005). The MALT forms a highly compartmentalised arm of the immune system and can be further divided into gastrointestinal associated lymphoid tissue (GALT), nasopharynx associated lymphoid tissue (NALT), and bronchiolar associated lymphoid tissue (BALT) (Davis, 2001). Although largely compartmentalised, there is a significant level of communication between braches of the MALT where stimulation is able to activate local, and systemic humoral and cellular responses (Neutra & Kozlowski, 2006). For example, vaccination targeting the NALT with a recombinant adenovirus was able to generate a specific immune response in the genital tract, while *S. pneumoniae* vaccination was also found to generate IgA antibodies at mucosal sites distal to the immunisation site (Janoff et al., 1999; Scott Gallichan & Rosenthal, 1995).

The NALT consists of antigen presenting cells as well as follicle associated epithelium rich in T and B cells situated immediately below the epithelium (Yusuf & Kett, 2017). Memory (M) cells specialise in particulate antigen uptake and transport antigen across the membrane for immunological sampling by the antigen presenting cells (APCs) (Illum, 2007). Soluble antigens are more likely to be recognised by the APCs directly (Sharma, Mukkur, Benson, & Chen, 2009).

This group of cell types allows for generation of local cellular and humoral responses (Yusuf & Kett, 2017). NALT vaccination has led to local germinal centres where reovirius specific IgA+ B cells proliferate providing evidence of locally produced plasma cells (Fujkuyama et al., 2012). In addition to local IgA production, NALT is able to generate a significant serum antibody response resulting in a multi factor immune response (Fujkuyama et al., 2012). While serum IgG is able to activate complement mediated killing and prevent systemic microbe

spread, IgA mediated antimicrobial effects are facilitated through different mechanisms (McFarland, Sant, Lybrand, & Beeson, 1999).

IgA is the second most abundant antibody isoform in the body largely present in the mucosa. Secreted IgA is a dimer resistant to degradation by proteases due to the heavy glycosylation of the constant (C) chain (Breedveld & van Egmond, 2019). The major role of secreted IgA in the mucosal defence is entrapment or steric hindrance of antigen, be it a toxin or microbe, preventing association with the mucosa in the first instance (Breedveld & van Egmond, 2019). Part of this protection is provided in the constant (C) chain where the glycosylation of the antibody dimer at the hinge region of the C chain can interfere with pathogen-mucosal interaction .This is evident where influenza virus attachment to the mucosa can be prevented by a unique glycosylation pattern of the hinge region of the IgA dimer (Maurer et al., 2018). The glycosylation has also been shown to prevent mucosa binding of a number of other bacterial species including certain strains of *E. coli* and *Helicobacter pylori* (Borén, Falk, Roth, Larson, & Normark, 1993; Schroten et al., 1998). In addition to neutralising functions, IgA is also able to operate intracellularly. Internalisation of IgA coated virus resulted in interaction with tripartite motif-containing protein 21 (TRIM21), a cytosolic antibody receptor that also binds IgG. Formation of the TRIM21, antibody-antigen complex targets the complex for proteasome destruction (Bidgood, Tam, McEwan, Mallery, & James, 2014).

Although intranasal delivery of the vaccines are able to capitalise on the highly vascularised nature and high concentration of immune cells in the MALT, the mediation of protection against a particular disease needs to be considered in the administration of the vaccine. In two independent studies, intranasal administration of various volumes of bioluminescent labelled bacteria, or 9mTc-labeled sulphide-colloid, resulted in different recovery profiles of the bacteria or radio isotope from the respiratory tract. Doses delivered in 50 µL resulted in the majority of recovery from the lungs and lower respiratory tract (LRT). However there was trace

amounts of bacteria/radio isotope in the upper respiratory tract (URT). Where volumes were lower than 10 µl, the bacteria or radio isotope were contained entirely to the upper respiratory tract (Miller et al., 2012; Southam, Dolovich, O'Byrne, & Inman, 2002).

While there is evidence protection against aerosol *Mtb* infection is only possible when intra nasal vaccines are delivered to the LRT, these studies have primarily used adenoviral vectors (Ronan, Lee, Tchilian, & Beverley, 2010; Song et al., 2010). LRT and URT immunisation with these adenoviral vectors has shown there is a distinct immune profile when vaccines are delivered to either site while only LRT vaccination stimulates lung resident memory T cells, which are recognised as an important mediator of protection (Park & Kupper, 2015).

1.8. PilVax

PilVax, short for pilus vaccine, is a novel peptide vaccine delivery strategy for the generation of highly specific mucosal immune responses. The platform utilises the known ability of *L. lactis* to generate protective immune responses to heterologous proteins expressed in the bacteria. PilVax however is aimed at targeting delivery of peptides or small proteins. To achieve this the pilus from the human exclusive pathogen, *Streptococcus pyogenes (S. pyogenes)* is expressed in *L. lactis* and is covalently anchored to the cell wall. Peptides of interest can be engineered within the immunogenic backbone monomer of pilus. This overcomes the disadvantages of peptide vaccines by stabilising the peptide within the immunogenic pilus structure and amplifying the peptide due to polymerisation of the pilus backbone monomer.

1.8.1 ***Streptococcus pyogenes pilus***

S. pyogenes is an exclusive human pathogen responsible for a wide variety of diseases. These range in severity from relatively mild or self-limiting disease such as pharyngitis to severe

invasive soft tissue infections such as necrotising fasciitis, or toxic shock syndrome (Cunningham, 2008). The bacterium is able to employ a large arsenal of virulence factors to establish these diseases with the pilus being one of the most important as it is involved in initial adhesion to host tissue (Cunningham, 2008).

Pili are long filamentous projections from the surface of the cell. They have been well characterised and understood in Gram negative bacteria with these structures playing key roles in pathogenesis, in particular in mediating attachment to host tissue (Sauer, Mulvey, Schilling, Martinez, & Hultgren, 2000). However due to how extremely thin pili can be (2-3 nm in *S. pyogenes*) the presence of these structures in Gram positive bacteria has only been relatively recently discovered (Mora et al., 2005) (Kang et al., 2007). The presence of pili in *S. pyogenes* was identified by searching the genome with a focus on the LPxTG motif. This motif is found in cell wall anchored proteins that belong to a family of microbial surface components recognizing adhesive matrix molecules (MSCRAMMs). Searching for genes that contain this motif that are adjacent to sortase genes resulted in the discovery of a highly variable 11 kilobase pathogenicity island. This has since become known as the fibronectin-binding, collagen binding T antigen (FCT) region and there is variability with this pathogenicity island which is present in in most *S. pyogenes* serotypes (Mora et al., 2005).

1.8.1.1 ***Pilus assembly***

The genes in the FCT cluster code for the proteins required for pilus formation. There are 6 FCT types. The pilus operon of M1 strains is contained within FCT-2, and M6 strains within FCT-1 (figure 1.4)

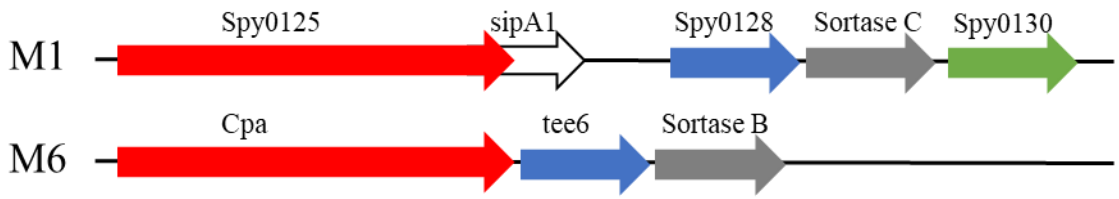

Figure 1.4: Schematic diagram of the pilus operon from the M1 and M6 strains of *S. pyogenes.*

In the M1 strain, the major pilin subunit is Spy0128 which under goes polymerisation to constitute the majority of the pilus structure. The polymerisation is carried out by sortase C1 (a transpeptidase). Spy0125 and Spy0130 are minor pilin proteins that function as the tip adhesin and cell wall anchor protein, respectively (figure 1.5 A) (Mora et al., 2005). SipA1 is a signal like peptidase required for pilus assembly, however, its specific mechanism of action is unknown (Young, Proft, Harris, Brimble, & Baker, 2014).

Pilus assembly is initiated following the secretions of the tip adhesin Spy0125, which is cleaved by sortase C between the threonine and glycine of the LPxTG motif in its C terminal domain resulting in a thioester intermediate. This undergoes nucleophilic attack by a terminal amino group within the lipid II protein in the cell wall, resulting in an isopetide bond (Proft & Baker, 2009). The Spy0128 subunits are also cleaved at the LPxTG motif at the C terminal and the threonine carboxylate linked to a lysine (K161) in the N terminal of the next pilin subunit through an isopeptide bond. Formation of this bond is catalysed by sortase C. Continual addition of the Spy0128 protein to this structure through covalent bonds results in the formation of the elongated pilus structure 2-3nm wide and >1µm in length. (Hendrickx, Budzik, Oh, & Schneewind, 2011; Proft & Baker, 2009). The resulting pili are covalently bound, high molecular weight proteins of varying lengths that display a characteristic laddering pattern in Western blots due to the differing size of the assembled pili. Pilus formation is terminated upon the addition of the cell wall anchor protein Spy0130 (Proft & Baker, 2009).

1.8.1.2 ***Pilus structure and integrity***

The crystal structure of Spy0128 has been solved revealing a 2 domain protein that largely consists of irregular all-β sheet secondary structures which are modified variants of the immunoglobulin fold that provides structural integrity (figure 1.5 B) (Kang et al., 2007). The Spy0128 structure is not susceptible to protease degradation as each subunit is covalently bound to the next. The sortase enzyme cross-links the side chains of a lysine and an asparagine (Lys36-Asn168 in the N domain; Lys179-Asn303 in the C domain), resulting in the formation of two isopeptide bonds per subunit, one in each domain. (Hendrickx et al., 2011; Kang et al., 2007). This was demonstrated by generation of recombinant Spy0128 that contained point mutations at this site to disrupt isopeptide bond formation. Recombinant Spy0128 with these mutation were susceptible to protease degradation (Kang, et al., 2007). The physiological significance of such strong bonds lies in the ability of the pilus to adhere to host surfaces despite major mechanical forces that might break a non-covalently linked structure, and resits degradation by host enzymes (Hendrickx et al., 2011).

The majority of *S. pyogenes* strains have a two domain major pillin structure like Spy0128. However backbone proteins from FCT-1 (eg M6 strain of *S. pyogenes*) have a unique 3-domain structure (figure 1.5). Like Spy0128, each domain the M6 major pilin consists of primarily β-sheet linked by variable loop regions. Unlike the M1 strain, however, these loop regions contain some degree of secondary structure (Paul G. Young et al., 2014).

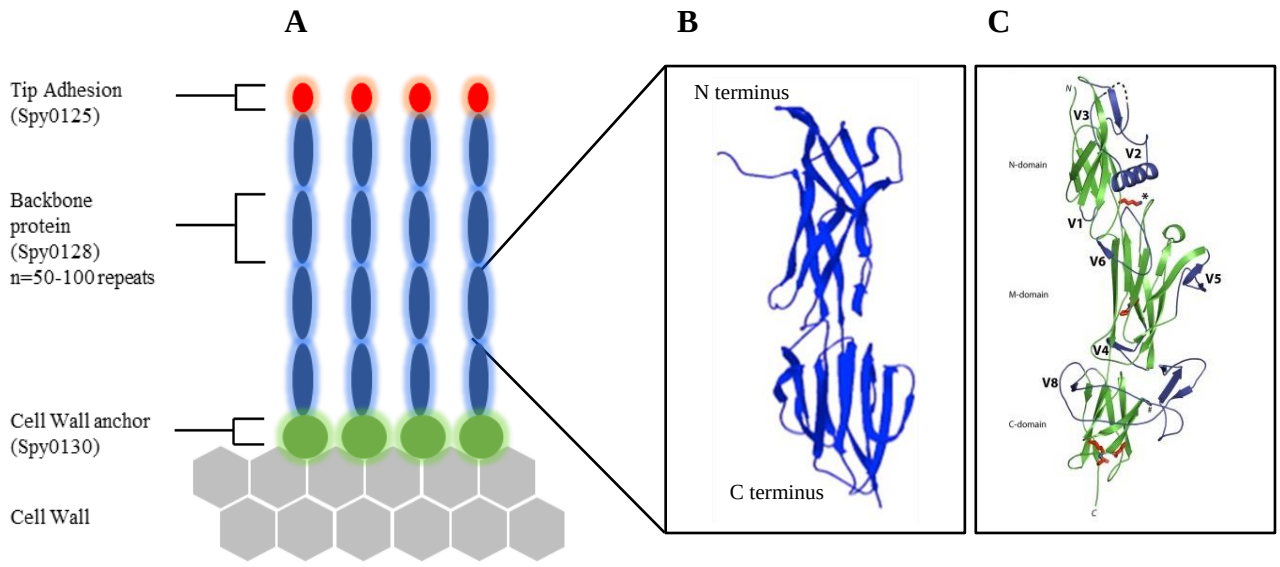

Figure 1.5: Schematic of *S. pyogenes* pilus and subunits.

A) Model of the *Streptococcus pyogenes* M1 pilus on the cell surface. B) Model of major pilin protein of the M1 strain (Spy0128) C) Model of major pilin protein of the M6 strain (tee6) (Kang, Coulibaly, Clow, Proft, & Baker, 2007; Paul G. Young et al., 2014)**. (**T6 model reproduced with permission).

1.8.2 ***Pilus immunogenicity***

Exposure to *S. pyogenes* results in a vigorous innate immune response when the bacterium comes into contact with host epithelial cells. It activates the production of pro inflammatory cytokines such as IL-8 and TGF-β and thus the recruitment of neutrophils, macrophages, and lymphocytes to the site of infection (Soderholm, Barnett, Sweet, & Walker, 2018). It has however been demonstrated that the adaptor protein tied to TLRs, MyD88 is required to be activated for *S. pyogenes* infection to induce cytokine production, triggering the recruitment of other cell types (Soderholm et al., 2018) (Hendrickx et al., 2011). Traditionally it has been assumed TLR2 was responsible for initiating the MyD88 signally pathway in *S. pyogenes* infection. This is because it has been implicated in the recognition of highly conserved pathogen associated molecular patterns (PAMPs) displayed on invading microorganisms and multiple ligands on gram positive bacteria. However it has also been shown that mice deficient in TLRs 2/4/9 are able to produce type I interferon through MyD88 dependent signalling

meaning there may be involvement of other TLRs in *S. pyogenes* infection (Gratz et al., 2008; Tsatsaronis, Walker, & Sanderson-Smith, 2014). Further mouse studies showed that TLR 2 and 13 are required to be knocked out to prevent *in vitro* macrophage mediated responses to *S. pyogenes.* Although TLR13 exists only in mice, it has an analogue TLR8 in humans that recognises rRNA (Fieber et al., 2015; Soderholm et al., 2018). Given the demonstrated ability of the pilus structure to generate protective antibodies by Mora et al 2005, it is likely it is immunogenicity is a result of recognition by one of these receptors (Mora et al., 2005).

1.8.3 ***Engineering peptides into PilVax***

PilVax, is a novel peptide delivery platform that harness the immunogenicity of the *S. pyogenes* pilus expressed in *L. lactis* to stimulate immune responses to a peptide of interest. The variable loop regions that link the β-sheet structures of the Spy0128 protein were the target sites for insertion of peptides into the M1 pilus structure (PilM1) (figure 1.6). These variable loop regions allowed for peptide insertion without disruption the secondary structure of the protein or pilus assembly (Wagachchi et al., 2018).

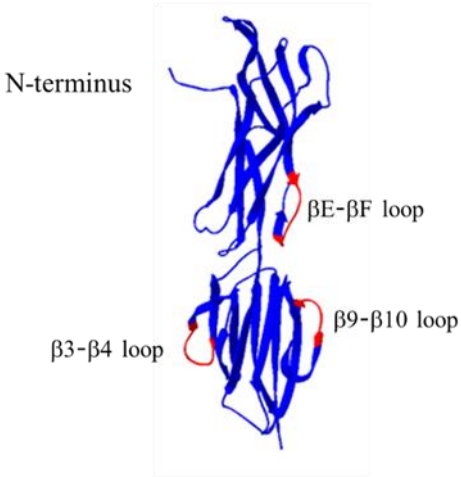

Figure 1.6: Variable loop regions of the M1 major pilin subunit targeted for peptide insertion (Wagachchi et al., 2018). Image licensed under creative commons 4.0 (CC BY 4.0).

The whole *S. pyogenes* M1_SF370 pilus operon containing peptide insertions within Spy0128 was then cloned into a shuttle vector allowing for expression on *L. lactis.* (Wagachchi et al., 2018).

The insertion of the peptide into three distinct loop regions, the β3-β4 loop, β9-β10 loop, and the βE- βF loop regions resulted in pilus assembly and formation on *L. lactis* (figure 1.7). This is seen as a characteristic high molecular weight laddering pattern seen by Western Blot analysis. Analyses by flow cytometry revealed the expression of the pilus to be slightly diminished with the addition of the $Ova_{324–339}$ peptide compared to *L. lactis* containing only the pilus with no peptides inserted (Wagachchi et al., 2018). Other loop regions were also tested but the pilus did not form in these constructs. These results suggest that these loop regions may be involved in structural integrity or successful assembly more than previously though. Interestingly in a 3D model of the Spy0128 protein, all three of the successful loop regions are on the same face of the protein structure.

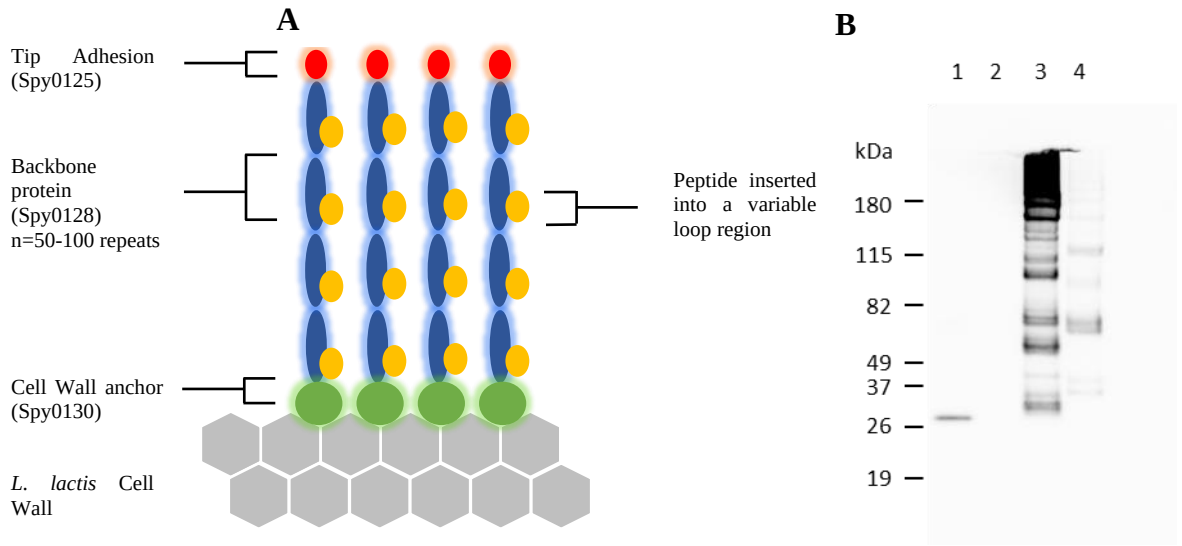

Figure 1.7: Schematic of PilVax

A) Schematic of the PilVax concept, showing the M1 pilus structure with a peptide inserted into a variable loop region and expressed on the surface of *L. lactis* B) Western blot probing for Spy0128, 1: recombinant Spy0128, 2: wild type *L. lacits* cell wall extract (CWE), 3: *L. lactis* expressing PilM1 CWE, 4: *L. lactis* expressing PilM1-Ova in the βE-βF loop region CWE (Wagachchi et al., 2018). Image licensed under creative commons 4.0 (CC BY 4.0).

Similar structural analysis of the T6 pilin subunit highlights the possibility of complete replacement of the V8 region. From a vaccine perspective this may mean larger peptides, or even whole protein antigens could be inserted without affecting pilus assembly.

Serum from mice vaccinated intranasally with a PilVax construct containing the $Ova_{324–339}$ peptide in the βE- βF loop region showed a significant specific IgG and IgA response to both the backbone Spy0128 protein, and the ovalbumin protein. However mice co vaccinated with *L. lactis* expressing the M1 pilus only and ovalbumin separately were not able to produce antibodies specific to the $Ova_{324–339}$ peptide. This suggests the immunogenicity of *L. lactis* and Spy0128 alone were not sufficient for generating peptide specific responses, rather the peptide must be contained within the pilus backbone protein. This reinforces the finding of Bermudez-Humaran et al 2004 mentioned earlier that found greatest immunogenicity is achieved when the structure of interest is in direct association with *L lactis* rather than separately. The high

titre of antibodies seen in the PilVax-OVA vaccinated mice was similar to the positive control group where mice were vaccinated with the mucosal adjuvant cholera toxin B mixed with Ova, systemic (serum) and mucosal (BAL and saliva) antibodies were observed. (Wagachchi et al., 2018).

Cellular immunity was not assessed in these studies because the model peptide $Ova_{324–339}$ binds specifically to the I-Ad MHC class II protein and thus a B cell epitope (McFarland, Sant, Lybrand, & Beeson, 1999; Wagachchi et al., 2018).

1.9. Aims

New prophylactic strategies are needed to address the global TB burden. Ag85B and ESAT-6 are promising vaccine targets against TB that could be delivered using the novel PilVax delivery platform.

The aim of this thesis is to test whether it is possible to use the PilVax system for delivery of a novel peptide vaccine in a model of an infectious disease.

The objectives are:

1. To optimise vaccinations for PilVax with regards to the humoral response. Different vaccination schedules will determine how the optimal antibody response is achieved.
2. Peptides from the ESAT-6 and Ag85B proteins have been selected for cloning in to the PilVax construct.
3. PilVax-Ag85B and PilVax-ESAT-6 constructs will be used to vaccinate mice according to the optimal vaccine schedule to determine the ability of PilVax to elicit a humoral response to these peptides.

4. PilVax-Ag85B and PilVax-ESAT-6 constructs will also be used to vaccinate mice in a schedule that optimises the T cell response and determine the cellular response to PilVax vaccinations. Peptide specific cells will be analysed as well as the cytokine response to re-stimulation with peptides.

This data will be used to determine if one of these PilVax constructs is suitable for use in a protection study to analyse if the humoral or cellular responses are protective.

The ability of the vaccine to elicit cellular and humoral responses to these peptides will also determine and shape what diseases PilVax may be able to be used with in future studies.

Chapter 2. Materials

2.1. Ethics approvals

Animal work carried out at the Vernon Jansen Unit (VJU) at the University of Auckland was approved by the University of Auckland Animal Ethics committee (UAAEC) (001664).

Animal work carried out at the Hercus Taieri Resource Unit (HTRU) at the University of Otago was approved by the University of Otago Animal Ethics committee (UOAEC) (64/2017).

2.2. Molecular biology

Solutions were prepared using Type 1 Mili-Q® water (Millipore).

2.2.1 ***Common reagents***

Phosphate Buffered Saline (PBS)	137 mM NaCl, 2.7 mM KCl, 10 mM Na_2HPO4, 1.8 mM KH_2PO4, pH 7.4
PBS-T	PBS + 0.1% (v/v) Tween-20 (Sigma Aldrich)
CCMB80 buffer	10 mM KOAc, 80 mM $CaCl_2$, 20 mM $MnCl_2$, 10 mM $MgCl_2$, 10% glycerol (Sigma Aldrich), pH 6.4

2.2.2 ***Primers***

All primers were ordered from Sigma Aldrich.

Table 2.1: Primer sequences.

Primer Name	5'-3' Sequence	Restriction sites
ESAT-6_P1.fw	CG**GATCC CTCGAG**ATGACAGAACAACAATGGAAT TTTGCTGGAATTGAAGCTG	*BamHI, XhoI*
ESAT-6_P1.rv	CG**GAATTC CTCGAG**TCCTTGAATAGCTGAAGCTGC AGCTTCAATTCCAGC	*EcoRI, XhoI*
ESAT-6_P2.fw	ACGCAC**GTCGAC**TATCAAGGTGTTCAACAAAAATG GGATGCTACTGCAAC	*SalI*
ESAT-6_P2.rv	ACGCAC**GTCGAC**TTGTAAAGCGTTATTAAGTTCTGT TGCAGTAGCATCCC	*SalI*
ESAT-6_P8.fw	CG**GATCC CTCGAG**CTTGCTCGTACTATTTCAGAAG CAGGTCAAGCTATGGCATC	*BamH1, XhoI*
ESAT-6_P8.rv	CG**GATCC GTCGAC**AGCAAACATACCAGTAACATTT CCTTCAGTAGATGCCATAGCTTGACC	*EcoRI, XhoI*
Ag85B.fw	CG**GATCC CTCGAG**TTTCAAGATGCTTATAATGCTG CAGGTGG	*BamHI, XhoI*
Ag85B.rv	CG**GAATTC CTCGAG**AAAAACAGCGTTATGTCCACC TGCAGCATTA	*EcoRI, SalI*
Spy0128.fw	GGAGCAGCCCTAACTAGTTTTGC	-
Spy0128.rv	GAGCTCCACCAACTGCTACAATTC	-

Restriction sites in blue, overlap underlined where applicable per primer pair. Restriction enzymes all sourced from New England Biolabs.

2.2.3 ***PCR reagents***

PCR Buffer (10X)	500 mM , 100 mM Tris.HCl (pH 9.0), 1% v/v Triton™ X-100 (Sigma Aldrich)
Taq Polymerase	5 Units/mL. Expressed and purified by Dr Ries Langly, The University of Auckland.

2.2.4 ***Gel electrophoresis***

Agarose	0.5-1% w/v Agarose (Bioline)
DNA loading dye (6x)	30% w/v glycerol (Sigma Aldrich), 0.25% w/v bromophenol blue (Sigma Aldrich), 0.25% w/v xylene cyanol (Serva)

2.2.5 ***Plasmids***

pLZ12KmP23R_PilM1_βE/βBF_*XhoI*	Modified shuttle vector that confers resistance to kanamycin. Contains the constitutive Lactococcus promoter P23R. The promoter is upstream of the operon for *S. pyogenes* M1 pilus assembly and formation (cloned by Dr Jacelyn Loh, The University of Auckland). The βE/βBF loop region of the pilus backbone subunit (Spy0128) was replaced with an *XhoI* restriction site by Dr Dasun Wagachchi (The University of Auckland).
pLZ12KmP23R_PilM1_β9/βB10_*XhoI*	Modified shuttle vector that confers resistance to kanamycin which also contains

	the constitutive Lactococcus promoter P23R. The promoter is upstream of the operon for *S. pyogenes* M1 pilus assembly and formation (cloned by Dr Jacelyn Loh, The University of Auckland). The β9/βB10 loop region of the pilus backbone subunit (Spy0128) was replaced with an *XhoI* site by Dr Dasun Wagachchi (The University of Auckland).
pLZ12KmP23R_PilM1_βE/βBF_OVA	Derivative of the above plasmid, with residues 323-339 from chicken ovalbumin cloned into the *XhoI* site by Dr Dasun Wagachchi (The University of Auckland).
pLZ12KmP23R_PilM6	Modified shuttle vector that confers resistance to kanamycin. Contains the constitutive Lactococcus promoter P23R. The promoter is upstream of the operon for *S. pyogenes* M6 pilus assembly and formation (cloned by Dr Jacelyn Loh, The University of Auckland).
pLZ12KmP23R_PilM6_ΔV8_ESAT-6	Derivative of the above plasmid, with the V8 region of the backbone protein (tee6) replaced with ESAT-6 (cloned by Dr Catherine Tsai, The University of Auckland).

pET-32a-3C-M1 Spy0128	Protein expression vector containing the Spy0128 gene from *S. pyogenes* M1. Cloned by Fiona Clow, The University of Auckland.

2.2.6 ***Bacteria strains***

Escherichia coli DH5α	*Escherichia coli* (*E. coli*) with genotype F– Φ80lacZΔM15 Δ(lacZYA-argF) U169 recA1 endA1 hsdR17 (rK–, mK+) phoA supE44 λ– thi-1 gyrA96 relA1. Used for cloning.
Escherichia coli BL21	*E. coli* with the genotype F– ompT gal dcm lon hsdSB (rBmB λ(DE3[lacI lacUV5-T7p07 ind1 sam7 nin5]) [malB+]K-12(λS) pLysS[T7p20 orip15A] (CmR) (Novagen). Used for protein expression.
Lactococcus lactis	MG1363 Wild Type Strain (Sourced from Dr Nick Heng, The University of Otago). Used for the heterologous expression of PilVax constructs.

2.2.7 ***Bacteria growth media***

Luria-Bertani medium (LB)	1.55% w/v Luria Broth base low salt (Duchefa Biochemie), 0.95% w/v NaCl

M17 medium with glucose (GM17)	3.725% w/v Difco M17 broth (BD Bioscience), 0.5% glucose
SOB medium	2% (w/v) bacto-tryptone (Oxoid), 0.5% yeast extract (Oxoid), 0.05% (w/v) NaCl, 0.018% (w/v) KCl, 1% (v/v) $MgCl_2$, pH 7.0
Agar plates	Liquid media as above supplemented with 1.5% Bacto Agar (BD Bioscience) and selective antibiotic as needed.

2.2.8 ***Selective antibiotics***

Table 2.2: Selective antibiotics used for cloning**.**

Antibiotic	Final working concentration	Supplier
Ampicillin (AMP)	100 μg/mL	Sigma Aldrich
Chloramphenicol (CM)	30 μg/mL	Sigma Aldrich
Kanamycin (KAN)	50 μg/mL for *E. coli* 200 μg/mL for *L. lactis*	Sigma Aldrich

2.3. Protein purification and analysis of heterologous M1 pilus expression

2.3.1 *Protein purification solutions*

Lysis buffer	25 mM Tris (pH 7.0), 300 mM, 10 mM $CaCl_2$, 10 mM imidazole, 0.1 mM PMSF, 1% Triton X-100 (Sigma Aldrich)
MCAC-0	25 mM Tris pH 7.0, 300 mM NaCl, 10 mM $CaCl_2$
MCAC-1000	25 mM Tris pH 7.0, 300 mM NaCl, 10 mM $CaCl_2$, 1 M imidazole
MonoQ solution A	20 mM Tris pH 8.0
MonoQ solution B	20 mM Tris pH 8.0, 1 M NaCl

2.3.2 *SDS PAGE and Western Blot solutions*

Cell Wall extract: Protoplast buffer	40% w/v sucrose, 10 mM $MgCl_2$, 100 mM K_2HPO_4, 2 mg/mL lysozyme (Sigma Aldrich), 40 U/mL mutanolysin (Sigma Aldrich)
2x loading dye	300 mM 2-mercaptoethanol (Scharlau), 125 mM Tris.HCl (pH 6.8), 20% glycerol (Sigma Aldrich), 4.1% SDS, 0.01% Bromophenol blue (Sigma Aldrich)
SDS-PAGE-resolving gel	1% w/v SDS, 375mM Tris.HCl (pH 8.8), 7.5-12.5% w/v acrylamide (Applichem), 1% w/v $(NH_4)_2S_2O_8$, 0.04% v/v TEMED (VWR International)

SDS-PAGE-stacking gel	1% w/v SDS, 125 mM Tris.HCl (pH 6.8), 5% w/v acrylamide (Applichem), 1% w/v $(NH_4)_2S_2O_8$, 0.04% v/v TEMED (VWR International)
SDS-PAGE-gel loading buffer	50 mM Tris.HCl (pH 6.8), 100 mM DTT, 2% w/v SDS, 1% w/v bromophenol blue (Sigma Aldrich), 10% v/v glycerol (Sigma Aldrich)
SDS-PAGE running buffer	25 mM Tris, 250 mM glycine, 0.1% w/v SDS
Coomassie blue	0.06% w/v Coomassie brilliant blue R-250 (Sigma Aldrich), 50% v/v drum ethanol (Thermo Fisher), 7.5% v/v glacial acetic acid (Scharlau)
Destain solution	8% v/v glacial acetic acid (Scharlau), 25% v/v drum ethanol (Thermo Fisher)
Tris-buffered saline (TBS)	50 mM Tris, 137 mM NaCl, 2.7 mM KCl
TBS-T	TBS plus 0.1% v/v Tween-20 (Sigma Aldrich)
TBS-Transfer buffer	25 mM Tris.HCl, 192 mM glycine, 20% (v/v) methanol (Merk), pH 8.3
Blocking solution	TBS-T plus 5% w/v skim milk powder (Anchor)
Probing solution	TBS-T plus 2.5% w/v skim milk powder (Anchor)

2.3.3 ***Flow cytometry reagents***

FACS blocking buffer	PBS, 3% FBS (GE healthcare), 5 mM EDTA
FACS buffer	PBS, 1% FBS (GE healthcare), 5 mM EDTA

2.3.4 ***Antibodies***

Table 2.3: Antibodies used in analysing heterologous expression of *S.pyogenes* M1 and M6 pilus in *L. lactis.*

	Species	Working dilution	Supplier
Anti-Spy0128	Rabbit	1:1000 (Western Blot) 1:100 (FACS)	Purified from rabbits vaccinated at the VJU, The University of Auckland
Anti-T6	Rabbit	1:1000 (Western Blot) 1:100 (FACS)	Purified from rabbits vaccinated at the VJU, The University of Auckland
Anti-rabbit IgG:HRP	Goat	1:10 000	BD Biosciences
Anti-rabbit IgG:FITC	Goat	1:1000	BD Biosciences

2.4. Mouse work

2.4.1 ***Mice***

Mice sourced from the VJU at The University of Auckland were either 5-6 week old female BALB/c or 7 week old male C57BL/6 mice housed in specific pathogen free conditions. Note: different strains were used for distinct experiments.

Mice sourced at the HTRU at the University of Otago were 7 week old male C57BL/6 mice housed in specific pathogen free conditions at the microbiology branch of the unit.

2.5. Antibody response analysis

2.5.1 *Proteins/peptides used*

Table 2.4: Proteins and peptides used to coat 96 well plates used for ELISAs.

	Sequence	Plate coating concentration	Supplier
rSpy0128	*See Appendix	1 µg/mL	Recombinant protein
rT6	*See Appendix	1 µg/mL	Recombinant protein
Ovalbumin	*See Appendix	1 µg/mL	Sigma-Aldrich
ESAT-6_P1	MTEQQWNFAGIEAAASAIQG	1 µg/mL	Genscript
ESAT-6_P2	YQGVQQKWDATATELNNALQ	1 µg/mL	Genscript
ESAT-6_P8	LARTISEAGQAMASTEGNVTGMFA,	1 µg/mL	Genscript
Ag85B	FQDAYNAAGGHNAVF	1 µg/mL	Genscript

2.5.2 *Antibodies*

Table 2.5: Secondary antibodies used in ELISAs.

	Species	Working dilution	Supplier
Anti-mouse IgG:HRP	Goat	1:10 000	BD Biosciences
Anti-mouse IgA:HRP	Goat	1:2000	BD Biosciences

2.6. Peptide specific T cell response analysis

2.6.1 *Tissue culture media*

Incomplete IMDM	IMDM (Gibo), 100 U/mL penicillin/streptomycin (Thermo Fisher) , 55 mM β-2-mercaptoethanol (VWR International)
Complete IMDM	Incomplete IMDM (Gibco), 0.5% FCS
Digestion media	Incomplete IMDM (Gibco), 2.4 mg/mL collagenase type I (Gibco), 0.12 mg/mL DNase I (Roche)

2.6.2 *Tetramer enrichment solutions*

FACS buffer	PBS, 1% FCS (Sigma Aldrich), 5 mM EDTA
MACS buffer	FACS buffer, 2 mM EDTA, 20 μg/mL DNase I (Roche)
Bead enrichment buffer	10% v/v anti APC microbeads (Miltenyi Biotech) in MACS buffer

2.6.3 ***Tetramer staining***

Table 2.6: Antibody panel used to detect CD4+ antigen specific cells of PilVax vaccinated mice.

Target	Fluorophore	Clone	Dilution	Supplier	Detector
CD3	FITC	17A2	1:400	BD Pharmigen	Blue 530/30
CD4	BB700	RM4-5	1:400	BD Horizon	Blue 710/50
CD44	BV421	IM7	1:800	BD Pharmingen	Violet 450/50
CD62L	BV510	MEL-14	1:200	BD Horizon	Violet 525/50
CD69	PE-CF594	H1.2F3	1:200	BD Pharmigen	Green 610/20
Live/Dead	FSV700	-	1:2000	BD Horizon	Red 730/45
FC block	-	-	1:10		
Ag85B MHC class II Tetramer IAb/FQDAYNAAG GHNAVF	APC	-	1:300	*	Red 670/14
ESAT-6_P1 MHC class II Tetramer IAb/QQWNFAGIE AAASA	APC	-	1:400	*	Red 670/14
hCLIP Tetramer	APC	-	1:400	*	Red 670/14

*: National Institute of Allergy and Infectious Disease Facility, Emory University, Atlanta, GA, USA.

2.6.4 ***Lymphocyte re-stimulation***

Table 2.7: Peptides used to re-stimulate lymphocytes isolated from PilVax immunised mice at 20μg/mL.

Peptide	Sequence
ESAT-6_P1	MTEQQWNFAGIEAAASAIQG
ESAT-6_P2	YQGVQQKWDATATELNNALQ
ESAT-6_P8	LARTISEAGQAMASTEGNVTGMFA
Ag85B	FQDAYNAAGGHNAVF

2.6.5 ***Cytokine staining***

Table 2.6: Antibody panel used to detect cytokine production of re-stimulated cells from PilVax vaccinated mice.

Target	Fluorophore	Clone	Dilution	Supplier	Detector
CD3	FITC	17A2	1:400	BD Pharmigen	Blue 530/30
CD4	BB700	RM4-5	1:400	BD Horizon	Blue 710/50
CD8	APC-cy7	53.67	1:400	BD Pharmigen	Red 780/60
IL-2	APC	JE56 5HH	1:50	Bio legend	Red 670/14
INF-γ	BV510	XM G1.2	1:200	BD Pharmigen	Violet 585/15
TNFα	BV711	MP6.XT2	1:100	BD	Violet 711
		2		Biosciences	
IL-17	BV650	TCII 18H	1:50	Bio legend	Violet 650
		10.1			
Live/Dead	FSV700	-	1:2000	BD Horizon	Red 730/45
Fc Block	-	-	1:10		

2.6.6 ***Flow cytometry reagents***

FACS buffer	PBS, 1% v/v FCS (Sigma Aldrich), 5 mM EDTA

Chapter 3. Methods

3.1. Bacteriology

Newly generated bacterial strains were stored at -80 ˚C in a 30% v/v glycerol stock. Existing, and new strains were streaked on to an agar plate for single colonies when required.

3.1.1 ***Growth conditions***

3.1.1.1 ***E. coli***

Unless otherwise specified, when plated for single colonies and cloning, *E. coli* was grown at 37 ˚C on LB agar containing the appropriate antibiotic as required. Liquid cultures were grown aerobically at 37 ˚C with aeriation in LB broth containing antibiotic as required for selection.

3.1.1.2 ***L. lactis***

Unless otherwise specified, when plated for single colonies, enumeration and cloning, *L. lactis* was grown at 28 ˚C on GM17 agar containing the appropriate antibiotic as required. Liquid cultures were grown anaerobically at 28 ˚C without agitation in GM17 broth containing antibiotic as required for selection.

3.2. Molecular biology

3.2.1 ***Polymerase chain reaction (PCR)***

3.2.1.1 ***Overlap PCR***

Peptide primers with overlapping 3’ ends, indicated in table 2.1, were annealed and amplified using a Master Cycler Nexus (Eppendorf). The reaction mix contained; 1x PCR buffer, 2.5 mM $MgCl_2$, 0.2 mM of each dNTP, 2 μM forward primer, 2 μm reverse primer, and 5 U Taq polymerase made up to 100 μl with MiliQ water.

Table 3.1: Thermal cycle used for generation of peptides.

Step	Temperature	Time
Denaturation	95 ˚C	40 seconds
Annealing	50 ˚C	45 seconds
Extension	72 ˚C	10 minutes

3.2.1.2 ***Single colony PCR***

Transformed bacteria were screened for uptake of insert DNA by colony PCR before sequencing. Colony PCR for newly generated plasmids used a primer pair including one external and one internal primer specific to the inserted DNA sequence. Colony PCR for transformation of sequenced plasmids only used internal primer pairs for the Spy0128 gene. Both were carried out with: 1x PCR buffer, 2.5 mM $MgCl_2$, 0.2 mM of each dNTP, 0.2 μM forward primer, 0.2 μM reverse primer and 2.5 U Taq polymerase and prepared up to 25 μL with MiliQ water. Using a sterile 200 μL pipette tip, the colony of interest was touched to transfer some colony to the tip, and mixed into the PCR mixture. To propagate each colony selected for further use, the tip was streaked onto a fresh selective agar plate and incubated appropriately depending on the species.

Table 3.2: Thermal cycles used in single colony PCR.

Step	Temperature	Time	Cycles
Initial denaturation	95 ˚C	10 minutes	1x
Denaturation	95 ˚C	30 seconds	25x for *E.coli* 35x for *L.lactis*
Annealing	50 ˚C	30 seconds	
Extension	72 ˚C	1 minute/kb	
Final extension	72 ˚C	10 minutes	1x

3.2.2 ***Gel electrophoresis***

PCR amplified DNA was mixed with 6x DNA loading dye and run on 1% w/v agarose gels prepared with TAE buffer and 1:10 000 SYBER red DNA gel stain (Invitrogen). The gel was run at 100 V and 400 mA for 20-30 minutes using a PowerPac Basic Power Supply (Bio Rad) and visualised with a ChemiDoc Imaging System (Bio-Rad). Samples were run alongside a 1 Kb plus DNA ladder (Invitrogen).

3.2.3 ***DNA purification***

Purified DNA quality and concentration was assessed by UV-Vis spectrophotometry using a NanoDrop 2000 (Thermo Fisher) before further use. Surplus DNA was stored at -20 ˚C following purification.

3.2.3.1 ***Plasmid purification***

2 mL (pET32a3c) or 10 mL (pLZ12KmP23R and its derivatives) were grown in an overnight culture of *E. coli* DH5α in LB containing the appropriate antibiotic at 37 ˚C and 200 rpm. Cells were pelleted by centrifugation at 4,500 g for 10 minutes and purified using a Nucleospin Plasmid Miniprep Kit (Macherey-Nagel) as per the manufacturer's instructions. (High copy protocol for pET32a3c vectors, low copy protocol for pLZ12KmP23R vector and its derivatives). DNA was eluted in 20 μL MiliQ water.

3.2.3.2 ***PCR product purification***

PCR products were purified using the QIAquick PCR purifcaiton kit (QIAGEN) as per the manufacturer's instructions. DNA was eluted in 20 μL of MiliQ water.

3.2.3.3 ***Gel extraction***

DNA to be extracted from an agarose gel was first run on a gel as in section 3.2.2. DNA was then visualised on a Dark Reader DR46B Transilluminator (Clare Chemical Research). The desired band was extracted with a sterile scalpel and the extracted agarose piece transferred to

a fresh 1.7 mL Eppendorf tube. The DNA was extracted using a QIAquick gel extraction kit (QIAGEN), according to the manufacturer's instructions.

3.2.4 ***Cloning techniques***

3.2.4.1 ***Restriction digest***

PCR products were digested following clean up as per section 3.2.3.2 and digested in the following mix: PCR product, 1 U of each required enzyme, 1x restriction enzyme buffer, made up to 20 µL with MiliQ water and incubated overnight at 37 ˚C. Reactions were stopped by heat inactivation according to manufacturer's instructions and digested DNA used directly in downstream applications.

800 ng of plasmid DNA was digested following purification (section 3.2.3.2) and digested in the same manner as PCR products. Where multiple enzymes (without compatible cut sites) were used to cut the DNA, reaction was heat inactivated as per the manufacturer's instructions and used directly in downstream applications. For single enzyme cuts and multiple enzymes that have compatible cut sites, DNA was run on an agarose gel as (section 3.2.2) and purified as per section 3.2.3.3 before being dephosphorylated.

3.2.4.2 ***Dephosphorisation***

Digested vector DNA was incubated with rAPid Alkaline Phosphatase (Roche) to prevent vector self-ligation by removing the 5' phosphate groups. Following digestion and gel purification of DNA, digested vector DNA was incubated with 1 U of rAPid Alkaline Phosphatase, 1 x Alkaline Phosphatase buffer, made up to 20 µL with MiliQ water. The mix was incubated at 37 ˚C for 30 minutes, followed by heat inactivation at 75 ˚C for 2 minutes. Vector DNA was used for ligation without any further purification.

3.2.4.3 ***Ligation***

Ligations were carried out overnight and maintained at 16 ˚C in a Mastercycler Nexus (Eppendorf) using the following reaction mix: 400 U T4 DNA ligase (New England Biolabs) 1x T4 DNA ligase buffer, 3:1 insert: vector DNA ratio made up to 10 µL with MiliQ water.

3.2.5 ***Transformation***

3.2.5.1 ***Preparing chemically competent E. coli cells***

A single colony of *E. coli* (DH5α or BL21) was inoculated in 2 mL of SOB media and grown overnight at 37 ˚C and 200 rpm. The culture was diluted 1:100 into fresh SOB and grown at 28 ˚C and 200 rpm to an OD_{600} of 0.2-0.3. (Approximately 2 hours for BL21 and 4 hours for DH5α). Cells were pelleted by centrifugation at 4, 000 g for 10 minutes at 4 ˚C, supernatant discarded, and cells suspended in ice cold CCMB80 buffer at a ratio of 32 mL per 100 mL of original culture. Following 20 minutes incubation on ice, cells were centrifuged as above and again suspended in fresh, ice cold CCM80 at a ratio of 4 mL per 100 mL of original culutre and left to incubate on ice for 20 minutes. Cells were then aliquoted and snap frozen in a dry ice/ethanol bath for storage at -80 ˚C until required.

3.2.5.2 ***Heat shock***

A 50 µL aliquot of competent *E. coli* (DH5α or BL21) cells were thawed on ice and mixed with 5 µL of ligation mixture. Following 10 minutes incubation on ice, the mixture was immersed in 42 ˚C water for 45 seconds and returned to ice for 2 minutes. 500 µL of LB was added to the mixture and cells were incubated at 37 ˚C for 30 minutes without agitation. The cells were then centrifuged for 5 minutes at 5, 000 g, and all but 100 µL of the supernatant removed. The cells were suspended in the remaining supernatant and plated onto an LB agar plate containing the appropriate antibiotic for overnight incubation at 37 ˚C.

3.2.5.3 ***Preparing electro competent L. lactis cells***

A single colony of *L. lactis* was used to inoculate an overnight 2 mL anaerobic culture of GM17 media and grown at 28 ˚C without agitation. The culture was diluted 1:50 into fresh GM17 media and grown anaerobically without agitation until and OD_{600} of 0.4 was reached (approximately 2 hours of growth). The cells were then centrifuged at 4, 000 g for 15 minutes at 4 ˚C and the supernatant discarded. Cells were washed twice with 4 mL of ice cold MiliQ water, and once with 2 mL of ice cold 50 mM EDTA. Cells were suspended in 400 μL of ice cold 0.3 M sucrose and used immediately.

3.2.5.4 ***Electroporation***

1 μg of DNA was incubated with 40 μL of electro competent *L. lactis* for 5 minutes on ice before being transferred to a pre chilled Micropulser (2mm gap) (BioRad) electroporation cuvette. The cells were pulsed at 2500 V (voltage), 25 μF (capacitance), 200 Ω (resistance) in a Gene Pulser Xcell (BioRad). Immediately following the pulse, 1 mL of GM17 was added to the bacteria and cells transferred to a 1.7 mL Eppendorf tube for incubation at 37 ˚C for 2 hours to allow for recovery. Bacteria were then centrifuged at 5, 000 g for 5 minutes and all but 100 μL of supernatant removed. The cells were suspended in the remaining amount and plated onto a GM17 agar plate and incubated for 36 hours at 28 ˚C.

3.2.6 ***Sequencing***

Sequencing was carried out by ABI Sequencing and Genotyping Services at Massey University, Palmerston North, New Zealand. The service used BigDye Sequencing Ready Reaction mix and cycle sequencing PCR with clean up using the X-Terminator system and capillary separation on the ABI3730 DNA analyser.

3.3. Protein purification

3.3.1 *Expression of Spy0128*

A single colony of *E. coli* BL21 containing a pET32a3c plasmid with the sequence for the Spy0128 gene (generated by Fiona Clow, The University of Auckland was inoculated into a 100 mL overnight culture of LB with the appropriate antibiotic and grown at 37 ˚C overnight at 200 rpm. This culture was used to inoculate a 1 L culture (1:10) of LB containing the appropriate antibiotic the following day and grown at 28 ˚C until an OD_{600} 0.6-0.8 was reached. Cells were induced to express protein with 0.1 mM IPTG and transferred to 37 ˚C and 200 rpm to grow for a further 5 hours. Cells were harvested by centrifugation at 4, 500 g for 30 minutes at room temperature and frozen at -20 ˚C after the supernatant was discarded.

3.3.2 *Purification by immobilised metal ion affinity chromatography (IMAC)*

The frozen pellets were resuspended in 10% w/v of lysis buffer and sonicated at 50 W for one minute using a Q700 sonicator (Qsonica). The cells were insulated with ice during the sonication process. The bacterial lysate was centrifuged at 10, 000 rpm for 30 minutes at 4 ˚C and the supernatant filtered using a 0.22 μm Millex-GP filter.

The nickel charged resin column (Bio-rad) was prepared by equilibrating with 10 column volumes (CVs) of MCAC-0. The filtered supernatant from the bacterial lysate was then passed over the column and subsequently washed with another 10 CVs of MCAC-0 washing buffer. The bound protein was eluted in a step-wise process using MCAC-0 containing a range of imidazole concentrations (50 mM to 500 mM). The protein sample eluted from IMAC was cut with 5 μg/mL 3c protease (in house) and 1.5 mM DTT to remove the thioredoxin tag prior to further purification. Spy0128 was further purified by anion exchange.

3.3.3 *Ion exchange (Anion) (Spy0128)*

Cut protein was dialysed into MonoQ buffer A at 4 ˚C for 48 hours prior to further purifications. Dialysed protein was purified using a fast protein liquid chromatography (FPLC) system with a Mono Q 4.6/100 PE column (GE Healthcare). The column was equilibrated with 5 CV mL MonoQ Buffer A before protein were eluted using a gradient of 0 to 100% MonoQ buffer B over 30 mL at a flow-rate of 2 mL/min. Eluted fractions were run on a SDS PAGE gel and the desired fraction dialysed into PBS at 4 ˚C.

3.3.4 *Denaturing SDS PAGE gel*

Denaturing sodium dodecyl sulfate polyacrylamide electrophoresis (SDS-PAGE) was carried out and gels cast using a Hoefer SE 245 Dual Caster (Amersham Biosciences) system. Gels were prepared by pouring resolving gel solution containing 7.5% -12.5% (w/v) acrylamide mix into the mould. Once set, stacking gel containing 5% (w/v) acrylamide was poured on top of the resolving gel and combs inserted to form wells. The resolving gel and stacking gel are both described in section 2.3.2. Once the gel was cast it was transferred to a Hoefer SE250 eletrophoresis unit (Amersham Biosciences) and submerged in running buffer.

Protein samples and cell wall extracts were mixed with 2x protein loading dye and boiled at 95 ˚C for 5 minutes before 10 μL of sample was loaded into the wells. Samples were electrophoresed alongside a 1 kb ladder (Invitrogen) either pre stained or unstained in running buffer at room temperature with a constant currant of 20mA using an EPS 301 power supply (Amersham Biosciences). Gels were then used for western blots (section 3.4.2) or stained for 1 hour at room temperature with Coomassie Blue solution with agitation. Coomassie blue was then removed and gel rinsed with MiliQ water before being placed in destaining solution for 1 hour at room temperature with agitation. The gel was imaged using a ChemiDoc imaging system.

3.4. Heterologous expression of *S. pyogenes* pilus in *L. lactis*

3.4.1 *Cell wall extract*

A single colony of the desired *L. lactis* clone was inoculated in a 15 mL overnight culture of GM17 with the appropriate antibiotic and grown anaerobically without agitation. Cells were harvested by centrifugation at 4,500 g for 15 minutes at 4 ˚C and supernatant removed. Cells were washed with 1 mL ice cold PBS and the pellets weighed. 0.1% w/v of ice cold protoplast buffer was used to suspend the cells before incubation at 37 ˚C for 3 hours with gentle rotation. Cells were pelted by centrifugation at 15, 000 g for 15 minutes at 4 ˚C and the supernatant collected and stored at -20 ˚C.

3.4.2 *Western Blot*

Cell wall extracts were run on an SDS-PAGE gel alongside a bench mark pre stained ladder and were transferred onto a nitrocellulose membrane using a TE77 semi-dry transfer unit (Hoefer) at 250 V and 50 A for 1 hour. The membrane was incubated for 1 hour at room temperature in blocking solution before being incubated with 1:1000 rabbit anti-Spy0128 or anti-T6 antibody in probing solution. The incubation period was 1 hour at room temperature. The nitrocellulose membrane was washed three times with TBS-T for 5 minutes then incubated with 1:10 000 goat anti-rabbit HRP (BD Biosciences) for one hour at room temperature. The membrane was washed three times with TBS for 5 minutes and then stained for 1 minute with ECL Detection Reagent (Amersham Biosciences). The nitrocellulose membrane was visualised using a ChemiDoc imaging system.

3.4.3 *Flow cytometry*

A single colony of the desired *L. lactis* clone was inoculated in a 1.5 mL overnight culture of GM17 with the appropriate antibiotic and grown anaerobically without agitation at 28 ˚C. Cells were harvested by centrifugation at 5, 000 g for 5 minutes at 4◦C and suspended in ice cold

PBS. Cells were diluted to an OD_{600} of 0.4 in 1 mL and washed with 1 mL of ice cold blocking buffer. They were then sonicated for 2 minutes using a SC-200-22 water bath and incubated on ice for 30 minutes. 200 μL aliquots of cells were then harvested by centrifuging at 5, 000 g for 5 minutes and suspended in 100 μL of FACS buffer containing1:100 anti-Spy0128 or anti-T6 antibody and incubated on ice for 30 minutes. Cells were washed twice with 200 μL of FACS buffer and suspended in 100 μL FACS buffer containing 1:1000 anti-rabbit IgG FITC. This was incubated on ice for 30 minutes and washed twice with 1mL FACS buffer. Cells were suspended in a final volume of 30 μL FACS buffer. The cells were fixed in 50 μL 4% paraformaldehyde (in PBS) and incubated at 37 ˚C for 10 minutes. 200 μL FACS buffer was added before samples were run on a BD LSR II flow cytometer. Data was analysed using FlowJo (FlowJo, LLC).

3.5. Vaccinations

3.5.1 *Vaccination dose/delivery Optimisation of PilVax-OVA antibody response*

5-6 week old female BALB/c mice were ordered from, and housed at the VJU at The University of Auckland. Four different vaccination schedules were to be tested using 5 mice each

Table 3.3: Vaccination schedule used to optimise PilVax-OVA humoral response.

Group	Dose	Volume	Vaccination Days
A	$1x10^8$	5 μL	0,1,2,14,15,16, 28,29,30,42,43,44
B	$1x10^8$	5 μL	2,16,30,44
C	$1x10^8$	50 μL	2,16,30,44
D	$3x10^8$	5 μL	2,16,30,44

All mice were euthanised two weeks following the final boost.

3.5.1.1 ***Vaccine aliquot preparation and enumeration***

Vaccine aliquots were prepared in advance, stored at -80 ˚C and thawed on the day of vaccination. A single colony of *L. lactis* pLZ12KmP23R_PilM1_βE/βF_OVA was used to inoculate an overnight 2 mL anaerobic culture of GM17 media and grown at 28 ˚C without agitation. The culture was diluted 1:50 into fresh, pre warmed GM17 media and grown anaerobically without agitation until and OD_{600} of 0.4-0.6 was reached. The cells were then centrifuged at 4, 000 g for 10 minutes at 4 ˚C and washed with PBS. After washing, cells were suspended to an OD of 10 in PBS + 10% glycerol and were divided into 500 μL aliquots for storage at -80 ˚C. One aliquot was titrated tenfold with 10 μL drops of the 10^{-6} to 10^{-8} dilutions plated onto GM17 Kanamycin 100 μg/mL plates in triplicate. This was incubated at 28 ˚C overnight to determine the CFU per aliquot.

3.5.1.2 ***Collection of pre immune serum***

Prior to vaccination a small serum sample was collected by tail bleeding. Mice were pre warmed with a heat lamp and restrained in a device with tail access. A single incision was made into a tail vein with a sterile scalpel and blood collected in a Microvette 500 Z-Gel tube (Starsted). Tissue paper and pressure was applied to the wound until bleeding had ceased, and serum was separated by centrifugation at 10, 000 g for 5 minutes and stored at -20 ˚C.

3.5.1.3 ***Collection of pre immune faeces***

Faecal pellets deposited from each mouse while restrained during the tail bleed were collected and stored on ice for same day processing. Pellets were weighed and suspended in 1 mL/100 mg faeces collection buffer, 1 mM PMSF in PBS. Pellets were squashed with pipette tips, and vortexed until homogenised then centrifuged at 10, 000 g for 5 minutes and the supernatant stored at -20 ˚C.

3.5.1.4 ***Vaccination delivery***

Immediately prior to vaccination, aliquots were thawed by adding 1 mL room temperature PBS and centrifuged at 10, 000 g for 5 minutes. The supernatant was discarded. Based off of the CFU per aliquot obtained from section 3.5.1.1, cells were suspended to the following concentrations for each of the groups:

Table 3.4: Concentration of each vaccination group to achieve desired dose.

Group	CFU/mL
A	$2x10^{10}$
B	$2x10^{10}$
C	$2x10^{9}$
D	$6x10^{10}$

Each vaccination group was transferred to a chamber and anaesthetised using isoflurane. Prior to immunisation each mouse was weighed, restrained and the appropriate volume of vaccine delivered to the left nostril and returned to their cage. Subsequent vaccinations were delivered to alternating nostrils. However for Group C where 50 μL was to be delivered, this was spilt into 25 μL in each nostril for all vaccinations. Mice weight and behaviour were continuously monitored throughout the experiment.

3.5.1.5 ***Euthanasia***

Mice were individually euthanised by asphyxiation with CO_2 after being transferred to a container with a lid in place. The chamber was filled with the gas and continued until breathing ceased. Death was confirmed by toe pinch.

3.5.2 ***Collection of samples post vaccination***

3.5.2.1 ***Serum***

Serum was collected via a cardiac puncture. Immediately following confirmation of death, mice were positioned ventrally. A 25 gauge needle on a 1 mL syringe was inserted at an oblique

angle below the mouse's left arm. Approximately 500mL blood was aspirated from the heart. Serum was collected in a Microvette 500 Z-Gel tube (Starsted) separated by centrifugation at 10,000 g for 5 minutes and stored at -20 ˚C.

3.5.2.2 ***Bronchiolar lavage (BAL)***

BAL fluids were collected by exposing the trachea following the cardiac puncture. A small opening was made in the cartilage and an 18 gauge needle attached to a 1 mL syringe (with 1 mL of PBS) was inserted. PBS was injected into the lungs and aspirated, with a typical recovery of at least 500 mL which was stored at -20 ˚C.

3.5.2.3 ***Oral wash***

Saliva was collected by moving the tongue of the mouse to one side and injecting 50 μL of PBS into the oral cavity and aspirating 3x. Typical recovery of PBS is greater than 30 μL and this was stored at -20 ˚C.

3.5.2.4 ***Faeces***

Faecal pellets were collected as in section 3.5.1.3.

3.5.3 ***Vaccination-Antibody response***

7 week old male C57BL/6 mice were ordered from, and housed at the VJU at the University of Auckland for vaccination as per the schedule of Group A described in section 3.5.1, with 5 mice per group.

Vaccine aliquots were prepared for each of the following PilVax constructs:

L. lactis pLZ12km2-PilM1_βE/βF_ESAT-6-P1 peptide (Residues 1-20)

L. lactis pLZ12km2-PilM1_ β9/β10 _ESAT-6-P2 peptide (Residues 51-70)

L. lactis pLZ12km2-PilM1_ βE/βF _ESAT-6-P8 peptide (Residues 72-95)

L. lactis pLZ12km2-PilM1_ βE/βF _Ag85B peptide (Residues 281-295

L. lactis pLZ12km2-PilM1_ βE/βF_OVA (Residues 323-339)

L. lactis pLZ12km2-PilM1 (no insert in PilM1 operon)

Vaccination and sample collection was carried out as described in section 3.5.3.

3.5.3.1 ***Nasal wash***

In addition to the samples collected in the previous section, mice in this study also had their nasal passage washed with PBS and collected. Following bronchiolar lavage, the mouse was held ventrally and 1 mL PBS injected anteriorly into the opening used for the lavage, and collected as it came out of the nose.

3.6. Vaccination-Peptide specific T cell response

7 week old male C57BL/6 were ordered from, and housed at the HTRU at the University of Otago.

The vaccination groups for experiment 1 are underlined while the following list contains all the vaccination groups for experiment 2:

L. lactis pLZ12Km2-PilM1_βE/βF_ESAT-6-P1 peptide (Residues 1-20)

L. lactis pLZ12Km2-PilM1_ β9/β10 _ESAT-6-P2 peptide (Residues 51-70)

L. lactis pLZ12Km2-PilM1_ βE/βF _ESAT-6-P8 peptide (Residues 72-95)

L. lactis pLZ12Km2-PilM1_ βE/βF _Ag85B peptide (Residues 281-295)

L. lactis pLZ12Km2-PilM1 (no insert in PilM1 operon)

L. lactis pLZ12Km2-PilM6 (no insert in PilM6 operon)

L. lactis pLZ12Km2-PilM6_ΔV8_ESAT-6 (full protein)

BCG

There were 7 mice per group in experiment 1, and 6 mice per group in experiment 2.

3.6.1 ***Vaccination protocol***

Vaccination aliquots for *L.lactis* strains were prepared and enumerated as described in section 3.5.1.1. The dose of *L. lactis* administered was $2x10^7$ CFU in 40 μL. (Protocol optimised by Kirman Lab at the University of Otago, Dunedin, New Zealand). Immediately prior to vaccination, aliquots were thawed as previously described in section 3.5.1.4 and suspended to a concentration of $5x10^8$ CFU/mL.

BCG vaccination aliquots were used from pre prepared aliquots in the Kirman lab at the University of Otago and inoculated at 10^6 CFU.

Mice were weighed and anesthetised with 87 mg/kg ketamine and 2.6 mg/kg xylazine in a 1:1 mixture injected subcutaneously with a 25 gauge needle. Once deep anaesthetic was confirmed mice were placed ventrally and 40 μL of the vaccine aliquot was slowly dispensed over the nose as it was inhaled by the mouse. Mice were closely monitored until full recovery had occurred, and strictly weight monitored for 3 days following immunisation or until recovery to baseline weight had been achieved.

Mice were vaccinated according to the following schedule, and euthanised 10 to 14 days following final boost. BCG vaccinated mice were vaccinated subcutaneously on day 0 only.

Table 3.5: Vaccination schedule of experiments analysing the cellular response.

Experiment	*L. lactis* CFU/mL	Vaccination days
Experiment 1	$5x10^8$	0,14,28
Experiment 2	$5x10^8$	0,14,36

3.6.2 ***Euthanasia***

Mice were euthanised by anaesthetic overdose with 15 mg/mL pentobarbitone injected intraperitoneal at 10 μL per gram of body weight. Death was confirmed by toe pinch.

3.6.3 ***Collection of samples***

Following confirmation of death the mouse was dissected open to expose the thoracic and abdominal cavity in a sterile manner within a class 2 biosafety cabinet.

3.6.3.1 ***Serum***

Serum was collected by aspiration from the inferior vena cava with a 25 gauge needle attached to a 1 mL syringe and transferred to a Microvette 500 Z-Gel tube (Starsted). Samples were stored on ice for same day processing (3.5.1.2).

3.6.3.2 ***Draining lymph node***

The mediastinal lymph node was located and once dissected out placed in in complete IMDM on ice for same day processing. Draining lymph nodes were pooled from each vaccination group.

3.6.3.3 ***Lungs***

Once the draining lymph node was removed, lungs were flushed remove circulating cells. This was done using 1 mL PBS in a 25 gauge needle and 1 mL syringe and injecting it into the right atrium of the heart. Lungs were dissected out using sterile scissors and placed into 3mL complete IMDM and stored on ice for same day processing.

3.6.4 ***Tissue processing***

Lungs were cut into small pieces with sterile scissors and placed into digestion media at 37 ˚C (5% CO_2). Digested lungs and lymph nodes (undigested) were transferred to a 70 μm cell strainer (Miltenye Biotech) that was positioned over a 50 mL falcon tube. The end of a syringe plunger was used to push the samples through the strainer, washing with 5 mL of complete

IMDM three times during the process. Cells were then centrifuged at 400 g for 8 minutes at 4 ˚C, the supernatant discarded, and suspended in 5 mL complete IMDM. 100 μL was taken for cell counting from each sample. 3 mL was taken for tetramer enrichment and staining, while 2 mL was taken for cytokine staining following stimulation with the cognate peptide.

3.7. Analysis of vaccinations-Antibodies

3.7.1 *Enzyme linked immunosorbent assays (ELISAs)*

Antibody titres of IgG and IgA present in serum, BAL, oral washes, nasal washes and faeces were determined by ELISA. Microloon 96-well ELISA plates (Grenier Bio-One) were coated with 100 μL of 1 μg/mL protein (Spy0128, Ovalbumin, Tee6) in PBS per well overnight at 4 ˚ C. For peptide ELISAs (ESAT-6_P1, ESAT-6_P2, ESAT-6_P8, Ag85B peptide) plates were incubated with 100 μL of 1 μg/mL peptide in Carbonate-Bicarbonate buffer (pH 9.4) at 37 ˚C for three house immediately prior to use. The plate was then washed three times with PBS-T before being blocked with 300 μL of 3% BSA and incubated for 15 minutes at room temperature. Following blocking, plates were washed three times with PBS-T and titrated samples added to the plate. Samples had been titrated in a separate 96 well microtitre plates as follows:

Sample	Starting dilution	Dilution
Serum	1:200	4x
BAL	1:50	4x
Oral Wash	1:50	4x
Nasal Wash	1:50	4x
Faeces	1:5	4x

Pre immune serum was diluted 1:100 and pre immune faeces were diluted 1:5

Samples were incubated on the plates in duplicate for 3 hours at room temperature and washed five times with PBS-T. 100 μL of either, goat anti-mouse anti-IgG HRP at 1:20 000, or goat anti-mouse anti-IgA HRP at 1: 2000 was added to each sample for a further 1 hour at room temperature. Plates were washed five times with PBS-T and 100 μL of room temperature TMB (life technologies) was added to each well. Plates were incubated for 5-10 minutes and the reaction stopped by adding 100 μL 1 M HCl to each well. Absorbance was read at 450 nm using an EnSpire 2300 plate reader (Perkin Elmer). End point titre was determined as the point where the mean absorbance was no more than three standard deviations above the mean absorbance of the pre immune serum or control wells.

3.8. Analysis of vaccinations-Peptide specific T cells

Serum collected from mice vaccinated at the University of Otago was also tested for humoral response by ELISA as described above.

3.8.1 ***Lymphocyte identification***

3.8.1.1 ***Tetramer staining***

Only groups for which there was a corresponding tetramer to the peptides contained in the PilVax constructs (or BCG) underwent the following process. Cells from section 3.6.4 were stained with the appropriate tetramer at dilutions indicated in table 2.6. 300 μL of tetramer of in FACS buffer was added to the cells in a 15 mL falcon tube and incubated at 37 ◦C for 30 minutes. A pooled sample from each group was also stained with the hCLIP tetramer as above in the dilution indicated in table 3.6.

3.8.1.2 ***Tetramer enrichment***

Cells were washed with 1 mL FACS buffer and centrifuged at 400 g for 8 minutes at 4 ◦C, after which the supernatant was discarded. Cells were suspended in 90 μL of bead enrichment buffer and incubated for 15 minutes at 4 ◦C in the dark following through mixing. Cells were washed

with 1 mL MACS buffer and centrifuged at 300 g for 10 minutes at 4 ˚C and the supernatant discarded. Cells were then suspended in 500 µL MACS buffer. Separation was carried out in an AutoMACS separator (Miltenyi biotech) using the 'POSSEL' separation setting and the positive fraction retained. The enriched cell populations were then transferred to 5 mL FACS tubes for cell surface staining. A small sample was taken for cell counting to determine number of cells following enrichment. Negative controls included PilVax-PilM1 vaccinated mice with no endogenous peptide, and staining a pooled sample from vaccination groups with endogenous peptide with the unrelated hCLIP tetramer to ascertain nonspecific tetramer binding.

3.8.1.3 ***Cell surface marker staining***

All staining was carried out in accordance with the dilutions indicated in the panel described in table 2.6.

Prior to cell surface staining tetramer enriched cells were incubated with Fc blocker and live dead stain for 30 minutes at 4 ˚C in 100 µL. Following which they were washed with 1 mL FACS buffer and centrifuged at 350 g for 5 minutes at 4 ˚C and the supernatant discarded. Cells were then stained with 100 µL of master mix of the remaining antibodies in the panel described in table 6 for 20 minutes on ice. They were then washed with 1 mL FACS buffer, centrifuged at 350 g for five minutes at 4 ˚C and the supernatant discarded. Cells were fixed by adding 100 µL of formalin and incubating at room temperature for 10 minutes before pelleting cells by centrifugation at for 6 minutes at 320 g at 4 ˚C. 200 µL was added to each sample prior to flow cytometry.

3.8.1.4 ***Flow cytometry***

Flow cytometry was carried out at the University of Otago Flow Cytometry facility, Dunedin, New Zealand using a BD LSRFortessa, (BD Biosciences) and analysed using Flow Jo (FlowJo, LLC). Gating was determined using FMOs.

3.8.2 *Cytokine production*

All staining in this section is carried out in accordance with the dilutions indicated in the panel described in in table 3.8.

3.8.2.1 ***Peptide stimulation***

24 well plates were seeded with 10^6 cells per well for each lung sample in 1 mL incomplete IMDM media. For draining lymph nodes this number of cells was obtained by pooling the draining lymph nodes from each vaccination group. 20 μg /mL cognate peptide in DMSO was added to the samples (Ag85B peptide to the BCG vaccine group). Samples were incubated at 37 ˚C, 5% CO_2 for 12 hours after which 10 μg/mL Brefeldin A was added to stop export of cytokines. Samples were incubated for a further 6 hours at 37 ˚C, 5% CO_2.

3.8.2.2 ***Cell Surface staining***

Prior to cell surface staining stimulated lymphocytes were harvested from the 24 well plate by vigorous pipetting and transferred to FACS tubes. Cells were pelleted by centrifugation at 350 g for 5 minutes at 4 ˚C. Cells were incubated with Fc blocker and live dead stain in a volume of 100 μL for 30 minutes at 4 ˚C. Cells were washed with 1 mL FACS buffer, centrifuged at 350 g for 5 minutes at 4 ˚C and the supernatant discarded. Cells were then stained with 100 μL of a master mix of antibodies for CD3, CD4, and CD8 at dilutions indicated in table 3.8 for 20 minutes on ice. Following this cells were washed with 1 mL FACS buffer and then fixed by adding 100 μL of formalin and incubating at room temperature for 10 minutes. Fixed cells were pelleted by centrifugation as above.

3.8.2.3 ***Intracellular staining***

Cells from the previous section had 500 μL of perm buffer added and were incubated on ice for 1 hour with agitation before the cells were pelleted by centrifugation for 5 minutes at 350 g at 4 ˚C. The supernatant discarded. Cells were stained with 100 μL of a master mix of antibodies for IL-2, IL-17, TNFα, and INF-γ was described table 8 for 1 hour on ice with

agitation. Cells were washed three times with 1mL Perm buffer and once with 1mL FACS buffer before being suspended in 200 μL FACS buffer and ready for flow cytometry as described in (3.8.1.4).

3.8.3 ***Statistical analysis***

Statistical analysis was carried out using Prism (GraphPad). Data was tested for normal distribution and variance prior to comparative analyses. Where these assumptions were met, t tests were carried out for comparison of two data sets, while one-way ANOVA using Tukey analysis was carried out for comparison of three or more data sets. If normality and variance assumptions were not met, and transforming the data to its logarithmic values did not correct for this, non-parametric tests were carried out. Mann Whitney tests were used to compare two data sets while the Kruskall Wallace test was used to compare three or more data sets.

3.8.4 ***Power calculations***

For studies conducted at the University of Auckland, mouse number per study was based off pervious work from the laboratory without consideration to power.

For studies conducted at the University of Otago, for immunogenicity studies a sample size of n=6/group would allow us to detect a difference in means of approximately 0.35 x 10^6 for the counts of live CD4 T-cells making cytokines between two groups. For the % of live CD4 T-cells making cytokines, a difference in means of 5.2% would be similarly detectable.

3.8.5 ***Antibody titrations***

Optimal monoclonal antibody staining concentrations were determined by single-staining lung cells from C57BL/6 mice.

Serial dilutions were carried out 1:2 with each antibody and concentrations ranging from 1:100-1:1600 for surface markers, and 1:25 to 1:200 for anti-cytokine monoclonal antibodies.

Surface staining was performed as described in section 3.8.1.3 for each dilution. For cytokine staining, lung cells were stimulated at $2x10^6$ cells/mL in a 24-well plate with complete IMDM containing 10 ng/mL phorbol-12-myristate-13-acetate (PMA; Sigma Aldrich) and 600 ng/mL ionomycin calcium salt (Sigma Aldrich) for 2 hours to stimulate cytokine production. Following stimulation, 10 ug/mL brefeldin A was added to each well and cells were incubated for a further 4 hours following which cells were washed, fixed and stained as in section 3.8.2.3 for each dilution. Unstained and viability-only controls were included for stimulated or unstimulated cells as appropriate.

Antibody concentrations were selected by gating on live lymphocytes, and comparing the population resolution (stain index) for each antibody between serial dilutions. Stain indices were calculated by division of the distance between negative and positive populations by the variance of the negative stained cell population, i.e. (MFI (pos) - MFI (neg)) / rSD (neg). Concentrations giving the highest stain index with minimal background staining were selected. Each lot of antibody was titrated independently.

Chapter 4. Cloning and expression

Initial work required the cloning of DNA sequences encoding the peptides of interest into PilVax, and transformation of these constructs into *L. lactis*. Heterologous expression of the pilus containing the peptides of interest was examined by Western blot and flow cytometry.

Analysis of the humoral response required the expression and purification of recombinant Spy0128 for detection of PilVax specific antibodies by ELISA.

4.1. PilVax cloning and expression

Tailoring PilVax for use as a vaccine against *Mtb* required the selection of peptides from the two proteins of interest, ESAT-6 and Ag85B. Three peptides were selected from the ESAT-6 protein and one from the Ag85B protein based off epitope mapping of these proteins in the literature (figure 4.1).

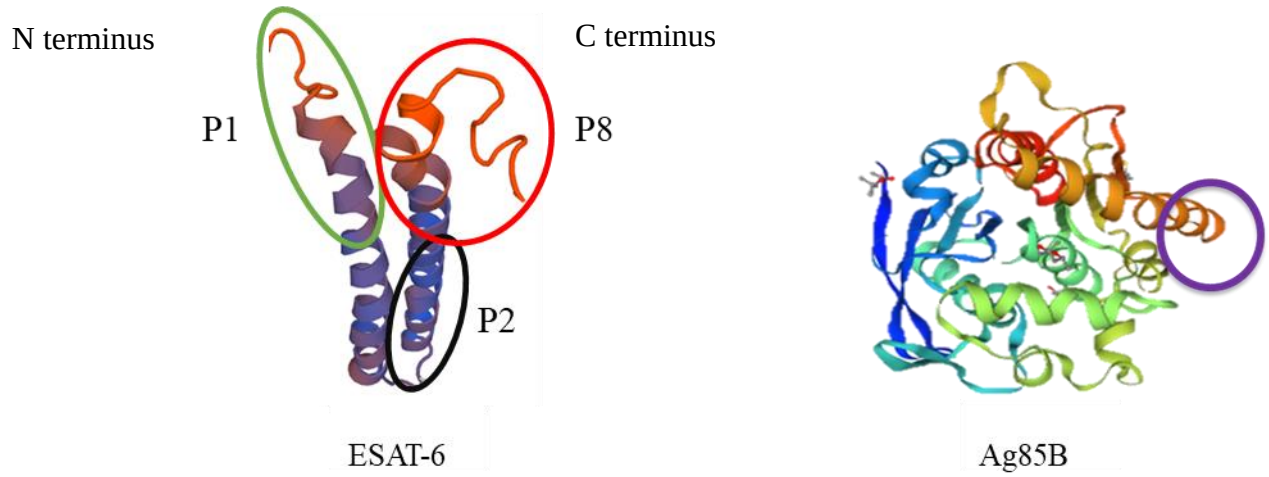

Figure 4.1: Peptides selected from ESAT-6 and Ag85B.

Peptides selected from the ESAT-6 and Ag85B proteins of *Mtb* for use in PilVax. Highlighted sections indicate the chosen peptide sequences in the protein structure (depicted using the SWISS model).

The DNA sequences encoding these peptides were to be cloned into the *S. pyogenes* serotype M1 Spy0128 gene at the regions encoding the βE-βF or β9-β10 loop regions (figure 4.2). Cloning of the full length ESAT-6 protein to replace the V8 loop region in the pilus of *S. pyogenes* serotype M6 was carried out by Dr Catherine Tsai at The University of Auckland (data not shown).

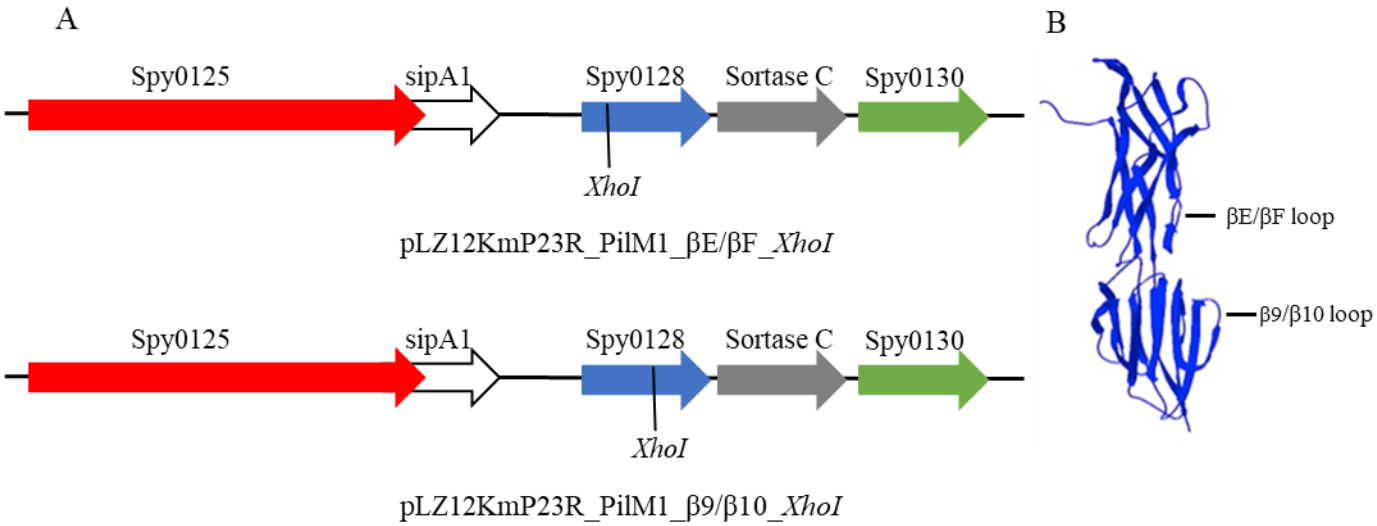

Figure 4.2: Schematic of PilVax cloning vectors and location of cloning sites in Spy0128 protein model.

A) Peptides selected from the ESAT-6 and Ag85B proteins of *Mtb* were cloned into to the *XhoI* site of either PilVax vector. B) Protein structure of Spy0128 (depicted using the SWISS model) indicating the loop regions where peptides were cloned into.

At the time of cloning these were the only loop regions known where insertion of a peptide did not terminate pilus assembly.

4.1.1 *Overlap PCR*

Selected peptides were amplified by overlap PCR as in section 2.2.1.1 (figure 4.3).

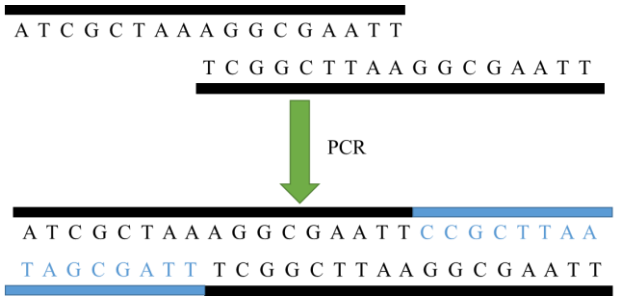

Figure 4.3: Schematic of overlap PCR for generation of DNA sequences of peptides for cloning into PilVax.

To generate peptide DNA sequences for PilVax, primers for each sequence were designed to overlap and thus anneal during PCR. The remaining peptide sequence was generated by Taq polymerase during the extension phase.

Peptide DNA sequences were too small to be visualised on high percentage agarose gels and were used under the assumption the PCR had been successful.

4.1.2 *Cloning into DNA sequence of Spy0128 βE-βF or β9-β10 loop regions*

Following amplification of the peptide DNA sequences by overlap PCR, DNA was digested and purified as described in section 2.2.4. The peptide DNA sequences were then purified and digested with *XhoI* and ligated with the pLZ12KmP23R_PilM1_βE/βF_*XhoI* or pLZ12KmP23R_PilM1_β9/β10_*XhoI* vectors. The DNA was transformed into *E. coli* (DH5α) by heat shock. Colonies were screened by single colony PCR using a combination of Spy0128 and peptide primers. For peptide DNA sequences in the βE-βF loop region Spy0128.fw and peptide.rv primers resulted in amplification of a 370 Kb DNA fragment, while Spy0128.rv and peptide.fw amplified a fragment of 850 Kb. Peptide DNA sequences in the β9-β10 loop region resulted in amplification of an 850 Kb DNA fragment with the Spy0128.fw and peptide.rv primer pair (figure 4.4).

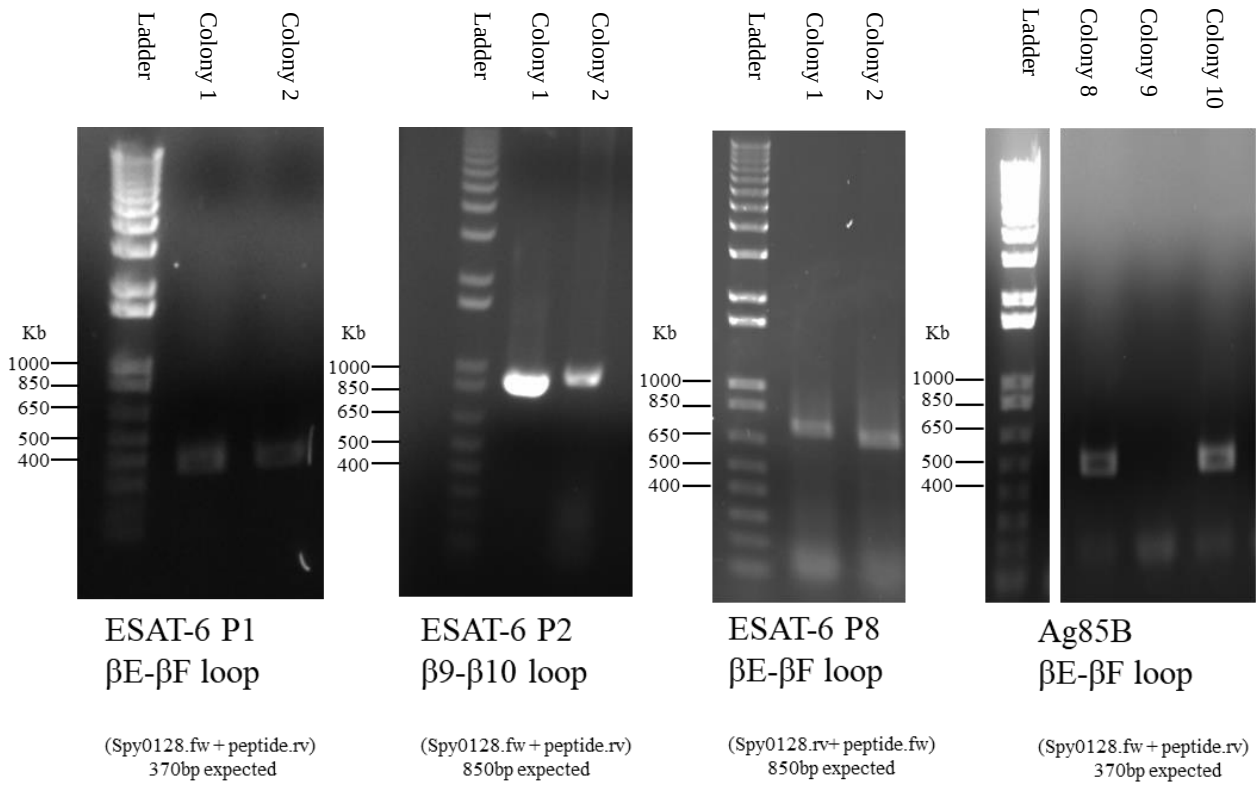

Figure 4.4: Single colony PCR screening for peptide DNA sequences in the pLZ12KmP23R_PilM1_βE/βF or pLZ12KmP23R_PilM1_β9/β10 plasmids in *E.coli* (DH5α).

The DNA sequence of each peptide was amplified by overlap PCR. The DNA was then cloned into the PilVax vectors and transformed into *E. coli* (DH5α). Colonies were screened by PCR with the primer pair indicated and electrophoresed on a 1% agarose gel. DNA was visualized using SYBER safe. Colonies with DNA fragments at the expected size for the primer pair used were selected for sequencing and downstream use.

Plasmid DNA from PCR positive colonies was purified and the sequence confirmed by sequencing using the ABI Sequencing and Genotyping Services at Massey University, Palmerston North, New Zealand. The first loop region the each peptide was successfully cloned into was used for further experiments.

4.1.3 *Transformation into L. lactis*

Plasmids identified by single colony PCR and confirmed correct by sequencing were electroporated into the *L. lactis* strain MG1363. Colonies were screened by single colony PCR using the Spy0128.fw and Spy0128.rv primers which amplified a fragment with an expected

size of 1kb (figure 4.5). All of the PilVax constructs were confirmed to be in *L. lactis* by colony PCR.

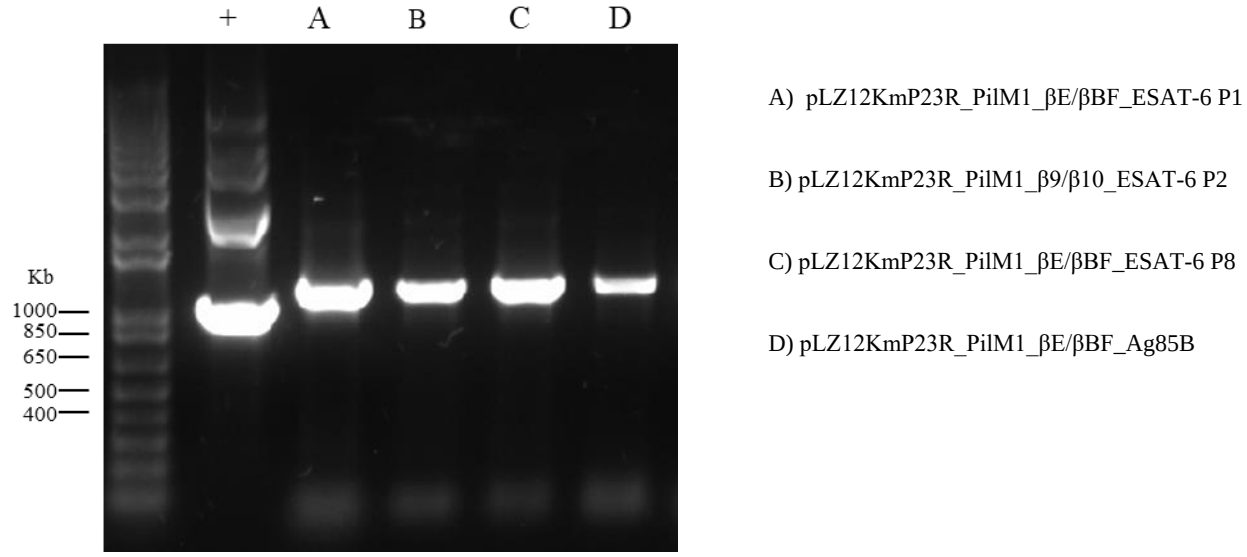

Figure 4.5: Single colony PCR screening for the Spy0128 gene containing an *Mtb* peptide DNA sequence in transformed *L. lactis* MG1363.

Sequence confirmed PilVax constructs were electroporated into *L. lactis* MG1363. Colonies were screened by PCR with the Spy0128.fw and Spy0128.rv primer pair and electrophoresed on a 1% agarose gel with a DNA fragment of 1 Kb expected. A positive control was also amplified using plasmid DNA as a template. DNA fragments were visualised with SYBR safe staining.

4.1.4 *Heterologous expression of pilus in L. lactis*

Once the plasmid containing the correct DNA sequence was confirmed in *L. lactis*, expression testing was carried out to ensure the pilus assembly and polymerisation was not terminated by insertion of the peptide. It was expected that insertion of peptides would lower the pilus expression as it has been demonstrated insertion of the $OVA_{324-339}$ peptide does interfere with pilus formation (Wagachchi et al., 2018). Western blots were used to confirm the expression of and polymerisation of the Spy0128 monomer in *L. lactis*.

Vaccine aliquots were prepared as in section 2.5.1.1 and stored at -80 ºC for all of the constructs confirmed in figure 4.5. Vaccine aliquots were also prepared for the *L. lactis* pLZ12Km2P23R-PilM6 (no insert in PilM6 operon).

L. lactis pLZ12Km2P23R-PilM6_ΔV8_ESAT-6 (full protein) constructs generated by Dr Catherine Tsai (The University of Auckland).

The cell wall extracts were analysed by Western Blot after separation by SDS PAGE on a 4%-12% gradient gel. PilM1 constructs were probed with rabbit anti-Spy0128 while the PilM6 constructs were probed with rabbit anti-T6 (figure 4.6).

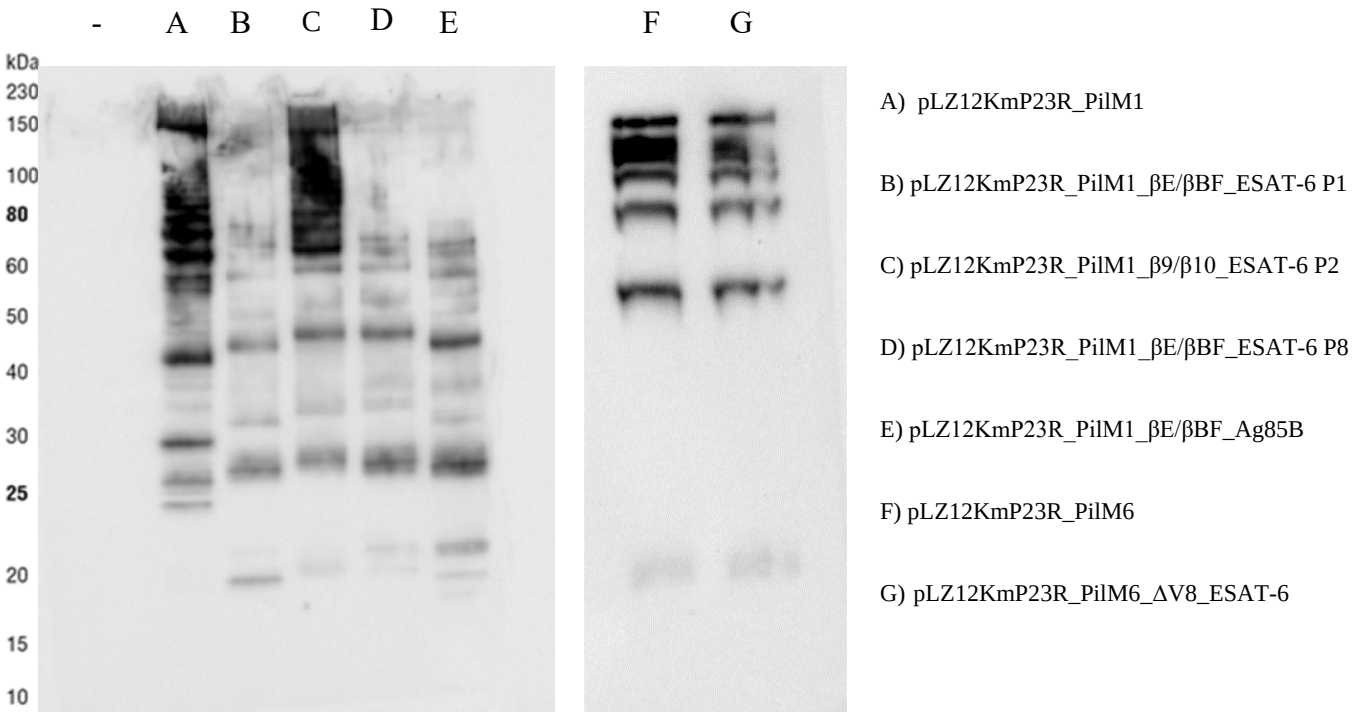

Figure 4.6: Western blot on cell wall extracts of *L. lactis* MG1363 strains containing PilVax constructs.

Cell wall extracts were prepared from frozen PilVax vaccine aliquots. Proteins were separated by SDS PAGE on a 4%-12% gradient gel and transferred to a nitrocellulose membrane. The membrane was probed with the relevant anti-major pilin subunit antibody and a secondary antibody conjugated to HRP. Pilus expression and polymerization was visualised using ECL detection. A cell wall extract from wild type *L. lactis* was used as a negative control.

Pilus polymerisation in *S. pyogenes* resulted in a distinct laddering pattern on Western blot analysis due to the generation of pili of various lengths and has previously been demonstrated in *L. lactis* (Wagachchi et al., 2018). *L. lactis* containing the M1 pilus with no peptide inserted (lane A) resulted in pilus formation with the distinct laddering pattern expected. Comparison

with pili that contain the *Mtb* peptides (lanes B-E) shows insertion of peptide does interfere with the amount of pilus expressed. Importantly however, it does not result in the termination of expression and polymerisation. The same trend was seen with the M6 pilus constructs (lane F-G) where insertion of the ESAT-6 protein did not terminate expression of the pilus despite fewer pili being detected.

Pilus expression was further analysed by flow cytometry. A frozen vaccine aliquot was stained as in section 3.4.3 and the fluorescence analysed using a BD LSR flow cytometer (figure 4.7).

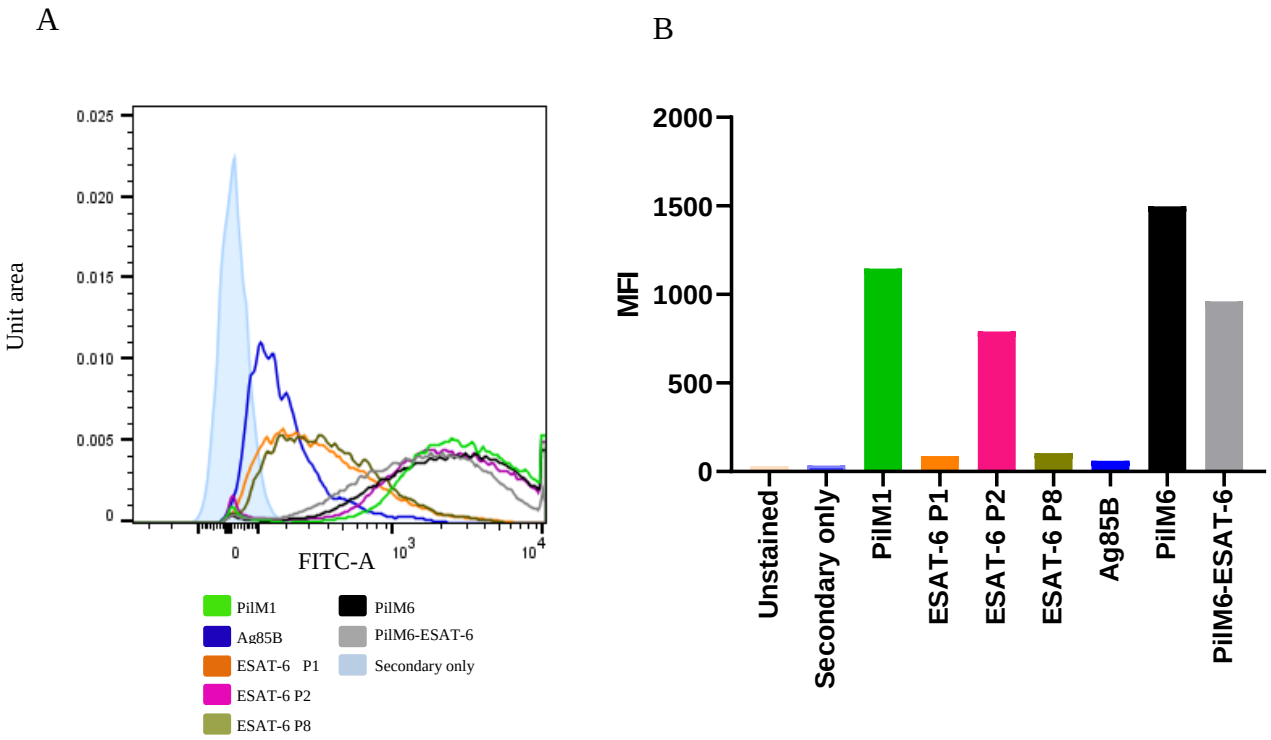

Figure 4.7: Flow cytometry analysis of PilVax vaccine aliquots.

Frozen vaccine aliquots were thawed and stained with anti-major pilin antibody and a secondary antibody conjugated to FITC. Fluorescence was analyzed using a flow cytometer. A) Distribution of fluorescent intensity and B) median fluorescent intensity (MFI) of each construct.

As expected the insertion of a peptide did diminish the level of pilus expression which is demonstrated comparing the median fluorescence intensity (MFI) of all new constructs to the parent construct (PilM1/PilM6).The smallest reduction in MFI is seen in with the insertion of the ESAT-6 P2 peptide, while the ESAT-6 P1, P8 and Ag85B peptides greatly diminished the

MFI. The pattern of expression seen here corresponds with the Western Blot carried out form the same batch of vaccine aliquots where pilus expression is diminished in the PilM1 strains. The insertion of ESAT-6 into the PilM6 construct did not have as drastic of an effect as some of the peptides in the PilM1 strain (figures 4.6 and 4.7).

4.1.5 ***Summary***

The DNA sequence of the peptides of interest from ESAT-6 and Ag85B were cloned primarily into the βE-βF loop region of the Spy0128 gene, with the exception of ESAT-6-P2, cloned into the β9-β10 loop region. Constructs were confirmed in *E. coli* by sequencing and transformed into *L. lactis*. Pilus expression was confirmed by Western blot and flow cytometry.

4.2. Expression and purification of Spy0128

For detection of anti-Spy0128 antibodies in the serum of vaccinated mice, recombinant protein will be used to coat ELISA plates. The pET expression vector containing Spy0128 in *E. coli* (BL21) was used to inoculate a 1 L cultures where protein was expressed and purified as in section 3.3.

The thioredoxin-tagged Spy0128 was isolated from the lysate by passing over a nickel sepharose column, and then eluted using MCAC-200. Fractions were analysed by SDS-PAGE (figure 4.8).

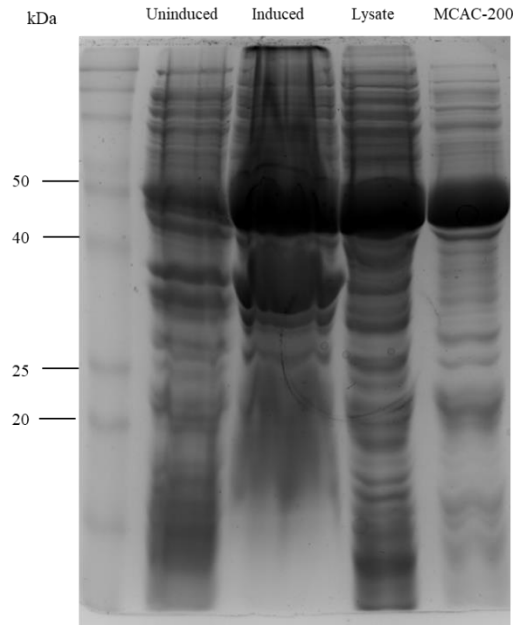

Figure 4.8: Expression and purification of recombinant Spy0128 using Ni^{2+} IMAC.

A 1L culture of *E. coli* (BL21) containing pET32a 3C_Spy0128 was induced to express recombinant Spy0128. The protein produced was soluble and passed over nickel sepharose beads. Recombinant Spy0128 was purified by elution with MCAC-200. The thioredoxin (12 kDa) tagged Spy0128 (35 kDa) are seen at 50 kDa on a 12.5% SDS PAGE gel visualised with coomassie blue stain.

Spy0128 was strongly induced and a remained in the lystate after sonication, thus was soluble.

The purified fraction collected from elution with MCAC-200 had a significant amount of other *E. coli* proteins eluted alongside it. For further purification the fraction was dialysed into anion exchange buffer (20 mM Tris pH 8.0) while being digested with 3C protease to remove the thioredoxin tag. The proteins were eluted in anion exchange purification with an increasing gradient of NaCl. Each peak was collected and run on a 12.5% SDS PAGE gel to identify the correct sized recombinant Spy0128 (35 kDa) (figure 4.9).

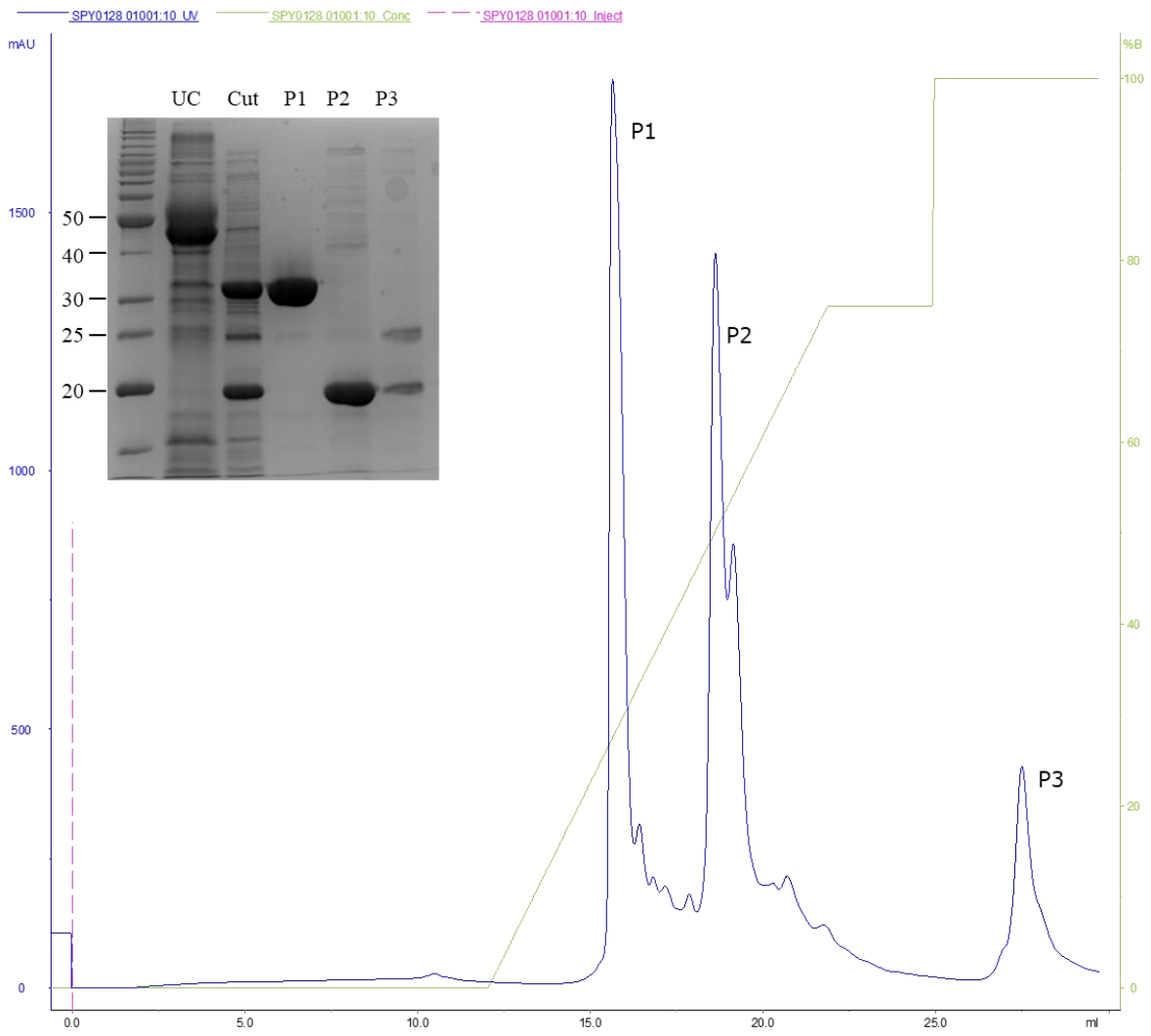

Figure 4.9: Purification of Spy0128 using anion exchange chromatography.

Elution profile of Spy0128 loaded onto a Mono Q 4.6/100 PE column, equilibrated with a buffer containing 20 mM TrisHCl (pH 8.0). Proteins were eluted using a gradient of 0 to 100% 20 mM TrisHCl, 1 M NaCl (pH 8.0). Each peak was collected and a sample run on a 12.5% SDS-PAGE gel and visualised using coomassie blue stain. The UC (uncut) lane contained the elution from the Ni^{2+} IMAC purification, while cut contains a sample of the protein after digestion with 3c protease before it was loaded on to the column. The 35 kDa protein eluted in peak 1 was the recombinant Spy0128.

4.2.1 ***Summary***

The fraction from peak 1 contained a protein band of the correct size for Spy0128. The recombinant protein had a concentration of 22.19 mg per litre. Recombinant Spy0128 was used to coat ELISA plates for the detection of antibodies against the pilus structure in vaccinated

mice. Detection of anti-T6 antibodies used recombinant T6 purified by Dr Jacelyn Loh (The University of Auckland.

4.3. Discussion

4.3.1 *ESAT-6 peptides*

As CD4+ T cells are able to confer protection to *Mtb* in mice, it was critical any selected peptides were T cell epitopes. The peptides selected represented a range of potential immunological responses. Literature searches identified ESAT-6 $_{1-20}$ (P1) and the ESAT-6 $_{51-70}$ (P2) peptides were potent T cell epitopes. (Kanaujia et al., 2004; A. S. Mustafa et al., 2000).

Analysis of serum from non-human primates infected with *Mtb* indicates the presence of antibodies against peptides of the ESAT-6 protein with significant levels of the anti-P2 and anti-ESAT-6$_{72-95}$ (P8) peptides antibodies detected (Kanaujia et al., 2004). This suggests a stratification in the immunogenicity of ESAT-6 peptides as peptides from the N-terminus are more of a T cell epitope while the more distal the peptide is, the more of a B cell epitope the peptide is. ESAT-6 P2, in the middle of the protein represents both a B and T cell epitope.

In order to test and generate a wide spectrum of immune responses from the ESAT-6 protein, these three epitopes were cloned into PilVax. Testing as wide of a range of ESAT-6 peptides is desirable as although the above T cell epitopes are well established in mice, the higher genetic variation in humans has resulted in the identification of various dominant T cell epitopes that differ in humans by geographic location (A. S. Mustafa et al., 2000).

Due to this human genetic diversity, rather than clone only peptides into PilVax, we did attempt to clone the entire ESAT-6 protein in the βE-βF loop region, however the construct did not express pilus (data not shown). This suggests there is an upper limit in terms of the size of what can be cloned into PilVax.

The pilus from the M6 serotype is different from the M1 with larger variable loop regions (figure 1.5). The V8 loop region was replaced by the DNA sequence for the entire ESAT-6 protein by Dr Catherine Tsai which did result in successful pilus expression. This allowed for the analysis of multiple ESAT-6 epitopes from one construct. However it was not cloned in time to be included in the main humoral vaccination study, but was included in the cellular response study.

4.3.2 ***Ag85B peptide***

Epitope mapping of the Ag85 complex of proteins identified the dominant epitope of both the Ag85A and Ag85B proteins to be from residues 241-260 (D'Souza et al., 2003). CD4+ T cells specific for the Ag85B $_{241-255}$ peptide were detected in vaccinated mice where there was protection against *Mtb* challenge in a mouse model suggesting a key role for this epitope (Bennekov et al., 2006). As it is a demonstrated T cell epitope the peptide was chosen for cloning into PilVax. It should be noted that the Ag85B protein sequence contains a 40 amino acid leading sequence that is cleaved from the protein once outside the cell. Although referring to the same amino acid sequence, Ag85B $_{241-255}$ refers to the sequence in the extracellular form of the protein, while Ag85B $_{281-295}$ refers to that same amino acid sequence in the cytosolic form of the protein. In this thesis the epitope inserted into Pilax was referred to as Ag85B $_{281-295}$.

Previous clinical trials of vaccines mentioned earlier have focused on the T cell specificity of the immune response analyzed. In many of these vaccines, Ag85B protein, and Ag85B$_{281-295}$ peptide specific CD4+ T cells have been detected through cytokine stimulation assays of purified lung and spleen cells (Luabeya et al., 2015; Vogelzang et al., 2014). Following VPM1002 vaccination up to 1000 CD4+ Ag85B$_{281-295}$ tetramer specific cells were detected when challenged with *Mtb* and implicated in protection. (Vogelzang et al., 2014).

Despite this epitope being able to confer protection to *Mtb* through memory T cells, the generation of antibodies against the Ag885B protein has not been extensively characterized in either the VPM1002 or H56 vaccine which both contain Ag85B. Passive immunization of mice with 'mycobacteria antigen specific antibodies' from VPM1002 vaccinated mice did not result in any noticeable effect in *Mtb* disease progression (Vogelzang et al., 2014). This suggests the antibodies that are generated, if they do play a role, is not in isolation but synergistic with other immune responses. As such the B cell epitopes of Ag85B are currently unknown, as is the role of Ag85B specific antibodies in *Mtb* protection.

Anti-Lipoarabinomannan IgA antibodies have been shown to block *Mtb* adhesion against colonization and enhance intracellular killing demonstrating a potential role for anti-cell wall component antibodies *Mtb* control (T. Chen et al., 2016). If the dominant B cell epitope is different to the T cell epitope, including both peptides into a Pilvax construct would maximize the potential to generate a comprehensive antibody and peptide specific cellular response to *Mtb*.

4.3.3 ***Cloning and expression***

The cloning of peptides into the PilVax constructs, although successful (figure 4.4), encountered a number of difficulties. Due to the manner in which PilVax was initially designed and cloned, only one restriction site was available for cloning peptides into the variable loop regions.

As cloning was carried out by a single digest with *XhoI* restriction sites, (or *SalI* which has complementary sticky ends) the peptide could insert in either the forward or reverse orientation. The reverse orientation of the peptide DNA sequence would have resulted the incorrect amino acid sequence. As transformation efficiency was quite low, possibly due to the 5 kb vs 50 bp size of the vector: insert, a significant number of clones were inserted in the wrong orientation.

This was one of the major hurdles in generating PilVax constructs, resulting in peptides only being inserted into a single loop region for these studies. Improvements in the cloning strategy have since been made by separating the Spy0128 gene from the pilus operon. Peptide DNA sequences can now be cloned into the 1 kb Spy0128 gene first, prior to inserting the gene back into the pilus operon within the pLZKm12P23R_PilM1 vector. This strategy has greatly improved transformation efficiency, allowing for higher throughput of peptide insertion.

Higher throughput generation of constructs would have also allowed for screening of a peptide in multiple loop regions to assess expression, as well the potential integration of multiple peptides at one or multiple sites to create a multivalent PilVax construct for analysis. The expression of the pilus in this scenario could however be further reduced in comparison to the PilVax constructs already generated. Inclusion of a known T cell, and B cell epitope in the PilVax construct could generate a holistic immune response and thus be highly beneficial in *Mtb* clearance.

The assembly of pilus was affected when a peptide was inserted (figure 4.6, 4.7). It was assumed that because the peptide DNA sequence is so small there would not be such large scale affects seen. However the sequence of the peptide is not in isolation as it inserted into a complex structure. Within the pilus the peptide will interact with the surrounding pilus the structure which, if significantly different in charge and hydrophobicity than the loop region it is replacing, could cause slight conformation changes to the structure. Any change may interfere with the efficiency with which sortase C is able to polymerise the pilus subunits potentially explaining the reduction in pilus assembly seen.

Computer modelling could be used to further analyse the affect specific peptide sequences have on the structure of the Spy0128 protein. Current cloning work has largely been on trial and error basis in regards to cloning proposed peptides into the Spy0128 monomer that do not

terminate pilus expression. This could be improved on by establishing a model using existing data where *Mtb* and non *Mtb* peptides have resulted in various levels of expression of the pilus (unpublished data). Structural analysis using such a model could elucidate what biochemical properties of a given peptide interact with the existing Spy0128 monomer and the pilus structure in such a way that results in the greatest level of pilus expression. This information could provide a guided peptide design for new PilVax vaccine candidate peptides and result in higher throughput cloning process.

Flow cytometry analysis of the PilVax constructs showed that pilus expression was overall lowest in the P1, P8 and Ag85B PilVax constructs, in comparison to other constructs (figure 4.7). The lack of Spy0128 monomers for primary antibody binding could explain this however flow cytometry cannot distinguish if this is due to shorter pilus being generated, or fewer pili across the cell. Western blot analysis showed a lack of high molecular weight bands in the P1, P8 and Ag85B constructs (figure 4.6) which indicates the pilus formed are of shorter length but could be confirmed by electron microscopy to visualise the pilus formation. The broad fluorescence distribution of the PilM1, P2, PilM6 and PilM6 ESAT-6 indicates a wide range of pilus length which correlates with the clear laddering pattern seen in the Western blot of the cell wall extract from these constructs (figure 4.6, 4.7).

The assumption was made that because the peptide/protein is encoded within the backbone monomer, the peptide will be expressed in a 1:1 ratio with the Spy0128/Tee6. Confirmation of peptide expression within the pilus structure could have been measured using specific anti-peptide or anti-ESAT-6, had these antibodies been available.

Cloning of the full ESAT-6 protein into the PilM6 pilus did not affect the pilus formation to the same degree as some peptides in the PilM1 pilus. There is comparable levels of pilus expression despite the insertion of a 95 amino acid protein which has the large capacity to

interfere with the pilus structure and polymerisation. The shape of ESAT-6, a hair pin loop of α helices with variable regions at the N and C terminus potentially allow the majority of the protein to naturally protrude away from the pilus. This closely replicates the V8 loop region which ESAT-6 replaced, which itself is protrudes away from the rest of the Tee6 protein.

4.3.4 ***Conclusion***

Peptides were selected from the ESAT-6 and Ag85B proteins based on their immunogenicity and cloned into the PilVax construct for testing as vaccine candidates. The result of this work has resulted in the streamlining of the cloning process to allow for a higher through put generation of peptide DNA sequences into PilVax. This would allow testing of the peptide DNA sequence in multiple loop regions to obtain the highest level of pilus expression possible in future constructs.

The insertion of peptide DNA sequences did affect the level of pilus expression however there is still pilus detectable by Western blot and flow cytometry analysis.

Chapter 5. Antibody response to PilVax

The aim of this chapter was to optimise the vaccine schedule to maximise the humoral response to PilVax using the previously characterised PilVax-OVA construct (Wagachchi et al., 2018). Previous work carried out with this construct initially used a vaccination dose of 1 x 10^8 CFU in 50µL. However, it was noted that delivery of this volume was technically more challenging and resulted in greater variance between mice (personal communication). Delivery to the nasal tissue (i.e. inoculum not entering the lungs) was also thought to be more amenable from a safety perspective. This chapter evaluated four different vaccination schedules using the model PilVax-OVA construct. The schedule that provided the best humoral response was then selected for testing the PilVax-*Mtb* constructs.

5.1. Vaccination optimisation

Four vaccination schedules were tested with PilVax-OVA. These four schedules were designed to determine the effect of inoculum dose and volume on specific humoral responses to the vaccine. The vaccine schedules were:

A) $1x10^8$ CFU in 5 µL, 3x per dose

B) $1x10^8$ CFU in 5 µL, 1x per dose

C) $1x10^8$ CFU in 50 µL, 1x per dose

D) $3x10^8$ CFU in 5 µL, 1x per dose.

Female BALB/c mice were vaccinated with PilVax-OVA, receiving four doses in total at the Vernon Janson Unit at the University of Auckland as in section 3.5.1

Serum, bronchial alveolar lavage, saliva, and faecal samples were collected for analysis.

5.1.1 *Serum antibodies*

Serum was collected from mice prior to every vaccination and titrated 1:100 to analyse the temporal serum IgG and IgA response to Spy0128 (figure 5.1).

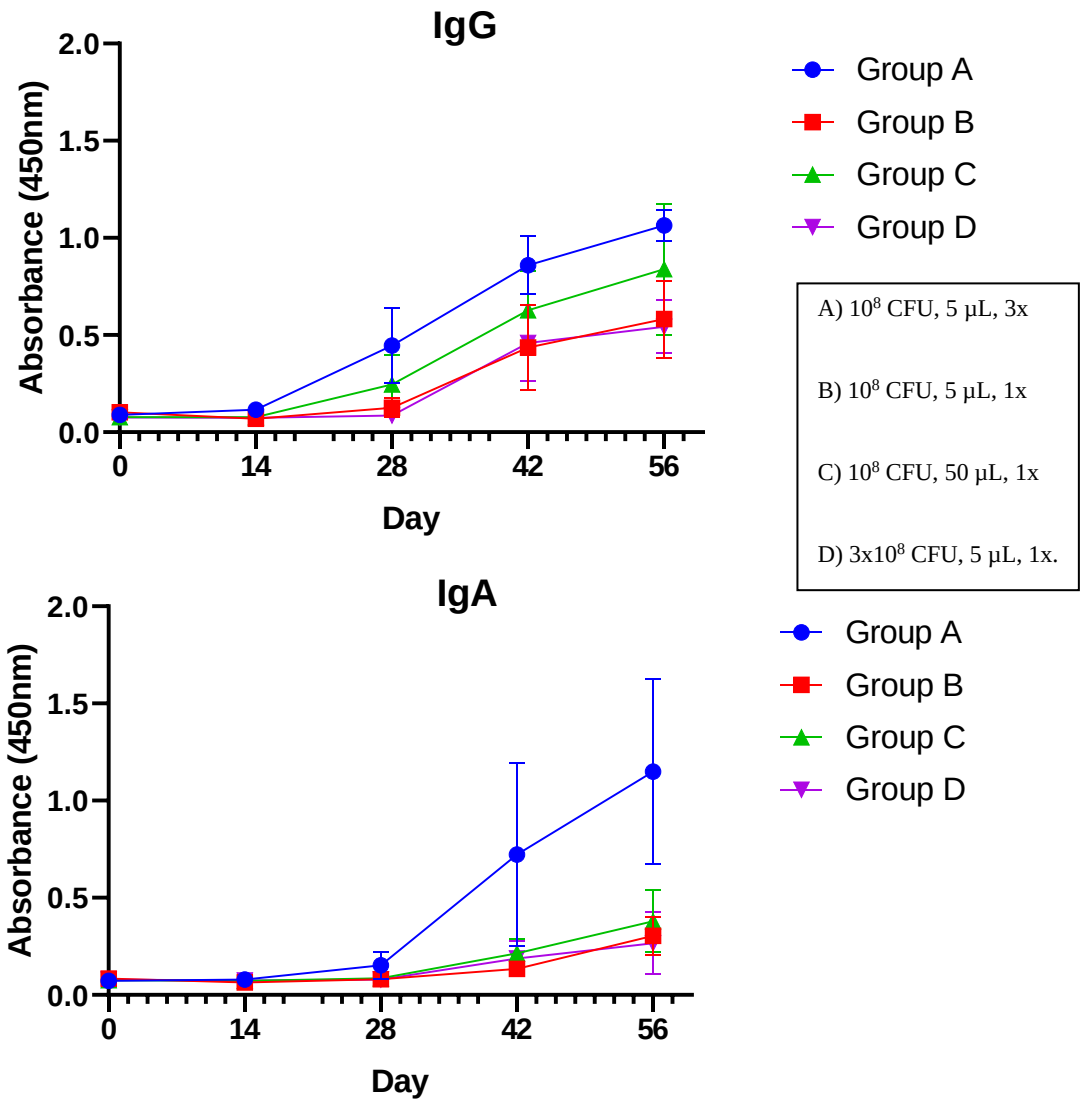

Figure 5.1: Temporal serum antibody response to PilVax-OVA vaccination groups

BALB/c mice (n=5) were immunised with PilVax-OVA using four different vaccination schedules with four immunisation rounds in total. Serum was collected prior to every boost. The presence of anti-Spy0128 IgG and IgA was determined by measuring absorbance at 450 nm in an ELISA where serum had been titrated 1:100. The mean and standard deviation of each group is shown.

The IgG response increased over time in all groups with reasonable variation within each group. At day 56 group A had the highest average absorbance at 450 nm, with the little variation within the group. However the mean fell within the standard deviation of group C. Vaccination with group A also resulted in the highest mean absorbance of IgA but there was a large amount of variation within the group. In contrast to IgG, there is a difference when comparing group A and C as the standard deviations did not overlap at day 56 and began to diverge from day 42. In terms of IgG and IgA responses both groups B and D have absorbance values consistently lower that groups A and C.

As there was no clear difference further analysis was carried out to quantify the level of antibody response to each vaccination group. The end point IgG and IgA titre was determined for Spy0128 and the OVA peptide by ELISA using recombinant Spy0128 generated in chapter 4, and ovalbumin protein (figure 5.2). End point titre was determined as the highest titration ± 3x the standard deviation of pre immune serum.

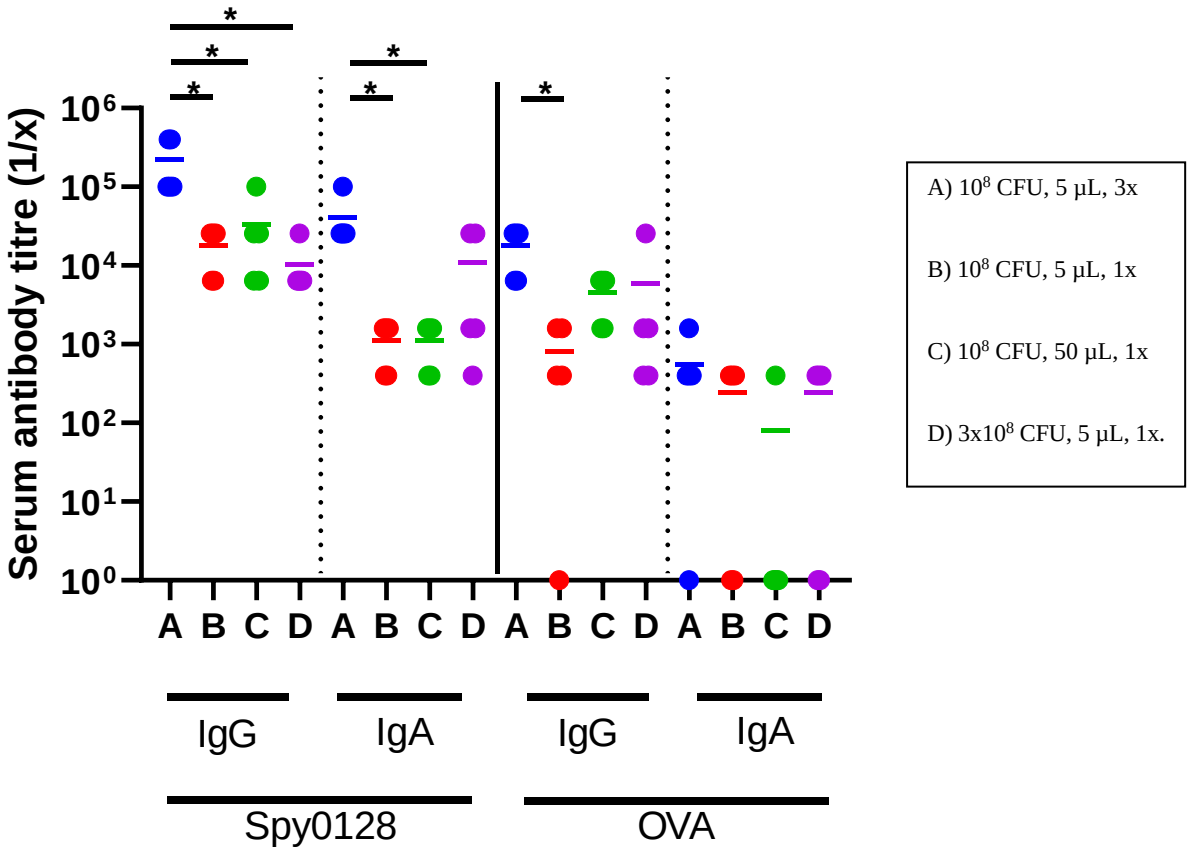

Figure 5.2: Serum end point titres in response to PilVax-OVA vaccination groups

BALB/c mice (n=5) were immunised with PilVax-OVA using four different vaccination schedules with four doses over 56 days. The IgG and IgA end point titre of Spy0128 and olvalbumin was determined by titrating serum from day 56 in an ELISA. End point titre was calculated as the highest titration ±3x the standard deviation of pre immune serum which had been diluted 1:100. Each data point represents the endpoint titre from an individual mouse. The mean of each group is shown as a horizontal line. * $p<0.05$ by way of One Way ANOVA using Tukey analysis.

The anti-Spy0128 IgG end point titre of group A was significantly higher than any of the other vaccination groups while the anti-Spy0128 IgA end point titre was significantly higher than groups B and C. The anti-OVA IgG end point titre was only significantly higher in group A when compared to group B. Anti-OVA IgA end point titre was not significantly different between any of the groups.

Group A consistently had the highest serum end point titres. To further analyse the humoral response to these vaccination schedules, antibodies from selected mucosal sites were also analysed.

5.1.2 *Mucosal antibodies*

In addition to serum collection on day 56, bronchial alveolar lavage (BAL) fluids, an oral wash (saliva) and faecal samples were collected and processed as in section 3.5. The IgA response to PilVax vaccination at these mucosal sites was analysed by ELISA (figure 5.3).

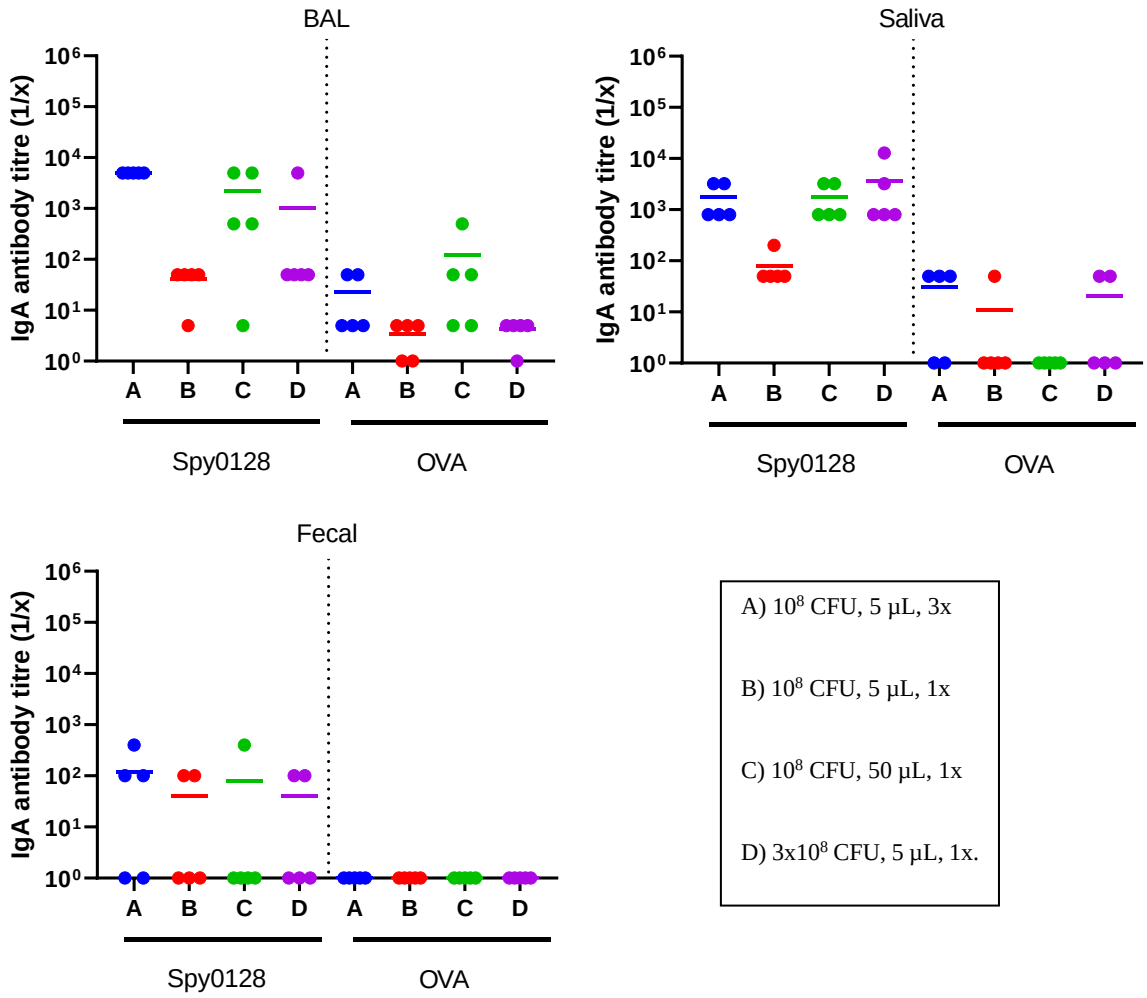

Figure 5.3: IgA end point titres at selected mucosal sites in response to PilVax-OVA vaccination groups

BALB/c mice (n=5) were immunised with PilVax-OVA using four different vaccination schedules with four doses over 56 days. IgA end point titre of anti-Spy0128 and anti-OVA was determined by titrating samples from day 56 in an ELISA. End point titre was calculated as the highest titration ±3x the standard deviation of the background for BAL and saliva, and of pre immune faeces for faecal samples. Pre immune faecal samples were diluted 1:5. Each data point represents the endpoint titre from an individual mouse. The mean of each group is shown as a horizontal line.

The anti-Spy0128 end point titre in the BAL fluids was highest in group A ($5x10^3$) with little variation within the group. The end point tire in group C was similar ($2.2x10^3$), however, there was more variability among mice in the group. Group C had a higher anti-OVA titre ($1.2x10^2$) than group A ($3.2x10^1$) but there was also greater variability within group C. Group B and D had lower titres for both antibody classes compared to the other two groups while also exhibiting less variability than group C.

Across both antibody classes, in the saliva and faecal samples, there was no significant difference between the vaccination groups. Interestingly there were no anti-OVA antibodies detected in saliva or faecal samples from group C. Additionally only one mouse had a detectable amount of anti-Spy0128 IgA antibody in the faeces. In contrast, the other vaccination groups had a higher level of anti-Spy0128 IgA in the faeces and higher anti-OVA IgA in the saliva sample than group C.

5.1.3 ***Summary***

Vaccination with 3 doses of $1x10^8$ bacteria in 5µL per boost resulted in the highest, least variable antibody end point titre in both serum and selected mucosal sites. Group A B and D exhibited lower variation in comparison to group C which has a dose delivery volume ten times larger than the other groups. For a high, and consistent antibody titre in serum and mucosa, vaccine schedule A will be used for further experiments.

5.2. Antibody response to PilVax

The aim of this section was to assess the ability of PilVax to elicit a humoral response against the PilVax constructs with *Mtb* peptides engineered into the loop regions of the Spy0128 protein generated in Chapter 4. The vaccination protocol that generates the highest antibody titre (analysed in section 5.1) was used in this study. The humoral response was analysed by ELISA to measure the end point titre of serum IgG and IgA to Spy0128 and the peptide of interest. The IgA end point titres at selected mucosal sites were also analysed.

Seven week old male C57BL/6 mice were ordered from the Vernon Jansen Unit (VJU) at the University of Auckland and immunised intranasally with the PilVax constructs generated in Chapter 4.

The vaccination groups were PilVax: ESAT-6-P1, ESAT-6-P2, ESAT-6-P8, Ag85B, with PilVax-OVA as a positive control, and-PilM1 (no insert in PilM1 operon) as a negative control.

5.2.1 ***Serum antibodies***

Two weeks following the final vaccination boost mice were euthanised and serum collected for analysis. Purified recombinant Spy0128 (section 4.2), ovalbumin protein, and synthetic peptides were used in an ELISA to analyse the level of IgG and IgA antibodies generated in response to PilVax vaccination. Serum was titrated to determine the end point titre (figure 5.4).

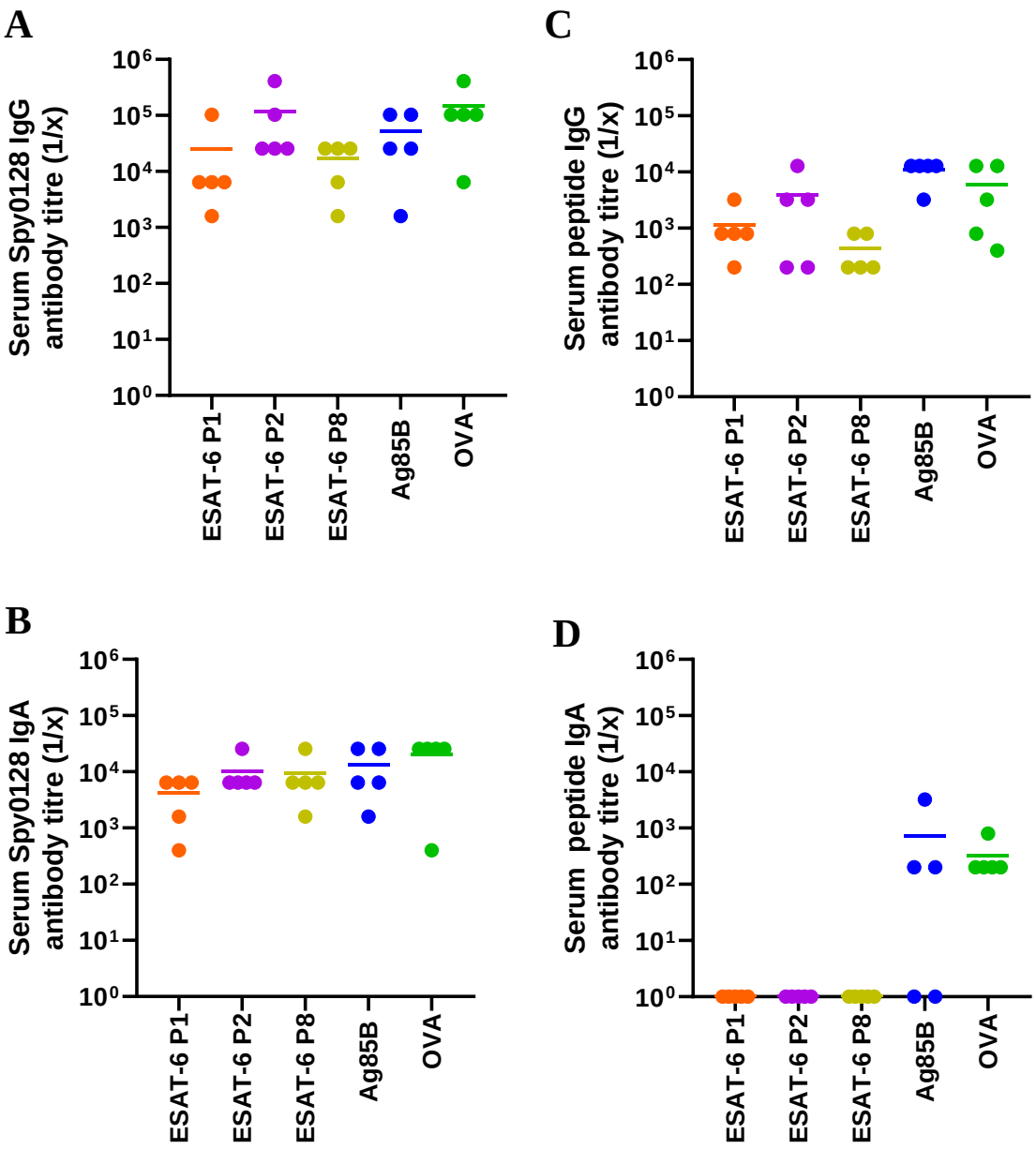

Figure 5.4: Serum anti-Spy0128 and anti-peptide IgG/IgA end point titres following PilVax-*Mtb* construct immunisation

C57BL/6 mice (n=5) were immunised and the serum end point titres of anti-Spy0128/anti-peptide IgG/IgA were determined by ELISA against rSpy0128, or cognate ovalbumin protein/synthetic peptides. Each data point represents the endpoint titre from an individual mouse. The mean of each group is shown as a horizontal line. End point titre was determined as highest titration ±3 x the standard deviation of pre immune serum which was titrated 1:100.

Vaccination with PilVax-*Mtb* constructs resulted in a high anti-Spy0128 IgG and IgA antibody titre across all constructs, similar to levels seen in previous studies with PilVax-OVA (figure 5.4 A/B). The anti-Spy0128 IgA end point titre was consistently 10 fold lower than the IgG

end point titre. The PilVax constructs with *Mtb* peptides have a similar anti-Spy0128 IgG and IgA end point titre to the previously characterised PilVax-OVA construct (figure 5.2).

The IgG anti-peptide end point titre was more variable across vaccination groups than what was seen with anti-Spy0128 antibodies (figure 5.4 C). Among the *Mtb* PilVax constructs, PilVax-Ag85B had the highest, and most consistent end point titre, similar to the anti-ovalbumin IgG end point titre in PilVax-OVA vaccinated mice. All peptide titres were below their corresponding anti-Spy0128. Only PilVax-Ova and PilVax-Ag85B generated any anti-peptide IgA antibodies (figure 5.4 D).

5.2.2 ***Mucosal antibodies***

Bronchiolar lavage (BAL) fluids, oral washes (saliva), nasal washes, and faecal samples were collected at the time of euthanasia as described in section 3.5. Purified recombinant Spy0128 ovalbumin protein, and synthetic peptides were used in an ELISA to analyse the presence of anti-Spy0128 and anti-peptide IgA antibodies generated at these sites. End point titres were determined by titrating the samples collected (figure 5.5).

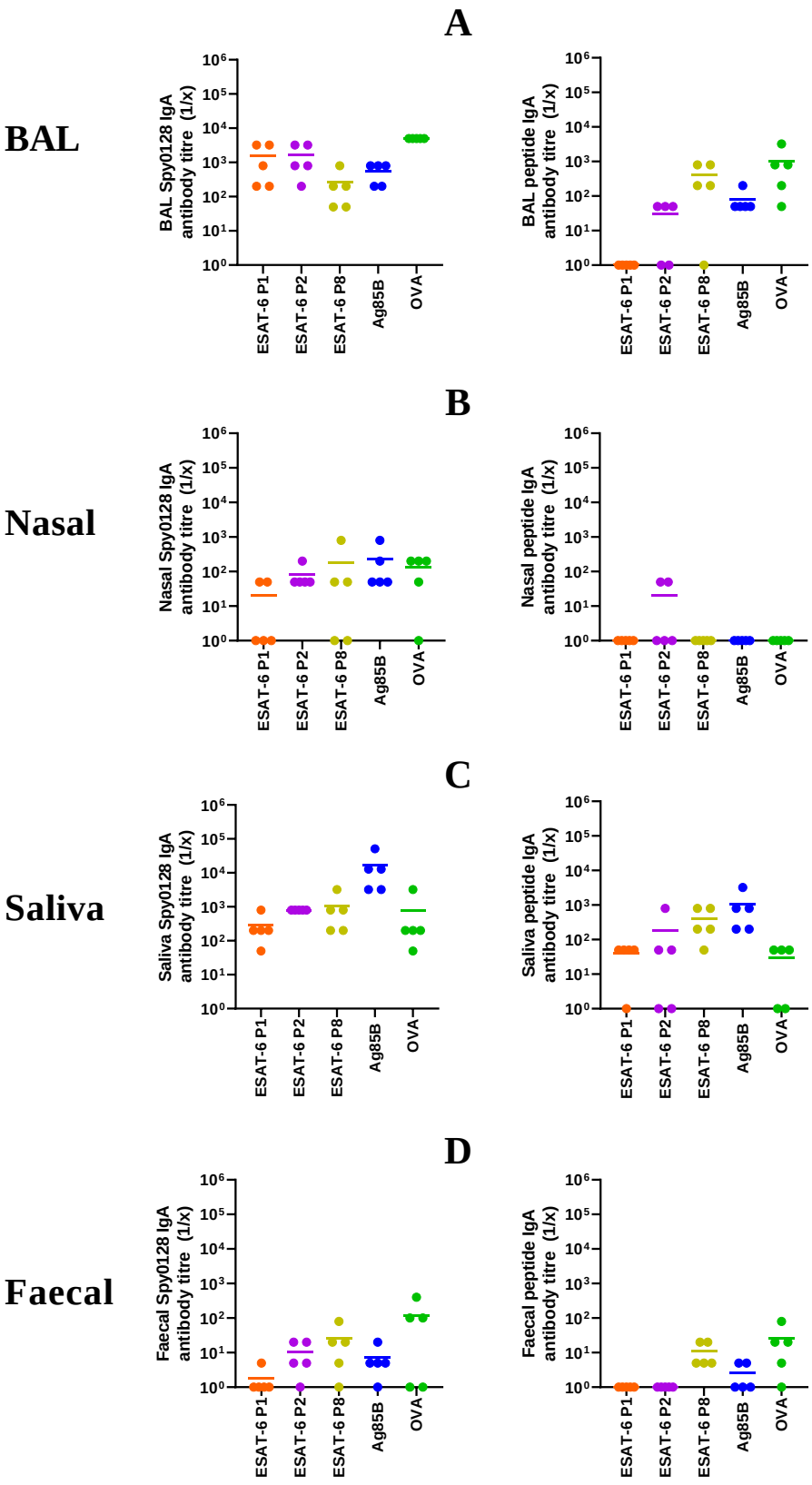

Figure 5.5: Mucosal anti-Spy0128 and anti-peptide IgA end point titres following PilVax immunisation.

C57BL/6 mice (n=5) were immunised and samples collected from selected mucosal sites. The end point titre of anti-Spy0128/anti-peptide IgA was determined by ELISA using rSpy0128, or cognate ovalbumin protein/synthetic peptides. Each data point represents the endpoint titre from an individual mouse. The mean of each group is shown as a horizontal line. End point titre was determined as highest titration ±3 x the standard deviation of the plate background for BAL, saliva, and nasal sites, and faecal pre immune samples which were titrated 1:5.

All vaccination groups had a similar end point titre of anti-Spy0128 IgA in BAL fluids (figure 5.5 A). PilVax-OVA vaccinated mice had the highest titre while the *Mtb* PilVax groups had more variation within the groups. Generation of peptide specific antibodies in BAL fluids was more variable. PilVax-ESAT-6 P1 vaccination resulted in no detectable antibodies with this assay, while the end point titre in the remaining groups was lower than the Spy0128 end point titre. PilVax-OVA vaccinated mice had the highest titre of peptide specific IgA antibodies generated in response to vaccination, followed by PilVax-ESAT-6 P8 vaccination, then both the PilVax-ESAT-6 P2 and PilVax-Ag85B vaccination groups (figure 5.5 A).

The end point titre of anti-Spy0128 antibodies in the nasal wash was typically at least 10 fold lower than in BAL fluids across all vaccination groups. PilVax-ESAT-6 P1 vaccinated mice had the lowest titre while the remaining groups were comparable to the PilVax-OVA vaccinated mice (figure 5.5 B). Only two mice in study had any detectable level of anti-peptide IgA in the nasal wash, which were seen in the PilVax-ESAT P2 group.

In the saliva recovered form *Mtb* PilVax vaccinated mice the mean end point titre of anti-Spy0128 was lowest in PilVax-ESAT-6 P1 vaccinated mice, followed by, in ascending order, PilVax-ESAT-6 P2 and PilVax-ESAT-6 P8, then PilVax-Ag85B vaccination (figure 5.5 C). PilVax-OVA vaccinated mice had an end point titre similar to the PilVax-ESAT-6 P2 and PilVax-ESAT-6 P8 vaccinated mice. The anti-peptide end point titre largely followed the same trend while approximately 10 fold lower (figure 5.5 C).

The end point titres in the faecal samples were the lowest out of all the mucosal sites tested. The mean anti-Spy0128 IgA titre among the PilVax-ESAT-6 vaccinated mice increased from the P1 to P8 while remaining lower than the mean seen in PilVax-Ova vaccinated mice (figure 5.5 D). Only the PilVax-ESAT-P8 vaccinated mice generated peptide specific IgA antibodies which were, again, lower than the titre seen in PilVax-OVA vaccinated mice. PilVax-Ag85B

vaccinated mice had an anti-Spy0128 and anti-peptide titre lower than both the PilVax-ESAT-6 P8 and PilVax-OVA vaccination groups (figure 5.5D).

5.2.3 ***Summary***

PilVax is able to generate systemic and local antibodies against *Mtb* peptides following vaccination.

Serum anti-Spy0128 IgG and IgA was generated at high levels across all *Mtb* PilVax vaccination groups at levels similar to the PilVax-OVA positive control. However there is more variability in the generation of anti-peptide IgG and IgA. Of the *Mtb* PilVax constructs, only PilVax-Ag85B vaccinated mice generated serum anti-peptide IgA. Anti-peptide IgG was detected for all groups with PilVax-Ag85B having the highest mean end point titre of the *Mtb* PilVax constructs.

Among the mucosal sites tested, the highest end point titres were detected in the BAL fluids, followed by the saliva, nasal wash, and faecal samples. Among the PilVax ESAT-6 peptide vaccinated mice, at all four mucosal sites, the PilVax-ESAT-6 P8 group frequently had the highest mean end point titre in both anti Spy0128 and anti-peptide IgA. This is followed by the PilVax-ESAT-6 P2 then PilVax-ESAT-6 P1 groups. PilVax-Ag85B vaccinated mice had a similar level of antibody response to the PilVax-ESAT P8 group, while both groups were often comparable to the PilVax-OVA positive control.

5.3. Antibody response to LRT vaccine delivery

A mouse study was carried out aimed at assessing the T cell response to PilVax vaccination using a vaccination schedule optimised in Dr Joanna Kirman's lab at the University of Otago (Chapter 6). Mice were vaccinated intransally with $2x10^7$ CFU delivered in 40 µL per boost with 3 doses in total over 42 days. This compares with the above study in section 5.2 where each dose was $1x10^8$ CFU delivered in 5 µL 3x per boost with four doses in total over 56 days.

End point serum from these mice was collected and the humoral response analysed. The vaccination groups for this study were: PilM1-PilVax-ESAT 6 P1, P2, P8, Ag85B, PilM1 (no peptide) and BCG (positive control). This experiment also had groups vaccinated with PilVax-PilM6 (no peptide) and PilM6-ESAT-6 (full protein) which were generated following the conclusion of the above study in section 1.2, thus not included there.

5.3.1 ***PilVax-PilM1 antibodies***

Two weeks following the final vaccination boost, mice were euthanised and serum collected for analysis. Purified recombinant Spy0128 and synthetic peptides were used for coating ELISA plates to analyse the level of IgG and IgA antibodies generated in response to PilM1-PilVax vaccination using the T cell vaccination schedule in section 3.6.1. Serum was titrated to determine the end point titre (figure 5.6).

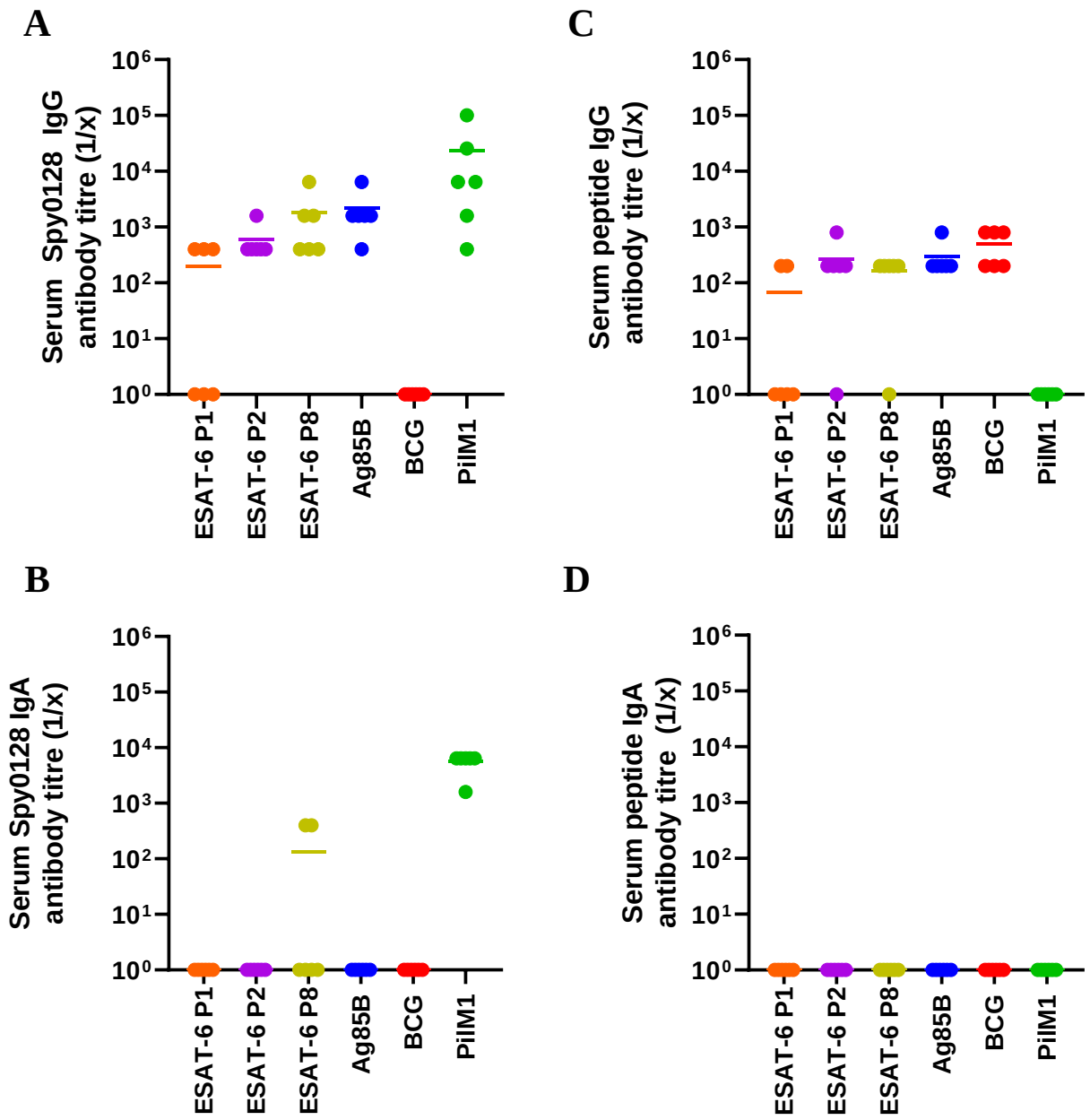

Figure 5.6: Serum anti-Spy0128 and anti-peptide IgG/IgA end point titres following PilVax immunisation using an alternative vaccination protocol.

C57BL/6 mice (n=6) were immunised and the serum end point titres of anti-Spy0128/anti-peptide IgG/IgA were determined by ELISA using rSpy0128, and cognate synthetic peptides. Each data point represents the endpoint titre from an individual mouse. The mean of each group is shown as a horizontal line. The mean of each group is shown. End point titre was determined as highest titration ±3 x the plate background.

Vaccination with this schedule resulted in an anti-Spy0128 and anti-peptide IgG end point titres at that are variable across all groups (figure 5.6 A/C). Vaccination with BCG, which expresses the Ag85B protein, resulted in a similar peptide specific IgG end point titre compared with the PilVax-Ag85B vaccinated mice which were only exposed to a peptide of the protein.

The end point IgG titres were at least 1000 fold lower compared to the previous vaccination schedule (figure 5.6 A/C).

The only group to have generated any significant anti-Spy0128 or anti-peptide IgA is the PilM1 vaccinated mice where anti Spy0128 IgA were detected (figure 5.6 B/D). This is however 10 fold lower compared with the end point tire seen in figure 5.6 B/D.

5.3.2 ***PilVax-PilM6 antibodies***

Two weeks following the final vaccination boost mice were euthanised and serum collected for analysis. Purified recombinant T6 (backbone monomer of the *S. pyogenes* M6 pilus) and synthetic peptides were used in an ELISA to analyse the level of IgG and IgA antibodies generated in response to PilM1-PilVax vaccination using the vaccination schedule in section 3.6.1. Serum was titrated to determine the end point titre (figure 5.7).

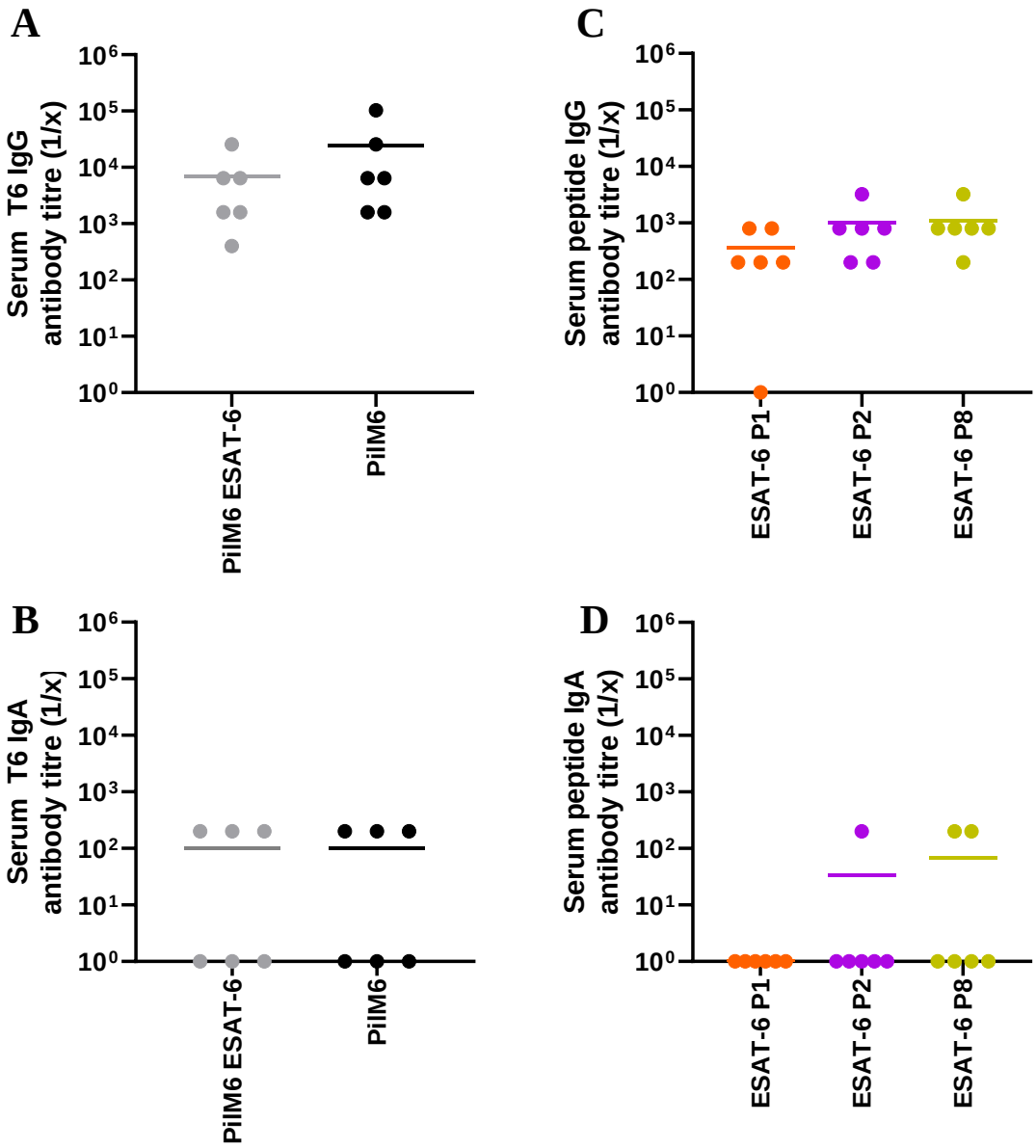

Figure 5.7: Serum anti-T6 and anti-peptide IgG/IgA end point titres following PilVax immunisation

C57BL/6 mice (n=6) were immunised and the serum end point titres of anti-T6/anti-peptide IgG/IgA were determined by ELISA using rT6, and synthetic peptides. Each data point represents the endpoint titre from an individual mouse. The mean of each group is shown as horizontal line. End point titre was determined as highest titration ±3 x the plate background.

Vaccination using the above schedule resulted in significant anti-T6 IgG end point titres in both PilVax-PilM6 constructs (figure 5.7 A). These titres are comparable to the anti-Spy0128 IgG titre seen when mice are vaccinated with the PilM1 Pilvax constructs (figure 5.4A). There was also an IgG response generated against all three of the ESAT-6 peptides tested in the PilVax-PilM6-ESAT-6 (full protein) vaccinated mice (figure 5.7 C). These end point titres are

comparable to the anti-peptide IgG titres generated in PilVax-ESAT-6 P1, P2 and P8 immunised mice (figure 5.4B).

There was a small anti-T6 IgA titre in some of the vaccinated mice in both groups, though not all mice had a detectable antibody response (figure 5.7 C). There was not a significant anti-peptide IgA response to any of the peptides tested (figure 5.7 D).

5.3.3 ***Summary***

Mice vaccinated with PilVax using a protocol optimised to generate a T cell response still generate anti-Spy0128 and anti-peptide specific IgG antibodies. However these antibodies are present at a lower level when compared to mice vaccinated using the previous schedule (section 4.2). There was also minimal/no vaccine-specific IgA antibodies detected.

These results demonstrated for the first time that PilVax-PilM6 constructs are able to generate serum anti -T6 IgG and IgA, as well as anti-peptide IgG antibodies.

5.4. Discussion

PilVax is a novel, *L. lactis* based, intranasal peptide delivery vaccine where the immune response has not been previously characterised. This chapter comprehensively explored the humoral response PilVax is able to generate. The level of local and systemic antibody response was analysed in response to vaccine delivery to different sites of the respiratory tract in order to generate the highest level of humoral activation. This was seen when vaccine delivery was confined to the upper respiratory tract (URT) (figures 5.2, 5.3). For comparison with adenoviral vectors targeting *Mtb* previously described, analysing the level of T cell response in these studies would have been beneficial, however, as it was not done this represents a limitation of these experiments in regards to *Mtb* potential. Despite this, data from these experiments does provide an insight into the humoral response against a series of PilVax constructs with variable

expression levels and peptide properties, and may provide useful insights for the development of vaccines against non *Mtb* pathogens.

5.4.1 ***Vaccine optimisation***

Anti-Spy0128 IgG in the serum was not detectable until day 28 when the vaccine was delivered as low volume, consecutive triple daily dose (group A) or high volume single dose (group C), while anti-Spy0128 IgA is not detected in either group until day 42 (figure 5.1). This lag in IgA production could be due to the time taken to undergo class switching. It also indicates multiple boosts of PilVax will be required to generate any form of immune response. While some *Mtb* studies have seen a decrease in compliance where multiple doses are required, these have been delivered by technically difficult methods such as intra dermal or intramuscular (J. Stanford et al., 2004). The needle free, and ease of delivery site access in PilVax may be able to overcome the limitations of requiring multiple boosts.

By day 56, low volume, consecutive triple daily dose (group A) and high volume single dose (group C) vaccinations had the highest mean absorbance value, which although quite variable provided a number of insights into the generation of antibodies. The increased response seen in immunisation with a low volume, consecutive triple daily dose is likely due to the repeated dosing per boost as a higher CFU confined to the URT (group D) does not increase the response generated (figures 5.1, 5.2, 5.3). The delivery to the lower respiratory tract (LRT) (group C) resulted in a more variable serum IgG response. This could be due to the technical difficulty of delivering a large dose to mice which may not provide the same challenge in humans.

There is already precedence for safe and efficacious nasal delivery of vaccines as shown in a recent clinical trial where the delivery is intranasal to support the generation of mucosal IgA against viral influenza. The trial influenza vaccine is delivered by nasal spray and has reached phase two trials where it is able to be safely administered, and result in the protective

seroconversion. Multiple doses, 14 days apart such as would be required for PilVax, has also been found to be tolerated, and results in better protective outcomes than a single dose (Lambkin-Williams et al., 2016). Development of an mucosal HIV vaccine has also demonstrated the safety and efficacy of administering an large intranasal vaccine dose of 350µL doses in non-human primates (Manrique et al., 2009). Given the demonstrated ability of PilVax to generate immune responses in mice following intranasal vaccination, there is precedent for this to be translated into humans through a number of potential dosing mechanisms. Given one of PilVax potential advantages is needle free easy delivery, a nasal spray is an attractive method of managing dosage in humans.

The production of serum IgA was clearly highest with repeated vaccination in the URT where, similar to serum IgG, the CFU is less relevant than the number of doses per boost (figures 5.1, 5.2, 5.3). This could be because repeated vaccination delivering PilVax to the NALT in a short time frame accelerates the signalling required to generate local and systemic IgA+ plasma cells.

These observations were largely confirmed by quantitative analysis of the level of antibody present at day 56 (figure 5.2). However the difference in the anti-Spy0128 IgA end point titre was not statistically significant between group A and D indicating perhaps the same serum anti-Spy0128 IgA can be achieved by increasing the CFU rather than the doses per boost.

However of more importance than the anti-Spy0128 response is the antibody response to the peptide of interest, in this case OVA. The end point titres of serum anti-OVA IgG and IgA were not significantly different (figure 5.2). The ability to generate both antibody isoforms in the serum is promising and would be of particular use against pathogens where systemic dissemination plays a major role in pathogenicity.

Pathogens where this may be of use include enterohemmorrhagic *Escherichia coli* (EHEC) for which there is currently no licensed vaccine. Pathogenesis is primarily due to the production

of Shiga toxins which, combined with a lack of treatment options and high mortality rate make this bacteria is a major health concern. Incorporating a peptide from Shiga toxins into PilVax could result in neutralizing antibodies and a reduction in EHEC morbidity. Current trials in mice have implicated musical IgA, and serum IgG as correlates of protection which PilVax is able to induce (Garcia-Angulo, Kalita, & Torres, 2013).

Neisseria gonorrhoeae is another bacteria where generation of a vaccine has been difficult and frustrated by the natural antigenic variability of the bacteria (Jerse, Bash, & Russell, 2014). Intranasal vaccination is able to induce antibodies in the genital tract in both mice and humans and although this was not tested in PilVax, the generation of mucosal antibodies at a number of distal mucosal sites is promising (Johansson, Wassén, Holmgren, Jertborn, & Rudin, 2001; Scott Gallichan & Rosenthal, 1995). The identification of a number of *Neisseria gonorrhoeae* antigens where antibodies are bactericidal, such as the Opa proteins and outer membrane secretins provide and insight into multiple peptides a PilVax construct could include(Cole & Jerse, 2009; Haghi, Peerayeh, Siadat, & Zeighami, 2012). Such a construct could potentially generate a specific immune response at the site of infection as well as serum antibodies. As there is no natural immunity gained from infection, correlates of protection have not been well defined, however the generation of multiple antibody isoforms has been implicated in protection (Jerse et al., 2014)

As the systemic response is a result of MALT activation and communication, all four vaccination schedules may have reached the peak serum titres possible by this route of vaccination. The level of serum antibodies required to induce protection were not tested as OVA is a model peptide not found in natural disease. Of interest would be if the level of serum antibodies produced by PilVax-OVA vaccination are protective in a model where OVA has been included as a peptide in disease models such as colorectal cancer models where B16 expression can be induced in cell lines.

As serum antibody production is a secondary function of the MALT stimulation, selected mucosal sites were also analysed for the amount of IgA produced. While anti-Spy0128 antibodies were detected at all three sites tested, the end point titre was variable. Low volume, consecutive triple daily dose vaccination (group A) delivered a high and consistent titre in the BAL fluids, while high volume single dose vaccination (group C) resulted in a more variable titre although the mean titre was still high. The anti-Spy0128 titres was not entirely reflected in the anti-OVA titres where, although URT vaccination (low volume, consecutive triple daily dose (group A)) delivered a consistent end point titre, it was lower than the tire seen in LRT vaccination (high volume single dose (group C)). The variation in end point titres is again potentially due to the difficulty in consistently delivering a single large dose of the vaccination in mice. The lower anti-OVA titres are likely due to the polyclonal nature of anti-Spy0128 antibodies generated vs the likely monoclonal anti-peptide antibodies. There are multiple epitopes across the Spy0128 protein where an immune response can be generated against, while the peptides inserted into the pilus represent only one epitope. The variation in end point titres is not likely related the level of pilus expression as these groups were all vaccinated with the same batch of PilVax-OVA vaccine aliquots where one aliquot was thawed and diluted to the required CFU required per group.

There is a lack of anti-OVA IgA in the faecal samples of all the groups (figure 5.3). This is however not unexpected as generally intranasal vaccination results in respiratory tract immune responses, whereas GALT stimulation requires oral administration (Holmgren & Czerkinsky, 2005). Alternative vaccination routes could be tested to further analyse PilVax's GALT stimulatory potential, however oral administration of a vaccine dose is challenging in mouse models.

Group A was selected as the vaccination schedule able to generate the highest, and most consistent antibody titres across a number of local and systemic sites.

5.4.2 ***Antibody response to Mtb PilVax constructs***

The humoral response to low volume, consecutive triple daily dose immunisation with a number of PilVax constructs with variable levels of expression, and a range of reported T and B cell epitopes was analysed.

The end point tire of serum anti-Spy0128 IgG and IgA is comparable across all groups while similar to the PilVax-OVA positive control (figure 5.4). This is despite an appreciable reduction in the level of pilus expression in some of the constructs (figures 4.6, 4.7). This indicates that production of serum anti-Spy0128 antibodies reaches saturation point at a relatively low level of pilus expression in *L. lactis*.

However, in comparison the level of anti-peptide serum antibodies is more variable and does not correlate well with the anti-Spy0128 end point titres (figure 5.4). While anti-Spy0128 antibodies are a measure of the successful delivery of the PilVax constructs to the immune system, the lack of correlation with the anti-peptide antibodies means the Spy0128 end point titres cannot be used as a proxy estimation of anti-peptide B cell activation. This is again possibly due to the multiple epitopes available for immune cell activation on the Spy0128 protein compared to the restricted peptide epitope potential. The immunogenicity of the Spy0128 protein and high antibody titres generated mean the protein could also be used as an adjuvant in other novel vaccines.

Any novel vaccine utilizing the immunogenicity of the Spy0128 would also likely be a peptide vaccine utilizing the PilVax platform. In the PilVax pilot study, administration of the OVA peptide and recombinant Spy0128 separately did not induce an OVA specific antibody response. This indicated the requirement for the peptide of interest to be incorporated within the Spy0128 protein to harness the adjuvant effect (Wagachchi et al., 2018). As shown in this thesis in chapter 5 and 6

, PilVax is able to generate peptide specific antibodies as well as peptide specific T cells.

Earlier discussion points in Chapter 4 centred on improving pilus expression through to cloning to find the loop region where expression would be highest. This data suggests that perhaps of more importance, is predicted immunogenicity of the peptide. However the ESAT-6 peptides did not demonstrate a significant increasing level of serum anti-IgG in peptides more distal to the N terminus as might have been expected, while there was no serum anti-peptide IgA detected. Unexpectedly, the highest anti-peptide end point titre was seen in the PilVax-Ag8B vaccinated mice where the peptide has been demonstrated as a potent T cell epitope with its B cell immunogenicity previously undescribed.

In the BAL fluids, nasal wash, saliva, and faecal samples, the end point titres did not correlate with the level of pilus expression of the PilVax construct nor with the predicted immunogenicity of the peptide. However the ability to generate peptide specific IgA antibodies at mucosal sites against a range of peptides does provide further evidence of PilVax's ability to stimulate the MALT. Of note is the ability to generate a response against more than just the previously characterised potent B cell epitope OVA.

Further investigations into the immunogenicity of each peptide in PilVax could be carried out to understand the mechanisms behind the low serum and peptide specific antibody response as the results obtained here appear to contradict previous assumptions in the literature. Insertion of multiple copies of the peptide into either the same loop region (ie peptides in tandem) or multiple loop regions of the pilus could overcome the lack of immune stimulation of characterised B cell epitopes seen in this study.

Serendipitous inclusion of two copies of the peptide into the βE-βF loop region during development of a PilVax construct targeting influenza allowed the comparison of one peptide copy versus two (Unpublished data). Following vaccination, the construct containing two

copies of the peptide resulted in a significantly higher anti-peptide antibody titre. Inclusion of two peptide copies per Spy0128 monomer doubles the number of peptide antigens in the PilVax construct which has shown potential to augment the immune response. Combining this with computer modelling of potential PilVax constructs mentioned in chapter 4 could indicate if inclusion of multiple copies of a given peptide per loop region is feasible without terminating pilus formation. Where it is possible, particularly in constructs with low pilus expression, could provide a method to increase peptide exposure and enhance the immune response generated.

The inability to produce serum anti peptide IgA in the majority of mice is potentially due to peptide specific factors as all of the different vaccination groups in section 5.1 generated a similar amount of anti-OVA IgA (figure 5.2). While these factors remain unknown, the ability of the OVA peptide to generate such a response is likely because the peptide binds specifically to the I-Ad MHC class II protein and is very well characterised, potent B cell epitope.

In this study, there was some peptide specific responses in the faecal samples however the titres were low. The lack of peptide specific antibodies in the faeces in section 5.1 and 5.2 does suggest the activation of GALT tissue in response to PilVax is low following this route of vaccination, which is not unexpected. Altering the route to take advantage of the characterised MALT communicate pathways by vaccinating orally could be tested to improve GALT IgA responses in the design of such a vaccine (Holmgren & Czerkinsky, 2005).

Although the role of antibodies is poorly understood in *Mtb* infection, there is a significant presence of antibody generating cells present in the *Mtb* induced granuloma (Phuah, Mattila, Lin, & Flynn, 2012). A recent study identified a role of serum anti-polysaccharide arabinomannan (a cell wall component) in the ability of sera from BCG immunised patients to impede of *Mtb* and BCG growth through opsonisation induced phagocytosis in an IgG dose dependent manner (T. Chen et al., 2016). The 2016 study only analysed titres by absorbance

value obtained in and ELISA so it is not known how the serum titres from Chen et al's study compare with the peptide specific titres obtained in this study (figure 5.5).

Anti-Ag85B serum IgG antibodies generated here may have a similar affect as anti-polysaccharide arabinomannan antibodies since Ag85B is also associated with the cell wall. BAL IgA antibodies could act to prevent *Mtb* binding during initial colonisation. During a post hoc analysis of the MVA85A study where Ag85A was delivered in an adenoviral vector, a correlation was found between the presence of Ag85A specific antibodies and a reduction in the risk of disease development in vaccinated infants (Fletcher et al., 2016). Further work could be carried out as to identify the specificity of such antibodies and if they are indeed protective. Confirmation of this would suggest perhaps the anti-Ag85B antibodies generated here could be of benefit in protection. The Ag85A and Ag85B proteins have 77% sequence homology and could conceivably share a common B cell epitope as they do already share a common T cell epitope (D'Souza et al., 2003). If the epitope is different, the inclusion of both peptides in a PilVax construct could conceivably generate a holistic immune response that may provide protection.

The serum peptide specific antibodies against ESAT-6 peptides P1 and P8 could neutralise the pore forming functions of the protein, as truncated forms of the protein are unable to insert in the membrane (Ma et al., 2015). In the extra cellular milieu, ESAT-6 P1, P2 or P8 antibodies could prevent the destructive interaction of the protein with basement epithelium and also prevent the immune modulatory functions by neutralising the protein. Although the level of mucosa specific antibodies generated here was not high (figure 5.5) such a neutralising role could be especially effective in the mucosa, where initial *Mtb* colonisation occurs. Intracellular anti-ESAT antibodies in macrophages could affect the cytosolic translation of the *Mtb* and target the protein for TRIM21 mediated destruction.

There is evidence that glycosylation of the Fc region of the antibody has an effect on the function of the antibodies that are generated. Patients with active, and latent TB have distinct glycosylation profiles of antibodies. Antibodies from patients with latent TB have enhanced effector functions resulting in greater levels of macrophage killing of *Mtb* (Lu et al., 2016). Isolation and analysis of antibodies from PilVax vaccinated mice would interesting in determining if the glycosylation of these antibodies is similar to that of antibodies from patients with latent *Mtb* and thus may have a protective role in *Mtb* infection.

5.4.3 ***Antibody response to vaccination with an alternative vaccine schedule***

The anti-Syp0128 serum IgG and IgA end point tires was lower than previous studies while the variability of the titres was to be expected as it was similar to the vaccination schedule of group C in section 5.1. The number of doses directly affects the production of antibodies an intranasal vaccinations and has already been shown in human trials where seroconversion occurs more frequently where multiple doses are administered (Lambkin-Williams et al., 2016), therefore the difference in titre seen is likely due to receiving one less dose than mice in section 5.2. As seen in figure 5.1, the level of antibody detected still increases with subsequent boosts after day 42. An extra boost may have resulted in anti Spy0128 titres comparable to previous studies. Interestingly with the peptide specific serum IgG, the same amount of anti-Ag85B$_{281\text{-}295}$ is detected in both PilVax-Ag85B and BCG vaccinate mice providing the first evidence PilVax may be able to generate an immune response similar to a known protective vaccine. However the role of antibody protection in BCG vaccinated mice is poorly understood and may not be of value.

Virtually no IgA is detectable in the serum other than anti-Spy0128 in the PilVax-PilM1 vaccinated mice. A further boost may increase result in the detection of any IgA as this was detected generated following the third boost in group C in section 5.1.

The lower antibody titres are also potentially due to the lower CFU of *L. lactis* delivered in this experiment, which is lower due to a difference in ethical approvals at different institutions. Although the production of antibodies seemed to be independent of pilus expression in section 5.2, it cannot be ruled out that the lack of IgA here is due to a lower CFU.

This study did not collect samples from mucosal sits so the generation of antibodies at those sties cannot be compared to previous work. However this study did include the PilM6 and PilM6-ESAT-6 constructs. These have not been previously tested so cannot be compared to previous data while ability of the M6 construct to generate mucosal antibodies also remains unknown. However this does provide evidence of that the T6 pilus structure can also be used in the design of novel vaccines and it may have a higher capacity to induce serum IgA antibodies (figure 5.7) compared to PilM1 vaccinations (figure 5.6).

Chapter 6. Peptide specific T cell response to PilVax

PilVax has been shown to elicit a humoral response but its ability to generate a cellular response has so far remained unknown (Wagachchi et al., 2018). The aim of the work in this chapter was to assess the ability of PilVax to elicit a T cell response by characterising the CD4+ peptide specific T cell response and the production of cytokines following stimulation with cognate peptide. In combination with results from previous chapters on the humoral response, these results were also expected to indicate which of the PilVax constructs would be the most promising candidates to continue to protection studies with. This work was carried out in collaboration with Dr Joanna Kirman at the University of Otago, Dunedin, New Zealand. Seven week old male C57BL/6 mice were ordered from the Hercus Taieri Resource Unit (HTRU) at the University of Otago and immunised intranasally with the PilVax constructs generated and described in previous chapters.

6.1. Pilot study of peptide specific T cell response to Ag85B

The initial pilot study aimed to demonstrate the ability of PilVax to generate a peptide specific T cell response. As the Ag85B is expressed in the BCG strains, the results presented provide a comparison of the immune response to the protein in its native from, and a peptide from the protein contained within the PilVax construct.

The vaccination groups for this study were:

L. lactis pLZ12Km2-PilM1_ βE/βF _Ag85B peptide (Residues 281-295), PilVax with a peptide from the Ag85B protein.

L. lactis pLZ12Km2-PilM1 (no insert in PilM1 operon), PilVax with no peptides to act as a negative control.

BCG as a positive control as *M. bovis* expresses Ag85B.

Each group contained 7 mice per group and was vaccinated as in 3.6.1

6.1.1 ***Pilot study vaccination results***

Mice were euthanised two weeks following the final boost and the lungs perfused with sterile PBS to ensure any cells detected were resident pulmonary populations, not circulating cells. Lungs were digested with collagenase type I and DNase. Digested lungs were then stained with Ag85B peptide specific MHC class II tetramer conjugated to the fluorophore APC. The tetramer cell population was enriched by addition of anti APC magnetic beads and passed through an automacs separator. The positive fraction was collected and stained with the antibody panel shown in table 3.6. A sample of cells from across groups was pooled and enriched with an unrelated tetramer (hCLIP) to rule out nonspecific binding. The stained positive fraction was analysed with a BD Fortessa flow cytometer and cells gated to identify the population of peptide specific CD4+ T cells (figure 6.1).

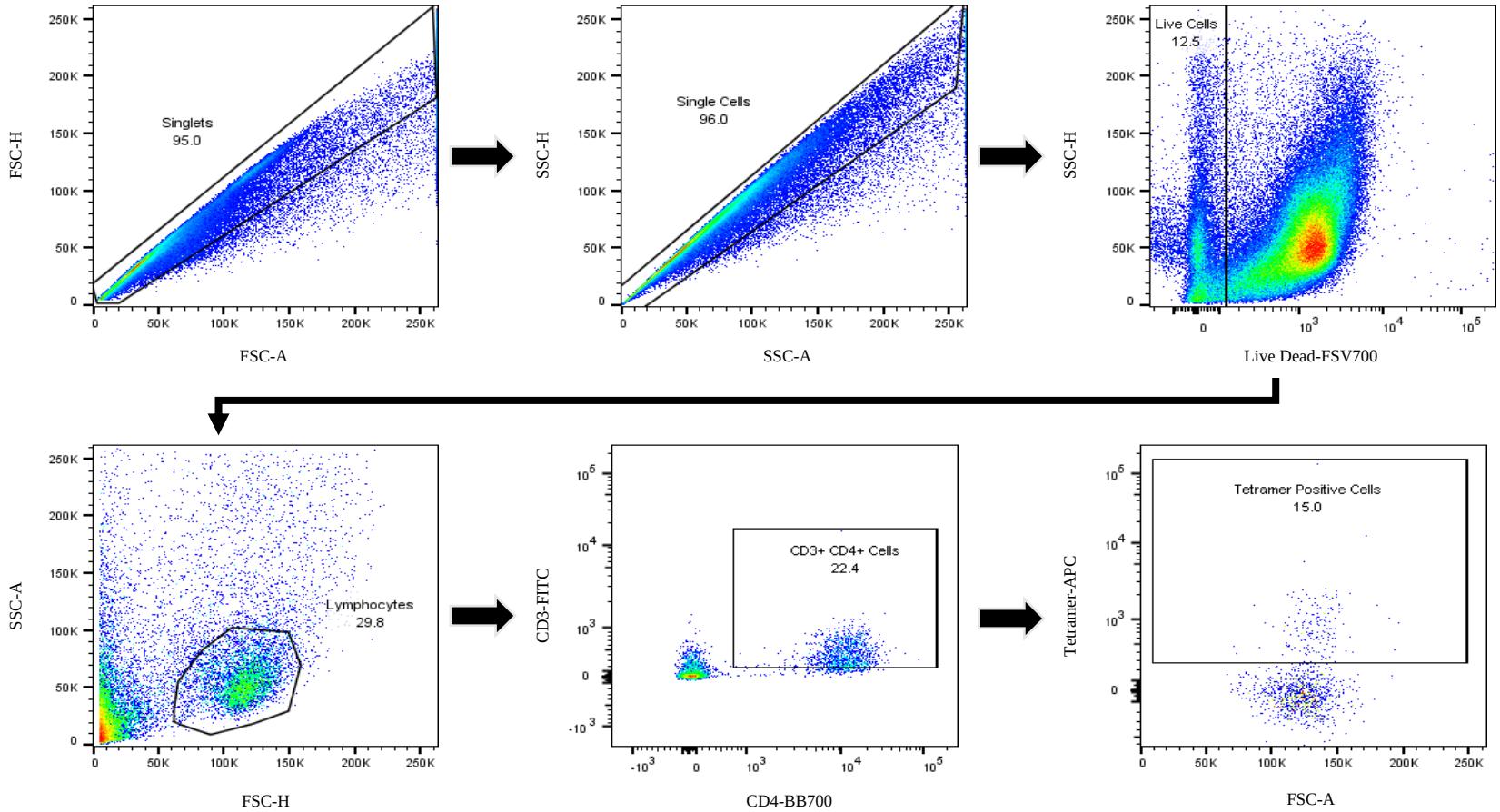

Figure 6.1: Flow cytometry of enzymatically digested lung cells following tetramer enrichment.

Dot blots show the gating strategy used to identify CD4+ T cells in immunised mice that were specific for the MHC class II molecule containing the Ag85B peptide following tetramer enrichment.

The total number of cells was determined by counting prior to tetramer enrichment. The number of CD4+ tetramer positive T cells per lung was determined by taking a sample of the positive fraction post automacs separation for counting to obtain the cell count in the enriched fraction. The proportion of each cell type identified by flow cytometry (6.1) was applied in a stepwise manner to the cell count to determine the number of tetramer positive cells per lung (figure 6.2). The number of tetramer positive cells was determined as a percentage of the total CD4+ cell population (figure 6.2 A) and also expressed as total number of tetramer positive cells per lung (figure 6.2 B).

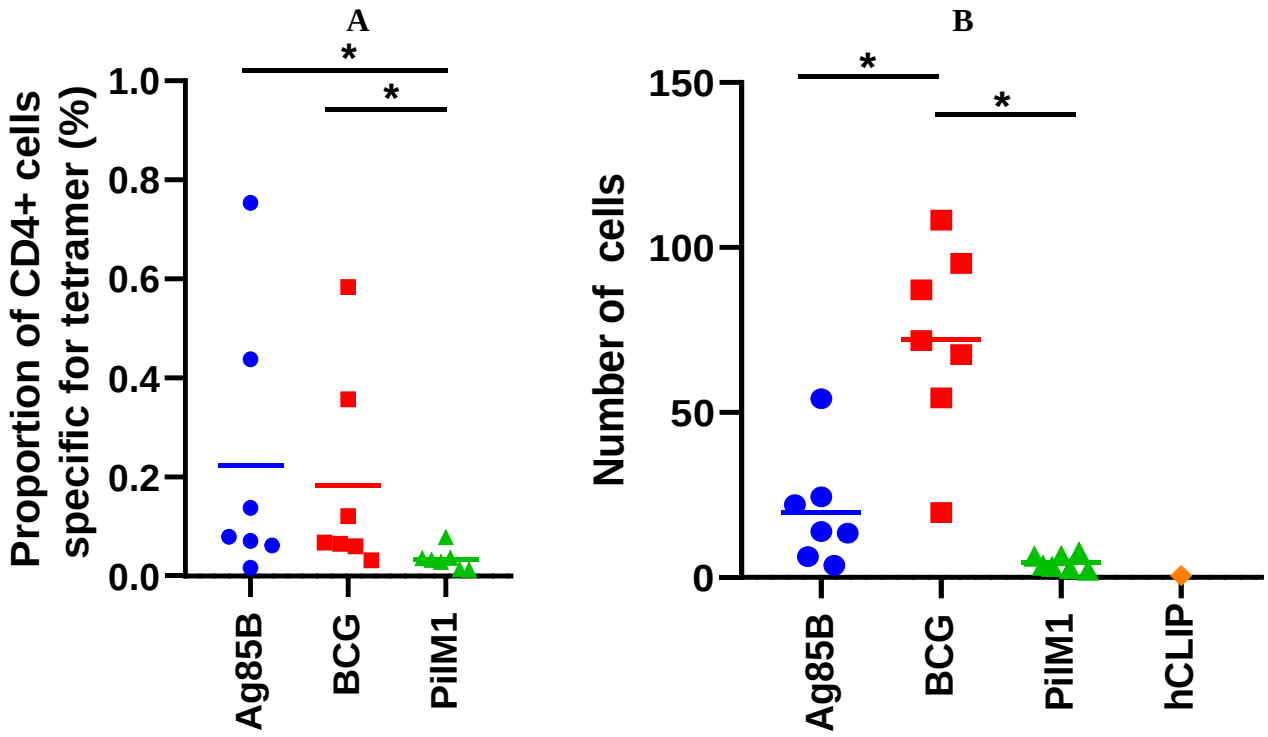

Figure 6.2: Comparison of peptide specific CD4+ T cells post vaccination.

C57BL/6 mice (n=7) were immunised and the proportion of peptide specific CD4+ T cells in the lungs (A) and total number of peptide specific CD4+ T cells in the lungs (B) were measured by flow cytometry and cell counts. Each data point represents cells from an individual mouse and the mean of each group is shown as a horizontal bar. Staining with hCLIP tetramer was used as a nonspecific control in a pooled sample of cells. *$p<0.05$ by way of ANOVA using Tukey analysis.

Following vaccination with PilVax, CD4+ peptide specific T cells were detectable in the lungs. There was a significant difference between the PilVax-Ag85B and BCG groups in terms of cell number with more peptide specific CD4+ T cells in the BCG vaccinated group. The mean of each group was higher than the negative control (PilM1) and the nonspecific binding. However only the BCG group was statistically significant. When tetramer-positive cells are expressed as a percentage of total CD4+ T cells, PilVax-Ag85B and BCG vaccination group resulted in a similar proportion of total CD4+ T cells specific for the peptide. Both groups were significantly higher than the PilM1 control group (figure 6.2 A).

6.1.2 ***Summary***

This pilot study showed the number of peptide specific CD4+ T cells generated as a proportion of the total number of CD4+ cells per lung was similar whether the immune system encounters the Ag85B protein in its native form on the BCG bacteria, or as a peptide of the protein contained in PilVax. This showed for the first time PilVax is able to generate a cellular response and provided the rational for expanding the next study to include other PilVax constructs.

6.2. Comprehensive analysis of lung resident T cell responses to PilVax vaccinations

As PilVax was demonstrated to elicit a T cell response, the next study expanded the PilVax immunisations to include the other PilVax constructs that had been generated. For PilVax constructs for which there was a tetramer to detect peptide specific CD4+ T cells, the phenotype of these peptide specific CD4+ T cells was analysed. In addition to peptide specific T cells, this chapter aimed to analyse the cytokine profile of CD3+ cells from the lungs of vaccinated mice when stimulated with cognate peptide. Vaccinations were carried in collaboration with Dr Joanna Kirman at the University of Otago.

6.2.1 *Peptide specific response in primary T cells*

The Ag85B MHC class II tetramer allowed for the detection of CD4+ peptide specific T cells in the BCG and Ag85B vaccination groups as in the pilot study, while the ESAT-6 P1 MHC class II Tetramer was used for the PilVax-ESAT-6 P1 and the PilM6-ESAT-6 vaccination groups.

As described in the pilot study, mice were euthanised following the final boost. The lungs were enzymatically digested, enriched for peptide specific cells and stained for cell surface markers. A sample of cells from across groups was pooled and enriched with a tetramer containing hCLIP to rule out nonspecific binding.

The cells were analysed with a BD fortessa flow cytometer and gated to identify the CD4+ peptide specific T cells (figure 6.3).

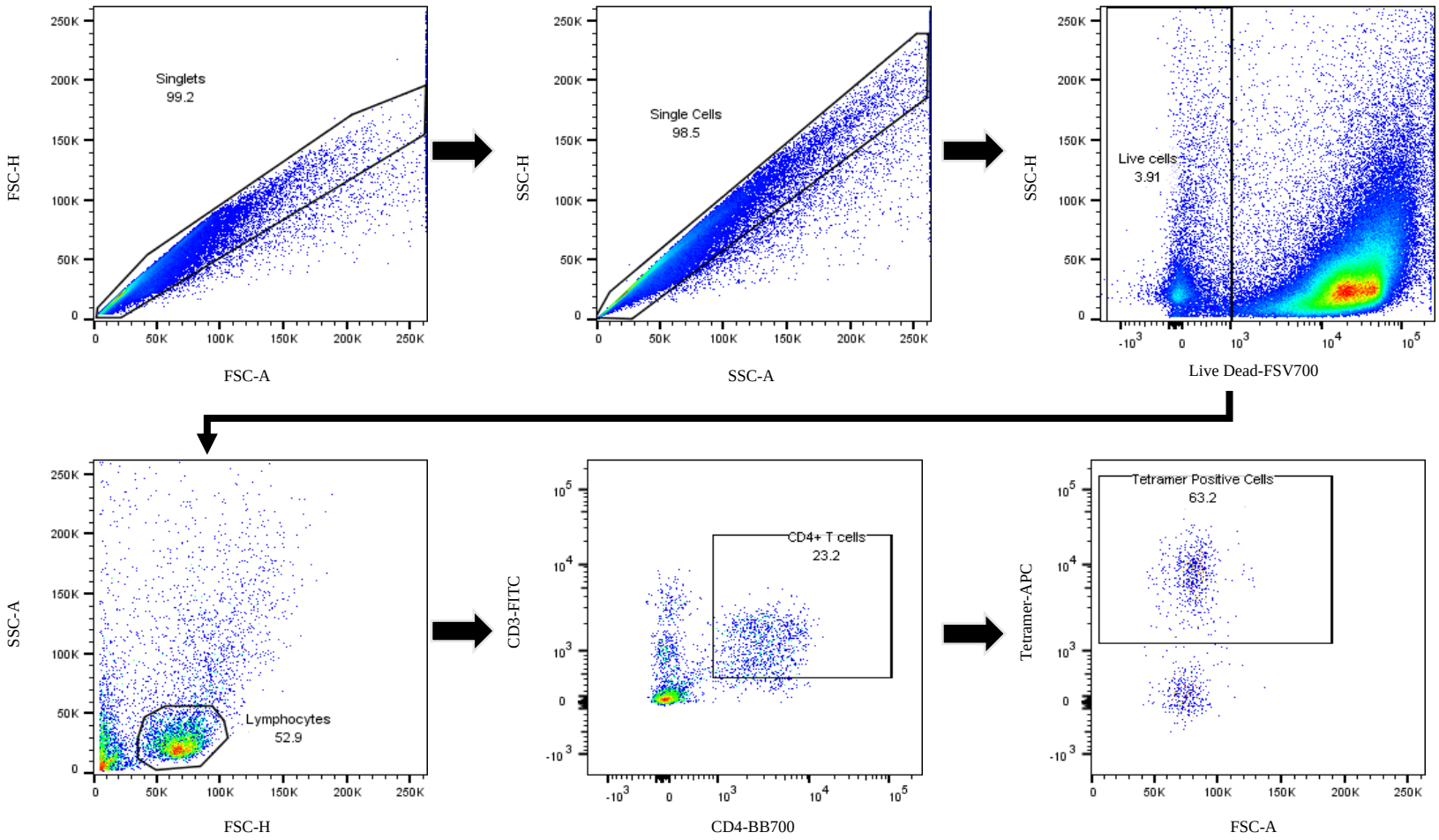

Figure 6.3: Flow cytometry of enzymatically digested lung cells following tetramer enrichment.

Dot blots show the gating strategy used to identify CD4+ T cells in immunised mice that were specific for the MHC class II molecule containing the Ag85B peptide following tetramer enrichment.

The number of CD4+ peptide specific T cells per lung was determined as in the pilot study by cell counts and flow cytometry.

The number of tetramer positive CD4+ T cells was determined as a percentage of the total CD4+ cell population (figure 6.4 A) and also expressed as total number of tetramer positive cells (figure 6.4 B).

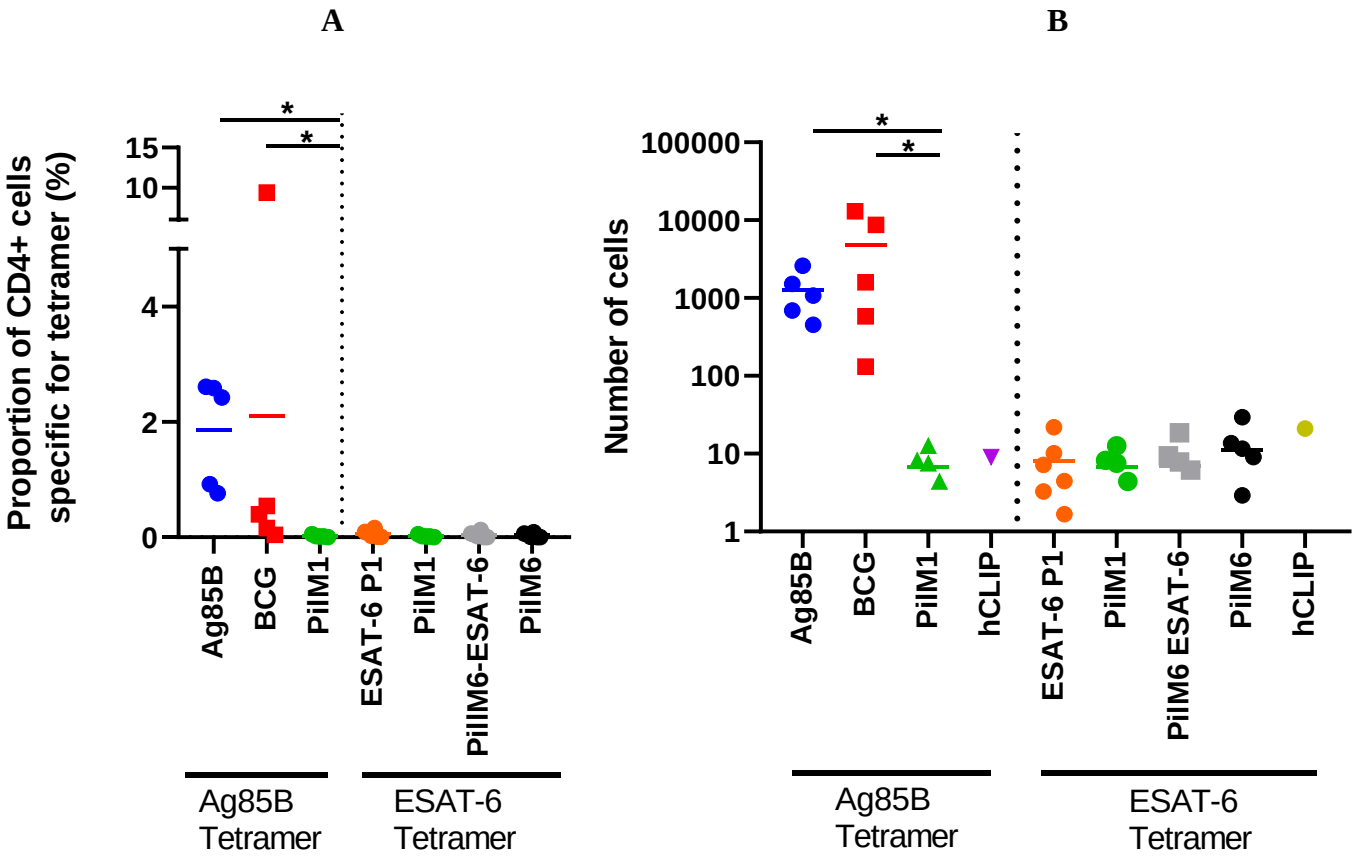

Figure 6.4: Comparison of peptide specific CD4+ T cells post vaccination.

C57BL/6 mice (n=6) were immunised and the proportion of peptide specific CD4+ T cells in the lungs (A) and total number of peptide specific CD4+ T cells in the lungs (B) were measured by flow cytometry and cell counts. Each data point represents cells from an individual mouse and the mean of each group is shown as a horizontal bar. Staining with hCLIP tetramer was used as a nonspecific control in a pooled sample of cells. A) *$p<0.05$ by way of Kruskall Wallace test B) *$p<0.05$ by way of ANOVA using Tukey analysis.

The proportion of CD4+ T cells in the lungs of vaccinated mice that were peptide specific was significantly higher than the negative control in both the PilVax-Ag85B and BCG vaccinated groups. In both groups, the mean percentage of total CD4+ T cells that were peptide specific was close to 2% (figure 6.4 A). The number of CD4+ peptide specific T cells was also significantly higher in the PilVax-Ag85B and BCG vaccinated mice when compared to PilM1 control group, and the nonspecific binding (figure 6.4 B). There was also no significant difference in the number of CD4+ peptide specific T cells between these vaccination groups.

In contrast, mice vaccinated with the PilVax-ESAT-6 P1 and PilVax-PilM6-ESAT-6 constructs did not have any detectable CD4+ peptide specific T cells in the lungs. Both vaccination groups resulted in 0% of total CD4+ T cells being peptide specific T cells. The number of peptide specific T cells was indistinguishable from their respective negative control and nonspecific binding.

As PilVax-ESAT-6 P1 and PilVax-PilM6-ESAT-6 vaccination did not result in any detectable CD4+ peptide specific T cells, these groups were not analysed any further in this section.

6.2.2 *Phenotypic determination of CD4+ peptide specific cells*

Cells determined to be CD4+ and peptide specific were further analysed using Flow Jo to assess selected cell surface markers. Although the PilM1 group has no CD4+ peptide specific cells, the values obtained correspond to nonspecific binding.

The immunological markers CD44, CD69 and CD62L and their expression in response to vaccination was examined among CD4+ peptide specific cells. Typically activated T cells are CD44+ while expression levels of CD62L can be used to discriminate T cell phenotype. $T_{Central\ Memory}$ cells are CD62L+ while $T_{Effector\ Memory}$ cells are CD62L (Baaten et al., 2010; S. Yang et al., 2011). CD69 is used to identify $T_{Resident\ Memory}$ cells (Cibrian & Sanchez-Madrid, 2017).

Large numbers of cells were found to express CD44, high levels of CD69 and low levels of CD62L (figure 6.5).

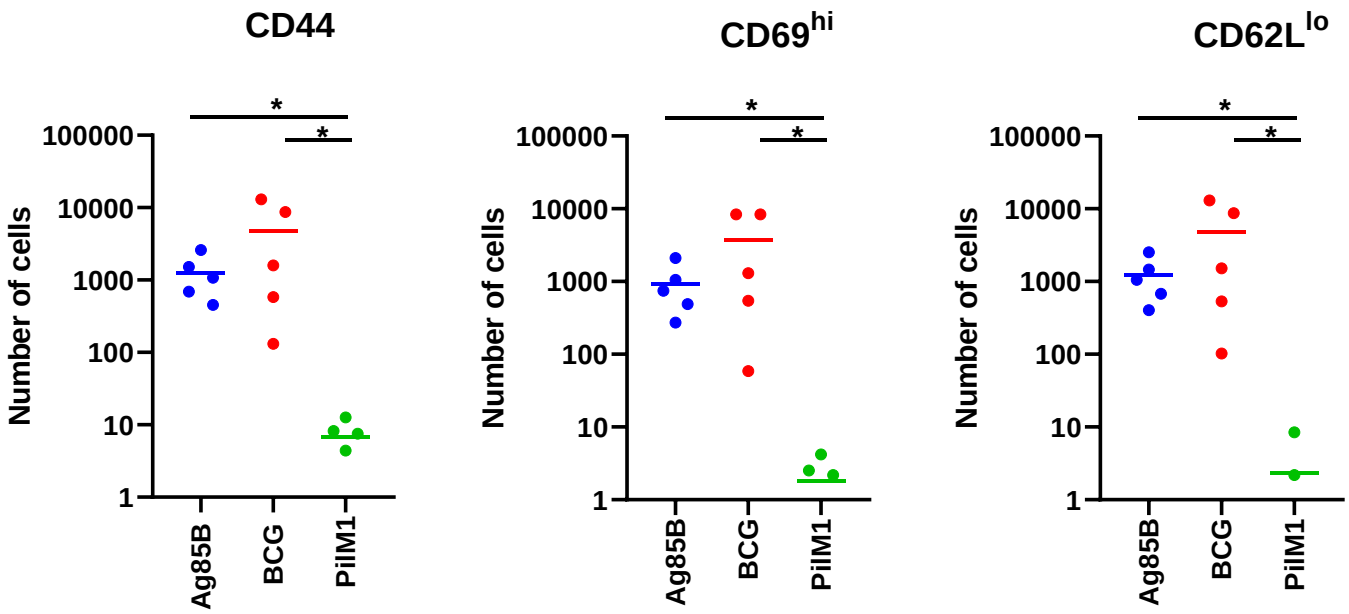

Figure 6.5: Expression of individual immunological cell surface markers on CD4+ peptide specific T cells.

Peptide specific CD4+ T cells from the lungs of vaccinated C57BL/6 mice (n=6) were analyzed for the level of expression of CD44, CD69 and CD62L. The number of cells expressing each marker was measured using flow cytometry. Each data point represents cells from an individual mouse and the mean of each group is shown as a horizontal bar. *$p<0.05$ by way of ANOVA using Tukey analysis.

Individually, almost all cells expressed CD44, high levels of CD69 and low levels of CD62L. These cell markers can also be used to determine T cell lineage. Boolean gating allowed the phenotype of CD4+ peptide specific T cells to be determined by analysing the combinations of each cell surface marker is being expressed (figure 6.6). In both vaccination groups almost 100% of cells expressed CD44 and a majority of cells expressed CD44 and high levels of CD69. The majority of cells displayed a T_{RM} phenotype ($CD44^{+}CD69^{hi}CD62L^{lo}$), 64.4% and 73.8% in the PilVax-Ag85B and BCG groups respectively. The next most common cells in both groups was T_{EM} ($CD44^{+}CD69^{lo}CD62L^{lo}$) (29.8% and 16.2%) while the remaining, and least common phenotype was T_{CM} ($CD44^{+}CD69^{lo}CD62L^{hi}$). In the PilVax-Ag85B group there

was a significant difference between the T_{EM} and T_{CM} cell populations while there was no difference in the BCG vaccinated mice.

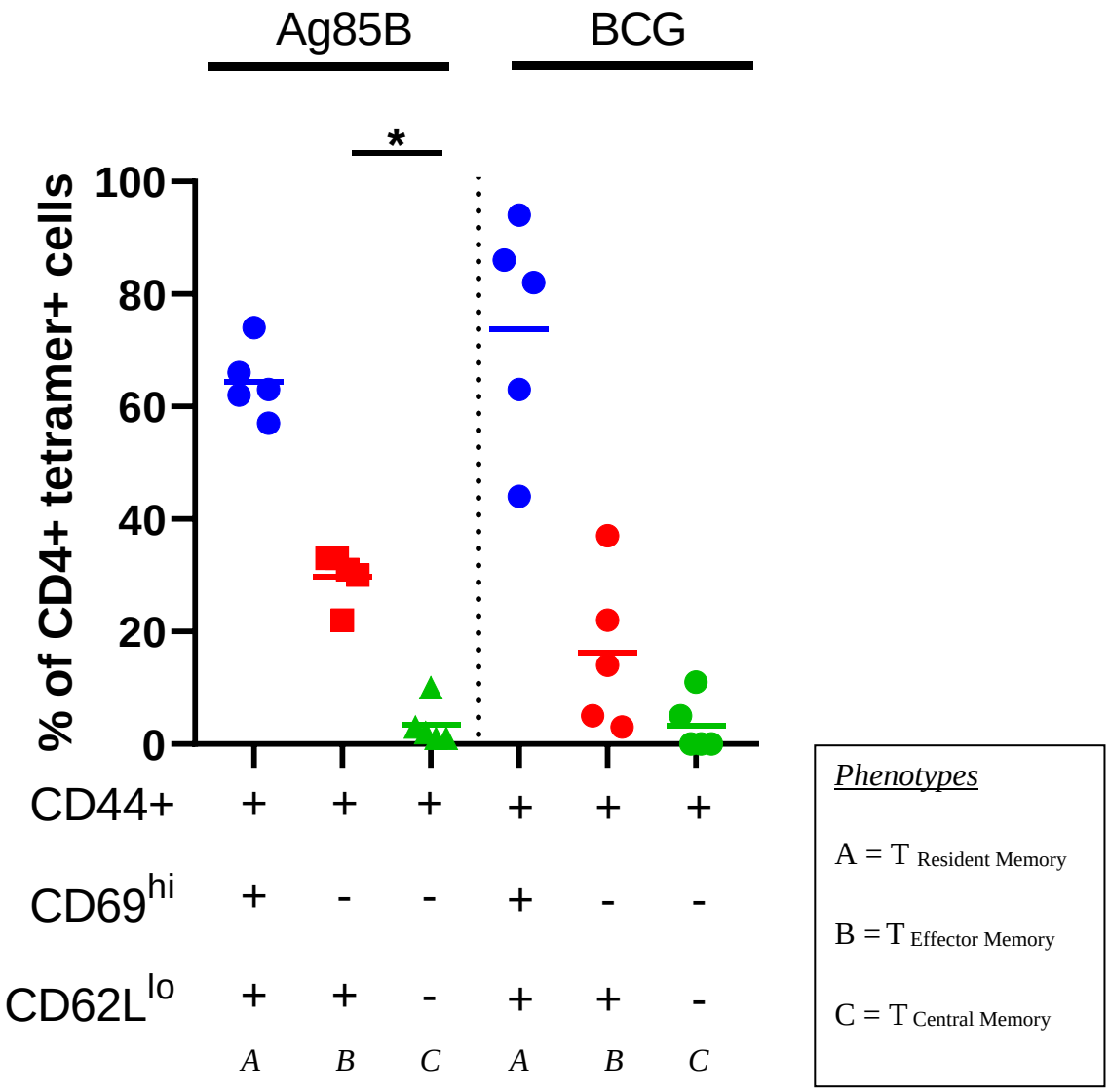

Figure 6.6: Phenotypical determination of CD4+ peptide specific T cells.

Percentage of total peptide specific CD4+ T cells from the lungs of vaccinated C57BL/6 mice (n=6) expressing combinations of each marker. Expression of CD44, CD69 and CD62L was measured using flow cytometry. Each data point represents cells from an individual mouse and the mean of each group is shown as a horizontal bar. *p<0.05 by way of Mann-Whitney test analysis.

In addition to CD4+ T cell specific responses this study also aimed to characterise the pulmonary T cell phenotypes, as well as measuring the cytokine response after re-stimulation with cognate peptide. Identifying the proportion of CD4+ and CD8+ T cell subsets was carried out to assess how PilVax was affecting the local lymphocyte population subsets. Lymphocytes were re-stimulated with cognate peptide to identify the function of PilVax induced peptide specific T cells.

Lymphocytes isolated from the lungs as in the previous section, were counted and seeded in a 24 well plate at 10^6 cells per well. Cells were incubated with 1 µg of cognate peptide and incubated at 37ºC for 12 hours. The PilM1 and PilM6 negative controls were pooled and incubated with each peptide individually.

Brefelden A was added at a final concentration of 10 µg/mL for 5 hours to stop the export of cytokines. Re-stimulated cells were harvested and stained for surface and intracellular markers as per the panel in table 3.8 and analysed using a BD LSRFortessa flow cytometer.

The vaccination groups for this portion of the experiment included all of the PilVax constructs generated and BCG.

6.2.3.1 ***T cell subsets***

The proportion of CD3+ T cell subsets was determined by analysis of the cell surface markers using flow cytometry. Cells were gated to identify the CD3+ T cell population and this population further characterised using CD4 and CD8 markers (figure 6.7). This analysis was able to identify CD4+, CD8+ and double negative (DN) CD3+ T cells.

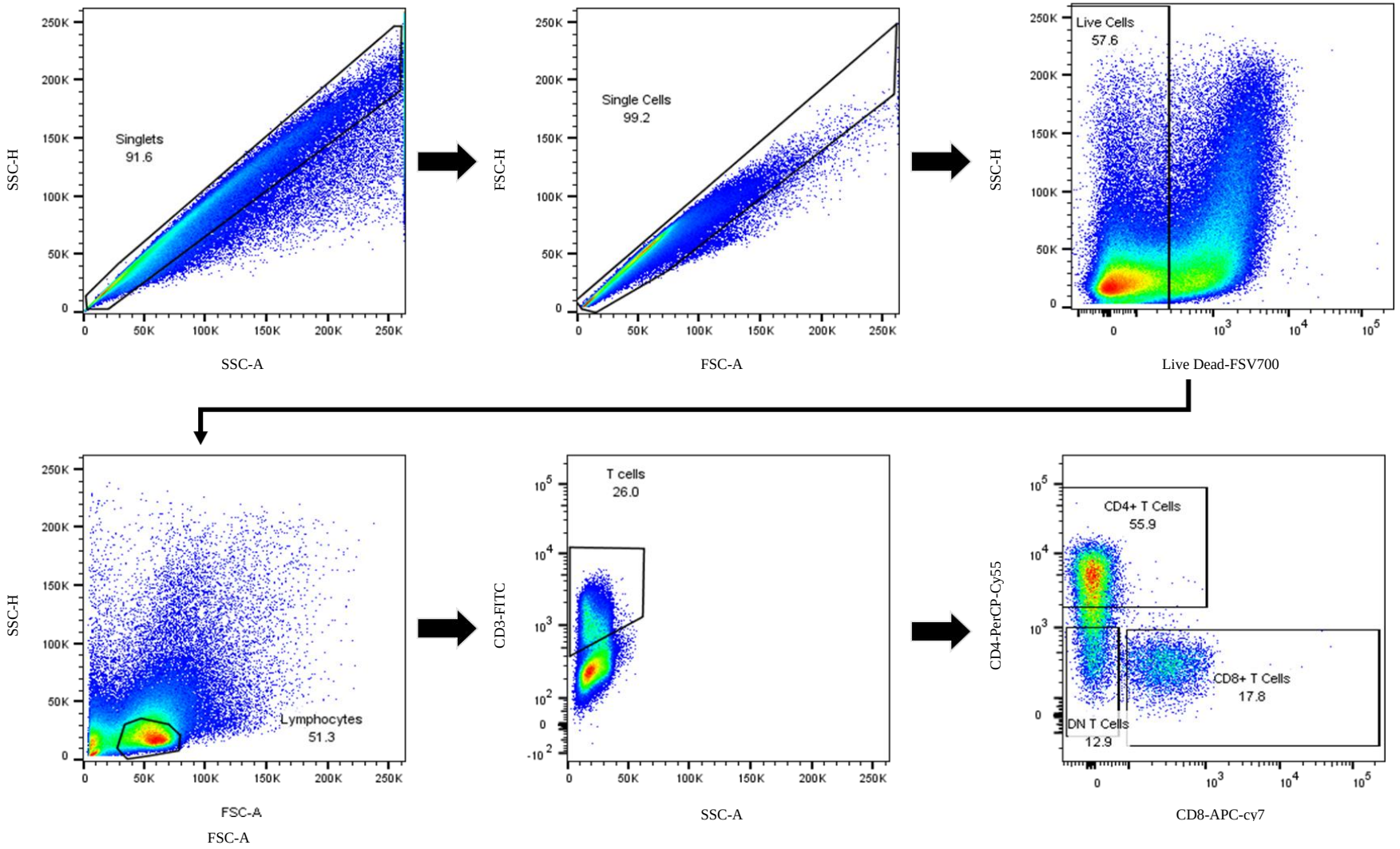

Figure 6.7: Flow cytometry on enzymatically digested lung cells following re-stimulated with cognate peptide.

Dot blots show the gating strategy used to identify subsets of CD3+ T cells in immunised mice following stimulation with cognate peptide.

The proportion of each CD3+ T cell subset (CD4+, CD8+ or double negative CD3+ cells) was determined for each mouse by gating the desired surface markers following flow cytomety and the mean of each subset from the BCG and PilVax constructs contaninng PilM1 + peptide vaccination groups plotted in figure 6.8.

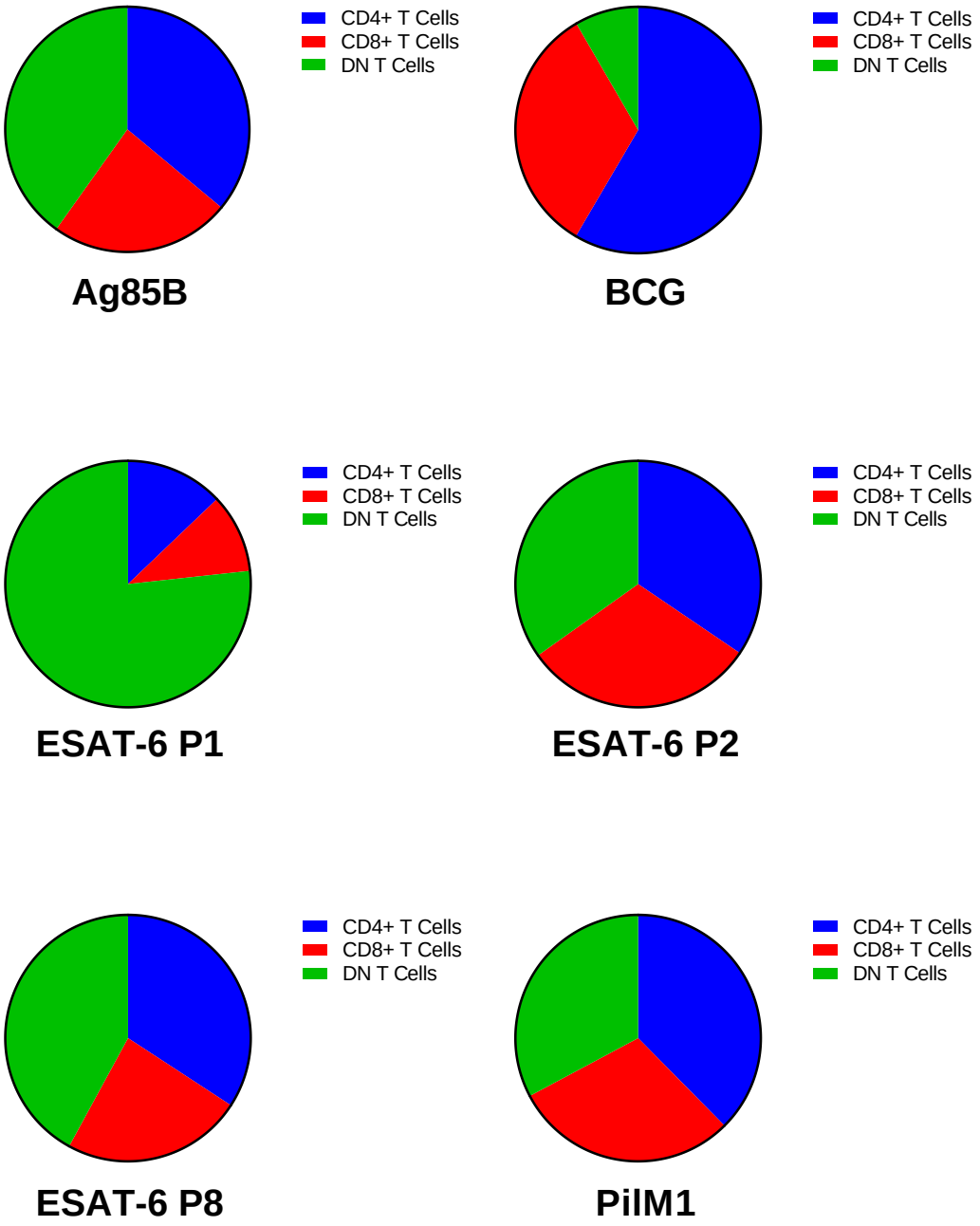

Figure 6.8: Proportion of pulmonary CD3+ T cell subsets in vaccinated mice vaccinated with PilVax-PilM1 constructs following re-stimulation with cognate peptide.

C57BL/6 mice (n=6) were immunised and pulmonary lymphocytes isolated following enzymatic digestion of the lungs. Cells were re-stimulated with their cognate peptide (PilM1 stimulated with each peptide individually) and the proportion of each CD3+ T cell subset was determined by flow cytometry. The mean of each CD3+ subset within each vaccination group is shown.

In the BCG vaccinated group, following stimulation with the Ag85B peptide the proportion of CD4+, CD8+, and double negative (DN) CD3+ T cells matched the distribution of cells that would be expceted in unvaccinated mice. The vast majority of cells were CD4+ T cells, with DN CD3+ cells accounting for a very small portion of the cell population. Mice vaccinated with PilVax however had a significantly altered distribtuion of CD3+ T cell subsets regardless of the peptide contained within it. The most profound effect was seen in PilVax-ESAT-6 P1 vaccinated mice where over 75% of the CD3+ cells were double negative, expressing neither CD4 or CD8. The remaining cells were relatively evenly split between CD4+ and CD8+ expression. The other peptides Ag85B, ESAT-6 P2, P8 were not as significantly altered compared to ESAT-6 P1, however the DN CD3+ T cells accounted for at least 30% of the cells present.

Cells from the PilVax-PilM1 vaccinated group also exhibited an altered CD3+ T cell subset. A sample of cells from these mice were pooled and incubated with each peptide indivudally. The mean of the proportion of CD3+ T cells from each peptide stimulation was obtained and displayed in figure 6.8.

The proportion of each CD3+ T cell subset was also determined in the same manner for the PilM6-ESAT-6 and PilM6 constructs (figure 6.9). Cells from the PilM6-ESAT-6 vaccinated mice were stimulated with each of the ESAT-6 peptides. The proportion of CD3+ T cell subsets was altered in commparion to BCG vaccinated mice (figure 6.8). The proportion of DN CD3+ T cells was increased when stimulated with all three peptides and less than half of the cells were CD4+.

Cells from the PilVax-PilM6 vaccinated group also exhibited an altered CD3+ T cell subset. A sample of cells from these mice were pooled and incubated with each peptide indivudally. The mean of the proportion of CD3+ T cells from each peptide stimulation was obtained and displayed in figure 6.9.

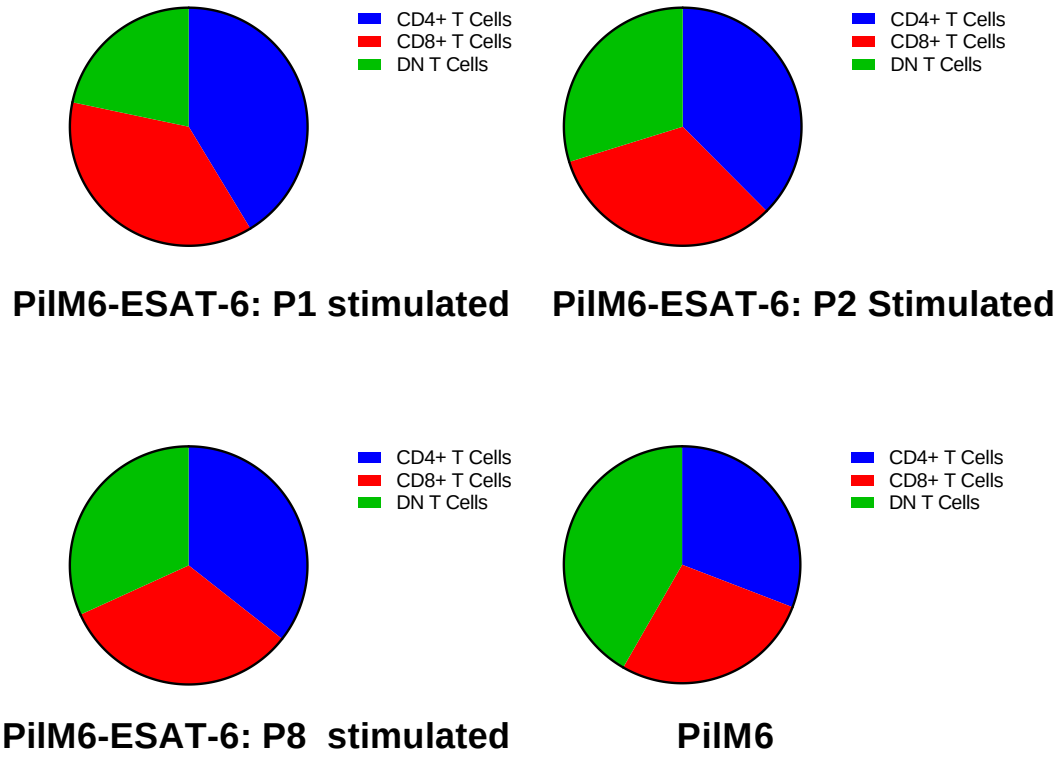

Figure 6.9: Proportion of pulmonary CD3+ T cell subsets in vaccinated mice vaccinated with PilVax-PilM6 constructs following re-stimulation.

C57BL/6 mice (n=6) were immunised and pulmonary lymphocytes isolated following enzymatic digestion of the lungs. Cells were re-stimulated with their cognate peptide (PilM6 stimulated with each peptide individually) and the proportion of each CD3+ T cell subset was determined by flow cytometry. The mean of each CD3+ subset within each vaccination group is shown.

6.2.3.2 ***Cytokine profile***

Re-stimulating cells from each vaccination group with their cognate peptide was carried out to analyse the production of selected cytokines to further characterise the cellular response. Each subset of CD3+ T cells identified previously were analysed for their production of certain cytokines using antibodies against IL-2, IL-17, INF-γ and TNFα.

Following identification of the T cell subsets through gating (figure 6.7) each population was further analysed by gating to identify the presence of the aforementioned cytokines (figure 6.10).

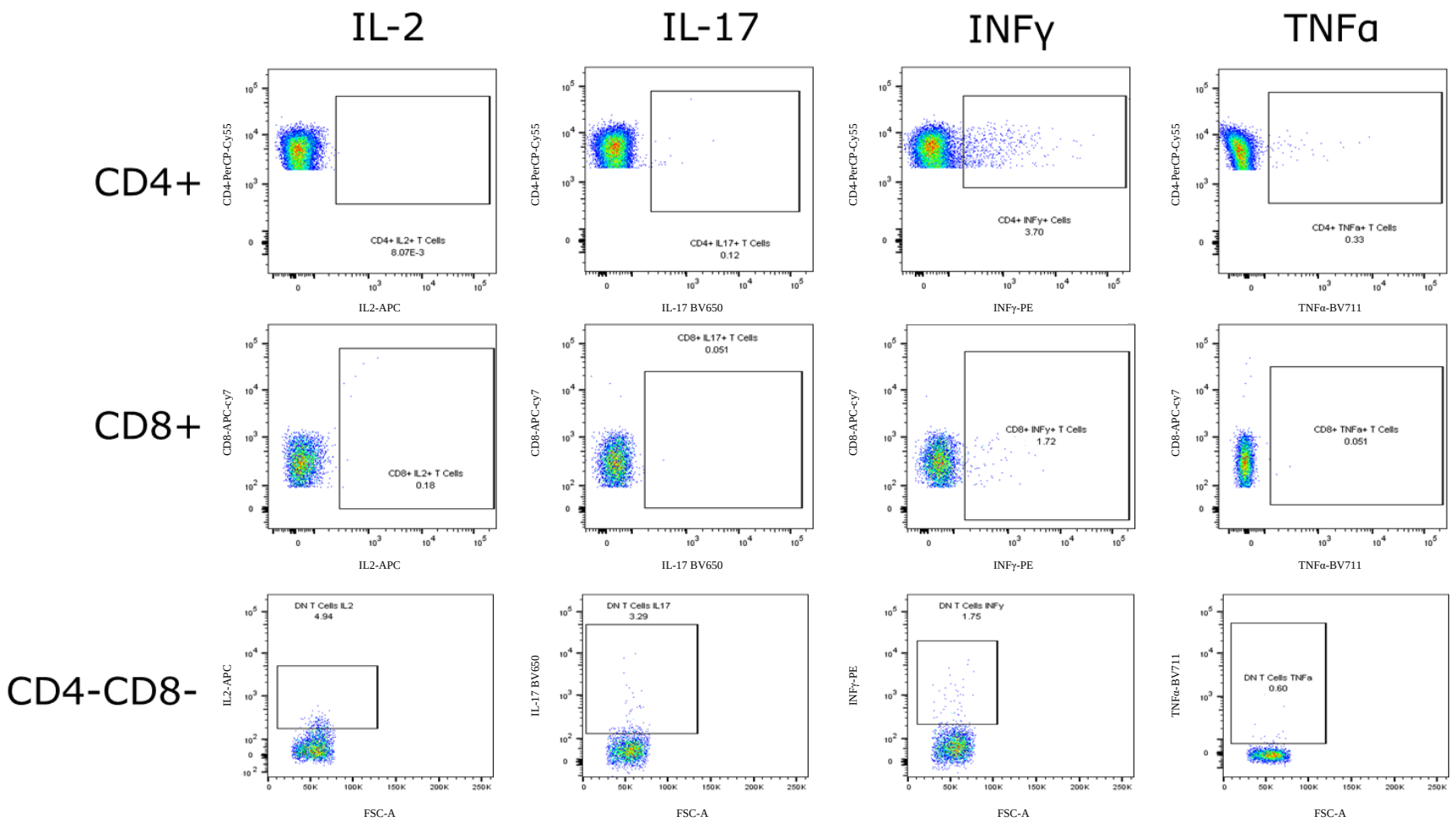

Figure 6.10: Flow cytometry on enzymatically digested lung cells following re-stimulated with cognate peptide for cytokine detection following the identification of CD3+ T cell subsets.

Dot blots show the gating strategy used to identify the production of cytokines in three distinct subsets of CD3+ T cells in immunised mice following stimulation with cognate peptide.

Boolean gating analysed the combinations of cytokines produced to detect cells that were producing a single, or multiple cytokines in each CD3+ T cell subset. Data was also analysed using t-SNE analysis in FlowJo (FlowJo LLC) however this did not provide insihgts into the analysis that Boolean gating was unable to identify (Appendix II. page 193).

Following re-stimulation, the majority of CD4+ T cells in PilVax-Ag85B and BCG vaccinated mice that produced cytokines only produced INF-γ (figure 6.11). The proportion of CD4+ T cells that expressed INF-γ was higher in BCG vaccinated mice while a small portion of cells from the PilVax-Ag85B vaccinated mice also produced INF-γ and IL-17. In either group no cells were producing three or four cytokines.

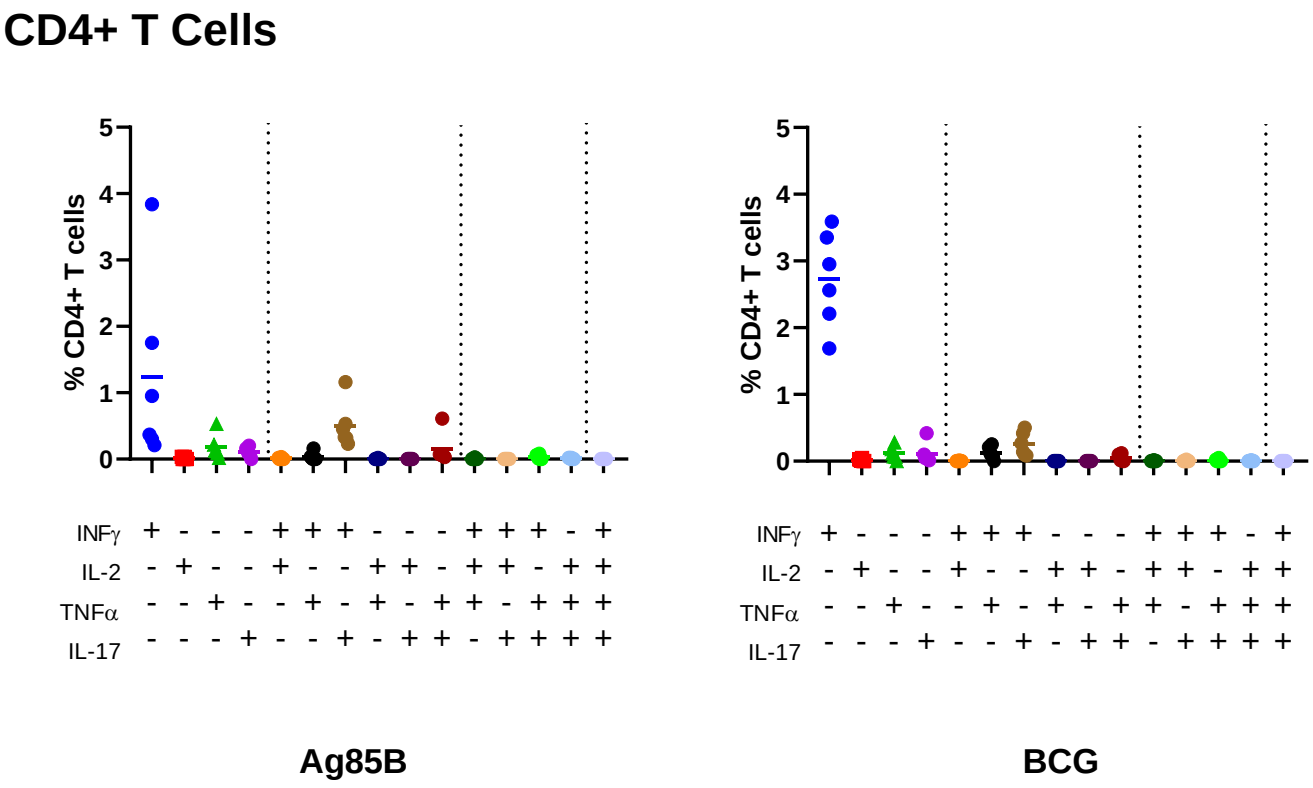

Figure 6.11: Cytokine profile of CD4+ T cells from the lungs of PilVax-Ag85B and BCG vaccinated mice.

CD4+ T cells from the lungs of vaccinated C57BL/6 mice (n=6) were analyzed for the production of IL-2, IL-17, INF-γ and TNFα. Production of cytokines was measured using flow cytometry and Boolean gating to determine the combinations of cytokines produced by cells. Each data point represents cells from an individual mouse and the mean of each group is shown as a horizontal bar.

Vaccination with the PilVax-ESAT-6 peptides resulted in the generation of CD4+ T cells that produced INF-γ /IL-17 following re-stimulation with cognate peptide (figure 6.12 A). The highest proportion of cells that were producing this cytokine combination was observed in PilVax-ESAT-6 P1 vaccinated mice, followed by PilVax-ESAT-6 P8 and then PilVax-ESAT-6 P2 vaccinated mice. Asterisks indicate where the mean of a given cytokine combination is higher than the mean when PilM1 was re-stimulated with the relevant peptide.

CD4+ T cells from mice vaccinated with the PilM6-ESAT-6 constructs did not produce cytokines following stimulation with the P2 or P8 peptide (figure 6.12 B). There was however a small proportion of cells that produced a multiple combinations of cytokines following stimulation with the P1 peptide (figure 6.12 B).

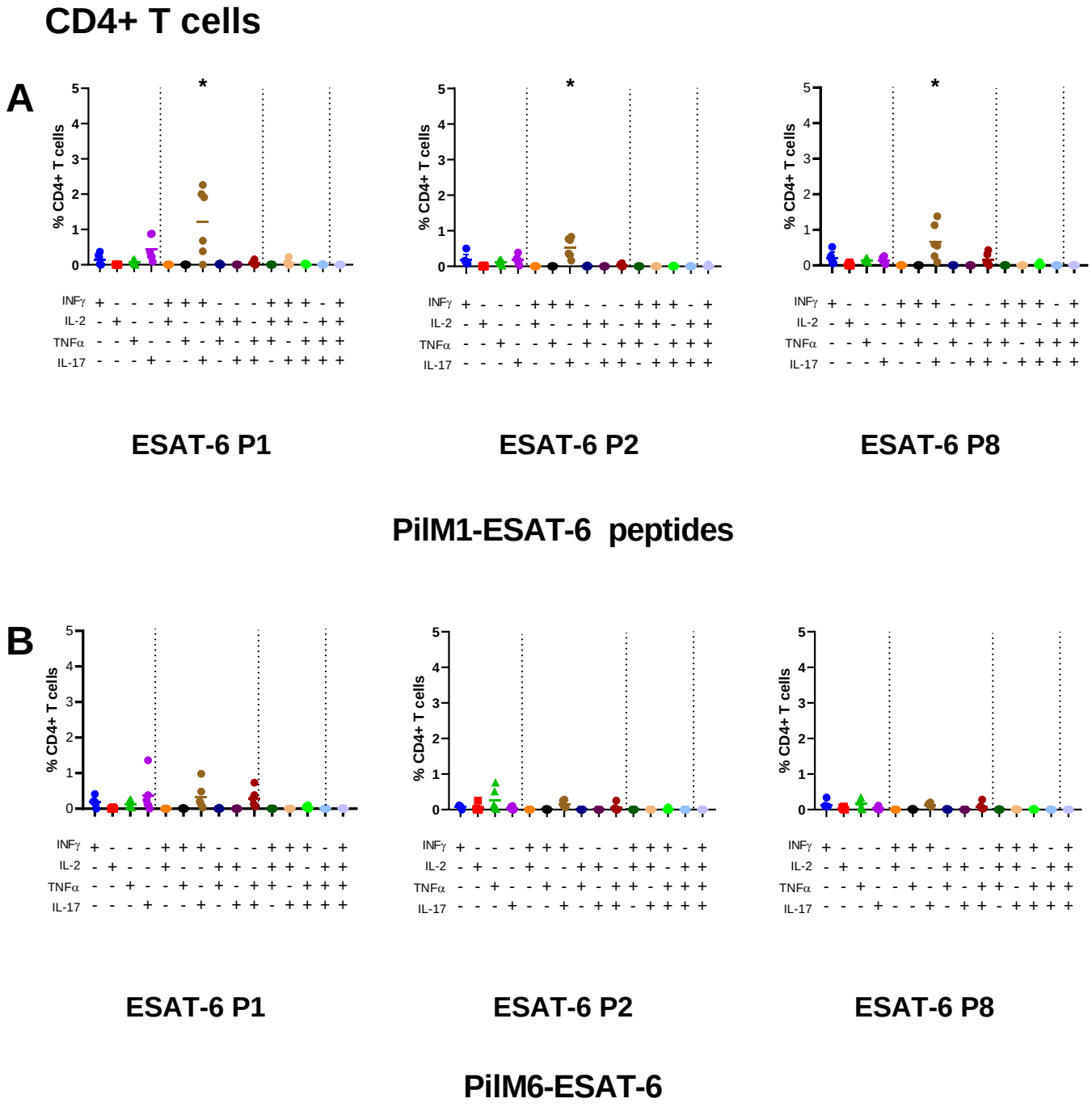

Figure 6.12: Cytokine profile of CD4+ T cells from the lungs PilVax-ESAT-6 vaccinated mice.

CD4+ T cells from the lungs of vaccinated C57BL/6 mice (n=6) were analyzed for the production of IL-2, IL-17, INF-γ and TNFα. Production of cytokines was measured using flow cytometry and Boolean gating to determine the combinations of cytokines produced by cells. Each data point represents cells from an individual mouse and the he mean of each combination is shown as a horizontal bar. Asterisks indicate where the mean of a given cytokine combination is higher than in re-stimulated PilM1.

The production of cytokines in CD8+ T cells from PilVax-Ag85B and BCG vaccinated mice was lower than in CD4+ T cells. In BCG vaccinated mice, the vast majority of CD8+ T cells producing cytokines were producing INF-γ following re-stimulation (figure 6.13). This proportion of cells producing INF-γ is higher than in PilVax-Ag85B where re-stiumlation does not appear to have resulted in the generation of a significant amount of CD8+ T cells producing INF-γ.

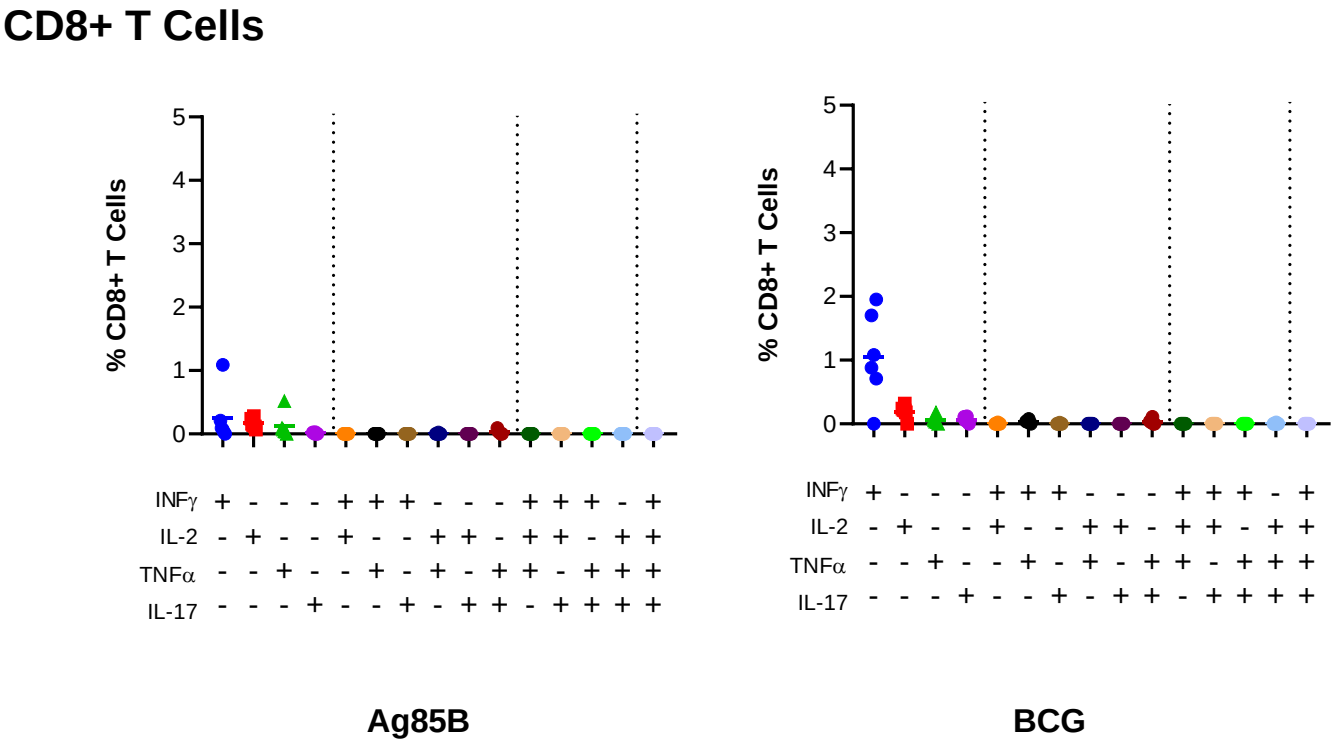

Figure 6.13: Cytokine profile of CD8+ T cells from the lungs of PilVax-Ag85B and BCG vaccinated mice.

CD8+ T cells from the lungs of vaccinated C57BL/6 mice (n=6) were analyzed for the production of IL-2, IL-17, INF-γ and TNFα. Production of cytokines was measured using flow cytometry and Boolean gating to determine the combinations of cytokines produced by cells. Each data point represents cells from an individual mouse and the mean of each groups is shown as a horizontal bar.

Vaccination with the PilVax-ESAT-6 peptides or PilM6-ESAT-6 did not result in the generation of CD8+ T cells that produced cytokines following re-stimulation with cognate peptide (figure 6.13).

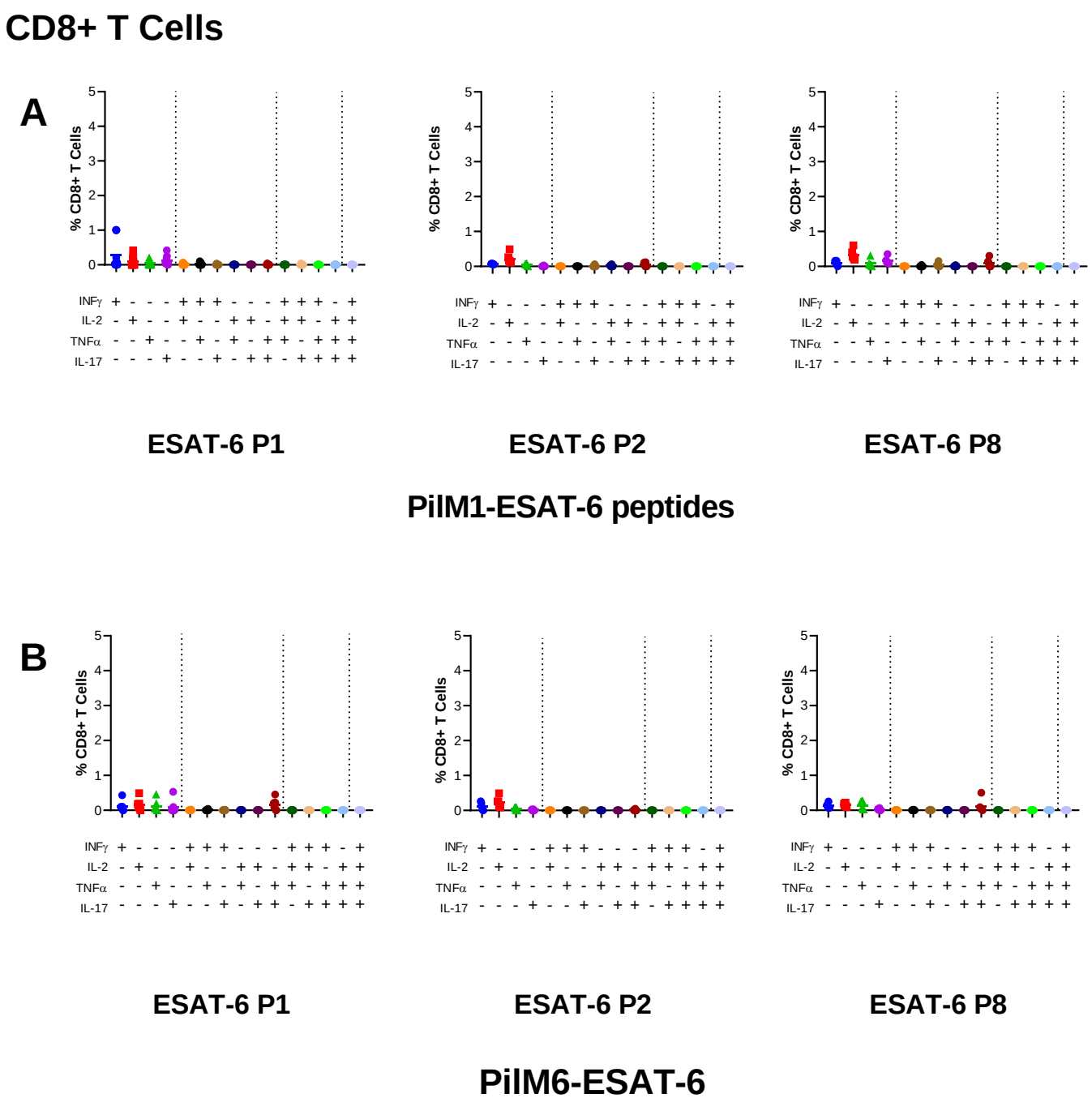

Figure 6.14: Cytokine profile of CD8+ T cells from the lungs PilVax-ESAT-6 vaccinated mice.

CD8+ T cells from the lungs of vaccinated C57BL/6 mice (n=6) were analyzed for the production of IL-2, IL-17, INF-γ and TNFα. Production of cytokines was measured using flow cytometry and Boolean gating to determine the combinations of cytokines produced by cells. Each data point represents cells from an individual mouse and the mean of each group is shown as a horizontal bar.

Analysis of CD3+CD4-CD8- T cells from PilVax-Ag85B and BCG vaccinated mice showed a borader range of cytokine production compated to CD4+ and CD8+ T cells (figure 6.15). The cells from both vaccination groups almost exclusively produced only one cytokine with all of the cytokines tested for detected. The production of cytokines was higher in the BCG vaccinated mice compared to PilVax-Ag85B vaccinated mice, athough the proportion of cells producing each cytokine was more variable among the former vaccination group.

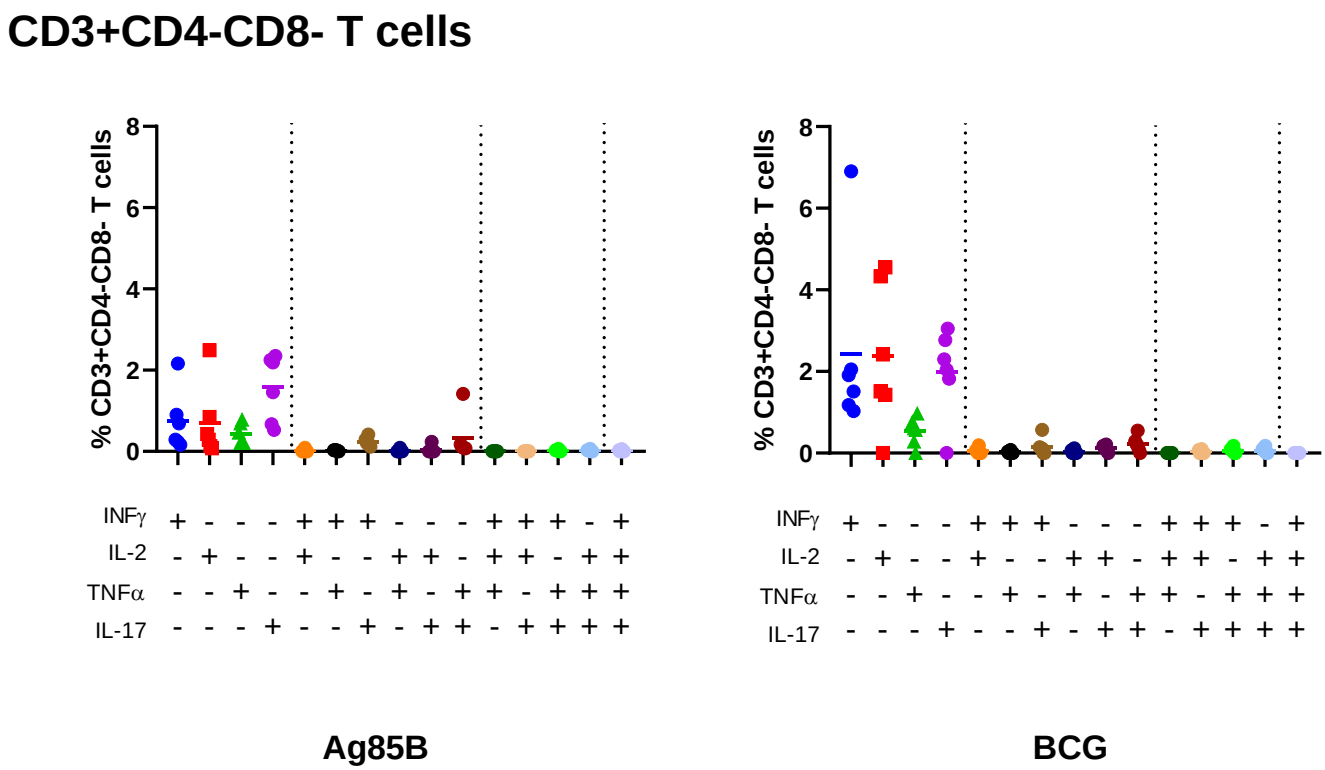

Figure 6.15: Cytokine profile of CD3+CD4-CD8- T cells from the lungs of PilVax-Ag85B and BCG vaccinated mice.

CD3+CD4-CD8- T cells from the lungs of vaccinated C57BL/6 mice (n=6) were analyzed for the production of IL-2, IL-17, INF-γ and TNFα. Production of cytokines was measured using flow cytometry and Boolean gating to determine the combinations of cytokines produced by cells. Each data point represents cells from an individual mouse and the mean of each group is shown as a horizontal bar.

PilVax-ESAT-6 vaccinated mice produced a broader range of cytokines following stimulation with cognate peptide compared to the CD4+ and CD8+ T cell populations (figure 6.16). Asterisks indicate where the mean of a given cytokine combination is higher than in re-stimulated PilM1.

In PilVax-ESAT-6 P1 mice vaccinated mice the highest proportion of CD3+CD4-CD8- T cells that produced cytokines only made IL-17 following restimulation with cognate peptide (figure 6.16 A). The mean proprotion of cells producing IL-17 following stimulation with P2 in PilVax-ESAT-6 P2 vaccinated mice is not higher than the mean when PilM1 is stimulated with the P2 peptide. In PilVax ESAT-6 P8 vaccinated mice the major proportion of cells producing cytokines produced INF-γ/IL-2.

CD3+CD4-CD8- T cells from mice vaccinated with the PilM6-ESAT-6 construct resulted in cells producing primarily INF-y and INF-y/TNFα when re-stimulated with the P1 peptide, and IL-17 alone when stimulated with the P2 or P8 peptide (figure 6.16 B).

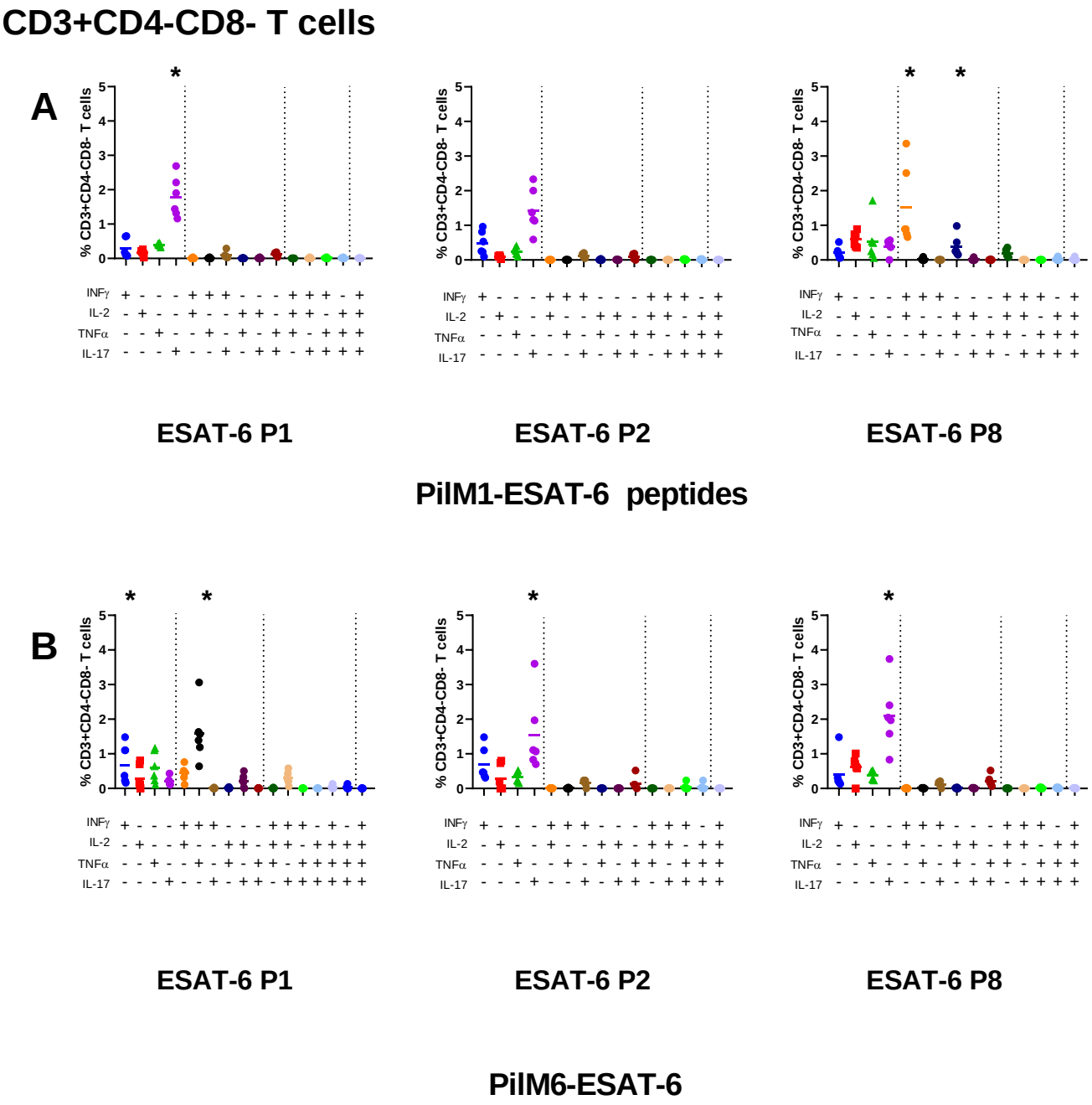

Figure 6.16: Cytokine profile of CD3+CD4-CD8- T cells from the lungs of PilVax-ESAT-6 vaccinated mice.

CD3+CD4-CD8- T cells from the lungs of vaccinated C57BL/6 mice (n=6) were analyzed for the production of IL-2, IL-17, INF-γ and TNFα. Production of cytokines was measured using flow cytometry and Boolean gating to determine the combinations of cytokines produced by cells. Each data point represents cells from an individual mouse and the mean of each group is shown as a horizontal bar. Asterisks indicate where the mean of a given cytokine combination is higher than in re-stimulated PilM1.

6.3. Peptide specific lymph node resident T cells

The expanded study also aimed to determine if there was localisation of peptide specific CD4+ T cells elsewhere in the mouse by investigating the presence of such cells in the mediastinal lymph node.

Prior to the dissection of the lungs from vaccinated mice, the mediastinal lymph node was dissected. Due to the low number of recoverable cells from the lymph nodes, for each vaccination group all six lymph nodes were pooled and analysed together rather than individually. The lymph nodes were not enzymatically digested but were processed in the same manner as the lungs with regards to tetramer enrichment, cell surface staining, and analysis on a BD Fortessa flow cytometer. The gating to identify was the same as for the lungs in both the pilot study (figure 6.1 and 6.3) and the number of CD4+ peptide specific T cells determined in the same manner previously described.

Peptide specific CD4+ T cells in the mediastinal lymph node were only detected in the BCG vaccination group, and the number of cells was higher than in the PilM1 negative control and nonspecific binding groups (figure 6.17).

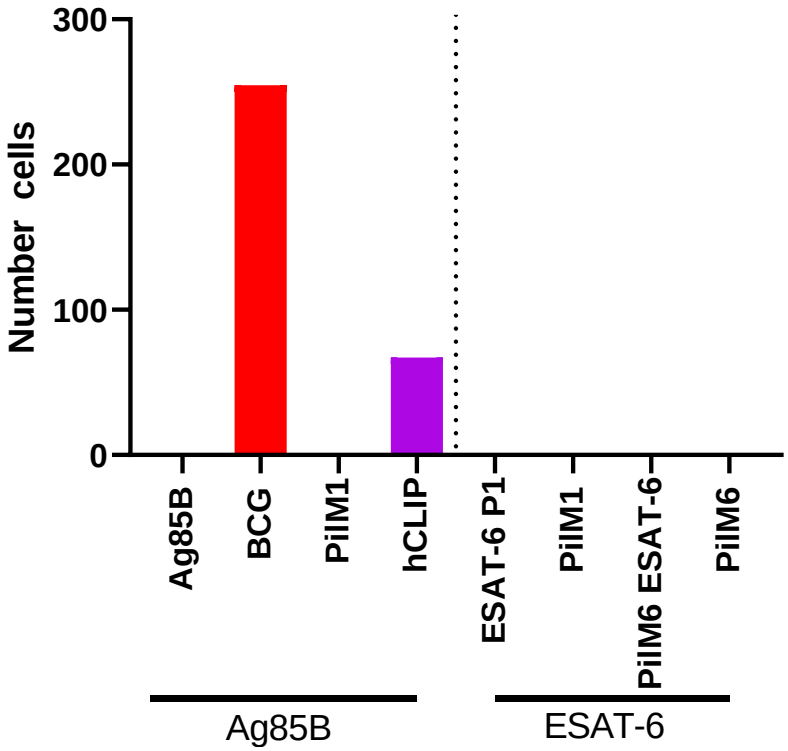

Figure 6.17: Comparison of lymph node CD4+ peptide specific T cells post vaccination.

C57BL/6 mice (n=6) were immunised and the number of peptide specific CD4+ T cells in the mediastinal lymph node was measured by flow cytometry and cell counts. The lymph nodes from each vaccination group were pooled and the number of cells detected is shown per vaccination group. Staining with hCLIP tetramer was used as a nonspecific control in a pooled sample of cells.

6.4. Summary

The pilot study revealed PilVax-Ag85B vaccination is able to elicit a T cell response similar to when mice are vaccinated with BCG in regard to the the proportion of pulmonary CD4+ T cells that are peptide specific. As a result the study was expanded to analyse all of the PilVax constructs that were generated in chapter 4.

Where a tetramer was avalible to detect peptide specific cells, the characteristics of CD4+ peptide specific cells in those vaccination groups further scrutinised. CD4+ peptide specifc pulmonary cells were dected in PilVax-Ag85B and BCG immunised mice. The proportion of peptide specific CD4+ T cells out of the total CD4+ T cell population was similar in both gorups, as was the absolute number of peptide specific CD4+ T cells. The major phenotype of these cells in both groups was $T_{\text{Resident Memory}}$ followed by $T_{\text{Effector Memory}}$ and $T_{\text{Central Memory}}$ respectively. No CD4+ peptide specific T cells were detected in mice vaccinated with PilVax-ESAT6 P1 or PilM6-ESAT-6.

For all of the PilVax constructs, following vaccination and restimulation with cognate peptide the pulmonary CD3+ T cell sub populations was determined with CD4 and CD8 antibodies. While BCG vaccinated mice exhibited a typical T cell subset distibution, all of the mice vaccinated with a PilVax construct had an elevated proportion of CD3+CD4-CD8- T cells regardless of the peptide contained within the construct. The largest altered distriubtion of T cell subsets was seen in PilVax-ESAT-6 P1 immunised mice where over 75% of the T cells were CD3+CD4-CD8-.

Analysis of the cytokines produced by each T cell subset post stimulation with cognate revealed production of cytokines was limited to CD4+ and CD3+CD4-CD8- T cells. The most signifiacnt production of cytokines occurred in BCG and PilVax-Ag85B vaccinated mice where the predominant cytokine was INF-γ in CD4+ T cells. Of the CD3+CD4-CD8- T cells

that produced cytokines, there were cells producing a single cytokine, with all of the cytokines tested detected. In both cases there was a higher proportion of cells producing cytokines in BCG vaccinated mice compared to PilVax-Ag85B vaccinated mice.

CD4+ peptide specifc cells were also found in the mediastinal lymph nodes of BCG vaccinated mice though they were unable to be detected in any other group.

6.5. Discussion

6.5.1 ***Pilot study***

To date the ability of PilVax to stimulate the cellular response had not been analysed. In the pilot study, mice were intinally vaccinated with only the PilVax-Ag85B and BCG. The presence of the Ag85B protein in *M. bovis* allows the BCG vaccinated mice to act as a positive control. The variability in number of specific CD4+ T cells in BCG vaccinated mice (figure 6.4) is reflected in other studies where BCG is administered as a single dose while vaccines administered as multiple doses such as H56/IC31, M72/AS01$_E$ and PilVax show a reduced variability in the number of specific T cells generated, (Rodo et al., 2019).

The presence of CD4+ Ag85B$_{281-295}$ specific cells in PilVax-Ag8B vaccinated mice provided the first evidence that PilVax is able to stimulate a T cell repsonse when the vaccine is delivered to the LRT. Although the number of CD4+ Ag85B$_{281-295}$ specific T cells was not high, as a proportion of total CD4+ T cells, the number of cells was comparible to BCG vaccinated mice. This indicates more cells were detected in BCG vaccinated mice due to the lungs from those mice having a higher cell number. In the subsequent study, the T cell resposne was further charaterised and expanded to include other vaccination groups.

6.5.2 ***Peptide specific pulmonary T cells***

6.5.2.1 ***PilVax-ESAT-6 constructs***

The vaccination groups that contained the ESAT-6_{1-20} peptide (P1, that matched the available tetramer) were included in this vaccination study on the basis that PilVax-Ag85B had demonstrated the ability of PilVax to generate peptide specific CD4+ T cells. ESAT-6_{1-20} tetramer-specific T cells were not detected in any immunisation group. However, as there is no positive control avaliable for this group, it could not be excluded that this was due to the technical failure of tetramer binding. As there was cytokine production following stimulation with cognate peptide this could also indicate the presence of CD4+ ESAT-6_{1-20} T cells, but at a level lower than the dection level of this assay. To definitivly understand this a positive control would be needed, either mice vaccinated with *Mtb* or *M. bovis* expressing ESAT-6. As both of these organisms would require PC3 containment, this is beyond the scope of this thesis.

6.5.2.2 ***PilVax-Ag85B and BCG vaccinated mice***

Analysis of the phenotypic markers CD44, CD69 and CD62L indicated the majority of tetramer positive cells expressed a T_{RM} phenotype in both PilVax-Ag85B and BCG vaccinated mice. This was confirmed with Boolean gating. The major difference observed between the two vaccination groups is a significant elevation in the T_{EM} population compared to the T_{CM} cell population in PilVax-Ag85B vaccinated mice.

In other studies, VPM1002 and BCG vaccination in mice induces a large number of T_{EM} that appear soon after vaccination but rapidly decline in number. The difference between VPM1002 and BCG vaccination lies in the longevity of the T_{CM} cellular population (Vogelzang et al., 2014). While the number of Ag85B peptide specific CD4+ T cells is similar in both BCG and VPM1002 vaccinated mice post challenge, the improved protection afforded by VPM1002 vaccination appears to lie in the phenotypic difference of the memory cells produced (Vogelzang et al., 2014). A prolonged T_{CM} cell population would result in a pool of Ag85B

specific cells with a high replicative capacity that would be able to quickly re-establish a T_{EM} cell population to home to the lungs an assist in controlling *Mtb* challenge. (Nieuwenhuizen et al., 2017). While the number of Ag85 peptide specific cells in PilVax-Ag85B and BCG vaccinated mice is similar to the numbers reported by Vogelzang et al 2014 following the VPM1002 and BCG vaccination, the phenotypic distribution seen in PilVax vaccinated mice is similar to BCG (figure 6.6). The localisation of Ag85B specific CD4+ T cells in the secondary lymphoid tissue in BCG vaccinated mice, but not PilAVax-Ag85B vaccinated mice (figure 6.17), combined with the higher proportion of T_{CM} cells in BCG vaccinated mice (figure 6.6) suggests PilVax may not have generated a long lived protective T_{CM} population as it is below the BCG 'baseline.' However it is not possible definitively conclude this without analysing the longevity of each memory phenotype in PilVax-Ag85B vaccinated mice. Additionally, as Vogelzang et al 2014 did not account for the role of T_{RM} cells, for comparative purposes these cells should also be analysed in VPM1002 vaccination. T_{RM} populations could reveal a further difference between VPM1002, PilVax, and BCG vaccination further explaining the potential differences in protection offered by each vaccine.

The presence of T_{RM} cells in PilVax vaccinated mice is promising as this cell type can rapidly respond to infection at the site of entry independent of recrutiment of additional T cells (Park & Kupper, 2015). These cells have shown to be protective in ther own right following BCG vaccination thus the ability of PilVax-Ag85B to stimulate a large proportion of this cell type is promising in regards to potential *Mtb* protection (Connor et al., 2010). Although present, T_{EM} cells have not typically been associated with protection against *Mtb* due to their lower replicative capacity and short term lives compared to the other cell types (Orme, 2010; Vogelzang et al., 2014; Wherry et al., 2003).

The T_{RM} cells detected in the BCG vaccinated group are relatively long lived, persisting six weeks after vaccination, however the longevitiy of these cells in PilVax-Ag85B vaccinated

mice is not currently known. Further work could assess the immune kinetics and longetivity of these cells in PilVax-Ag85B vaccinated mice compared to BCG vaccinated mice. Without knowing the kinetics of PilVax-Ag85B specific CD4+ T cells in mice it is not known if the mice in this study are being compared at similar time points in the development of peptide specific CD4+ T cells.

A recent study with a version of the H56 vaccine has demonstrated the number of H56 peptide specific cells two weeks post final immunisation is slightly higher (10^4) than the number of Ag85B tetramer specific cells in figure 6.4 in both the PilVax-Ag85B vaccination group and BCG vaccination groups (10^3) (Joshua S. Woodworth et al., 2019). These H56 specific cells were sustained with a one to two log reduction in number twenty two weeks post final immunisation which may provide insight into the longevity of PilVax induced T cell populations.

The vaccination regime used here utilised two subcutaneous immunisations and one intranasal dose. Interestingly, while this regime appeared to induce a larger, sustained T_{RM} population, this did not provide any extra protection in terms of CFU reduction following *Mtb* challenge compared to mice that received three subcutaneous doses (Joshua S. Woodworth et al., 2019). This suggests that a larger pool of anti-*Mtb* antigen T_{RM} cells does not necessarily contribute to improved protection where a vaccine already generates a smaller pool of these cells. It indicates the number of T_{RM} cells may not be able to be used as a reliable correlate of protection. Woodworth et al 2019 however did not interrogate the kinetics of the various phenotypes of H56 antigen specific memory T cells over time (Joshua S. Woodworth et al., 2019).

In another murine model, in BCG vaccinated mice the number of Ag85B specific CD4+ T cells peaked at 10^3 four weeks post vaccination and had decreased by one log twenty weeks post vaccination (Vogelzang et al., 2014). The mice used in this thesis were five weeks post

vaccination and the number of peptide specific cells had therefore likely peaked and was declining in number. Vogelzang et al 2014 also determined kinetics of Ag85B specific CD4+ T_{EM} and T_{CM} cells over time however did not investigate the role of T_{RM} cells. 5 weeks post vaccination the number of T_{EM} had decreased significantly from their peak one week post immunisation, while the number of T_{CM} remained steady over the time course of interest. This is reflected in figure 6.6 where the proportion of T_{EM} cells is lower and BCG vaccinated mice compared to PilVax-Ag85B, while the proportion of T_{CM} is slightly higher. Analysis of the longevity of T_{CM} and T_{RM} cells generated by PilVax vaccination could reveal a pathway by which PilVax-Ag85B vaccination may result in a different outcome compared with BCG.

The lack of a significant difference between the T_{EM} and T_{CM} T cell populations seen the BCG group compared to PilVax-Ag85B immunised mice has a number of possible explainations (figure 6.6). The time between vaccination and analysis was different between the two vaccination groups. The BCG mice were vaccinated once on day 0 then analysed on day 42. The immune response in these mice may have been consolidating toward a memory response with cells trafficking away from the lung and toward the draining lymph node. Evidence that supports this is the reduction in the T_{EM} cell population and the presence of Ag85B $_{281\text{-}295}$ CD4+ T cells detected in the lymph node of BCG vaccinated mice, but absent in the PilVax-Ag85B vaccinated mice (figure 6.17). Secondly, the BCG vaccinated mice only received one dose of the vaccniation where as PilVax vaccinated mice received multiple doses. This is because it takes multiple doses of PilVax to stimulate an immune response (chapter 5 figure 5.1). While the time since last vaccination differs between groups may explain why there is a different cell composition, it may also be an artifact of the reduction in variability offered by increasing the number of doses. This could be addressed by analysing PilVax-immunised mice 42 days after the final boost and analysing the presence of peptide specific cells in the periphery.

PilVax differs from other vaccines in trials (figure 1.1) due to the intransal route of delivery. Aerosol H56 vaccination in non-human primate models shows vaccination results in higher bacterial clearance than subcutaneous highlighting the benefit of PilVax mucosal delivery (Wong, Agger, Andersen, & Flynn, 2016). Additionally, mucosal BCG delivery results in superior protection against *Mtb* infection, inducing a further log reduction of *Mtb* following challenge compared to sub cutaneous BCG vaccination (Perdomo et al., 2016). The delivery route alone may offer enhanced protection against Mtb despite a similar peptide specific T cell response observed (figure 6.6, 6.11).

Increased protection observed in mucosal BCG delivery is associated with an influx of Ag85B peptide specific cells into the lungs, peaking 28 days post immunisation and remaining elevated for three weeks (Perdomo et al., 2016). The peak of $5x10^3$ cells is of a similar magnitude to PilVax-Ag85B vaccination at a similar time point following final vaccination (figure 6.6). Adoptive transfer the infiltrating T_{RM} cells resulted in protection against *Mtb* challenge (Perdomo et al., 2016). This adoptive transfer did deplete CD4+ and CD8+ T cells prior to transfer without a naïve cell transfer as a control which may question the validity this result due to concerns with adoptive transfer models as described previously.

The protective role of resident memory cells has demonstrated independently of adoptive transfer models by treating vaccinated mice with fingolimod, which blocks the trafficking of T cells into the lung prior to challenge. This showed a population lung resident (T_{RM}) cells alone is sufficient for protection against intranasal BCG challenge (Connor et al., 2010). Although PilVax-Ag85B did not generate a significant T_{CM} population at the time point the immune response was interrogated, the T_{RM} phenotype generated appears to play a role in protection. The Ag85B peptide specific T_{RM} generated could be sufficient to protect against *Mtb* challenge, and provided they are a sustained population, and could improve upon the current sub cutaneous BCG vaccination.

Where protection has been attributed to T_{RM} cells, such as mucosal BCG delivery, the major cytokine production measured is CD4+ cells producing only INF-γ (Perdomo et al., 2016). Though the proportion of CD4+ T cells producing INF-γ in PilVax-Ag85B mice is slightly lower than BCG vaccinated mice (figure 6.11), it is possible that if these cells are largely the T_{RM} cells identified in figure 6.6, protection is able to be achieved with PilVax-Ag85B.

As any novel *Mtb* vaccine is not likely to entierly replace BCG vaccination further studies could also include a vaccination group to analyse if boosting with PilVax-Ag85B is able to increase the exisiting response to BCG vaccination (Andersen & Doherty, 2005). The vaccine candidate MIP when administered as an aerosol boost two months following BCG vaccination has shown to result in a increase the production of INF-γ while also resulting in a sustained, significant reduction in bacterial load following *Mtb* challenge compared to BCG alone in a guinea pig model (Scriba et al., 2016). In mice BCG/MPI administration results in a further log reduction in pulmonary bacterial load following challenge compared to BCG alone (Saqib et al., 2016). This improves the response to MIP vaccination alone which results in a similar level of protection as BCG (Gupta et al., 2012). Although the protective capacity of PilVax is yet to be defined, there is precedent for novel vaccine candidates to be able to boost an existing response. Testing the ability of PilVax to act as a booster could use Saqib et al 2016's model and vaccine mice with BCG and begin the PiVax immunisation six weeks later, in addition to and BCG and PilVax only control.

There is also scope to expand the parameters measured by assessing the bacterial dissemination and load in other tissue when challenged with *Mtb* such as the spleen, as frequently analysed in other vaccine candidates. Spleenocytes could also be re-stimulated in addition to pulmonary lymphocytes to test T cell functionality. Where we have stimulated cells with the specific peptide of interest, others have used *Mtb* cell lysates (DAR-901 and MIP) which could also be included in such a study to provide a directly comparable data to existing literature (Masonou

et al., 2019; Saqib et al., 2016). However as PilVax only has one *Mtb* epitope, this may not yield a different level of stimulation with cognate peptide. Nevertheless it would be useful in assessing the ability of the peptide specific cells generated to respond to Ag85B protein in its native form.

This data shows the ability to generate peptide specific T cell respononses. Although the protective capacity of these cells it unknown there is justification to carry out a protection study

6.5.3 ***T cell subsets***

During the gating process to identify CD4+ and CD8+ T cell subsets, an unusally high proportion of CD3+CD4-CD8- double negative (DN) T cells was observed. Further examination revealed a large portion of the CD3+ cells in PilVax vaccinated mice were of this phenotype.

The function of DN T cells has remained poorly characterised. The role of DN T cells has been suggested as a regulatory T cell subset, and represent approximately 1-3% of the peripheral blood mononucelar cells in healthy individuals (Fischer et al., 2005; Sieling et al., 2000; Z.-X. Zhang, Yang, Young, DuTemple, & Zhang, 2000). Eleveated levels of this T cell subtype have also been closely assoicated with autoimmune diseases such as lupus. DN Tcells have also been linked to chronic activation of T cells (Grishkan, Ntranos, Calabresi, & Gocke, 2013; Sieling et al., 2000; D. Zhang et al., 2007). In a recent demonstration of this, CD3+CD4+ T cells were continually exposed to anti CD3/CD28 beads. Following repeated exposure to these beads that cause T cell activation, CD4 was down regulated leading to the rapid expansion of a DN T cell population (Grishkan et al., 2013). The DN population appeared after a minumum of three stimulations, while the cells expressed a high amount of IL-17 and INF-γ.

Proliferation of this cell population has been previously observed where pneumonic delivery of *Francisella tularensi*s live vaccine strain (LVS) resulted in the proliferation of DN T cells.

This was not seen with intradermal delivery of the same vaccine. This suggests the route of vaccine delivery affects the generation of the immune response. (Cowley et al., 2005). In multiple studies, DN T cells have potently mediated protection against intracellular pathogens, including *Mtb* largely through large scale secretions of IL-17 and INF-γ. Interstingly these cells were also able to confer the same protection in adoptive transfer studies (Cowley et al., 2005). These cells have also been described a proliferating in the the spleen of pneumonically vaccinated mice which phenotypic markers assoicated with memory T cells (Cowley et al., 2005; Cowley, Meierovics, Frelinger, Iwakura, & Elkins, 2010). Futher PilVax studies could also investigate the spleen of vaccinated mice for the presence of memory T cells at that site to assess the longevity of the immune response. The mulit-dose delivery of PilVax may cause the down regualtion of CD4 in the pulmonary T cells following multiple exposures to the PilVax *L. lactis* and explain the expansion of DN T cells. The proporation of DN CD3+ T cells in PilVax vaccinated mice does not seem to correlate with the level of pilus expression, suggesting that it may be exposure to *L. lactis* that promotes this expansion. Vaccinating mice with wild type *L. lactis* that has no pilus, could address this.

The percentage of level IL-17 and INF-γ producing DN T cells of PilVax-Ag85B and BCG vaccinated was similar (figure 6.15). However the larger proportion of DN T cells in PilVax vaccinated mice would indicate a larger amount of these cytokines was produced from the PilVax-Ag85B vaccinated mice. In PilVax-ESAT-6 vaccinated mice there is a clear trend of elvation in IL-17 production when cells are stimulated with cognate peptide (figure 6.16). This provides evidence that altough no CD4+ peptide specific T cells were detected, the immune activation here may warrant the inclusion of these constructs in a protection study as the tetramer staining may have failed.

The increased presence of DN T cells could be an explanation as to why mucosal vaccination delivered to the LRT appears to provide greater protection against pulmonary TB than more

traditional parenteral vaccination. This puts PilVax at a major advantange as the immune response generated does appear to skew toward what could be considered an ideal response in terms of *Mtb* protection.

However from this data it is not possible to tell if the appearance of these cells is the result of sustained stimulation and CD4+ downregulation as suggested by Grishkan et al 2013, due to a component of the vaccine itself, or as a result of stimulation with cognate peptide. The PilM1 negative control contains both the *S. pyogenes* pilus and *L. lactis* making it impossible to determine if either of these PilVax components is alone responsible for this effect or the repeated LRT delivery of antigen. As the cells were all stimulated before analysis there is no data providing information about the pre stimulation state of the lymphocytes. Additionally the staining to identify the peptide specific T cells (figure 6.3) did not stain for CD8 so is not possible to infer such information from other data sets. As the majority of other *Mtb* vaccine candidates are delivered intramuscular or subcutaneous, an increase in the proportion of double negative pulmonary T cells in these vaccine trials has not been previously described. (Das et al., 2016; Desel et al., 2011; Penn-Nicholson et al., 2015; L. Zhang et al., 2016) Given the findings of Grishkan et al 2013, it is likely the DN T cell population is a result of down regulation of CD4 as a result of repeated stimulation (Grishkan et al., 2013).

6.5.4 ***Cytokine Profiles***

The production of a number of cytokines was analaysed following stimulation of pulmonary cells with cognate peptide. INF-γ, TNFα and IL-17 have critical roles in control of *Mtb* infection, while IL-2 is marker of T cell activation (Domingo-Gonzalez, Prince, Cooper, & Khader, 2016).

The profiles of CD4+ T cells from PilVax-Ag85B and BCG vaccinated mice were similar as both produced INF-γ, while PilVax-Ag85B vaccinated mice also induced a number of cells

that produced INF-γ and IL-17 (figure 6.11). While previous studies have simply used INF-γ production as a correlate of protection, it has proved to not be the case as seen in the MVA85A vaccination study (Tameris et al., 2013). Of note here is the population of PilVax-Ag85B lung cells secreting both INF-γ and IL-17 following re-stimulation with cognate peptide. Further characterisation of the cytokines in the *Mtb* response have suggeseted an important correlate of protection in INF- γ and IL-17 secreting *Mtb* specific memory T cells which appear to have been generated here (Domingo-Gonzalez et al., 2016). Adoptive transfer of such cells has been shown to provide protection against *Mtb* infection, and the presence of such cells through mucosal vaccination improves BCG protection (Monin et al., 2015). Promisingly, these cells have been shown to be long lived, persisting for up to two years and may provide long term protection potential (Lindenstrøm et al., 2012).

In contrast, the majority of other vaccine candidates in clinical trials produce CD4+ T cells that are polyfunctional and protection afforded by these vaccines has been attributed to these polyfunctional T cells (Desel et al., 2011; Masonou et al., 2019; Saqib et al., 2016; L. Zhang et al., 2016). In these studies, the amount of cytokine produced was not necessarily higher than BCG vaccination rather a marked increase in the number of polyfuncational T cells has been attributed to the protective capacity. This is evident in the DAR-901 vaccine where the amount of cytokine produced upon stimulation was actually lower than BCG vaccination, however there was a noticeable increase in the proportion of polyfuncational T_{EM} cells attributed to protection (Masonou et al., 2019). These vaccine candidate studies however re-stimulate cells with whole *Mtb* cell lysate, where as we used cognate peptide. Where VPM1002, MIP, DAR-901, and Vaccae™ consist of multiple epitopes providing multiple epitopes for T cell recognition in vaccination and re-stimulation. PilVax is limited to a single peptide which could explain the differences in cytokine detection. This represents a potential limitation of PilVax as in response to stimulation with *Mtb* cell lysate, there is only one epitope to stimulate vaccine induced cells compared to the multiple epitopes available to other vaccine induced cells. Due to this, the same level of cytokine response may not be achieved.

Due to the lack of a definitive correlate of protection, it is difficult to predict how the PilVax immune response correlates with protection. Even among advanced vaccine candidates predicted mechanisms of protection differ. VPM1002 is thought to mediate protection thorough T_{CM} cell populations, while DAR-901 protection is attributed to T_{EM} cells (Desel et al., 2011; Masonou et al., 2019; Vogelzang et al., 2014). In VPM1002 studies the T_{EM} cells declined quickly in both vaccine candidate and BCG groups, while T_{CM} did not persist in VPM1002 vaccinated mice. If DAR-901 protection is mediated by T_{EM} cells, it could fail to induce lifelong protection in the same way as BCG. Without knowing the longevity of each memory phenotype in PilVax-Ag85B vaccinated mice it is difficult to predict how the cells identified in figure 6.6 may correlate to immunity.

A major limitation when comparing vaccine candidates is the lack of a standardised method to quantify peptide specific cells, cytokine responses, and a standardised phenotypic characterisation of memory T cells generated. While T_{CM} and T_{EM} are often characterised, the role of T_{RM} cells has not been studied in depth in pre-clinical studies. This is possibly due to a number of these studies being carried before the role of T_{RM} cells was defined in *Mtb* protection with the first indications of their importance not becoming apparent until recently (Park & Kupper, 2015; Perdomo et al., 2016; Sakai et al., 2014).

Previously INF-γ had been identified as a key correlate of protection as mice and humans deficient in this cytokine were extremely susceptible to fatal *Mtb* infections (Flynn et al., 1993; Ottenhoff, Kumararatne, & Casanova, 1998). As such INF-γ had been used as a major indicator of *Mtb* vaccine candidate protection in various trials. However the MVA85A vaccine candidate, which is able to induce a high level of INF-γ in humans, failed to boost protection more than BCG in neonates (Tameris et al., 2013). This called into question the ability to use INF-γ alone as a reliable correlate of protection and the subsequent search for a cytokine signature that correlates with *Mtb* protection has not yielded success. As such it is impossible to predict based on the cytokine profile from PilVax vaccination if protection is likely.

There is the production of a significant amount of INF-γ in CD4+ T cells in PilVax-Ag85B vaccinated mice, however PilVax-Ag85B vaccination lacks the polyfuncational cytokine profile where a single cell produces INF-γ, TNFα and IL-2, which seen in many other vaccine candidates. However this could be due to the limitations of the experimental design discussed below (p184). The only polyfunctional cells induced by PilVax-Ag85B vaccination was CD4+ T cells producing both INF-γ and IL-17, which are absent in BCG vaccinated mice (figure 6.11). IL-17 production has been implicated in the superior protection VPM1002 vaccination is able to confer compared to BCG while mice deficient in IL-17 production have impaired control of *Mtb* infection (Desel et al., 2011; Freches et al., 2013). Though unable to confer protection in its own right, Il-17 is able to confer partial protection against *Mtb* infection(Wozniak, Saunders, Ryan, & Britton, 2010). The presence of IL-17 and INF-γ producing CD4+ T cells in PilVax-Ag85B vaccinated mice could provide a pathway for PilVax-Ag85B vaccination to result in a greater level of Mtb protection compared to BCG.

Even though MVA85A did not enhance BCG protection in neonates, the design of this trial was perhaps flawed as neonatal BCG vaccination is where short term protection is actually acquired, so a lack of improvement in the existing immune response in this population should not be dismissed. To truly test its efficacy in neonates in this trial would be unethical as MVA85A would have to be administered on its own without BCG, and compared to the proven BCG vaccination, placing those neonates at risk of *Mtb* infection. Though this study has prompted a search for further correlates, INF-γ production should not be ignored.

Since natural *Mtb* infection does not result in prolonged immunity, it is not possible to easily determine what could correlate to protection. Previously INF-γ production was the major focus of vaccine trials, however this has since been expanded due to a lack of translation of this correlate protection into human trials. Based off of data obtained from studies of current vaccine candidates, the presence of a sustained CD4+ $T_{CM,}$ a sustained local CD4+ T_{RM} cells response, INF-γ and IL-17, and polyfunctional T cells appear to be critical. Despite CD8+ T_{RM} cells being implicated in

protection against intracellular pathogens and in Vaccae™, the focus remains on CD4+ mediated immunity as a longitudinal study of a number of vaccines in the clinical pipeline (figure 1.1) did implicated CD4+ T cells as the most significant correlate of enhanced protection in most vaccine candidates (Rodo et al., 2019; Schenkel et al., 2014). However, a true correlate of protection will not be revealed until a successful preventive vaccine is discovered.

The presence of $Ag85B_{281-295}$ specific CD4+ T cells and INF-γ/IL-17 producing cells is promising as a potential correlate of protection. These cells are also present in PilVax-ESAT-6 P1, P2 and P8 vaccinated mice (figure 6.12). This suggests that CD4+ ESAT-6 P1 cells were generated but were not detected due to technical failure of the tetramer staining. Conversley, as they are in all three PilVax-ESAT-6 peptide, and PilVax-Ag85B vaccinated mice could be due to the *L lactis* or pilus. Futher control groups could be included in future studies, both *L. lactis* with no pilus and a PBS vaccination group to determine if this is the case. The lack of INF- γ and IL17 secreting *Mtb* specific cells in PilVax-PilM6-ESAT-6 vacicnated mice could be due to the presentation ESAT-6 as a protein rather than peptide. Re-stimulation with the ESAT-6 protein may yeild a different result.

Only INF-γ was detected in CD8+ T cells from BCG vaccinated mice, while the remaning vaccination groups did not have any appreicable level of any cytokine production (figure 6.13). However INF-γ alone is not a good meausre of *Mtb* protective capaicty and the role of CD8+ T cells in *Mtb* infection is not well established.

The DN T cell cytokine profile was discussed in section 6.5.3 however it is worth mentioning the induction of INF-γ and IL-17 among this cell population and the protection adoptive transfer of these cells is able to permit (Cowley et al., 2005). PilVax-Ag85B is able to induce two subsets, CD4+ and DN T cells that produce INF-γ and IL-17 which have indivdually shown to be able to transfer protection in addptive transfer, and that can enhance BCG vaccination.

The high IL-17 production of DN T cell population in the PilVax-PilM6-ESAT-6 peptides, and PilM6-ESAT-6 protein vaccined mice suggests these constructs may be more immunogenic than previously suggested (figure 6.16). The generation of peptide specifc antibodies (chapter 5) and cytokine production seen here demonstrates that these contructs are more immunogenic than the tetramer staining suggests and warrant further investigation.

PilVax-Ag85B is certainly a promising candidate vaccine for protection studies. This data also provides justification for assseing what effect BCG and PilVax-Ag85B vacciation is able to elicit. BCG is able to generate a protection which seen across a number of studies. The addition of DN T and CD4+ T cells that produce INF-γ and IL-17 as in PilVax vaccination, may provide a more roubst, long lived protective response than previously seen.

A limitation of the cytokine analysis carried out in this study was that only one time point was analysed post-stimulation with cognate peptide. This can affect which cytokines are detected, as for example, TNFα is stored as a membrane associated homotrimer ready for rapid release which may have gone undetected by this assay (Domingo-Gonzalez et al., 2016). Additionally the samples here only looked at the production of cytokines that remained intracellular following the addition of Brefelden A to stop the export of cytokines from the cell. Analysis of cytokines in the supernatant could have provided more data on the total production of cytokines across the entire timeframe of the re-stimulation. Of greater value would be to analyse the cytokines across a number of time points and analyse the supernatent and intracellular production.

Chapter 7. Future Directions

PilVax has shown an ability to stimulate the MALT and generate peptide specific humoral and cellular responses. It has been demonstrated for the first time that PilVax is able to induce T cell specific responses through vaccinating with the PilVax-Ag85B construct. It should be noted that despite the low level of pilus expression in this construct, the level of T cell detection and activation is similar to BCG vaccinated mice. Further work could add additional copies of the peptide to the construct to try and boost the peptide specific immune response generated.

A number of questions remain about the other PilVax constructs generated for *Mtb* vaccination. In particular the PilVax-ESAT-6 P1 construct where, although CD4+ specific T cells were not detected, there is a large proliferation of DN T cells that produce INF-γ and IL-17. Although it can not be proven definitively without a positive control, the failure to detect ESAT-$6_{1\text{-}20}$ specific CD4+ T cells could be a technical problem. This construct could be worth further investigation due to the DN T cell potential in control of *Mtb* infection.

A study to assess the protective capacity of PilVax could be carried out that combines the information obtained in both the studies conducted here. A further round of vaccination may enhance the IgA response generated in addition to the T cell response already seen. The additional dose could be beneficial in production of IgA, but also further stimulate DN T cell proliferation which the literature suggests may be beneficial in controlling *Mtb* infection.

For protective studies a sample size of n=8/group would provide 80% power to detect a difference of approximately 0.5 (on the common log scale) for colony forming units (CFU) in lungs between the two groups, based on an estimated pooled standard deviation of 0.35 from previously collected data, when using a two-sided test at the 0.05 level. This effect is considered to be of practical importance. For context, a difference of approximately 1.0 (on the

common log scale) is typically observed for CFU between BCG-vaccinated and unvaccinated groups of mice.

Age and sex matched C57BL/6 mice should be vaccinated closely replicating the vaccination schedule and dose in section 6.2. The study should include a BCG vaccinated positive control group. Although mucosal BCG vaccination results in superior protection, in a human context the vaccine is delivered subcutaneously thus for translational purposes this positive control should also be delivered by this route in murine protection study (Perdomo et al., 2016). The timing of the BCG vaccination should be altered from section 6.2, to be at the same time as the final PilVax vaccination to provide a more direct comparison of time since completion of vaccination to challenge.

The PilVax-Ag85B and PilVax-ESAT-6 P1 group should be included in a protection study. PilVax-Ag85B due to the peptide specific antibodies, peptide specific CD4+ T cells, and cytokine production demonstrated throughout this thesis. Despite the lack of ESAT-6 P1 tetramer cells detected in this study (figure 6.4), the detection of peptide specific antibodies (figure 5.4, 5.5 and 5.6) suggest the peptide is not conformationally restricted when contained within the PilVax construct. Stimulation with cognate peptide also resulted in the production of INF-γ and TNFα producing CD4+ T cells, two cytokines that are critical in *Mtb* protection. In addition to this, as other studies have detected the presence of ESAT-6 P1 specific CD4+ T cells, this indicates that perhaps the failure to detect these cells here is due to a technical failure of the tetramer staining (Joshua S. Woodworth et al., 2019).

Negative control groups should include a group vaccinated PilVax-PilM1, to ensure any effects seen cannot be attributed to the pilus structure or *L. lactis*. A group of non-vaccinated mice should also be included that contains more than an n of 8. A portion of this larger group would be sacrificed immediately following *Mtb* challenge to determine pulmonary *Mtb* colonisation

by homogenising the lungs and spleen, plating on Middlebrook 7H11 agar and incubating at 37ºC for 2-3 weeks to determine CFU.

As BCG is a successful vaccination in its own right in protecting infants and children against *Mtb* infection it is unlikely to be replaced by PilVax alone (Andersen & Doherty, 2005). A model for testing the boosting effect a novel vaccine BCG has already been validated where mice are vaccinated with BCG and rested for two months prior to vaccination (Saqib et al., 2016). Inclusion of such a group would determine if PilVax is able to improve on any potential protection offered by BCG alone, and if so, in combination with the results in this thesis may elucidate how this occurs providing insight into potential correlates of protection.

Six weeks following completion of vaccination, mice should be challenged with 10^6 aerosolised *Mtb* and monitored for a further six weeks for vital health signs such as weight and behaviour. Survival compared to negative controls can be compared and after 6 weeks, remaining mice would be sacrificed. Bacterial load would be determined by plating lungs and spleen homogenates on Middlebrook 7H11 agar prior to incubation at 37ºC for 2-3 weeks to determine CFU. Assessing these two sties allows the determination of the ability of PilVax to control pulmonary infection as well as limit *Mtb* dissemination. A one log reduction in bacterial load on top of the reduction observed in BCG vaccinated is generally considered good protection, despite not resulting in sterilising immunity and resulting in a bacterial load of 10^4 CFU remaining (Gong, Liang, & Wu, 2018).

The expansion of antibodies could also be analysed by collecting serum samples at time points throughout the experiment and determine the end point titres against PilVax-peptide specific antibodies in each vaccination group. The sampling of mucosal sites could also be carried out at the experimental end point and antibody titres compared to previous data. Increases in peptide specific antibodies following challenge would indicate a potential role in the protection

against *Mtb* infection. The function of these antibodies could be analysed by purifying peptide specific antibodies and analysing the a glycan profile as described by Lu et al 2016 (Lu et al., 2016). If the glycan profile is similar to that identified in patients with latent *Mtb* infection, it could indicate the expanded population of Pilvax specific antibodies is playing a role in any suppression of *Mtb* that may be observed.

Should PilVax vaccination prove protective, there is the possibility of carrying on with further efficacy trials into non-human primates. However further assessing the immune response in PilVax vaccinated mice that have been challenged would also be beneficial. Determining the kinetics and expansion of pulmonary T cell phenotypes prior to and during infection and further analysis of the major cytokine production during *Mtb* infection could also be carried out. Together these data sets could provide insight into what is responsible for the protection by comparing how memory T cell phenotypes and cytokine responses differ between PilVax, BCG and other vaccine candidate vaccinations.

However if PilVax is able to elicit protection, it is worth mentioning that a significant limitation of PilVax lies in the fact that it is a genetically modified organism (GMO). This has major implications for downstream applications and use as a vaccine with regulatory and environmental challenges if it proves to be a protective peptide delivery system.

At least one study has addressed this and provided a proof of concept for a non GMO lactic acid bacteria delivery platform. Immune responses can be generated when a recombinant protein expressing a LysM domain is expressed separately in *E. coli*, and then bound to the cell wall of lactic acid bacteria. The lactic bacteria with recombinant protein attached to the cell wall via LysM domain binding were used in the immunisation study (A. D. Mustafa et al., 2018). Such a method could be advantageous for PilVax as although the majority of the immune responses observed appear to be independent of the level of pilus expression,

controlling the amount of pilus bound the surface of the *L lactis* may prove beneficial in terms of quality control.

For a *S. pyogenes* pilus based vaccine *E. coli* cannot be used as pilus assembly only occurs in the presence of a Gram positive housekeeping sortase. However work is underway in lab to adapt PilVax to memopath technology where the pilus is attached to the cell surface bacteria like particles (BLPs) that are essentially heat killed *L. lactis* (Bosma et al., 2006). PilVax could be heat killed however this process has the potential to strip the cell wall proteins and damage the pilus structure making addition of the pilus construct post heat killing more desirable. The pilus will be modified with the LPxTG motif of the cell wall anchor protein (Spy0125) replaced with a protein anchor (PA) that has a high affinity for the peptidoglycan of the cell wall. The replacement of the LPxTG motif will result in the pilus being retained in the cytoplasm where it is able to be recovered and mixed with the BLPs where binding is instant though not covalent. Controlling the amount of pilus per vaccine dose would improve the consistency per dose and negate any potential batch to batch variation in pilus expression in the current form.

In parallel to the memopath technology there is also the potential to utilise a nisin inducible expression system. The pilus in its current form is expressed constitutively under the lactococcal P23 promoter however nisin controlled expression (NICE) could be used. In this case the pilus protein expression would be under tight regulation but able to be induced to express much larger quantities than constitute expression. The expression is in proportion to the amount of inducing agent added providing more control in the standardisation of amount of antigen delivered per dose. This could provide an alternative means of quality control to BLPs (Bahey-El-Din, 2012; Mierau & Kleerebezem, 2005). Although *L. lactis* utilising this system are still a GMO, the implication selective marker is lactose which is already in the food chain. This compares to the current PilVax design where there is a selective antibiotic marker which can not be released into the environment.

Conclusion

By studying the immune response to vaccination with PilVax constructs with a range of *Mtb* epitopes, we have identified at least one construct that is able to induce a significant cellular and humoral response. The production of peptide specific CD4+ T cells is similar to that seen in BCG vaccination and the majority of these cells are resident memory cells, a subtype critical in *Mtb* control. PilVax also resulted in the generation of a number of INF-γ and IL-17 secreting double negative CD3+ T cells which have been implicated in *Mtb* clearance and control. Additionally, vaccination generates peptide specific serum and mucosal antibodies. This thesis has assessed the immunogenicity of a number of PilVax constructs targeting *Mtb*, and provided evidence that PilVax-Ag85B should be used in a protection study to analyse the protective capacity of the PilVax vaccination.

Appendix I

Spy0128 Sequence

MKLRHLLLTGAALTSFAATTVHGETVVNGAKLTVTKNLDLVNSNALIPNTDFTFKIEPDT
TVNEDGNKFKGVALNTPMTKVTYTNSDKGGSNTKTAEFDFSEVTFEKPGVYYYKVTEEKI
DKVPGVSYDTTSYTVQVHVLWNEEQQKPVATYIVGYKEGSKVPIQFKNSLDSTTLTVKKK
VSGTGGDRSKDFNFGLTLKANQYYKASEKVMIEKTTKGGQAPVQTEASIDQLYHFTLKDG
ESIKVTNLPVGVDYVVTEDDYKSEKYTTNVEVSPQDGAVKNIAGNSTEQETSTDKDMTIT
FTNKKDFEVPTGVAMTVAPYIALGIVAVGGALYFVKKKNA

T6 Sequence

MLACLAILAVVGLGMTRVSALSKDDTAQLKITNIEGGPTVTLYKIGEGVYNTNGDSFINF
KYAEGVSLTETGPTSQEITTIANGINTGKIKPFSTENVSISNGTATYNARGASVYIALLT
GATDGRTYNPILLAASYNGEGNLVTKNIDSKSNYLYGQTSVAKSSLPSITKKVTGTIDDV
NKKTTSLGSVLSYSLTFELPSYTKEAVNKTVYVSDNMSEGLTFNFNSLTVEWKGKMANIT
EDGSVMVENTKIGIAKEVNNGFNLSFIYDSLESISPNISYKAVVNNKAIVGEEGNPNKAE
FFYSNNPTKGNTYDNLDKKPDKGNGITSKEDSKIVYTYQIAFRKVDSVSKTPLIGAIFGV
YDTSNKLIDIVTTNKNGYAISTQVSSGKYKIKELKAPKGYSLNTETYEITANWVTATVKT
SANSKSTTYTSDKNKATDNSEQVGWLKNGIFYSIDSRPTGNDVKEAYIESTKALTDGTTF
SKSNEGSGTVLLETDIPNTKLGELPSTGSIGTYLFKAIGSAAMIGAIGIYIVKRRKA

Ovalbumin Sequence

MGSIGAASMEFCFDVFKELKVHHANETIFYCPIAIMSALAMVYLGAKDSTRTQINKVVRF
DKLPGFGDSIEAQCGTSVNVHSSLRDILNQITKPNDVYSFSLASRLYAEERYPILPEYLQ
CVKELYRGGLEPINFQTAADQARELINSWVESQTNGIIRNVLQPSSVDSQTAMVLVNAIV
FKGLWEKAFKDEDTQAMPFRVTEQESKPVQMMYQIGLFRVASMASEKMKILELPFASGTM
SMLVLLPDEVSGLEQLESIINFEKLTEWTSSNVMEERKIKVYLPRMKMEEKYNLTFVLMA
MGITDVFSSSANLSGISSAESLKISQAVHAAHAEINEADREVVGSAEAGVDAASVSEEFR
ADHPFLFCIKHIATNAVLFFGRCVSP

Appendix II

Data from chapter 6 was also visualised using t-SNE analysis carried out using FlowJo (FlowJo, LLC). The analysis did not provide further insights into the pulmonary lymphocyte production of cytokines following stimulation with cognate peptide beyond the Boolean gating strategy used. Data below represents a sample of t-SNE data as a reference.

t-SNE analysis of peptide specific T cells-CD4+ T cells

CD4+ T cell populations from PilVax-Ag85B vaccinated mice samples were concatenated using FlowJo and then t-SNE analysis run (A). Populations 1, 2, and 3 were identified by overlaying cytokine production gates onto the t-SNE plot (B). Each population was interrogated for cytokines produced (C). The same process was carried out for BCG CD4+ T cells (D-F). Boolean gating of this data is seen in figure 6.11

PilVax-Ag85B

t-SNE plot of concatenated
PilVax-Ag85B CD4+ T cells

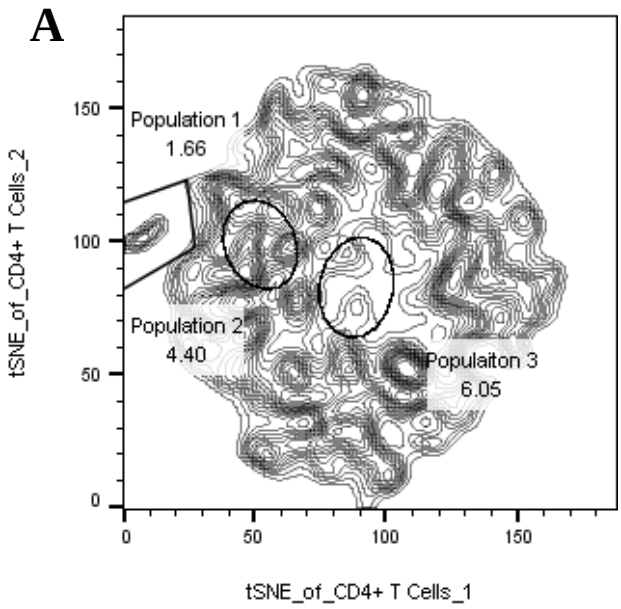

concat_1_Ag85B-CD4+ T cells.fcs
CD4+ T Cells
33377

B

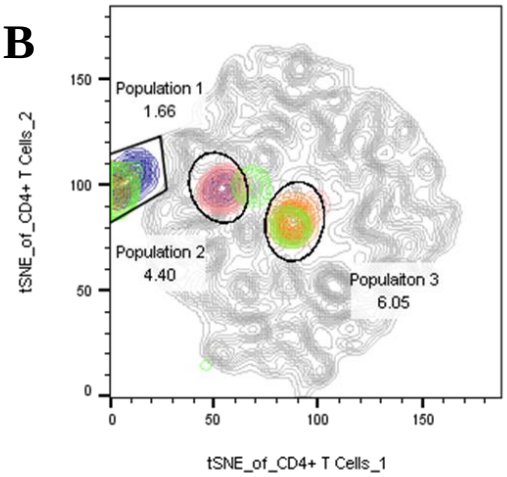

	Sample Name	Subset Name	Count	Freq. of Parent
	concat_1_Ag85B-CD4+ T cells.fcs	CD4+ IL2+ T Cells	9.00	0.027
	concat_1_Ag85B-CD4+ T cells.fcs	CD4+ TNFa+ T Cells	120	0.36
	concat_1_Ag85B-CD4+ T cells.fcs	CD4+ IL17+ T Cells	229	0.69
	concat_1_Ag85B-CD4+ T cells.fcs	CD4+ INFy+ Cells	558	1.67
	concat_1_Ag85B-CD4+ T cells.fcs	CD4+ T Cells	33377	100

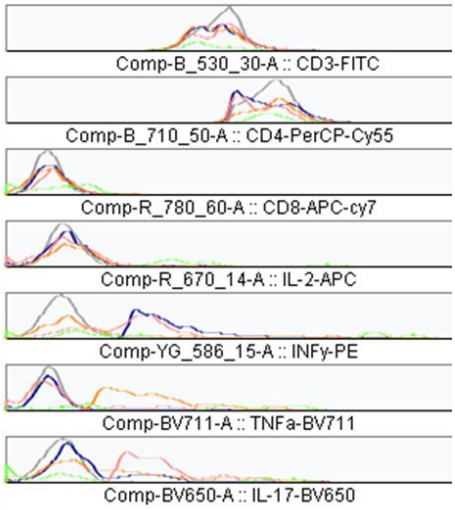

C

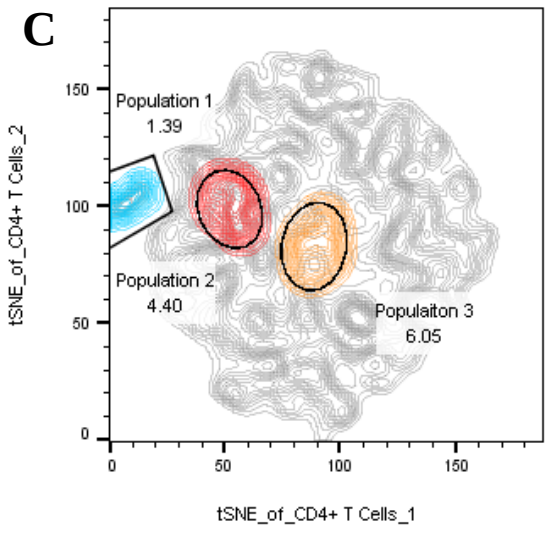

	Sample Name	Subset Name	Count	Freq. of Parent
	concat_1_Ag85B-CD4+ T cells.fcs	Populaiton 3	2019	6.05
	concat_1_Ag85B-CD4+ T cells.fcs	Population 2	1467	4.40
	concat_1_Ag85B-CD4+ T cells.fcs	Population 1	463	1.39
	concat_1_Ag85B-CD4+ T cells.fcs	CD4+ T Cells	33377	100

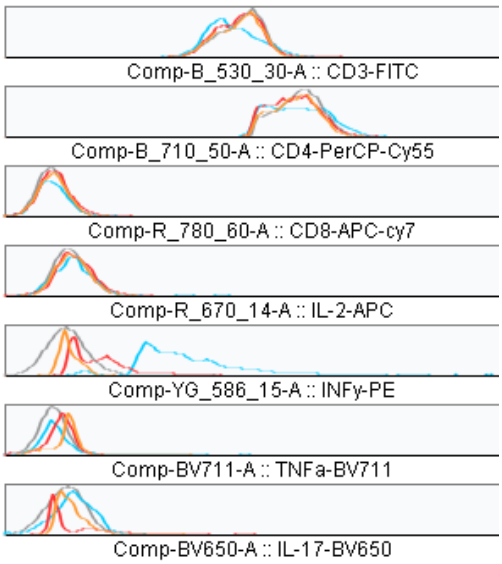

BCG

t-SNE plot of concatenated
BCG CD4+ T cells

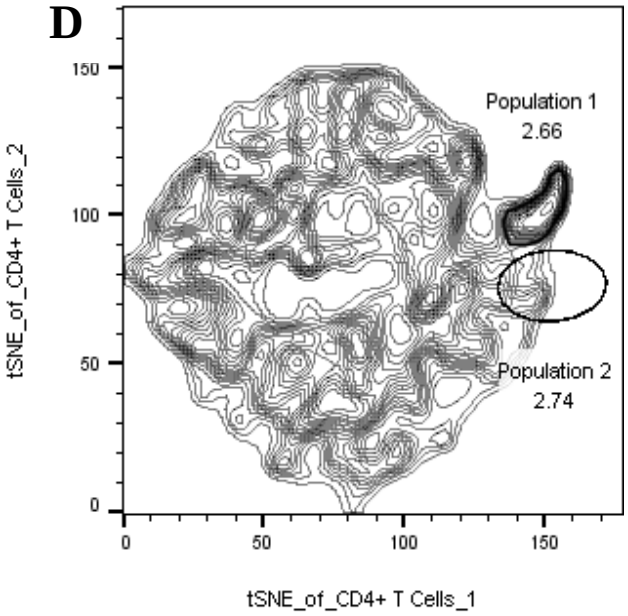

concat_1_BCG CD4+ T cells.fcs
CD4+ T Cells
33105

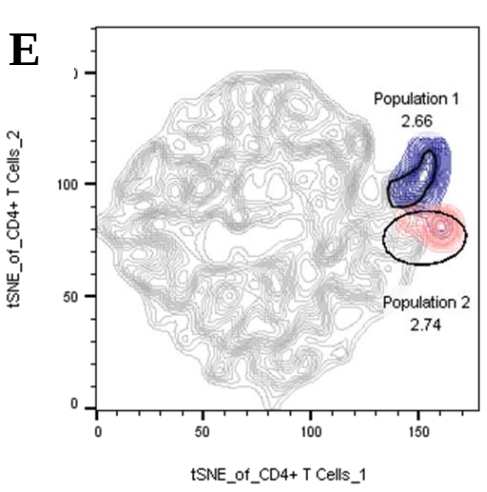

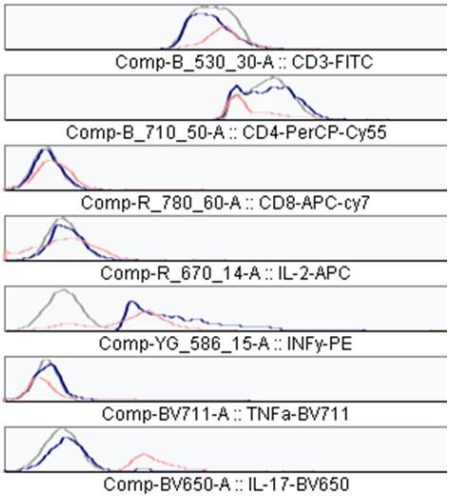

	Sample Name	Subset Name	Count	Freq. of Parent
	concat_1_BCG CD4+ T cells.fcs	CD8+ IL2+ T Cells	0	0
	concat_1_BCG CD4+ T cells.fcs	CD8+ TNFa+ T Cells	0	0
	concat_1_BCG CD4+ T cells.fcs	CD4+ IL17+ T Cells	87.0	0.26
	concat_1_BCG CD4+ T cells.fcs	CD4+ INFy+ Cells	1017	3.07
	concat_1_BCG CD4+ T cells.fcs	CD4+ T Cells	33105	100

F

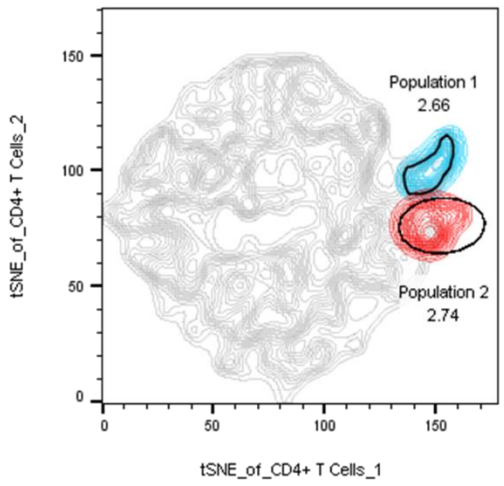

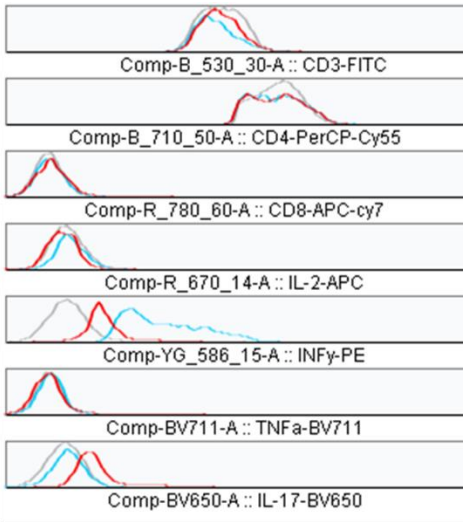

	Sample Name	Subset Name	Count	Freq. of Parent
	concat_1_BCG CD4+ T cells.fcs	Population 2	907	2.74
	concat_1_BCG CD4+ T cells.fcs	Population 1	879	2.66
	concat_1_BCG CD4+ T cells.fcs	CD4+ T Cells	33105	100

t-SNE analysis of peptide specific T cells

CD3+ cell populations from PilVax-Ag85B vaccinated mice samples were concatenated using FlowJo and then t-SNE analysis run (G). CD4+,CD8+, and CD3+CD4-CD8- were identified by overlaying cytokine production gates onto the t-SNE plot (H). The same process was carried out for BCG CD4+ T cells (I-J). Boolean gating of this data is seen in figure 6.8

t-SNE plot of concatenated
PilVax-Ag85B T cells

G

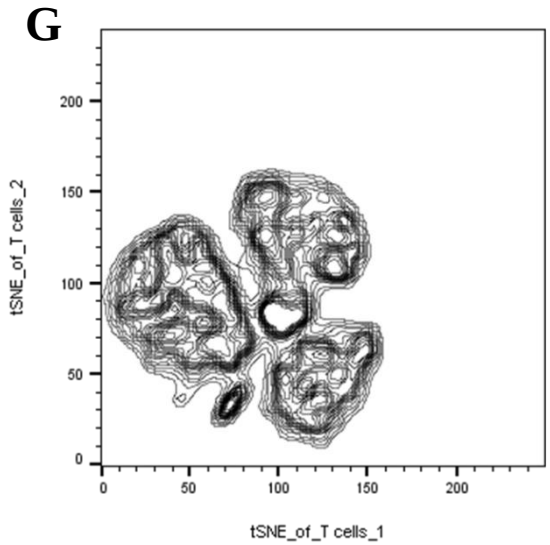

concat_1_Ag85B T cells.fcs
T cells
99265

H

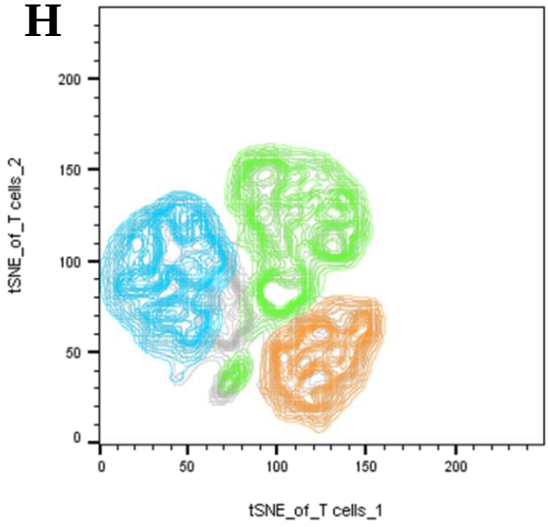

	Sample Name	Subset Name	Count	Freq. of Parent
	concat_1_Ag85B T cells.fcs	DN T Cells	37210	37.5
	concat_1_Ag85B T cells.fcs	CD8+ T Cells	22148	22.3
	concat_1_Ag85B T cells.fcs	CD4+ T Cells	33377	33.6
	concat_1_Ag85B T cells.fcs	T cells	99265	100

t-SNE plot of concatenated
BCG T cells

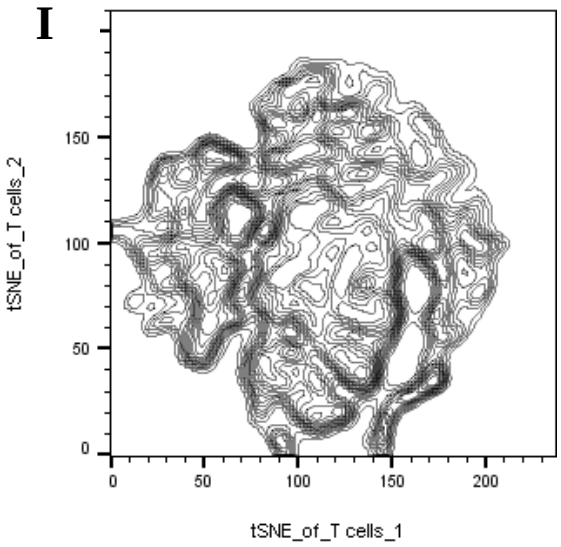

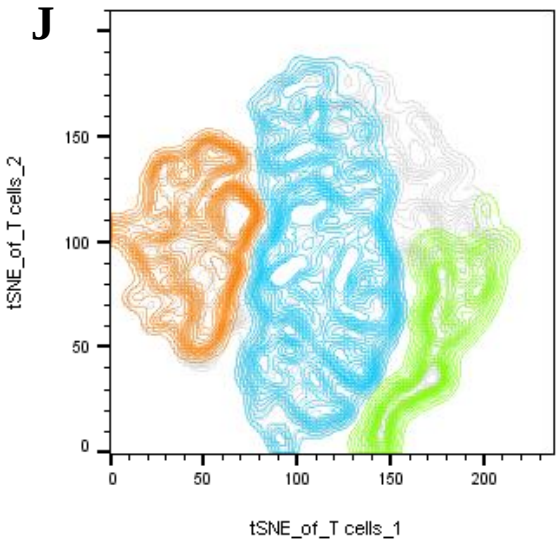

concat_1_BCG T cells.fcs
T cells
61756

	Sample Name	Subset Name	Count	Freq. of Parent
	concat_1_BCG T cells.fcs	DN T Cells	7314	11.8
	concat_1_BCG T cells.fcs	CD8+ T Cells	14146	22.9
	concat_1_BCG T cells.fcs	CD4+ T Cells	33105	53.6
	concat_1_BCG T cells.fcs	T cells	61756	100

References

Aagaard, C., Hoang, T. T., Izzo, A., Billeskov, R., Troudt, J., Arnett, K., . . . Dietrich, J. (2009). Protection and polyfunctional T cells induced by Ag85B-TB10.4/IC31 against *Mycobacterium tuberculosis* is highly dependent on the antigen dose. *PLoS One, 4*(6), 5930.

Abou-Zeid, C., Ratliff, T. L., Wiker, H. G., Harboe, M., Bennedsen, J., & Rook, G. A. (1988). Characterization of fibronectin-binding antigens released by *Mycobacterium tuberculosis* and *Mycobacterium bovis* BCG. *Infect Immun, 56*(12), 3046-3051.

Ancelet, L., Rich, F. J., Delahunt, B., & Kirman, J. R. (2012). Dissecting memory T cell responses to TB: Concerns using adoptive transfer into immunodeficient mice. *Tuberculosis, 92*(5), 422-433.

Andersen, P., Andersen, A. B., Sorensen, A. L., & Nagai, S. (1995). Recall of long-lived immunity to *Mycobacterium tuberculosis* infection in mice. *J Immunol, 154*(7), 3359-3372.

Andersen, P., Askgaard, D., Ljungqvist, L., Bentzon, M. W., & Heron, I. (1991). T-cell proliferative response to antigens secreted by *Mycobacterium tuberculosis*. *Infect Immun, 59*(4), 1558-1563.

Andersen, P., & Doherty, T. M. (2005). The success and failure of BCG - implications for a novel tuberculosis vaccine. *Nat Rev Microbiol, 3*(8), 656-662.

Andersen, P., & Kaufmann, S. H. (2014). Novel vaccination strategies against tuberculosis. *Cold Spring Harb Perspect Med, 4*(6), a018523.

Arbonés, M. L., Ord, D. C., Ley, K., Ratech, H., Maynard-Curry, C., Otten, G., . . . Teddert, T. F. (1994). Lymphocyte homing and leukocyte rolling and migration are impaired in L-selectin-deficient mice. *Immunity, 1*(4), 247-260.

Armitige, L. Y., Jagannath, C., Wanger, A. R., & Norris, S. J. (2000). Disruption of the genes encoding antigen 85A and antigen 85B of *Mycobacterium tuberculosis* H37Rv: effect on growth in culture and in macrophages. *Infect Immun, 68*(2), 767-778.

Baaten, B. J., Li, C.-R., & Bradley, L. M. (2010). Multifaceted regulation of T cells by CD44. *Communicative & integrative biology, 3*(6), 508-512.

Bahey-El-Din, M. (2012). *Lactococcus lactis*-based vaccines from laboratory bench to human use: an overview. *Vaccine, 30*(4), 685-690.

Belisle, J. T., Vissa, V. D., Sievert, T., Takayama, K., Brennan, P. J., & Besra, G. S. (1997). Role of the major antigen of *Mycobacterium tuberculosis* in cell wall biogenesis. *Science, 276*(5317), 1420-1422.

Bennekov, T., Dietrich, J., Rosenkrands, I., Stryhn, A., Doherty, T. M., & Andersen, P. (2006). Alteration of epitope recognition pattern in Ag85B and ESAT-6 has a profound influence on vaccine-induced protection against *Mycobacterium tuberculosis*. *Eur J Immunol, 36*(12), 3346-3355.

Berg, S., Starbuck, J., Torrelles, J. B., Vissa, V. D., Crick, D. C., Chatterjee, D., & Brennan, P. J. (2005). Roles of conserved proline and glycosyltransferase motifs of EmbC in biosynthesis of lipoarabinomannan. *J Biol Chem, 280*(7), 5651-5663.

Bermudez-Humaran, L. G., Cortes-Perez, N. G., Le Loir, Y., Alcocer-Gonzalez, J. M., Tamez-Guerra, R. S., de Oca-Luna, R. M., & Langella, P. (2004). An inducible surface presentation system improves cellular immunity against human papillomavirus type 16 E7 antigen in mice after nasal administration with recombinant lactococci. *J Med Microbiol, 53*(Pt 5), 427-433.

Berthet, F. X., Rasmussen, P. B., Rosenkrands, I., Andersen, P., & Gicquel, B. (1998). A *Mycobacterium tuberculosis* operon encoding ESAT-6 and a novel low-molecular-mass culture filtrate protein (CFP-10). *Microbiology, 144 (Pt 11)*, 3195-3203.

Bosma, T., Kanninga, R., Neef, J., Audouy, S. A., van Roosmalen, M. L., Steen, A., . . . Leenhouts, K. (2006). Novel surface display system for proteins on non-genetically modified Gram-positive bacteria. *Appl Environ Microbiol, 72*(1), 880-889.

Brandt, L., Oettinger, T., Holm, A., Andersen, A. B., & Andersen, P. (1996). Key epitopes on the ESAT-6 antigen recognized in mice during the recall of protective immunity to *Mycobacterium tuberculosis*. *J Immunol, 157*(8), 3527-3533.

Brennan, P. J., & Nikaido, H. (1995). The envelope of mycobacteria. *Annu Rev Biochem, 64*, 29-63.

Cambier, C. J., Falkow, S., & Ramakrishnan, L. (2014). Host evasion and exploitation schemes of *Mycobacterium tuberculosis*. *Cell, 159*(7), 1497-1509.

Chen, A., Engel, P., & Tedder, T. F. (1995). Structural requirements regulate endoproteolytic release of the L-selectin (CD62L) adhesion receptor from the cell surface of leukocytes. *J Exp Med, 182*(2), 519-530.

Chen, T., Blanc, C., Eder, A. Z., Prados-Rosales, R., Souza, A. C., Kim, R. S., . . . Achkar, J. M. (2016). Association of human antibodies to arabinomannan with enhanced mycobacterial opsonophagocytosis and intracellular growth reduction. *J Infect Dis, 214*(2), 300-310.

Cibrian, D., & Sanchez-Madrid, F. (2017). CD69: from activation marker to metabolic gatekeeper. *Eur J Immunol, 47*(6), 946-953.

Clark, R. A. (2015). Resident memory T cells in human health and disease. *Science translational medicine, 7*(269), 269rv261-269rv261.

Colditz, G. A., Brewer, T. F., Berkey, C. S., & et al. (1994). Efficacy of BCG vaccine in the prevention of tuberculosis: Meta-analysis of the published literature. *JAMA, 271*(9), 698-702.

Cole, J. G., & Jerse, A. E. (2009). Functional characterization of antibodies against *Neisseria gonorrhoeae* opacity protein loops. *PLoS One, 4*(12), e8108-e8108.

Connor, L. M., Harvie, M. C., Rich, F. J., Quinn, K. M., Brinkmann, V., Le Gros, G., & Kirman, J. R. (2010). A key role for lung-resident memory lymphocytes in protective immune responses after BCG vaccination. *Eur J Immunol, 40*(9), 2482-2492.

Content, J., de la Cuvellerie, A., De Wit, L., Vincent-Levy-Frebault, V., Ooms, J., & De Bruyn, J. (1991). The genes coding for the antigen 85 complexes of *Mycobacterium tuberculosis* and *Mycobacterium bovis* BCG are members of a gene family: cloning, sequence determination, and genomic organization of the gene coding for antigen 85-C of *M. tuberculosis*. *Infect Immun, 59*(9), 3205-3212.

Corthesy, B., Boris, S., Isler, P., Grangette, C., & Mercenier, A. (2005). Oral immunization of mice with lactic acid bacteria producing *Helicobacter pylori* urease B subunit partially protects against challenge with *Helicobacter felis*. *J Infect Dis, 192*(8), 1441-1449.

Cowley, S. C., Hamilton, E., Frelinger, J. A., Su, J., Forman, J., & Elkins, K. L. (2005). CD4−CD8− T cells control intracellular bacterial infections both in vitro and in vivo. *J Exp Med, 202*(2), 309-319.

Cowley, S. C., Meierovics, A. I., Frelinger, J. A., Iwakura, Y., & Elkins, K. L. (2010). Lung CD4−CD8− double-negative T cells are prominent producers of IL-17A and IFN-γ during primary respiratory murine infection with *Francisella tularensis* live vaccine strain. *The Journal of Immunology, 184*(10), 5791.

Cuevas-Cordoba, B., Juarez-Eusebio, D. M., Almaraz-Velasco, R., Muniz-Salazar, R., Laniado-Laborin, R., & Zenteno-Cuevas, R. (2015). Mutation at embB codon 306, a potential marker for the identification of multidrug resistance associated with

ethambutol in *Mycobacterium tuberculosis*. *Antimicrob Agents Chemother, 59*(9), 5455-5462.

Cunningham, M. W. (2008). Pathogenesis of Group A Streptococcal infections and their sequelae. *Adv Exp Med Biol, 609*, 29-42.

D'Souza, S., Rosseels, V., Romano, M., Tanghe, A., Denis, O., Jurion, F., . . . Huygen, K. (2003). Mapping of murine Th1 helper T-Cell epitopes of mycolyl transferases Ag85A, Ag85B, and Ag85C from *Mycobacterium tuberculosis*. *Infect Immun, 71*(1), 483-493.

Das, S., Chowdhury, B. P., Goswami, A., Parveen, S., Jawed, J., Pal, N., & Majumdar, S. (2016). *Mycobacterium indicus pranii* (MIP) mediated host protective intracellular mechanisms against tuberculosis infection: Involvement of TLR-4 mediated signaling. *Tuberculosis, 101*, 201-209.

Derrick, S. C., & Morris, S. L. (2007). The ESAT6 protein of *Mycobacterium tuberculosis* induces apoptosis of macrophages by activating caspase expression. *Cell Microbiol, 9*(6), 1547-1555.

Desel, C., Dorhoi, A., Bandermann, S., Grode, L., Eisele, B., & Kaufmann, S. H. (2011). Recombinant BCG ΔureC hly+ induces superior protection over parental BCG by stimulating a balanced combination of type 1 and type 17 cytokine responses. *J Infect Dis, 204*(10), 1573-1584.

Dieye, Y., Hoekman, A. J., Clier, F., Juillard, V., Boot, H. J., & Piard, J. C. (2003). Ability of *Lactococcus lactis* to export viral capsid antigens: a crucial step for development of live vaccines. *Appl Environ Microbiol, 69*(12), 7281-7288.

Domingo-Gonzalez, R., Prince, O., Cooper, A., & Khader, S. A. (2016). Cytokines and chemokines in *Mycobacterium tuberculosis* infection. *Microbiol spectr, 4*(5)

Edelson, B. T., & Unanue, E. R. (2001). Intracellular antibody neutralizes Listeria growth. *Immunity, 14*(5), 503-512.

Escuyer, V. E., Lety, M. A., Torrelles, J. B., Khoo, K. H., Tang, J. B., Rithner, C. D., . . . Chatterjee, D. (2001). The role of the embA and embB gene products in the biosynthesis of the terminal hexaarabinofuranosyl motif of *Mycobacterium smegmatis* arabinogalactan. *J Biol Chem, 276*(52), 48854-48862.

Fieber, C., Janos, M., Koestler, T., Gratz, N., Li, X. D., Castiglia, V., . . . Kovarik, P. (2015). Innate immune response to *Streptococcus pyogenes* depends on the combined activation of TLR13 and TLR2. *PLoS One, 10*(3), e0119727.

Fischer, K., Voelkl, S., Heymann, J., Przybylski, G. K., Mondal, K., Laumer, M., . . . Mackensen, A. (2005). Isolation and characterization of human antigen-specific TCR αβ+ CD4-CD8- double-negative regulatory T cells. *Blood, 105*(7), 2828-2835.

Fletcher, H. A., Snowden, M. A., Landry, B., Rida, W., Satti, I., Harris, S. A., . . . McShane, H. (2016). T-cell activation is an immune correlate of risk in BCG vaccinated infants. *Nat Commun, 7*, 11290.

Flynn, J. L., Chan, J., Triebold, K. J., Dalton, D. K., Stewart, T. A., & Bloom, B. R. (1993). An essential role for interferon gamma in resistance to *Mycobacterium tuberculosis* infection. *J Exp Med, 178*(6), 2249-2254.

Freches, D., Korf, H., Denis, O., Havaux, X., Huygen, K., & Romano, M. (2013). Mice genetically inactivated in interleukin-17A receptor are defective in long-term control of *Mycobacterium tuberculosis* infection. *Immunology, 140*(2), 220-231.

Fuchs, M., Kampfer, S., Helmsing, S., Spallek, R., Oehlmann, W., Prilop, W., . . . Hust, M. (2014). Novel human recombinant antibodies against *Mycobacterium tuberculosis* antigen 85B. *BMC Biotechnol, 14*, 68.

Garcia-Angulo, V. A., Kalita, A., & Torres, A. G. (2013). Advances in the development of enterohemorrhagic *Escherichia coli* vaccines using murine models of infection. *Vaccine, 31*(32), 3229-3235.

Giri, P. K., Verma, I., & Khuller, G. K. (2006). Enhanced immunoprotective potential of *Mycobacterium tuberculosis* Ag85 complex protein based vaccine against airway *Mycobacterium tuberculosis* challenge following intranasal administration. *FEMS Immunol Med Microbiol, 47*(2), 233-241.

Gomes, M. S., Paul, S., Moreira, A. L., Appelberg, R., Rabinovitch, M., & Kaplan, G. (1999). Survival of *Mycobacterium avium* and *Mycobacterium tuberculos*is in acidified vacuoles of murine macrophages. *Infect Immun, 67*(7), 3199-3206.

Gong, W., Liang, Y., & Wu, X. (2018). The current status, challenges, and future developments of new tuberculosis vaccines. *Hum Vaccin Immunother, 14*(7), 1697-1716.

Gordon, S. V., & Parish, T. (2018). Microbe profile: *Mycobacterium tuberculosis*: Humanity's deadly microbial foe. *Microbiology, 164*(4), 437-439.

Gratz, N., Siller, M., Schaljo, B., Pirzada, Z. A., Gattermeier, I., Vojtek, I., . . . Kovarik, P. (2008). Group A Streptococcus activates type I interferon production and MyD88-dependent signaling without involvement of TLR2, TLR4, and TLR9. *J Biol Chem, 283*(29), 19879-19887.

Grishkan, I. V., Ntranos, A., Calabresi, P. A., & Gocke, A. R. (2013). Helper T cells down-regulate CD4 expression upon chronic stimulation giving rise to double-negative T cells. *Cell Immunol, 284*(1-2), 68-74.

Grosset, J. (1978). The sterilizing value of rifampicin and pyrazinamide in experimental short-course chemotherapy. *Bull Int Union Tuberc, 53*(1), 5-12.

Gupta, A., Ahmad, F. J., Ahmad, F., Gupta, U. D., Natarajan, M., Katoch, V. M., & Bhaskar, S. (2012). Protective efficacy of *Mycobacterium indicus pranii* against tuberculosis and underlying local lung immune responses in guinea pig model. *Vaccine, 30*(43), 6198-6209.

Haghi, F., Peerayeh, S. N., Siadat, S. D., & Zeighami, H. (2012). Recombinant outer membrane secretin PilQ406–770 as a vaccine candidate for serogroup B *Neisseria meningitidis*. *Vaccine, 30*(9), 1710-1714.

Haile, Y., Bjune, G., & Wiker, H. G. (2002). Expression of the mceA, ESAT-6 and hspX genes in *Mycobacterium tuberculosis* and their responses to aerobic conditions and to restricted oxygen supply. *Microbiology, 148*(Pt 12), 3881-3886.

Harboe, M., Oettinger, T., Wiker, H. G., Rosenkrands, I., & Andersen, P. (1996). Evidence for occurrence of the ESAT-6 protein in *Mycobacterium tuberculosis* and virulent *Mycobacterium bovis* and for its absence in *Mycobacterium bovis* BCG. *Infect Immun, 64*(1), 16-22.

Harth, G., Lee, B. Y., Wang, J., Clemens, D. L., & Horwitz, M. A. (1996). Novel insights into the genetics, biochemistry, and immunocytochemistry of the 30-kilodalton major extracellular protein of *Mycobacterium tuberculosis*. *Infect Immun, 64*(8), 3038-3047.

Hendrickx, A. P. A., Budzik, J. M., Oh, S.-Y., & Schneewind, O. (2011). Architects at the bacterial surface - sortases and the assembly of pili with isopeptide bonds. *Nature Reviews Microbiology, 9*, 166.

Holmgren, J., & Czerkinsky, C. (2005). Mucosal immunity and vaccines. *Nature Medicine, 11*, S45.

Houben, D., Demangel, C., van Ingen, J., Perez, J., Baldeón, L., Abdallah, A. M., . . . Peters, P. J. (2012). ESX-1-mediated translocation to the cytosol controls virulence of mycobacteria. *Cellular Microbiology, 14*(8), 1287-1298.

Houben, E. N., Korotkov, K. V., & Bitter, W. (2014). Take five - Type VII secretion systems of Mycobacteria. *Biochim Biophys Acta, 1843*(8), 1707-1716.

Huang, C. Y., & Hsieh, W. Y. (2017). Efficacy of *Mycobacterium vaccae* immunotherapy for patients with tuberculosis: A systematic review and meta-analysis. *Hum Vaccin Immunother, 13*(9), 1960-1971.

Huygen, K., Lozes, E., Gilles, B., Drowart, A., Palfliet, K., Jurion, F., . . . et al. (1994). Mapping of TH1 helper T-cell epitopes on major secreted mycobacterial antigen 85A in mice infected with live *Mycobacterium bovis* BCG. *Infect Immun, 62*(2), 363-370.

Jerse, A. E., Bash, M. C., & Russell, M. W. (2014). Vaccines against gonorrhea: current status and future challenges. *Vaccine, 32*(14), 1579-1587.

Johansson, E.-L., Wassén, L., Holmgren, J., Jertborn, M., & Rudin, A. (2001). Nasal and vaginal vaccinations have differential effects on antibody responses in vaginal and cervical secretions in humans. *Infect Immun, 69*(12), 7481.

Kanaujia, G. V., Motzel, S., Garcia, M. A., Andersen, P., & Gennaro, M. L. (2004). Recognition of ESAT-6 sequences by antibodies in sera of tuberculous nonhuman primates. *Clin Diagn Lab Immunol, 11*(1), 222-226.

Kang, H. J., Coulibaly, F., Clow, F., Proft, T., & Baker, E. N. (2007). Stabilizing isopeptide bonds revealed in gram-positive bacterial pilus structure. *Science, 318*(5856), 1625-1628.

Kinhikar, A. G., Verma, I., Chandra, D., Singh, K. K., Weldingh, K., Andersen, P., . . . Laal, S. (2010). Potential role for ESAT6 in dissemination of *M. tuberculosis* via human lung epithelial cells. *Mol Microbiol, 75*(1), 92-106.

Kohama, H., Umemura, M., Okamoto, Y., Yahagi, A., Goga, H., Harakuni, T., . . . Arakawa, T. (2008). Mucosal immunization with recombinant heparin-binding haemagglutinin adhesin suppresses extrapulmonary dissemination of *Mycobacterium bovis* Bacillus Calmette-Guérin (BCG) in infected mice. *Vaccine, 26*(7), 924-932.

Kondratieva, T. K., Rubakova, E. I., Linge, I. A., Evstifeev, V. V., Majorov, K. B., & Apt, A. S. (2010). B cells delay neutrophil migration toward the site of stimulus: tardiness critical for effective Bacillus Calmette-Guerin vaccination against tuberculosis infection in mice. *J Immunol, 184*(3), 1227-1234.

Lambkin-Williams, R., Gelder, C., Broughton, R., Mallett, C. P., Gilbert, A. S., Mann, A., . . . Burt, D. (2016). An intranasal proteosome-adjuvanted trivalent influenza vaccine is safe, immunogenic & efficacious in the human viral influenza challenge model. Serum IgG & mucosal IgA Are important correlates of protection against illness sssociated with infection. *PLoS One, 11*(12), e0163089.

Leroux-Roels, I., Leroux-Roels, G., Ofori-Anyinam, O., Moris, P., De Kock, E., Clement, F., . . . Ballou, W. R. (2010). Evaluation of the safety and immunogenicity of two antigen concentrations of the Mtb72F/AS02(A) candidate tuberculosis vaccine in purified protein derivative-negative adults. *Clin Vaccine Immunol, 17*(11), 1763-1771.

Lienhardt, C., & Zumla, A. BCG: the story continues. *The Lancet, 366*(9495), 1414-1416.

Lin, P. L., Dietrich, J., Tan, E., Abalos, R. M., Burgos, J., Bigbee, C., . . . Andersen, P. (2012). The multistage vaccine H56 boosts the effects of BCG to protect cynomolgus macaques against active tuberculosis and reactivation of latent *Mycobacterium tuberculosis* infection. *J Clin Invest, 122*(1), 303-314.

Lindenstrøm, T., Woodworth, J., Dietrich, J., Aagaard, C., Andersen, P., & Agger, E. M. (2012). Vaccine-induced th17 cells are maintained long-term postvaccination as a distinct and phenotypically stable memory subset. *Infect Immun, 80*(10), 3533-3544.

Lu, L. L., Chung, A. W., Rosebrock, T. R., Ghebremichael, M., Yu, W. H., Grace, P. S., . . . Alter, G. (2016). A functional role for antibodies in tuberculosis. *Cell, 167*(2), 433-443.e414.

Luabeya, A. K. K., Kagina, B. M. N., Tameris, M. D., Geldenhuys, H., Hoff, S. T., Shi, Z., . . . Hussey, G. D. (2015). First-in-human trial of the post-exposure tuberculosis vaccine H56:IC31 in *Mycobacterium tuberculosis* infected and non-infected healthy adults. *Vaccine, 33*(33), 4130-4140.

Ma, Y., Keil, V., & Sun, J. (2015). Characterization of *Mycobacterium tuberculosis* EsxA membrane insertion: roles of N- and C-terminal flexible arms and central helix-turn-helix motif. *J Biol Chem, 290*(11), 7314-7322.

Mackay, L. K., Braun, A., Macleod, B. L., Collins, N., Tebartz, C., Bedoui, S., . . . Gebhardt, T. (2015). Cutting edge: CD69 interference with sphingosine-1-phosphate receptor function regulates peripheral T cell retention. *The Journal of Immunology, 194*(5), 2059.

Mahairas, G. G., Sabo, P. J., Hickey, M. J., Singh, D. C., & Stover, C. K. (1996). Molecular analysis of genetic differences between *Mycobacterium bovis* BCG and virulent *M. bovis*. *J Bacteriol, 178*(5), 1274-1282.

Malhotra, I., Ouma, J., Wamachi, A., Kioko, J., Mungai, P., Omollo, A., . . . King, C. L. (1997). In utero exposure to helminth and mycobacterial antigens generates cytokine responses similar to that observed in adults. *J Clin Invest, 99*(7), 1759-1766.

Mannam, P., Jones, K. F., & Geller, B. L. (2004). Mucosal vaccine made from live, recombinant *Lactococcus lactis* protects mice against pharyngeal infection with *Streptococcus pyogenes*. *Infect Immun, 72*(6), 3444.

Manrique, M., Kozlowski, P. A., Wang, S. W., Wilson, R. L., Micewicz, E., Montefiori, D. C., . . . Aldovini, A. (2009). Nasal DNA-MVA SIV vaccination provides more significant protection from progression to AIDS than a similar intramuscular vaccination. *Mucosal Immunology, 2*(6), 536-550.

Masonou, T., Hokey, D. A., Lahey, T., Halliday, A., Berrocal-Almanza, L. C., Wieland-Alter, W. F., . . . von Reyn, C. F. (2019). CD4+ T cell cytokine responses to the DAR-901 booster vaccine in BCG-primed adults: A randomized, placebo-controlled trial. *PLoS One, 14*(5), e0217091.

Mawa, P. A., Nkurunungi, G., Egesa, M., Webb, E. L., Smith, S. G., Kizindo, R., . . . Elliott, A. M. (2015). The impact of maternal infection with *Mycobacterium tuberculosis* on the infant response to Bacille Calmette-Guérin immunization. *Philosophical transactions of the Royal Society of London. Series B, Biological sciences, 370*(1671), 20140137.

McFarland, B. J., Sant, A. J., Lybrand, T. P., & Beeson, C. (1999). Ovalbumin(323-339) peptide binds to the major histocompatibility complex class II I-A(d) protein using two functionally distinct registers. *Biochemistry, 38*(50), 16663-16670.

Mercenier, A., Muller-Alouf, H., & Grangette, C. (2000). Lactic acid bacteria as live vaccines. *Curr Issues Mol Biol, 2*(1), 17-25.

Mierau, I., & Kleerebezem, M. (2005). 10 years of the nisin-controlled gene expression system (NICE) in *Lactococcus lactis*. *Appl Microbiol Biotechnol, 68*(6), 705-717.

Monin, L., Griffiths, K. L., Slight, S., Lin, Y., Rangel-Moreno, J., & Khader, S. A. (2015). Immune requirements for protective Th17 recall responses to *Mycobacterium tuberculosis* challenge. *Mucosal Immunology, 8*(5), 1099-1109.

Mora, M., Bensi, G., Capo, S., Falugi, F., Zingaretti, C., Manetti, A. G. O., . . . Telford, J. L. (2005). Group A Streptococcus produce pilus-like structures containing protective antigens and Lancefield T antigens. *Proceedings of the National Academy of Sciences, 102*(43), 15641-15646.

Mustafa, A. D., Kalyanasundram, J., Sabidi, S., Song, A. A., Abdullah, M., Abdul Rahim, R., & Yusoff, K. (2018). Proof of concept in utilizing in-trans surface display system of *Lactobacillus plantarum* as mucosal tuberculosis vaccine via oral administration in mice. *BMC Biotechnol, 18*(1), 63.

Mustafa, A. S., Oftung, F., Amoudy, H. A., Madi, N. M., Abal, A. T., Shaban, F., . . . Andersen, P. (2000). Multiple epitopes from the *Mycobacterium tuberculosis* ESAT-6 antigen are

recognized by antigen-specific human T cell lines. *Clin Infect Dis, 30 Suppl 3*, S201-205.

Mwau, M., Cebere, I., Sutton, J., Chikoti, P., Winstone, N., Wee, E. G., . . . Hanke, T. (2004). A human immunodeficiency virus 1 (HIV-1) clade A vaccine in clinical trials: stimulation of HIV-specific T-cell responses by DNA and recombinant modified vaccinia virus Ankara (MVA) vaccines in humans. *J Gen Virol, 85*(Pt 4), 911-919.

Nieuwenhuizen, N. E., Kulkarni, P. S., Shaligram, U., Cotton, M. F., Rentsch, C. A., Eisele, B., . . . Kaufmann, S. H. E. (2017). The recombinant Bacille Calmette-Guerin vaccine VPM1002: Ready for clinical efficacy testing. *Front Immunol, 8*, 1147.

Oettinger, T., Jorgensen, M., Ladefoged, A., Haslov, K., & Andersen, P. (1999). Development of the *Mycobacterium bovis* BCG vaccine: review of the historical and biochemical evidence for a genealogical tree. *Tuber Lung Dis, 79*(4), 243-250.

Olafsdottir, T. A., Lingnau, K., Nagy, E., & Jonsdottir, I. (2009). IC31, a two-component novel adjuvant mixed with a conjugate vaccine enhances protective immunity against pneumococcal disease in neonatal mice. *Scand J Immunol, 69*(3), 194-202.

Olsen, A. W., Hansen, P. R., Holm, A., & Andersen, P. (2000). Efficient protection against *Mycobacterium tuberculosis* by vaccination with a single subdominant epitope from the ESAT-6 antigen. *Eur J Immunol, 30*(6), 1724-1732.

Onwueme, K. C., Vos, C. J., Zurita, J., Ferreras, J. A., & Quadri, L. E. (2005). The dimycocerosate ester polyketide virulence factors of mycobacteria. *Prog Lipid Res, 44*(5), 259-302.

Orme, I. M. (1988). Characteristics and specificity of acquired immunologic memory to *Mycobacterium tuberculosis* infection. *J Immunol, 140*(10), 3589-3593.

Orme, I. M. (2010). The Achilles heel of BCG. *Tuberculosis (Edinb), 90*(6), 329-332.

Orme, I. M., & Collins, F. M. (1983). Protection against *Mycobacterium tuberculosis* infection by adoptive immunotherapy. Requirement for T cell-deficient recipients. *J Exp Med, 158*(1), 74-83.

Ottenhoff, T. H. M., Kumararatne, D., & Casanova, J.-L. (1998). Novel human immunodeficiencies reveal the essential role of type-1 cytokines in immunity to intracellular bacteria. *Immunology Today, 19*(11), 491-494.

Palma, C., Iona, E., Giannoni, F., Pardini, M., Brunori, L., Fattorini, L., . . . Cassone, A. (2008). The LTK63 adjuvant improves protection conferred by Ag85B DNA-protein prime-boosting vaccination against *Mycobacterium tuberculosis* infection by dampening IFN-γ response. *Vaccine, 26*(33), 4237-4243.

Pape, J. W., Liautaud, B., Thomas, F., Mathurin, J. R., St Amand, M. M., Boncy, M., . . . Johnson, W. D., Jr. (1983). Characteristics of the acquired immunodeficiency syndrome (AIDS) in Haiti. *N Engl J Med, 309*(16), 945-950.

Park, C. O., & Kupper, T. S. (2015). The emerging role of resident memory T cells in protective immunity and inflammatory disease. *Nature Medicine, 21*, 688.

Peake, P., Gooley, A., & Britton, W. J. (1993). Mechanism of interaction of the 85B secreted protein of *Mycobacterium bovis* with fibronectin. *Infect Immun, 61*(11), 4828-4834.

Peng, X., & Sun, J. (2016). Mechanism of ESAT-6 membrane interaction and its roles in pathogenesis of *Mycobacterium tuberculosis*. *Toxicon, 116*, 29-34.

Penn-Nicholson, A., Geldenhuys, H., Burny, W., van der Most, R., Day, C. L., Jongert, E., . . . Scriba, T. J. (2015). Safety and immunogenicity of candidate vaccine M72/AS01E in adolescents in a TB endemic setting. *Vaccine, 33*(32), 4025-4034.

Perdomo, C., Zedler, U., Kühl, A. A., Lozza, L., Saikali, P., Sander, L. E., . . . Kupz, A. (2016). Mucosal BCG vaccination induces protective lung-resident memory T cell populations against tuberculosis. *mBio, 7*(6), e01686-01616.

Petricevich, V. L., Ueda, C., Alves, R. C., da Silva, M. A., Moreno, C., Melo, A. R., & Dias da Silva, W. (2001). A single strain of *Mycobacterium bovis* Bacillus Calmette-Guerin (BCG) grown in two different media evokes distinct humoral immune responses in mice. *Braz J Med Biol Res, 34*(1), 81-92.

Phuah, J. Y., Mattila, J. T., Lin, P. L., & Flynn, J. L. (2012). Activated B cells in the granulomas of non-human primates infected with *Mycobacterium tuberculosis*. *Am J Pathol, 181*(2), 508-514.

Pilon, J. L., Rhyan, J. C., Wolfe, L. L., Davis, T. R., McCollum, M. P., O'Rourke, K. I., . . . Nol, P. (2013). Immunization with a synthetic peptide vaccine fails to protect mule deer *Odocoileus hemionusrom* chronic wasting disease. *J Wildl Dis, 49*(3), 694-698.

Prendergast, K. A., Counoupas, C., Leotta, L., Eto, C., Bitter, W., Winter, N., & Triccas, J. A. (2016). The Ag85B protein of the BCG vaccine facilitates macrophage uptake but is dispensable for protection against aerosol *Mycobacterium tuberculosis* infection. *Vaccine, 34*(23), 2608-2615.

Proft, T., & Baker, E. N. (2009). Pili in Gram-negative and Gram-positive bacteria - structure, assembly and their role in disease. *Cell Mol Life Sci, 66*(4), 613-635.

Rahman, M. J., Dégano, I. R., Singh, M., & Fernández, C. (2010). Influence of maternal gestational treatment with mycobacterial antigens on postnatal immunity in an experimental murine model. *PLoS One, 5*(3), e9699-e9699.

Raynaud, C., Laneelle, M. A., Senaratne, R. H., Draper, P., Laneelle, G., & Daffe, M. (1999). Mechanisms of pyrazinamide resistance in mycobacteria: importance of lack of uptake in addition to lack of pyrazinamidase activity. *Microbiology, 145 (Pt 6)*, 1359-1367.

Reed, M. B., Domenech, P., Manca, C., Su, H., Barczak, A. K., Kreiswirth, B. N., . . . Barry, C. E., 3rd. (2004). A glycolipid of hypervirulent tuberculosis strains that inhibits the innate immune response. *Nature, 431*(7004), 84-87.

Rezvani, K., Yong, A. S. M., Mielke, S., Jafarpour, B., Savani, B. N., Le, R. Q., . . . Barrett, A. J. (2011). Repeated PR1 and WT1 peptide vaccination in Montanide-adjuvant fails to induce sustained high-avidity, epitope-specific CD8+ T cells in myeloid malignancies. *Haematologica, 96*(3), 432.

Ritz, N., & Curtis, N. (2009). Mapping the global use of different BCG vaccine strains. *Tuberculosis, 89*(4), 248-251.

Rodo, M. J., Rozot, V., Nemes, E., Dintwe, O., Hatherill, M., Little, F., & Scriba, T. J. (2019). A comparison of antigen-specific T cell responses induced by six novel tuberculosis vaccine candidates. *PLoS Pathog, 15*(3)

Rodríguez, A., Tjärnlund, A., Ivanji, J., Singh, M., García, I., Williams, A., . . . Fernández, C. (2005). Role of IgA in the defense against respiratory infections: IgA deficient mice exhibited increased susceptibility to intranasal infection with *Mycobacterium bovis* BCG. *Vaccine, 23*(20), 2565-2572.

Rook, G. A., & Hernandez-Pando, R. (1996). The pathogenesis of tuberculosis. *Annu Rev Microbiol, 50*, 259-284.

Rouse, D. A., DeVito, J. A., Li, Z., Byer, H., & Morris, S. L. (1996). Site-directed mutagenesis of the katG gene of *Mycobacterium tuberculosis:* effects on catalase-peroxidase activities and isoniazid resistance. *Mol Microbiol, 22*(3), 583-592.

Ryndak, M., Wang, S., & Smith, I. (2008). PhoP, a key player in *Mycobacterium tuberculosis* virulence. *Trends Microbiol, 16*(11), 528-534.

Sakai, S., Kauffman, K. D., Schenkel, J. M., McBerry, C. C., Mayer-Barber, K. D., Masopust, D., & Barber, D. L. (2014). Cutting edge: control of *Mycobacterium tuberculosis* infection by a subset of lung parenchyma-homing CD4 T cells. *J Immunol, 192*(7), 2965-2969.

Sancho, D., Gómez, M., & Sánchez-Madrid, F. (2005). CD69 is an immunoregulatory molecule induced following activation. *Trends in Immunology, 26*(3), 136-140.

Saqib, M., Khatri, R., Singh, B., Gupta, A., Kumar, A., & Bhaskar, S. (2016). *Mycobacterium indicus pranii* as a booster vaccine enhances BCG induced immunity and confers higher protection in animal models of tuberculosis. *Tuberculosis, 101*, 164-173.

Sauer, F. G., Mulvey, M. A., Schilling, J. D., Martinez, J. J., & Hultgren, S. J. (2000). Bacterial pili: molecular mechanisms of pathogenesis. *Curr Opin Microbiol, 3*(1), 65-72.

Schenkel, J. M., Fraser, K. A., Beura, L. K., Pauken, K. E., Vezys, V., & Masopust, D. (2014). Resident memory CD8 T cells trigger protective innate and adaptive immune responses. *Science, 346*(6205), 98.

Schön, T., Juréen, P., Giske, C. G., Chryssanthou, E., Sturegård, E., Werngren, J., . . . Ängeby, K. A. (2009). Evaluation of wild-type MIC distributions as a tool for determination of clinical breakpoints for *Mycobacterium tuberculosis*. *Journal of Antimicrobial Chemotherapy, 64*(4), 786-793.

Scorpio, A., & Zhang, Y. (1996). Mutations in pncA, a gene encoding pyrazinamidase/nicotinamidase, cause resistance to the anti-tuberculous drug pyrazinamide in tubercle bacillus. *Nat Med, 2*(6), 662-667.

Scott Gallichan, W., & Rosenthal, K. L. (1995). Specific secretory immune responses in the female genital tract following intranasal immunization with a recombinant adenovirus expressing glycoprotein B of herpes simplex virus. *Vaccine, 13*(16), 1589-1595.

Scriba, T. J., Kaufmann, S. H., Henri Lambert, P., Sanicas, M., Martin, C., & Neyrolles, O. (2016). Vaccination against tuberculosis with whole-cell mycobacterial vaccines. *J Infect Dis, 214*(5), 659-664.

Sharma, S. K., Katoch, K., Sarin, R., Balambal, R., Kumar Jain, N., Patel, N., . . . Rani, R. (2017). Efficacy and safety of *Mycobacterium indicus pranii* as an adjunct therapy in category II pulmonary tuberculosis in a randomized trial. *Sci Rep, 7*(1), 3354.

Siegrist, M. S., & Bertozzi, C. R. (2014). Mycobacterial lipid logic. *Cell Host Microbe, 15*(1), 1-2.

Sieling, P. A., Porcelli, S. A., Duong, B. T., Spada, F., Bloom, B. R., Diamond, B., & Hahn, B. H. (2000). Human double-negative T Cells in systemic lupus erythematosus provide help for IgG and are restricted by CD1c. *The Journal of Immunology, 165*(9), 5338.

Skeiky, Y. A., Alderson, M. R., Ovendale, P. J., Guderian, J. A., Brandt, L., Dillon, D. C., . . . Reed, S. G. (2004). Differential immune responses and protective efficacy induced by components of a tuberculosis polyprotein vaccine, Mtb72F, delivered as naked DNA or recombinant protein. *J Immunol, 172*(12), 7618-7628.

Skinner, M. A., Yuan, S., Prestidge, R., Chuk, D., Watson, J. D., & Tan, P. L. (1997). Immunization with heat-killed *Mycobacterium vaccae* stimulates CD8+ cytotoxic T cells specific for macrophages infected with *Mycobacterium tuberculosis*. *Infect Immun, 65*(11), 4525-4530.

Smith, J., Manoranjan, J., Pan, M., Bohsali, A., Xu, J., Liu, J., . . . Gao, L. Y. (2008). Evidence for pore formation in host cell membranes by ESX-1-secreted ESAT-6 and its role in *Mycobacterium marinum* escape from the vacuole. *Infect Immun, 76*(12), 5478-5487.

Soderholm, A. T., Barnett, T. C., Sweet, M. J., & Walker, M. J. (2018). Group A Streptococcal pharyngitis: Immune responses involved in bacterial clearance and GAS-associated immunopathologies. *J Leukoc Biol, 103*(2), 193-213.

Somoskovi, A., Parsons, L. M., & Salfinger, M. (2001). The molecular basis of resistance to isoniazid, rifampin, and pyrazinamide in *Mycobacterium tuberculosis*. *Respir Res, 2*(3), 164-168.

Sorensen, A. L., Nagai, S., Houen, G., Andersen, P., & Andersen, A. B. (1995). Purification and characterization of a low-molecular-mass T-cell antigen secreted by *Mycobacterium tuberculosis*. *Infect Immun, 63*(5), 1710-1717.

Sreejit, G., Ahmed, A., Parveen, N., Jha, V., Valluri, V. L., Ghosh, S., & Mukhopadhyay, S. (2014). The ESAT-6 protein of *Mycobacterium tuberculosis* interacts with β-2-microglobulin (β2M) affecting antigen presentation function of macrophage. *PLoS Pathog, 10*(10), e1004446-e1004446.

Stanford, J., Stanford, C., & Grange, J. (2004). Immunotherapy with *Mycobacterium vaccae* in the treatment of tuberculosis. *Front Biosci, 9*, 1701-1719.

Stanford, J. L., Stanford, C. A., Grange, J. M., Lan, N. N., & Etemadi, A. (2001). Does immunotherapy with heat-killed *Mycobacterium vaccae* offer hope for the treatment of multi-drug-resistant pulmonary tuberculosis? *Respir Med, 95*(6), 444-447.

Sterne, J. A., Rodrigues, L. C., & Guedes, I. N. (1998). Does the efficacy of BCG decline with time since vaccination? *Int J Tuberc Lung Dis, 2*(3), 200-207.

Suliman, S., Luabeya, A. K. K., Geldenhuys, H., Tameris, M., Hoff, S. T., Shi, Z., . . . Group, H. T. (2019). Dose pptimization of H56:IC31 vaccine for tuberculosis-endemic populations. A double-blind, placebo-controlled, dose-selection trial. *Am J Respir Crit Care Med, 199*(2), 220-231.

Tameris, M., McShane, H., McClain, J. B., Landry, B., Lockhart, S., Luabeya, A. K., . . . Mahomed, H. (2013). Lessons learnt from the first efficacy trial of a new infant tuberculosis vaccine since BCG. *Tuberculosis (Edinb), 93*(2), 143-149.

Telenti, A., Philipp, W. J., Sreevatsan, S., Bernasconi, C., Stockbauer, K. E., Wieles, B., . . . Jacobs, W. R., Jr. (1997). The emb operon, a gene cluster of *Mycobacterium tuberculosis* involved in resistance to ethambutol. *Nat Med, 3*(5), 567-570.

Thakur, A., Mikkelsen, H., & Jungersen, G. (2019). Intracellular pathogens: Host immunity and microbial persistence strategies. *Journal of immunology research, 2019*, 1356540-1356540.

Tsatsaronis, J. A., Walker, M. J., & Sanderson-Smith, M. L. (2014). Host responses to Group A Streptococcus: cell death and inflammation. *PLoS Pathog, 10*(8), e1004266.

Unsoeld, H., & Pircher, H. (2005). Complex memory T-cell phenotypes revealed by coexpression of CD62L and CCR7. *Journal of virology, 79*(7), 4510-4513.

Van Der Meeren, O., Hatherill, M., Nduba, V., Wilkinson, R. J., Muyoyeta, M., Van Brakel, E., . . . Tait, D. R. (2018). Phase 2b controlled trial of M72/AS01(E) vaccine to prevent tuberculosis. *The New England journal of medicine, 379*(17), 1621-1634.

van der Wel, N., Hava, D., Houben, D., Fluitsma, D., van Zon, M., Pierson, J., . . . Peters, P. J. (2007). *M. tuberculosis a*nd *M. leprae* translocate from the phagolysosome to the cytosol in myeloid cells. *Cell, 129*(7), 1287-1298.

Villena, J., Medina, M., Vintiñi, E., & Alvarez, S. (2008). Stimulation of respiratory immunity by oral administration of *Lactococcus lactis*. *Canadian Journal of Microbiology, 54*(8), 630-638.

Vogelzang, A., Perdomo, C., Zedler, U., Kuhlmann, S., Hurwitz, R., Gengenbacher, M., & Kaufmann, S. H. (2014). Central memory CD4+ T cells are responsible for the recombinant Bacillus Calmette-Guerin ΔureC::hly vaccine's superior protection against tuberculosis. *J Infect Dis, 210*(12), 1928-1937.

Volkman, H. E., Pozos, T. C., Zheng, J., Davis, J. M., Rawls, J. F., & Ramakrishnan, L. (2010). Tuberculous granuloma induction via interaction of a bacterial secreted protein with host epithelium. *Science, 327*(5964), 466-469.

von Reyn, C. F., Lahey, T., Arbeit, R. D., Landry, B., Kailani, L., Adams, L. V., . . . Waddell, R. (2017). Safety and immunogenicity of an inactivated whole cell tuberculosis vaccine

booster in adults primed with BCG: A randomized, controlled trial of DAR-901. *PLoS One, 12*(5), e0175215-e0175215.
Wagachchi, D., Tsai, J.-Y. C., Chalmers, C., Blanchett, S., Loh, J. M. S., & Proft, T. (2018). PilVax – a novel peptide delivery platform for the development of mucosal vaccines. *Scientific Reports, 8*(1), 2555.
Wells, J. M., & Mercenier, A. (2008). Mucosal delivery of therapeutic and prophylactic molecules using lactic acid bacteria. *Nat Rev Microbiol, 6*(5), 349-362.
Wells, W. F., Ratcliffe, H. L., & Grumb, C. (1948). On the mechanics of droplet nuclei infection; quantitative experimental air-borne tuberculosis in rabbits. *Am J Hyg, 47*(1), 11-28.
Wherry, E. J., Teichgraber, V., Becker, T. C., Masopust, D., Kaech, S. M., Antia, R., . . . Ahmed, R. (2003). Lineage relationship and protective immunity of memory CD8 T cell subsets. *Nat Immunol, 4*(3), 225-234.
Wiker, H. G., & Harboe, M. (1992). The antigen 85 complex: a major secretion product of *Mycobacterium tuberculosis*. *Microbiol Rev, 56*(4), 648-661.
Williams, A., Reljic, R., Naylor, I., Clark, S. O., Falero-Diaz, G., Singh, M., . . . Ivanyi, J. (2004). Passive protection with immunoglobulin A antibodies against tuberculous early infection of the lungs. *Immunology, 111*(3), 328-333.
Wong, E. A., Agger, E. M., Andersen, P., & Flynn, J. L. (2016). Vaccination route has an impact on level of protection of non-human primates from tuberculosis. *The Journal of Immunology, 196*(1 Supplement), 146.121.
Woodworth, J. S., Christensen, D., Cassidy, J. P., Agger, E. M., Mortensen, R., & Andersen, P. (2019). Mucosal boosting of H56:CAF01 immunization promotes lung-localized T cells and an accelerated pulmonary response to *Mycobacterium tuberculosis* infection without enhancing vaccine protection. *Mucosal Immunology, 12*(3), 816-826.
Woodworth, J. S., Cohen, S. B., Moguche, A. O., Plumlee, C. R., Agger, E. M., Urdahl, K. B., & Andersen, P. (2017). Subunit vaccine H56/CAF01 induces a population of circulating CD4 T cells that traffic into the *Mycobacterium tuberculosis*-infected lung. *Mucosal Immunology, 10*(2), 555-564.
WorldHealthOrganisation. (2018). *Global tuberculosis report 2018*.
Wozniak, T. M., Saunders, B. M., Ryan, A. A., & Britton, W. J. (2010). *Mycobacterium bovis* BCG-Specific Th17 cells confer partial protection against *Mycobacterium tuberculosis* infection in the absence of gamma interferon. *Infect Immun, 78*(10), 4187.
Xu, L. J., Wang, Y. Y., Zheng, X. D., Gui, X. D., Tao, L. F., & Wei, H. M. (2009). Immunotherapeutical potential of *Mycobacterium vaccae* on *M. tuberculosis infection* in mice. *Cell Mol Immunol, 6*(1), 67-72.
Yang, H., & Kim, D. S. (2015). Chapter One - Peptide immunotherapy in vaccine development: From epitope to adjuvant. In R. Donev (Ed.), *Advances in Protein Chemistry and Structural Biology* (Vol. 99, pp. 1-14): Academic Press.
Yang, S., Liu, F., Wang, Q. J., Rosenberg, S. A., & Morgan, R. A. (2011). The shedding of CD62L (L-selectin) regulates the acquisition of lytic activity in human tumor reactive T lymphocytes. *PLoS One, 6*(7), e22560. 10.1371/journal.pone.0022560
Young, P. G., Moreland, N. J., Loh, J. M., Bell, A., Atatoa Carr, P., Proft, T., & Baker, E. N. (2014). Structural conservation, variability, and immunogenicity of the T6 backbone pilin of serotype M6 *Streptococcus pyogenes*. *Infect Immun, 82*(7), 2949-2957.
Young, P. G., Proft, T., Harris, P. W., Brimble, M. A., & Baker, E. N. (2014). Structure and activity of *Streptococcus pyogenes* SipA: a signal peptidase-like protein essential for pilus polymerisation. *PLoS One, 9*(6), e99135.
Yusuf, H., & Kett, V. (2017). Current prospects and future challenges for nasal vaccine delivery. *Hum Vaccin Immunother, 13*(1), 34-45.

Zhang, D., Yang, W., Degauque, N., Tian, Y., Mikita, A., & Zheng, X. X. (2007). New differentiation pathway for double-negative regulatory T cells that regulates the magnitude of immune responses. *Blood, 109*(9), 4071-4079.

Zhang, L., Jiang, Y., Cui, Z., Yang, W., Yue, L., Ma, Y., . . . Qian, A. (2016). *Mycobacterium vaccae* induces a strong Th1 response that subsequently declines in C57BL/6 mice. *Journal of veterinary science, 17*(4), 505-513.

Zhang, Y., Heym, B., Allen, B., Young, D., & Cole, S. (1992). The catalase—peroxidase gene and isoniazid resistance of *Mycobacterium tuberculosis*. *Nature, 358*(6387), 591-593.

Zhang, Y., Scorpio, A., Nikaido, H., & Sun, Z. (1999). Role of acid pH and deficient efflux of pyrazinoic acid in unique susceptibility of *Mycobacterium tuberculosis* to pyrazinamide. *J Bacteriol, 181*(7), 2044-2049.

Zhang, Z.-X., Yang, L., Young, K. J., DuTemple, B., & Zhang, L. (2000). Identification of a previously unknown antigen-specific regulatory T cell and its mechanism of suppression. *Nature Medicine, 6*(7), 782-789.

Zimhony, O., Cox, J. S., Welch, J. T., Vilcheze, C., & Jacobs, W. R., Jr. (2000). Pyrazinamide inhibits the eukaryotic-like fatty acid synthetase I (FASI) of *Mycobacterium tuberculosis*. *Nat Med, 6*(9), 1043-1047.